UDK 624+69(05) = 862 CODEN: GDVIAE ISSN 0350-2465

Volumen 78 / Volume 78
Str. 245 - 296 / pp. 245 - 296
Svibanj 2026. Zagreb / May 2026 Zagreb

Časopis Hrvatskog saveza građevinskih inženjera
Journal of the Croatian Association of Civil Engineers
Journal des Kroatischen Verbandes der Bauingenieure

Sadržaj / Contents

5/2026

Znanstveni i stručni članci / Scientific and Professional Papers

UDK 624+69(05) = 862 CODEN: GDVIAE ISSN 0350-2465

Sadržaj / Contents / Inhalt

5/2026

Stručno-informativni prilozi / Professional news items

Vijesti / News

UDK 624+69(05) = 862

CODEN: GDVIAE

Impressum

Osnivač i izdavač
Hrvatski savez građevinskih inženjera
Berislavićeva 6, 10000 Zagreb

Adresa uredništva
Zagreb, Berislavićeva 6
Tel: +385 1 48-72-502
e-mail: gradjevinar@hsgi.org
www.casopis-gradjevinar.hr

Glavni i odgovorni urednik
Prof.dr.sc. **Stjepan Lakušić**
Sveučilište u Zagrebu
e-mail: stjepan.lakusic@grad.unizg.hr

Urednici - novinari
Tanja Vrančić
Anđela Bogdan

Tehnički urednik
Tanja Vrančić

Informatička podrška
Ivo Haladin
Katarina Vranešić

Lektori i prevoditelji
Nataše Bunijevac Krlić (hrvatski jezik)
Sanda Dominković (hrvatski jezik)
Studio Nixa Prijevodi (engleski jezik)
Editage Author Services

Časopis Građevinar referiraju:
The Thomson Reuters services - Science Citation Index Expanded (poznat kao SciSearch®) i Journal Citation Reports/Science Edition, od siječnja 2008), ICONDA-Stuttgart, CITIS LTD-Dublin, CIRIA-London, ENGINEERING INFORMATION Inc-New York, BATIMENT, TRAVAUX PUBLICS - Francuska, Stroit'el'stvo i arhitektura - Referativniji žurnal - Moskva, HRIS ABSTRACT-Washington, DOCUMENTATION WASSER-Düsseldorf

Časopis GRAĐEVINAR sufinancira Ministarstvo znanosti, obrazovanja i mladih Republike Hrvatske

Svi objavljeni članci u časopisu recenzirani su.
Časopis izlazi mjesečno.
Naklada: 2500 primjeraka

Pretplata
Godišnja pretplata:
za Hrvatsku (47,78 EUR);
za inozemstvo (120 EUR + poštarina).
Pretplata za studente u Hrvatskoj (15, 93 EUR).

Žiro račun
HSGI, OIB: 57450863852,
Zagreb, Berislavićeva 6
Broj računa: 2360000-1101426005

Print
Tiskara Zelina d.d.

Oblikovanje
Modulor Studio

Naslovna stranica:
Miami Stadium, DIBS
(https://www.dibs-parking.com/blog/your-ultimate-guide-to-hard-rock-stadium-s-epic-summer-2025-lineup)
Atlanta Stadium, HOK
(https://parametric-architecture.com/hok-mercedes-benz-stadium/?srsltid=AfmBOooR13eME4y9bV-fzm_3hA8JsSi_V3DsD5fHqOU3-Id3K_i9KEiq#Project_Details)

Napomena:

Od broja **1/2012** GRAĐEVINARA, svi se radovi tiskaju na hrvatskom jeziku kao i dosada, no u online izdanju svi su radovi osim na hrvatskom u cijelosti i na engleskom jeziku. Na taj način časopis GRAĐEVINAR pomaže autorima da se rezultati njihovih znanstvenih istraživanja te njihove vrijedne spoznaje i iskustva što je moguće više približe znanstvenoj i stručnoj javnosti i to ne samo na području hrvatskoga govornog područja već na području cijele međunarodne znanstvene i stručne zajednice. Od siječnja 2012. u časopisu Građevinar primjenjuje se dvostruko slijepa recenzija (engl. **double blind review**). Od broja 1/2014 svi radovi umjesto dosadašnjeg UDK broja imaju DOI broj. Za pretraživanje radova prema DOI broju preporuča se koristiti servis http://dx.doi.org.

HSGI
Hrvatski savez građevinskih inženjera

GRAĐEVINAR
IF 2024 = 0,9

UDK 627.13.001.4:551.464. CODEN: GDVIAE ISSN 0350-2465

Impressum

Founder and Publisher
Croatian Association of Civil Engineers
Berislaviceva 6, 10000 Zagreb, Croatia

Editorial office
Zagreb, Berislaviceva 6
Phone: +385 1 48-72-502
e-mail: gradjevinar@hsgi.org
www.casopis-gradjevinar.hr

Editor-in-Chief
Prof. **Stjepan Lakušić**
University of Zagreb
e-mail: stjepan.lakusic@grad.unizg.hr

Editors - Journalists
Tanja Vrančić
Anđela Bogdan

Technical Editor
Tanja Vrančić

IT Support
Ivo Haladin
Katarina Vranešić

Linguistic Advisers and Translators
Nataše Bunijevac Krlić (Croatian)
Sanda Dominković (Croatian)
Studio Nixa Prijevodi (English)
Editage Author Services

Abstracting and Indexing
The Thomson Reuters services: Science Citation Index Expanded (also known as SciSearch®) and Journal Citation Reports/ Science Edition, from January 2008), ICONDA-Stuttgart, CITIS LTD-Dublin, CIRIA-London, ENGINEERING INFORMATION Inc-New York, BATIMENT, TRAVAUX PUBLICS-France, Stroit'el'stvo i arhitektura - Referativniji žurnal - Moskva, HRIS ABSTRACT-Washington, DOCUMENTATION WASSER-Düsseldorf

Journal GRAĐEVINAR is co-financed by the Ministry of Science, Education and Youth of the Republic of Croatia

All papers published in journal have been reviewed.
Journal published monthly
Circulation: 2500 copies

Subscriptions
Yearly subscription fee:
for Croatia (47,78 EUR)
for other countries (120 EUR + shipping cost).
Subscription for students in Croatia (15,93 EUR).

Foreign account
Bank name and adress: Zagrebacka banka, Paromlinska 2, Zagreb
Account Holder's Name: HSGI
SWIFT Code: ZABA HR 2X
IBAN: HR 732360000 1101426005

Print
Tiskara Zelina d.d.

Design
Modulor Studio

Journal cover:
Miami Stadium, DIBS
(https://www.dibs-parking.com/blog/your-ultimate-guide-to-hard-rock-stadium-s-epic-summer-2025-lineup)
Atlanta Stadium, HOK
(https://parametric-architecture.com/hok-mercedes-benz-stadium/?srsltid=AfmBOooR13eME4y9bV-fzm_3hA8JsSi_V3DsD5fHqOU3-Id3K_i9KEiq#Project_Details)

Note:

As of the first issue of GRAĐEVINAR for 2012, all papers are printed in Croatian language as usual, but the online edition of the journal features full versions of all papers in English language as well. In this way, GRAĐEVINAR will help the authors to present results of their scientific research and their valuable ideas and experience to the scientific and professional community, not only in areas where Croatian language is in use, but also throughout the entire international scientific and professional community. As of January 2012, the journal has DOUBLE BLIND REVIEW process. Since the issue 1/2014, all papers will have the DOI number instead of the current UDK number. The use of the service http://dx.doi.org is recommended for finding papers according to their DOI number.

HSGI
Croatian Association of Civil Engineers

GRAĐEVINAR
IF 2024 = 0,9

UDK 624+69(05) = 862 CODEN: GDVIAE ISSN 0350-2465

Urednički odbor

Potpora časopisu

UDK 627.13.001.4:551.464. CODEN: GDVIAE ISSN 0350-2465

Editorial board

Supported by

Primljen / Received: 30.10.2025.
Ispravljen / Corrected: 3.5.2026.
Prihvaćen / Accepted: 7.5.2026.
Dostupno online / Available online: 10.6.2026.

Praćenje seizmičke aktivnosti nakon potresa u Petrinji 2020. godine

Autori:


Izv.prof.dr.sc. **Josip Stipčević**
jstipcevic.geof@pmf.hr
Autor za korespondenciju


Krešimir Kuk, mag.phys.-geophys.
kreso.kuk@gfz.hr


Izv.prof.dr.sc. **Iva Dasović**
iva.dasovic@gfz.hr


Dr.sc. **Dinko Šindija**
dsindija@gmail.com


Dr.sc. **Kristina Šariri**
ksariri@gfz.h


Dr.sc. **Marin Sečanj**
msecanj@gfz.hr


Prof.dr.sc. **Davorka Herak**
davorka.herak@gfz.hr


Akademik **Marijan Herak**
marijan.herak@gfz.hr

Sveučilište u Zagrebu
Prirodoslovno-matematički fakultet
Geofizički odsjek

Izvorni znanstveni rad

Josip Stipčević, Krešimir Kuk, Iva Dasović, Dinko Šindija, Kristina Šariri, Marin Sečanj, Davorka Herak, Marijan Herak

Praćenje seizmičke aktivnosti nakon potresa u Petrinji 2020. godine

Niz potresa na području Petrinje započeo je u ponedjeljak 28. prosinca 2020. u 6:28 po lokalnome vremenu (CET) potresom magnitude M_L = 5,1 (M_W = 4,9), koji se osjetio na većemu dijelu središnje Hrvatske. Epicentar se nalazio jugozapadno od Petrinje, u blizini sela Strašnika. Ubrzo su uslijedili potresi lokalne magnitude 4,6 u 7.49 te magnitude 3,8 u 7:51 u istome epicentralnom području, kao i niz slabijih potresa. Nažalost, ti relativno snažni potresi pokazali su se tek prethodnim potresima, jer je već sljedećeg dana, 29. prosinca 2020. u 12:19, zabilježen još jači potres lokalne magnitude 6,2 (M_W = 6,4), također s epicentrom u blizini Strašnika. Temelj ove studije čini velika količina prikupljenih seizmoloških podataka. Za analizu novoprikupljenog skupa podataka korišteni su klasični postupci analize te napredne metode strojnog učenja. Time je dobiven znatno proširen seizmički katalog s više od 50.000 potresa. Analiza seizmičnosti potvrđuje da su najveći potresi usklađeni s glavnim desnim Petrinjskim rasjedom, s pomakom po pružanju, no evolucija naknadnih potresa pokazala je da je preraspodjela naprezanja aktivirala brojne sekundarne rasjede, što je dovelo do složene prostorne i vremenske raspodjele seizmičnosti. Rezultati pružaju detaljan seizmološki uvid u procese u tome žarišnom području unutar tektonske ploče.

Ključne riječi:
Petrinja, potres, naknadni potresi, seizmička mreža, strojno učenje

Original research paper

Josip Stipčević, Krešimir Kuk, Iva Dasović, Dinko Šindija, Kristina Šariri, Marin Sečanj, Davorka Herak, Marijan Herak

Monitoring seismic activity following 2020 Petrinja earthquake

The series of earthquakes in the Petrinja area began on Monday, 28 December 2020, at 6:28 a.m. local time (CET), with an earthquake of magnitude M_L = 5.1 (M_W = 4.9), which was felt across most of central Croatia. Its epicentre was southwest of Petrinja, near Strašnik village. This was soon followed by earthquakes of local magnitude 4.6, 7:49 a.m. and magnitude 3.8 at 7:51 a.m. in the same epicentral area, as well as a series of weaker earthquakes. Unfortunately, these relatively strong earthquakes proved to be just foreshocks, as an even stronger earthquake of local magnitude 6.2 (M_W = 6.4) occurred the next day, 29 December 2020, at 12:19 p.m., also with an epicentre near Strašnik. The cornerstone of this study is the vast amount of seismological data collected. We used both manual and advanced machine learning techniques to analyse the newly collected dataset. This resulted in a substantially expanded seismic catalogue with over 50,000 events. Seismicity analysis confirms that the largest events align with the primary dextral strike-slip Petrinja Fault; however, the aftershock pattern evolved, revealing that stress redistribution activated numerous secondary faults, leading to a complex spatial and temporal distribution of seismicity. The findings provide a detailed seismological record and crucial insights into the tectonic processes of this intraplate region.

Key words:
Petrinja, earthquake, aftershock, seismic network, machine learning

1. Uvod

Potres kod Petrinje (M_W = 6,4; M_L = 6,2) od 29. prosinca 2020. jedan je od najvažnijih potresa koji su se dogodili u Hrvatskoj u posljednjih nekoliko stoljeća. Dan ranije glavnome potresu prethodio je snažan potres (M_W = 4,9; M_L = 5,0), dok se najveći naknadni potres (M_W = 4,7; M_L = 4,9) dogodio 6. siječnja 2021. Seizmičnost područja i detaljne analize poznatog potresa kod Pokupskog iz 1909. prikazane su, naprimjer, u [1, 2].

Prema [1], glavni potres prouzročio je velika razaranja u epicentralnome području. Podrhtavanje se osjetilo diljem Hrvatske i Slovenije te u velikome dijelu Bosne i Hercegovine, Srbije, Mađarske, Italije, Austrije i Slovačke, uz sedam smrtnih slučajeva. Trešnja tla izazvala je brojne sekundarne pojave, uključujući likvefakciju, erupcije mulja, pješčane vulkane, klizišta te više od stotinu vrtača u blizini sela Mečenčana, jugoistočno od epicentra (slika 1.). Dodatni podaci o utjecaju, štetama i povezanim pojavama navedeni su, naprimjer, u [3-9]. Taj veliki potres s pomakom po pružanju rasjeda unutar tektonske ploče privukao je znatnu pozornost međunarodne seizmološke zajednice. Preliminarna analiza ranih opažanja prikazana je u [10], dok su brojna kasnija istraživanja bila usredotočena na karakterizaciju seizmičkog izvora (npr. [11-16]). Promjene Coulombova naprezanja nakon glavnog potresa analizirane su u [1, 14, 15, 17]. Nekoliko studija analiziralo je i *InSAR* satelitske podatke radi interpretacije površinskih deformacija (npr. [14, 15, 18, 19]). Detaljna prostorno-vremenska analiza petrinjskoga potresnog niza tijekom prvih šest mjeseci, uključujući relokaciju više od 13.800 potresa uz primjenu prostorno varijabilnih staničnih korekcija, procjenu epistemičke nesigurnosti lokacija, izračun mehanizama žarišta te usporedbu različitih modela rasjeda, prikazana je u [1]. U ovome radu ukratko je prikazana tektonika područja i opisana brza uspostava privremenih seizmoloških postaja nakon glavnog potresa. Nadalje, prikazana je seizmičnost epicentralnog područja Petrinje u razdoblju 2020. – 2024. Za praćenje seizmičnosti primijenjene su dvije vrste identifikacije potresa u seizmogramima: klasične metode (osobna analiza iskusnog seizmologa) i metode strojnog učenja. Opći cilj ovog rada jest prikazati seizmološki rad koji se obavljao pet godina nakon petrinjskog potresa.

2. Tektonika i geološka građa

Područje središnje Hrvatske, uključujući područje Petrinje, nalazi se u prijelaznoj zoni između strukturnih jedinica Unutarnjih Dinarida i jugozapadnog dijela Panonskog bazena. To je područje od razdoblja kasne jure pa sve do danas bilo izloženo višestrukim tektonskim fazama, što je rezultiralo složenom geološkom građom i geodinamičkim okružjem. Današnje suženje prostora između Jadranske mikroploče i Europe najvećim se dijelom događa unutar područja Vanjskih Dinarida, a djelomično se prenosi i na Unutarnje Dinaride te na prijelazno područje Dinaridi – Panonski bazen [20]. Aktivna kompresija, smjera SSI-JJZ, u istraživanome području potvrđena je rješenjima žarišnih mehanizama potresa [21] te geodinamičkim modeliranjem. U razdoblju od kasne krede do ranog paleogena šire područje Petrinje bilo je dio sjevernog ogranka Neotethysa, poznatog kao Savski ocean, te je bilo podvrgnuto kontinuiranoj subdukciji preostale oceanske kore pod kontinentalnu koru Euroazijske ploče. Postupnim zatvaranjem Savskog oceana formirana je Savska suturna zona (SSZ) [22, 23]. Regionalno izdizanje, boranje i napredovanje navlaka Unutarnjih Dinarida prema JZ, uz taloženje sintektonskih naslaga, bilo je aktivno sve do srednjeg eocena [20, 22]. U nastavku formiranja navlaka prema JZ i predgorju započelo je formiranje borano-navlačnog pojasa Vanjskih Dinarida. Pretpostavlja se da je glavna tektonska faza u formiranju Vanjskih Dinarida trajala od sredine eocena i tijekom oligocena, kada su se u predgorskome bazenu taložile sintektonske flišne i prominske naslage.

U sjevernome dijelu Unutarnjih Dinarida tijekom miocena došlo je do prelaska iz kompresijskog u ekstenzijski režim naprezanja te je dio navlačnih rasjeda duž Savske suturne zone invertiran u normalne rasjede. U krovinskim krilima tih rasjeda formiran je niz tektonskih polugraba, koje su napredovanjem ekstenzije postupno formirale Savsku depresiju [22]. Savska depresija počela se otvarati tijekom ranog miocena (oko 18 Ma). Istodobno sa spuštanjem krovinskih krila normalnih rasjeda iz podinskih krila tih rasjeda postupno su se prema površini izdigle starije stijene iz podloge, predmiocenske starosti, u obliku ekstenzijskih metamorfnih doma na JZ rubu Savske depresije.

Otvaranje miocenskih bazena regionalnih i lokalnih razmjera bilo je praćeno taloženjem sintektonskih te posttektonskih sedimentnih jedinica koje se danas djelomično nalaze na površini duž rubova Savske depresije. U Savskoj depresiji rana miocenska sinriftna faza trajala je do srednjeg miocena (oko 13,5 mil. god., prema [24]). Njezinim završetkom, krajem sarmata, u JZ dijelu Panonskog bazena uslijedila je postriftna faza termalne subsidencije, koja je trajala do kraja panona (oko 11,6 – 4,5 mil. god.), tijekom koje su u Savskoj depresiji taloženi lapori i pješčenjaci velike debljine. Krajem panona u Panonskome bazenu uslijedila je promjena iz ekstenzijskog u kompresijski režim tektonskoga naprezanja (npr. [24]).

Završetak faze termalne subsidencije i početak naknadne faze suženja nisu bili jednoliki unutar panonskoga bazenskog sustava, ni prostorno ni vremenski. U sjeverozapadnome i središnjemu dijelu Savske depresije ta je faza započela krajem miocena ili u ranome pliocenu (oko 6 Ma; [24, 22]), djelomično tektonskom inverzijom brojnih normalnih rasjeda formiranih za ranog miocena, a djelomično formiranjem reversnih rasjeda tijekom pliocena i kvartara, pretežno s pružanjem SZ-JI u središnjemu dijelu Savske depresije [22] te SI-JZ u njezinu sjevernom dijelu, u blizini granice s bazenom Hrvatskog zagorja [25]. Ti su rasjedi lokalno povezani s rasjedima s pomakom po pružanju, desni rasjedi s pružanjem SZ-JI i lijevi rasjeda s pružanjem SI-JZ. Neki od njih i danas su aktivni, što potvrđuju korelacije geoloških i seizmoloških podataka [26].

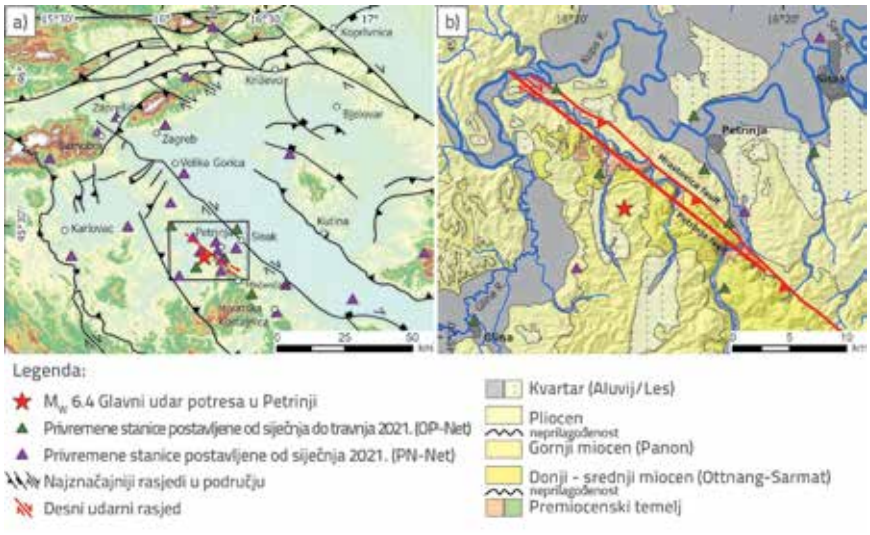

Slika 1. Tragovi rasjeda preuzeti su iz [20, 23, 25]; Pojednostavljena geološka karta širega petrinjskog epicentralnog područja, temeljena na Osnovnoj geološkoj karti, listovi Sisak [27] i Bosanski Novi [28]

Šire epicentralno područje, tj. područje petrinjskog niza potresa 2020. – 2021. pruža se u smjeru SZ-JI u duljini od približno 20 km, na udaljenosti od oko 7 km JZ od grada Petrinje (slika 1.). To područje pripada Hrastovičkoj gori, najizraženijoj morfološkoj strukturi u okolici Petrinje, s najvišim vrhom Cepelišć (415 m n.m.). Prema podacima s geološke karte [27], ta struktura predstavlja asimetričnu antiklinalu s blagim nagibom JZ te strmim nagibom SI krila koje je omeđeno Hrastovičkim rasjedom, koja se pruža SZ-JI (slika 1.b). Iako se pomak po tome rasjedu smatrao normalnim [27], tijekom potresa 1909. i naknadnih potresa 2020. opažen je reversni pomak, što otvara pitanje predstavlja li dio reljefa od oko 300 m komponentu navlačenja kroz više seizmičkih ciklusa [21]. Jezgru i strmije SI krilo antiklinale mjestimično izgrađuju stijene gornjokredne i eocenske starosti, koje većim dijelom diskordantno prekrivaju mlađe naslage miocenske i pliocenske starosti koje su jasno izražene u blago nagnutome jugozapadnom krilu antiklinale (slika 1.b). Najmlađe naslage u istraživanome području čine kvartarni šljunci, pijesci, prahovi i gline taloženi u poplavnoj ravnici rijeke Kupe i duž njezinih pritoka, lokalno povezani s lesnim naslagama koje su uglavnom očuvane u dolinama, ali se pojavljuju i na većim nadmorskim visinama u blizini vrha Hrastovičke gore.

Zbog jačine potresa i specifične geološke građe u širemu epicentralnom području uočen je velik broj sekundarnih učinaka potresa, odnosno koseizmičkih deformacija na površini kao što su likvefakcija, pukotine, klizišta i urušne vrtače (npr. [3, 29-31]).

3. Seizmografske mreže

Kada se dogodi snažan potres, od presudne je važnosti da seizmološka zajednica brzo reagira uspostavom guste mreže privremenih instrumenata za praćenje u širemu epicentralnom području. Takva konfiguracija ključna je za detekciju i najslabijih podrhtavanja, od kojih bi mnoga inače ostala nezabilježena. Mogućnost preciznog lociranja i vrlo malih potresa neophodna je za razumijevanje veličine i prostornog dosega aktiviranih rasjednih struktura. Točno određivanje dubine žarišta jedan je od najzahtjevnijih aspekata analize potresa, jer je riječ o parametru koji je najteže precizno odrediti. Taj se problem može ublažiti povećanjem gustoće i osjetljivosti mreže seizmografa, uz poseban naglasak na postavljanje postaja u neposrednoj blizini epicentralnog područja. Nadalje, kako se najveći broj naknadnih potresa javlja neposredno nakon glavnog udara, tako je brza instalacija instrumenata u pogođenome području ključna za njihovo odgovarajuće bilježenje.

Na početku petrinjskoga potresnog niza seizmička mreža u području rijeke Kupe bila je relativno rijetka, pri čemu su se dvije postaje najbliže glavnome potresu nalazile na udaljenostima od 32 i 36 km (plavi trokuti na slici 2.).

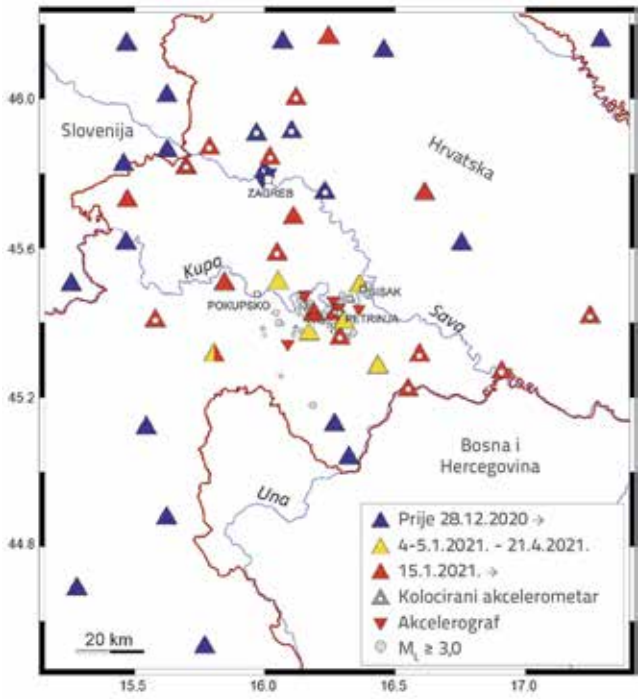

Slika 2. Seizmičke postaje u široj okolici epicentralnog područja petrinjskog potresa nakon instalacije mreža OP-Net (žuti trokuti) i PN-Net (crveni trokuti, širokopojasne postaje). Plavi trokuti označavaju širokopojasne postaje u sastavu hrvatske CR mreže, privremene zagrebačke mreže te slovenske (SL) i mađarske (HU) mreže. Mali obrnuti trokuti označavaju akcelerografe. Bijeli krugovi unutar simbola označavaju postaje s kolociranim akcelerometrima. Prilagođeno prema [1]

Srećom, 4. i 5. siječnja 2021. u epicentralnome području postavljena je privremena mreža od šest postaja (OP-Net; žuti trokuti na slici 2.) u suradnji Nacionalnog instituta za oceanografiju i primijenjenu geofiziku – OGS (Italija) i Geofizičkog odsjeka Prirodoslovno-matematičkoga fakulteta Sveučilišta u Zagrebu, i to unatoč ograničenjima putovanja uzrokovanima pandemijom bolesti COVID-19. Ubrzo nakon toga, sredinom siječnja 2021., započela je instalacija petrinjske mreže (PN-Net; crveni simboli na slici 2.) korištenjem novonabavljenih instrumenata hrvatske Seizmološke službe (vidi poglavlje 3.2. i [1] za detalje). U nastavku ukratko su opisani postavljanje instrumenata i druge terenske aktivnosti nakon glavnoga petrinjskog potresa i u ranoj fazi niza naknadnih potresa.

3.1. Brza instalacija instrumenata (OP-Net)

Zbog serije potresa u Zagrebu, koja je započela 22. ožujka 2020. glavnim potresom magnitude M_w = 5,3 (M_L = 5,5), i uspostave pripadajuće lokalne mreže seizmografa krajem 2020. hrvatski seizmolozi nisu raspolagali slobodnim instrumentima za postavljanje nakon potresa u području Banovine. Kako bi se taj problem riješio, seizmolozi s Geofizičkog odsjeka PMF-a u Zagrebu brzo su uspostavili suradnju s kolegama iz Nacionalnog instituta za oceanografiju i primijenjenu geofiziku – OGS (Italija). U sklopu te suradnje OGS je ustupio šest seizmografa, opremljenih integriranim akcelerometrom, za brzu instalaciju u epicentralnome području. Ta suradnja bila je ključna za osiguravanje žurne instalacije instrumenata za praćenje seizmičke aktivnosti.

Slika 3. Primjeri instaliranih privremenih postaja: a) Privremene postaje u Sisku i b) Taborištu opremljene kratkoperiodnim instrumentom (seizmograf s integriranim akcelerometrom *Lunitek Sentinel-Geo*) iz mreže OP-Net; c) Privremena postaja mreže PN-Net na petrinjskome groblju s kolociranim seizmometrom *Kinemetrics MBB-2* (siva izolacijska kutija) i akcelerometrom *Kinemetrics ETNA2* (ispod zelene izolacijske kutije); d) Akcelerometar u izolacijskoj kutiji prikazan izbliza

Samo šest dana nakon glavnog potresa i unatoč epidemiološkim ograničenjima, 4. i 5. siječnja 2021. pet od tih instrumenata postavljeno je na ključnim lokacijama u Banovini, i to u Hotnji, Sisku, Taborištu, Novome Selu Glinskom i Mečenčanima (slika 2., [32]). Osim toga jedan širokopojasni seizmometar postavljen je na Petrovoj gori 4. siječnja. Strateško raspoređivanje i brza instalacija te privremene mreže znatno su unaprijedili postojeću stalnu seizmičku mrežu u tome području, poboljšavajući azimutalnu pokrivenost i omogućujući dodatna opažanja lokalnih potresa. To je bilo osobito važno jer je smanjilo nesigurnost i nestabilnost u određivanju lokacije potresa, posebno dubine žarišta (vidi sliku 4.). Poboljšana pokrivenost omogućila je pouzdanije lociranje i manjih potresa, čime su dobiveni vrijedni podaci o seizmičkoj aktivnosti u regiji. Pet kratkoperiodičnih instrumenata OP-Net mreže radilo je do sredine travnja 2021., kada su deinstalirani i vraćeni u Italiju.
Ta suradnja ne samo da je pridonijela boljemu razumijevanju seizmičnosti područja Banovine, već je naglasila važnost međunarodne suradnje u seizmologiji. Brzom uspostavom privremene mreže visokokvalitetnih seizmičkih postaja prikupljeni su ključni podaci o lokalnim potresima koji su neophodni za opisivanje svojstava naknadnih potresa i za buduće procjene seizmičke opasnosti u regiji.

3.2. Privremena seizmografska mreža Petrinja (PN-Net)

Nakon početne instalacije šest postaja mreže OP-Net, hrvatska Seizmološka služba pri Geofizičkome odsjeku PMF-a u Zagrebu primila je znatna financijska sredstva od Vlade Republike Hrvatske (putem Ministarstva znanosti i obrazovanja) za nabavu kompleta seizmoloških instrumenata. U vrlo kratkome roku nabavljeno je 20 modernih seizmometara s pripadajućim AD pretvornicima i jedinicama za pohranu podataka i 20 akcelerometara s potrebnom dodatnom opremom. Instrumenti su brzo nabavljeni i isporučeni kako bi se omogućilo pravodobno instrumentalno bilježenje naknadnih potresa u području Petrinjskog rasjeda. Oprema je promptno testirana i konfigurirana, a prvi instrumenti postavljeni su na teren već nekoliko tjedana nakon glavnog potresa.
U početnoj fazi instrumenti su postavljeni u neposrednome epicentralnom području, u gradu Petrinji te u naseljima Brestu Pokupskom, Hrastovici, Mošćenici, Hrvatskom Čuntiću, Gori i Novom Farkašiću. U sljedećoj fazi privremene seizmološke postaje instalirane su u širemu epicentralnom području na pet lokacija (Pobrđani, Jasenovac, Lasinja,

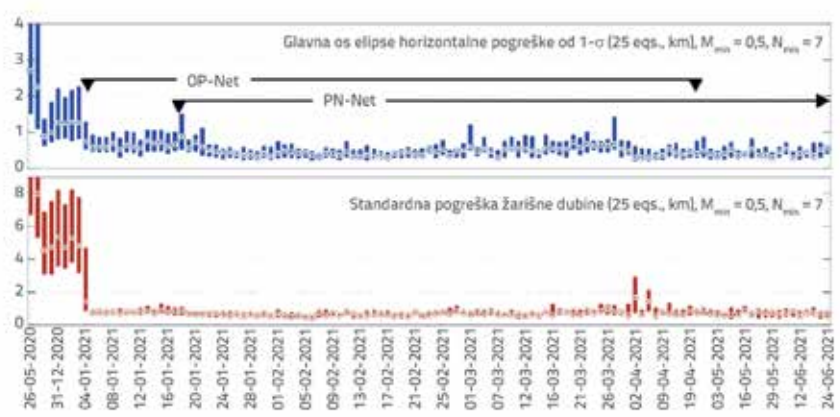

Slika 4. Vremenska evolucija radijusa pouzdanosti 1σ za lokacije žarišta, procijenjena pomoću nepreklapajućih kliznih prozora od 25 uzastopnih potresa tijekom prvih šest mjeseci petrinjskoga potresnog niza. Uključeni su jedino potresi lokalne magnitude $M_L \geq 0,5$, locirani s najmanje sedam nastupnih vremena potresnih faza. Zaokružene točke označavaju medijane, dok stupci prikazuju raspon između 25. i 75. percentila. Razdoblja rada privremenih mreža prikazana su u gornjemu dijagramu

Omanovac i Čazma) kako bi se osigurali podaci sa širega geografskog područja u odnosu na epicentre potresa. Nekoliko instrumenata postavljeno je i u širemu području Zagreba (Marija Bistrica, Samobor, Žumberak, Ladvenjak i dr.) radi praćenja naknadnog niza zagrebačkog potresa od 22. ožujka 2020., koji je još uvijek bio aktivan. Tijekom sljedećih mjeseci redovito su se terenski obilazile mobilne mreže radi prikupljanja podataka i provjere ispravnosti rada postaja. U tome razdoblju prikupljene su stotine gigabajta vrijednih seizmoloških podataka. U kasnijoj fazi nabavljeni su novi serverski sustavi te je uspostavljena izravna veza za prijenos podataka sa svih privremenih postaja do operativnog centra u Zagrebu u stvarnome vremenu.

3.3. Učinkovitost privremenih seizmografskih mreža

Rad mreže OP-Net, a potom i PN-Net, imao je znatan utjecaj na pouzdanost određivanja lokacija naknadnih potresa. Kao što je to prikazano na slici 4., uspostava mreže OP-Net povećala je pouzdanost određivanja epicentara za približno 50 %, dok je prosječna nesigurnost dubine žarišta smanjena s oko ±5 km na manje od ±1 km. Pouzdanost lokacija dodatno je poboljšana uspostavom mreže PN-Net.

4. Praćenje seizmičnosti nakon glavnog potresa

Kao što je istaknuto u prethodnome poglavlju, brza i učinkovita reakcija na snažan potres od ključne je važnosti, što podrazumijeva žurnu uspostavu guste privremene seizmičke mreže u blizini aktivirane rasjedne zone. Takvo unapređenje mreže ključno je za detekciju vrlo slabih naknadnih potresa te predstavlja osnovnu strategiju za poboljšanje točnosti lociranja potresa, osobito dubine njegova žarišta. Dobiveni podaci visoke razlučivosti neophodni su za razjašnjavanje složene tektonike potresnog niza. U slučaju petrinjskih potresa takvo unaprijeđeno praćenje bilo je ključno za kartiranje prostorne razdiobe seizmičnosti u tome području. Iako su najveći potresi jasno povezani s glavnom seizmogenom strukturom – desnim Petrinjskim rasjedom s horizontalnim pomakom – pouzdano lociranje tisuća naknadnih potresa pokazalo je da se brojni manji potresi pojavljuju i duž više sekundarnih rasjeda aktiviranih preraspodjelom tektonskih napetosti. Zato su brza uspostava mreže OP-Net i poslije mreže PN-Net bile presudne za detaljno definiranje geometrije rasjeda i razumijevanje ukupnog dosega aktivirane zone.

U nastavku prikazane su dvije komplementarne analize temeljene na bogatome skupu seizmičkih podataka prikupljenih tijekom nekoliko godina nakon glavnoga petrinjskog potresa. Prvo su opisani rezultati klasične, manualne analize seizmograma prikupljenih sa stalnih i privremenih mreža, a zatim rezultati automatske analize primjenom dubokih neuronskih mreža za detekciju potresnih signala, uz naglasak na prednostima i nedostacima tog pristupa u odnosu na klasičnu analizu.

4.1. Katalog petrinjskoga potresnog niza na temelju klasične analize seizmograma

U ovome poglavlju prikazani su rezultati analize seizmograma prikupljenih u razdoblju od 28. prosinca 2020. do 31. prosinca 2024., a koju su obavili seizmolozi s dugogodišnjim iskustvom. U nastavku rada takva se analiza naziva klasičnom analizom. Tijekom tog razdoblja u širemu epicentralnom području Petrinje locirano je 19.570 potresa (slika 5.). Lokacije iz prvih šest mjeseci aktivnosti preuzete su iz kataloga [1], dok su za kasnije razdoblje (srpanj 2021. – prosinac 2024.) korišteni podaci iz Hrvatskog kataloga potresa – CEC, prema [33]; posljednja revizija 2025.). Najveći potresi jasno su povezani s glavnom seizmogenom strukturom – desnim Petrinjskim rasjedom (crvena linija na slici 5., gore). Međutim, prostorna raspodjela seizmičnosti pokazuje da su se brojni naknadni potresi pojavljivali i duž sekundarnih rasjeda aktiviranih preraspodjelom naprezanja nakon glavnog potresa (vidi [1]). To uključuje potresne izvore između Siska i Petrinje, u blizini sela Donjeg Vukojevca, sjeveroistočno i zapadno od Gline, u području Donjeg Selkovca i Donjeg Žirovca te zapadno od Mečenčana.

Uvid u razdiobu hipocentara daje šest presjeka (A – F) prikazanih u donjem dijelu slike 5. Oni uključuju samo pouzdano locirane potrese koji zadovoljavaju kriterije navedene u opisu slike. Većina hipocentara koncentrirana je na dubinama između 5 i 15 km. Presjeci upućuju na nekoliko aktiviranih rasjeda, koji su svi subvertikalni ili strmo nagnuti prema sjeveroistoku. Presjek D dodatno sugerira postojanje strukturnog diskontinuiteta ili odvajanja unutar zone Petrinjskog rasjeda na dubini od približno 11 km. Detaljnija analiza tih značajki izlazi izvan okvira ovog rada.

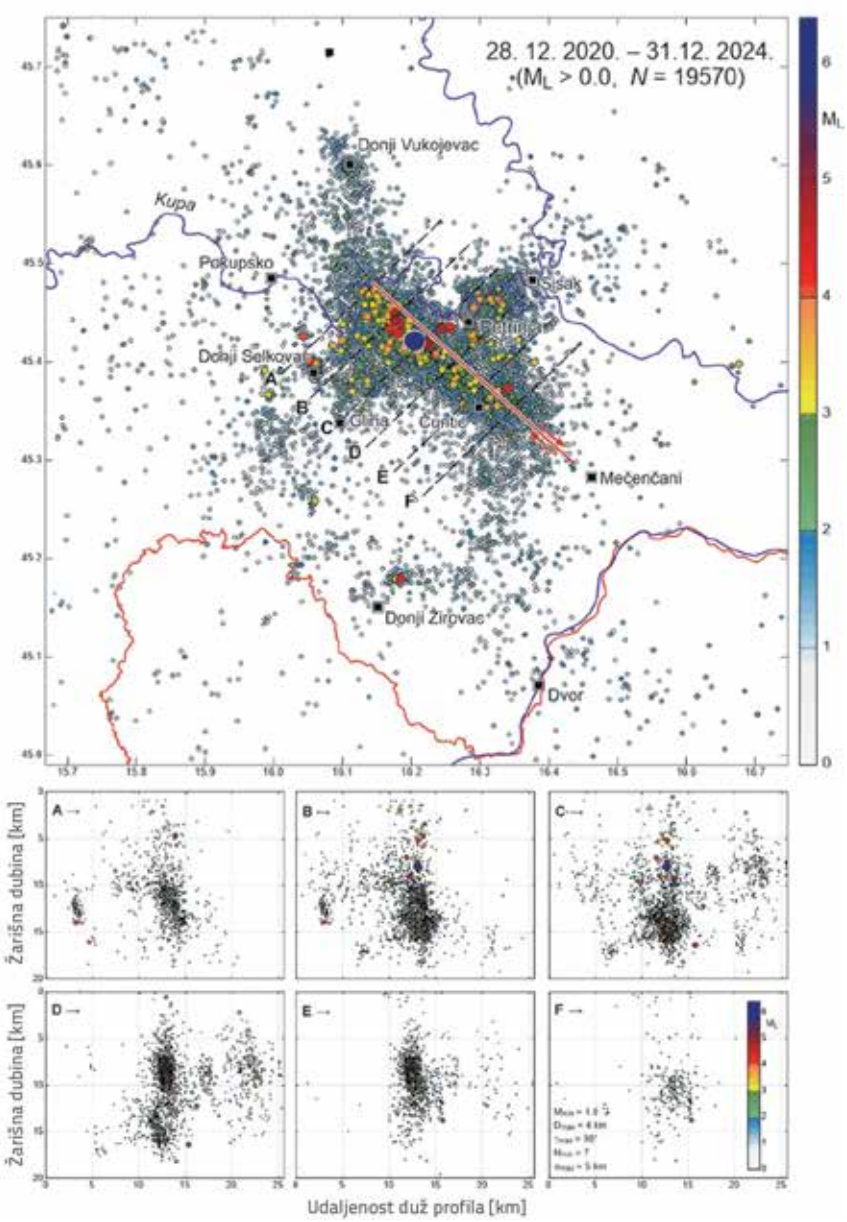

Slika 5. Gore: Epicentri svih 19.570 potresa magnitude M_L > 0,0 iz petrinjskoga potresnog niza (2020. – 2024.). Veličina simbola i boja skalirani su prema magnitudi. Crvena linija prikazuje pojednostavljeni površinski trag Petrinjskog rasjeda, a strelice označavaju relativno gibanje blokova. Isprekidane crne linije označavaju položaje presjeka A – F. Dolje: Presjeci A – F prikazuju vertikalne profile hipocentara potresa koji zadovoljavaju uvjete navedene u presjeku F (minimalna magnituda M_{min} = 1,0; maksimalna udaljenost od profila D_{max} = 4 km; maksimalni azimutni razmak postaja γ_{max} = 90°; minimalni broj faza za lociranje N_{min} = 7; maksimalna dopuštena standardna pogreška hipocentra σ_{max} = 5 km)

Vremenska evolucija potresnog niza prikazana je na slici 6. U prva četiri dana (28. – 31. prosinca 2020.) seizmičnost je bila gotovo u cijelosti ograničena na Petrinjski rasjed, koji se aktivirao u duljini od približno 20 km, pružajući se jugozapadno od rijeke Kupe prema Čuntiću. Važno je napomenuti da su već u toj ranoj fazi bili aktivni i udaljeniji izvori, uključujući područja sjeveroistočno od Petrinje, istočno od Velike Soline te u blizini Donjeg Žirovca, oko 25 km od Petrinjskog rasjeda. Najveći dio aktivnosti (oko 65 % svih lociranih potresa) zabilježen je tijekom 2021. Tijekom tog razdoblja naknadni potresi proširili su se preko Kupe, definirajući difuznu rasjednu zonu približno smjera S–J, obilježenu uglavnom potresima manjih magnituda, pretežno južno od Donjeg Vukojevca. Istodobno je pojačana aktivnost na jugoistočnome segmentu Petrinjskog rasjeda, s produženjem prema selu Mečenčanima, čime je ukupna duljina aktiviranoga rasjednog segmenta povećana na više od 30 km. Najjača aktivnost tijekom 2021., osim uz sam Petrinjski rasjed, zabilježena je između Siska i Petrinje, uz dodatne potrese magnitude $M_L \geq 4{,}0$ u blizini Velike Soline i Donjeg Žirovca.

U razdoblju od 2022. do 2024. seizmička aktivnost u sjeverozapadnome dijelu zone naknadnih potresa i na području Sisak – Petrinja postupno se smanjivala, dok se većina aktivnosti zadržala u jugoistočnome dijelu zone, istočno i sjeverozapadno od Čuntića (grozdovi A i B na slici 6.). Tijekom 2022. početno linearno poravnanje epicentara duž Petrinjskog rasjeda razvilo se u oblik konkavan prema sjeveroistoku. Ta promjena odražava kontinuiranu aktivnost unutar uskog pojasa između Gline i Donjeg Vukojevca te u grozdu označenome slovom "B" na slici 6., smještenome pretežno u sjeveroistočnome bloku zone Petrinjskog rasjeda. To je u suprotnosti s aktivnošću duž glavnog rasjeda (npr. grozd A i sjeverozapadni segment), gdje se većina hipocentara nalazi u jugozapadnome bloku.

Katalog potresa za petrinjski niz pokazuje potpunost za $M_L \geq 1{,}0$ (vidi sliku 7.a) počevši od 30. prosinca 2020., odnosno oko 13 sati nakon glavnog potresa kako bi se izbjeglo početno razdoblje u kojemu su brojni mali potresi bili prikriveni učestalim jačim događajima. Gutenberg-Richterov koeficijent b = 0,96 nešto je veći od vrijednosti b = 0,91 koja je navedena u radu [1] za prvih šest mjeseci i $M_L \geq 1{,}2$. Parametri modificiranoga Omorijeva zakona, koji opisuju opadanje učestalosti naknadnih potresa, ostali su stabilni tijekom cijelog niza, odnosno koeficijenti dobiveni za četverogodišnje razdoblje (slika 7.b) gotovo su jednaki onima

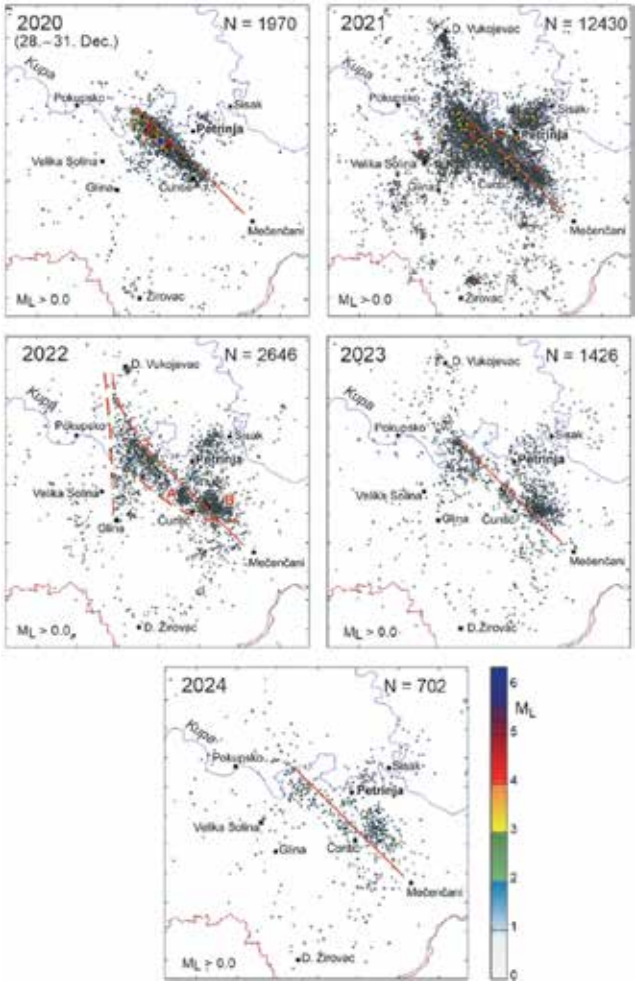

Slika 6. Epicentri potresa iz petrinjskoga potresnog niza prema godinama (2020. – 2024.). Ukupan broj lociranih potresa s M_L > 0,0 unutar svakog dijagrama prikazan je u gornjemu desnom kutu. Puna crvena linija označava pojednostavljeni trag Petrinjskog rasjeda. Isprekidane linije označavaju uočene trendove

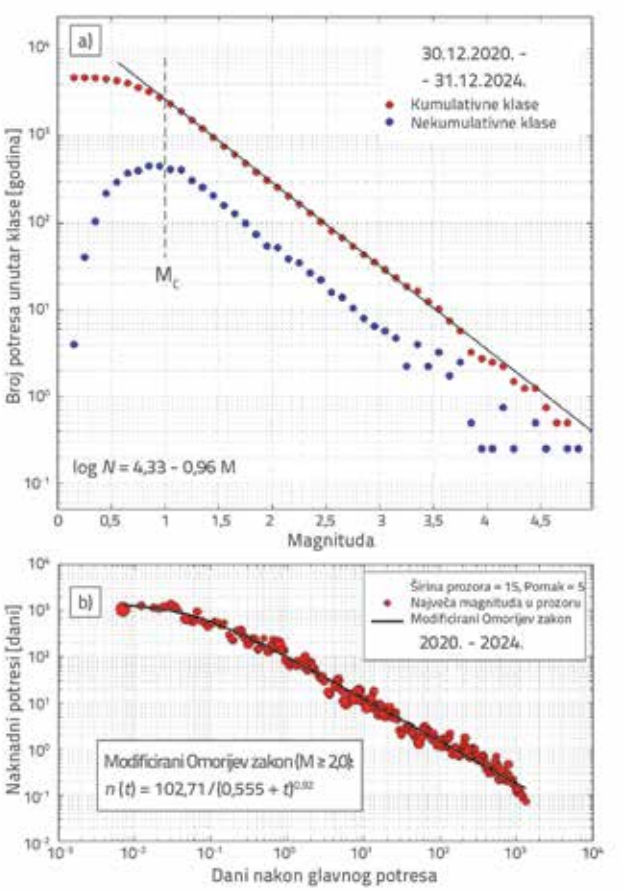

Slika 7. a) Razdioba frekvencije i magnitude za petrinjski potresni niz (2020. – 2024.), bez glavnog potresa; b) Modificirani Omorijev zakon – vremenska promjena aktivnosti naknadnih potresa ($M_L \geq 2,0$) petrinjskog niza (2020. – 2024.)

iz prvih šest mjeseci [1]. To upućuje na postupno smanjenje aktivnosti u nadolazećim godinama, pri čemu se povratak na približnu razinu prije 2020. očekuje tek oko 2038.

4.2. Automatska detekcija i lociranje potresa

Povećanje gustoće seizmičkih mreža poput slučaja prikazanog u radu dovelo je do znatnog povećanja količine podataka, a time i vremena potrebnog za njihovu klasičnu stručnu obradu. Posljednjih godina metode strojnog učenja (ML) pokazale su se kao učinkovita i pouzdana alternativa tradicionalnim pristupima obradi podataka [34-36]. Glavni razlozi za to uključuju brzinu obrade, pri čemu se jedan dan kontinuiranih podataka može analizirati u samo nekoliko minuta, što je osobito važno za manje ili slabije financirane institucije. Osim toga ML metode omogućuju ujednačenu točnost i kvantifikaciju nesigurnosti u određivanju faza, detekciju potresa manjih magnituda te bolje prepoznavanje nailazaka potresnih faza na seizmogramima s izraženim šumom.

U ovome radu prikazani su tijek obrade i početni rezultati analize seizmičkih podataka iz gotovo dviju godina primjenom strojnog učenja, i to za razdoblje od početka potresnog niza do kraja studenoga 2022. [37]. Kontinuirani zapisi seizmograma iz mreža CR, OP-Net i PN-Net analizirani su pomoću duboke neuronske mreže za detekciju potresa *EQTransformer* [36], trenirane za detekciju potresa i određivanje dolazaka P-valova i S-valova na bazi podataka *INSTANCE* [38]. Detektirane faze potom su povezane s pojedinim potresom, a početne lokacije potresa određene su pomoću asocijatora *PyOcto* [39]. Te su lokacije dodatno poboljšane primjenom algoritma *NonLinLoc* [40], uz korekcije vremena putovanja specifične za pojedini izvor (SSST; [41]). Vjerojatnosti koje daje *EQTransformer* korištene su i za određivanje nepouzdanosti vremena nailazaka, pri čemu su fazama s većom vjerojatnošću pridijeljene manje nepouzdanosti. Početna analiza *EQTransformerom*, uz niski prag detekcije od 0,05 za P-valove i S-valove, rezultirala je s ukupno 8.953.730 detektiranih seizmičkih faza (6.588.039 P-faza i 2.365.691 S-faza). Nakon primjene kriterija za povezivanje faza, uključujući

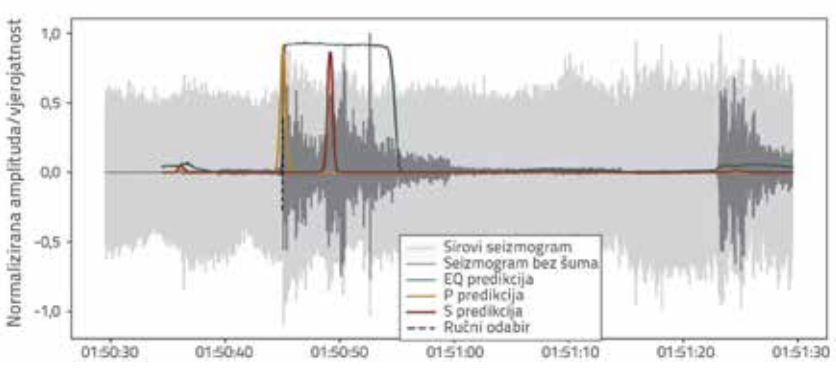

Slika 8. Primjer detekcije i određivanja faza pomoću algoritma *EQTransformer* na seizmogramu s postaje PN03 (OP-Net) s jakim šumom. Prikazani su sirovi (sivo) i filtrirani (crno) seizmogram, vjerojatnost detekcije potresa (zeleno) te vjerojatnosti P-faze (žuto) i S-faze (crveno), zajedno s ručno određenim dolaskom (crna isprekidana linija). Potres se dogodio 20. siječnja 2021. u 01:50:38 UTC i smatra se novootkrivenim, jer nije uključen u Hrvatski katalog potresa

minimalni broj faza po potresu (pet prije instalacije OP-Net mreže odnosno sedam nakon 4. siječnja 2021.), dobivene su 943.844 valjane faze (53 % P-faza i 47 % S-faza). Time je formiran katalog od 50.305 potresa lociranih u istraživanome području. Većina tih potresa (68 %) dogodila se do kraja lipnja 2021.

Kako bi se osiguralo da novi katalog dobiven dubokim učenjem predstavlja stvarne potrese, provjeren je u odnosu na Hrvatski katalog potresa – CEC ([33]; najnovija revizija iz 2025.) za isto razdoblje istraživanja. Događaji su klasificirani kao "podudarni", ako su se njihova vremena nastanka razlikovala za manje od dvije sekunde od onih u CEC-u. Za događaje bez odgovarajućeg podudaranja u ručnome katalogu primijenjeni su dodatni kriteriji kvalitete: azimutalni razmak postaja manji od 150°, najmanje deset povezanih seizmičkih faza i glavna poluos elipsoida pouzdanosti (prema procjeni *NonLinLoca*) manja od 20 km.

Primjer takvog potresa i toga kako funkcioniraju detekcija i odabir faze pomoću *EQTransformera* prikazan je za stanicu PN03 iz OP-Net mreže (slika 8.). Dvominutni seizmogram odgovara događaju s vremenom nastanka 20. siječnja 2021. u 01:50:38 UTC, klasificiranome kao novoidentificirani jer ga nema u Hrvatskome katalogu potresa (ali je prisutan u manualno obrađenom skupu podataka samo s odabirom P-faze). Unatoč visokoj razini šuma, *EQTransformer* uspješno je detektirao događaj i identificirao dolaske i P i S s vršnim vjerojatnostima od 0,93 odnosno 0,87. Za usporedbu prikazan je i seizmogram bez šuma dobiven metodom uklanjanja/dekompozicije na temelju duboke neuronske mreže [42], koji ilustrira temeljnu strukturu signala i sposobnost modela da prema zadanim postavkama izvuče korisne informacije iz podataka sa šumom.

Usporedbom s Hrvatskim katalogom potresa (CEC) utvrđeno je da je podudarno 86 % potresa. Od 50.305 događaja u novome ML katalogu i 22.386 događaja u CEC-u 19.225 ih je zajedničkih, dok 3161 CEC događaj nije detektiran. Identificirano je i 31.080 novih potresa, od kojih 9184 zadovoljavaju stroge kriterije kvalitete i smatraju se pouzdanim detekcijama (slika 9.). Ti su potresi prostorno koncentrirani uz petrinjski rasjedni sustav i sukladni su s prostornom razdiobom naknadnih potresa. Većina hipocentara nalazi se u gornjih 15 km kore, s izraženim grupiranjem na dubinama od 5 do 10 km. Te su dubine u prosjeku nekoliko kilometara pliće nego u manualnome katalogu, što je trend koji je također uočen u prethodnim studijama strojnog učenja [42].

Rezultati pokazuju da pristup strojnim učenjem uspješno reproducira većinu klasično identificiranih potresa, uz znatno proširenje kataloga.

5. Žarišni mehanizmi

Kako bi se pružio uvid u složene tipove rasjedanja koji su povezani s petrinjskom rasjednom zonom nakon potresa 2020., u nastavku ukratko su prikazana dostupna rješenja žarišnih mehanizama dobivenih iz polariteta prvih pomaka do kraja 2024., kako su prikazani u katalogu CroFMS [21].

Kao što je to već uočeno u [1], najveći potresi duž Petrinjskog rasjeda pokazuju pretežno rasjedanje s pomakom po pružanju

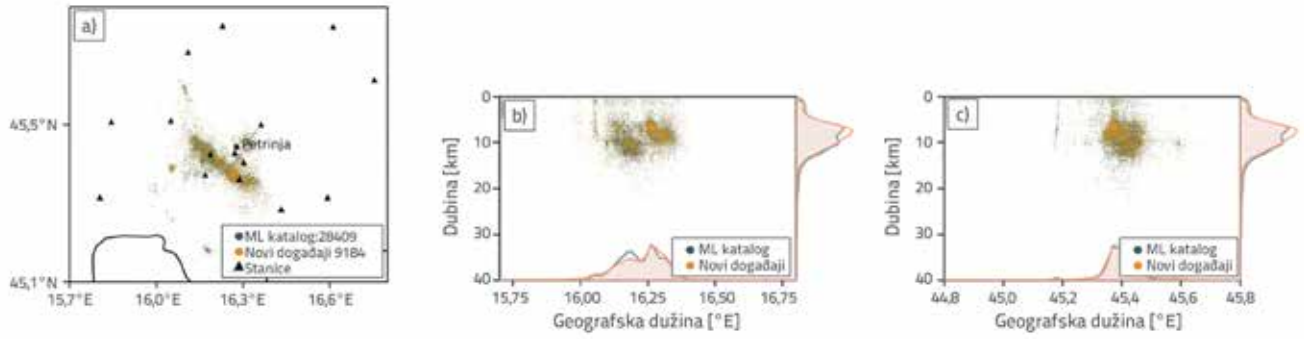

Slika 9. a) Karta s 28.409 potresa iz kataloga dobivenog metodama strojnog učenja. Novi, visokopouzdano locirani potresi označeni su narančastom bojom; Vertikalni presjeci koji prikazuju razdiobu dubina potresa iz ML kataloga u ovisnosti o: b) geografskoj dužini; c) geografskoj širini, uz istaknute novootkrivene potrese

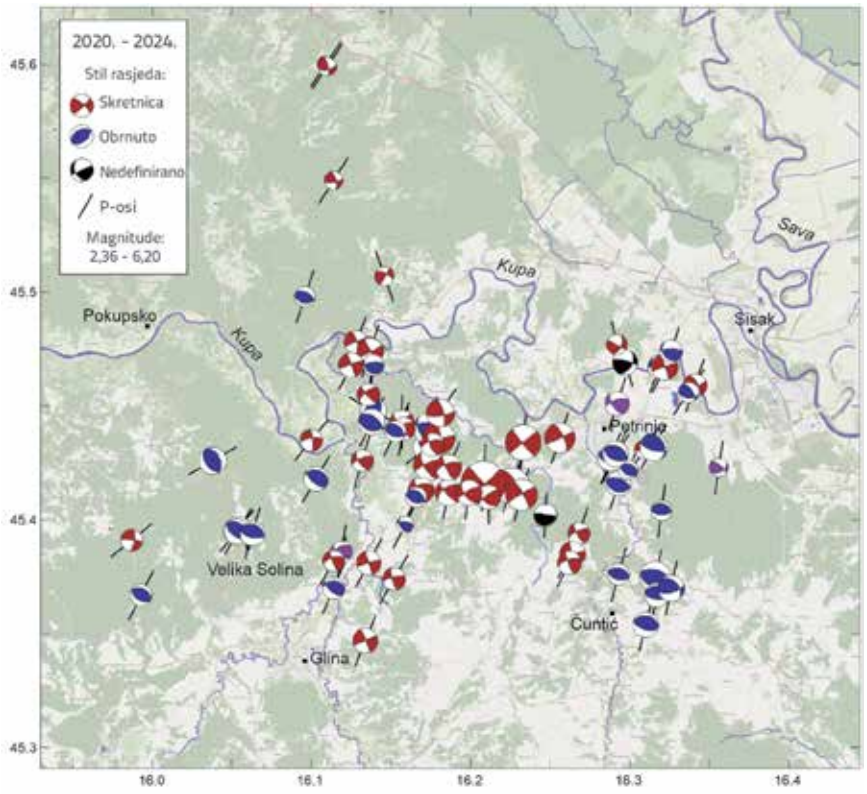

Slika 10. Rješenja žarišnih mehanizama (FMS) u razdoblju 2020. – 2024. iz kataloga CroFMS [21]. Rješenja su prikazana stereografskom projekcijom na donju hemisferu. Boja kompresijskih kvadranata označava tip rasjedanja (vidi legendu). Kratke crne linije označavaju orijentaciju P-osi. Veličina simbola *beach-ball* skalirana je prema magnitudi u rasponu prikazanom u legendi. Prikazana su samo rješenja kvalitete ≥ 2

(slika 10.). Međutim, gotovo jednak broj naknadnih potresa dogodio se na reversnim rasjedima, osobito u blizini Velike Soline te u grozdovima sjeveroistočno od Čuntića i jugoistočno od Petrinje. U radu [1] pokazano je i da je raspodjela rasjedanja s pomakom po pružanju i reversnog rasjedanja u skladu s promjenama Coulombove napetosti uzrokovanima glavnim potresom.

Smjer P-osi, koji je većinom orijentiran u pravcu JJZ–SSI, usporediv je sa smjerom maksimalnoga horizontalnog naprezanja (S_{Hmax}) u tome području [21]. Zanimljivo je da P-os glavnog potresa ima gotovo smjer S-J, što upućuje na prosječnu rotaciju P-osi u nizu naknadnih potresa od oko 16° u smjeru kazaljke na satu [1].

6. Rasprava i zaključci

Sveobuhvatna analiza petrinjskoga potresnog niza u razdoblju 2020. – 2024., potpomognuta klasičnim i naprednim metodama strojnog učenja, pruža znatno unaprijeđen uvid u seizmičke i tektonske procese aktivne u toj važnoj prijelaznoj zoni između Unutarnjih Dinarida i jugozapadnog dijela Panonskog bazena.

Ključni element ovog istraživanja bila je brza i koordinirana uspostava privremenih seizmičkih mreža, posebno talijansko-hrvatske mreže OP-Net te naknadno mreže PN-Net. Njihova uspostava nadopunila je nedovoljno gustu stalnu mrežu, što je rezultiralo znatnim povećanjem broja postaja i kvalitete podataka. Povećana gustoća mreže bila je presudna za smanjenje nepouzdanosti u lociranju žarišta potresa, osobito njihove dubine, što je ključno za pouzdano kartiranje rasjednih ploha (slika 4.).

Nažalost, potres je pogodio područje koje prethodno nije bilo dovoljno pokriveno seizmičkim mjerenjima, ponajviše zbog ograničenih financijskih sredstava. Posebno je nedostatak instrumenata za mjerenje jake trešnje tla (akcelerografa) označio propuštenu jedinstvenu priliku za prikupljanje podataka o ubrzanju tla u bliskome polju velikog potresa s pomakom po pružanju rasjeda. Takvi bi podaci predstavljali iznimno vrijedan doprinos bazi akcelerograma u Hrvatskoj. Ipak, postavljanje OP-Net mreže, koja uključuje i geofone i akcelerografe, a potom i PN-Net mreže, omogućilo je bilježenje ubrzanja tijekom najjačega naknadnog potresa 6. siječnja 2021. te tijekom svih kasnijih većih potresa.

Mogućnost brze instalacije instrumenata omogućila je bilježenje najintenzivnijeg razdoblja naknadnih potresa neposredno nakon glavnog udara. Nadalje, velika količina podataka učinkovito je obrađena primjenom metoda strojnog učenja, čime je seizmički katalog proširen za više od 50 %, uz uspješnu detekciju tisuća potresa male magnitude koji nisu bili identificirani klasičnom analizom. Time je potvrđena vrijednost naprednih metoda u praćenju potresne aktivnosti nakon glavnog potresa.

Detaljna analiza gotovo 20.000 klasično lociranih i više od 50.000 potresa detektiranih metodama strojnog učenja (slike 5. i 9.) potvrđuje da su se najveći potresi dogodili duž Petrinjskog rasjeda, aktivne strukture u složenoj prijelaznoj zoni između Dinarida i Panonskog bazena. Međutim, razdioba seizmičnosti s vremenom je postajala sve složenija, pri čemu je preraspodjela napetosti nakon glavnog potresa aktivirala brojne sekundarne rasjede koji se protežu izvan neposredne zone glavnog rasjeda. Iako se potresna aktivnost općenito smanjuje u skladu s modificiranim Omorijevim zakonom (slika 7.b), što upućuje na postupni povratak na pozadinsku razinu oko 2038., neki grozdovi još su aktivni u jugoistočnim dijelovima zone.

Analiza žarišnih mehanizama (katalog CroFMS) upućuje na složenu interakciju različitih tipova rasjedanja (slika 10.). Dok najveći potresi pokazuju očekivano rasjedanje s pomakom po pružanju, znatan broj naknadnih potresa karakterizira reverzno rasjedanje. Ta heterogena raspodjela u skladu je s promjenama

Coulombove napetosti uzrokovanima glavnim potresom, čime se potvrđuju suvremeni modeli statičkog iniciranja rasjedanja. Dodatno, uočena je važna pojava rotacije P-osi: dok su P-osi naknadnih potresa usklađene s regionalnim maksimalnim horizontalnim naprezanjem (S_{Hmax}), one pokazuju zamjetnu rotaciju u odnosu na P-os glavnog potresa. Ta rotacija pruža važan uvid u svojstva lokalnog naprezanja i njegove varijabilnosti. Zaključno, pet godina intenzivnog praćenja seizmičnosti nakon petrinjskog potresa rezultiralo je iznimno detaljnim i pouzdanim razumijevanjem toga znatnog potresa s pomakom po pružanju koji se dogodio unutar tektonske ploče. Uspješna suradnja i brza uspostava seizmičkih mreža, uz primjenu naprednih metoda strojnog učenja, omogućile su stvaranje iznimno bogatog skupa podataka. On upućuje na primarne i sekundarne rasjede aktivirane tijekom potresnog niza te pruža snažne dokaze da je heterogeno rasjedanje povezano s naknadnim potresima izravna i predvidiva posljedica preraspodjele tektonskih napetosti. Dobiveni uvidi u geometriju i kinematiku petrinjskoga rasjednog sustava, produktivnost naknadnih potresa i kratkoročne varijacije tektonskih napetosti važni su za unaprjeđenje modela seizmičke opasnosti. Oni omogućuju pouzdaniju karakterizaciju glavnih seizmogenih rasjeda, uključujući parametre koji definiraju vjerojatnost da se na njima dogodi potres, maksimalne očekivane magnitude i tipične mehanizme žarišta. Time se stvara čvršća osnova za deterministično modeliranje realističnih scenarija potresa na području Banovine, što doprinosi razvoju dugoročnih strategija smanjenja seizmičkog rizika u središnjoj Hrvatskoj.

Zahvala

Seizmološka služba pri Geofizičkome odsjeku Prirodoslovno-matematičkoga fakulteta Sveučilišta u Zagrebu zahvaljuje Vladi Republike Hrvatske i Ministarstvu znanosti i obrazovanja na financijskoj potpori za nabavu kompleta seizmoloških instrumenata za praćenje seizmičnosti: 20 modernih seizmometara i 20 akcelerometara s pripadajućom opremom. Seizmolozi iz Geofizičkog zavoda "Andrija Mohorovičić" zahvaljuju kolegama iz Nacionalnog instituta za oceanografiju i primijenjenu geofiziku – OGS (Italija) na pomoći i ustupanju šest seizmografa s integriranim akcelerometrima za brzu instalaciju. Postajama stalne hrvatske mreže i mobilnog fonda (PN-Net) upravljala je hrvatska Seizmološka služba. Ovaj rad podržala je Europska unija – NextGenerationEU putem Nacionalnog plana za oporavak i otpornost 2021. – 2026. Institucionalna potpora bila je od Prirodoslovno-matematičkoga fakulteta Sveučilišta u Zagrebu (GIGA). Automatska detekcija i lociranje potresa provedeni su u sklopu projekta "Geofizičko-seizmološka istraživanja potresom ugroženih područja u RH i razvoj atenuacijskih relacija predviđanja seizmičkog gibanja tla – CRONOS", financiranog iz Norveškog financijskog mehanizma (2014. – 2021., projekt 04-UBS-U-0002/22-90). Privremenim postajama OP-Net mreže upravljali su seizmolozi Geofizičkog zavoda "Andrija Mohorovičić". Zahvaljujemo svim kolegama koji su sudjelovali u postavljanju i održavanju postaja te u analizi seizmograma i podataka.

LITERATURA

[1] Herak, M., Herak, D.: Properties of the Petrinja (Croatia) earthquake sequence of 2020–2021–Results of seismological research for the first six months of activity. Tectonophysics, 858 (2023), Paper No. 229885, https://doi.org/10.1016/j.tecto.2023.229885

[2] Herak, D., Herak M.: The Kupa Valley (Croatia) Earthquake of 8 October 1909 - 100 Years Later, Seismological Research Letters 81 (2010), pp. 30–36, https://doi.org/ 10.1785/gssrl.81.1.30

[3] Pollak, D., Gulam, V., Novosel, T., Avanić, R., Tomljenović, B., Hećej, N., Terzić, J., Stipčević, J., Bačić, M., Kurečić, T., Dolić, M.: The preliminary inventory of coseismic ground failures related to December 2020–January 2021 Petrinja earthquake series, Geologia Croatica, 74(2) (2021), pp. 189-208, https://doi.org/10.4154/gc.2021.08

[4] Tomac, I., Vlahovic, I., Parlov, J., Matoš, B., Matešic, D., Kosovic, I., Pavicic, I., Frangen, T., Terzic, J., Pavelic, D.: Geotechnical Reconnaissance and Engineering Effects of the December 29, 2020, M6. 4 Petrinja, Croatia Earthquake, and Associated Seismic Sequence, Technical report of Geotechnical Extreme Event Reconnaissance (GEER) Association: Petrinja, Croatia, 2021, pp. 49-96, https://doi.org/10.18118/G63T0

[5] Tomac, I., Kovačević Zelić, B., Perić, D., Domitrović, D., Štambuk Cvitanović, N., Vučenović, H., Parlov, J., Stipčević, J., Matešić, D., Matoš, B., Vlahović, I.: Geotechnical reconnaissance of an extensive cover-collapse sinkhole phenomena of 2020–2021 Petrinja earthquake sequence (Central Croatia), Earthquake spectra, 39 (2023) 1, pp. 653-686, https://doi.org/10.1177/87552930221115759

[6] Atalić, J., Uroš, M., Šavor Novak, M., Demšić, M., Baniček, M., Kadić, A., Oreb, J.: The Croatian Centre for Earthquake Engineering: establishment, activities and future opportunities, in 3rd European Conference on Earthquake Engineering & Seismology (3ECEES), (2022), pp. 2088-2097

[7] Atalić, J., Demšić, M., Baniček, M., Uroš, M., Dasović, I., Prevolnik, S., Kadić, A., Šavor Novak, M., Nastev, M.: The December 2020 magnitude (Mw) 6.4 Petrinja earthquake, Croatia: seismological aspects, emergency response and impacts, Bulletin of earthquake engineering, 21 (2023) 13 , pp. 5767-5808, https://doi.org/10.1007/s10518-023-01758-z

[8] Mihaljević, I., Zlatović, S.: Embankments damaged in the magnitude Mw 6.4 Petrinja earthquake and remediation, Geosciences, 13 (2023) 2, Paper No. 48, https://doi.org/ 10.3390/geosciences13020048

[9] Mijić, Z., Zlatović, S., Montgomery, J., Ziotopoulou, K., Gjetvaj, V.: Liquefaction effects in the 2020 Mw 6.4 Petrinja, Croatia, earthquake, Soil Dynamics and Earthquake Engineering, 193 (2025), Paper No. 109262 https://doi.org/ 10.1016/j.soildyn.2025.109262

[10] Markušić, S., Stanko, D., Penava, D., Ivančić, I., Bjelotomić Oršulić, O., Korbar, T., Sarhosis, V.: Destructive M6. 2 Petrinja earthquake (Croatia) in 2020 - Preliminary multidisciplinary research, Remote Sensing, 13 (2021) 6, Paper No. 1095, https://doi.org/ 10.3390/rs13061095

[11] Kastelic, V., Atzori, S., Carafa, M., Govorčin, M., Herak, D., Herak, M., Matoš, B., Stipčević, J., Tomljenović, B.: Petrinja Seismogenic Source and its 2020-2021 Earthquake Sequence (central Croatia). in EGU General Assembly Conference Abstracts (2021), Paper No. EGU21-16585

[12] Baize, S., Amoroso, S., Belić, N., Benedetti, L., Boncio, P., Budić, M., Cinti, F.R., Henriquet, M., Jamšek Rupnik, P., Kordić, B., Markušić, S.: Environmental effects and seismogenic source characterization of the December 2020 earthquake sequence near Petrinja, Croatia, Geophysical Journal International, 230 (2022) 2, pp. 1394-1418, https://doi.org/ 10.1093/gji/ggac123

[13] Henriquet, M., Kordic, B., Métois, M., Lasserre, C., Baize, S., Benedetti, L., Spelić, M., Vukovski, M.: Rapid remeasure of dense civilian networks as a game-changer tool for surface deformation monitoring: The case study of the Mw 6.4 2020 Petrinja Earthquake, Croatia, Geophysical Research Letters, 49 (2022) 24, Paper No. e2022GL100166, https://doi.org/10.1029/2022GL100166

[14] Xiong, W., Yu, P., Chen, W., Liu, G., Zhao, B., Nie, Zh., Qiao, X.: The 2020 Mw 6.4 Petrinja earthquake: a dextral event with large coseismic slip highlights a complex fault system in northwestern Croatia, Geophys. J. Int., 228 (2022), pp. 1935–1945, https://doi.org/10.1093/gji/ggab440

[15] Zhu, S., Wen, Y., Gong, X., Liu, J.: Coseismic and Early Postseismic Deformation of the 2020 Mw 6.4 Petrinja Earthquake (Croatia) Revealed by InSAR, Remote Sensing, 15(10) (2023), 2617. https://doi.org/10.3390/rs15102617

[16] Žilić, I., Causse, M., Vallee, M., Markušić, S.: High Stress Drop and Slow Rupture During the 2020 MW6.4 Intraplate Petrinja Earthquake, Croatia, Journal of Geophysical Research-Solid Earth, 130 (2025) 1, 10.1029/2024JB029107

[17] Sardeli, E., Michas, G., Pavlou, K., Zaccagnino, D., Vallianatos, F.: Spatiotemporal properties of the 2020–2021 Petrinja (Croatia) earthquake sequence, Journal of Seismology, 28 (2024) 4, pp. 899-920, https://doi.org/ 10.1007/s10950-024-10228-1

[18] Bjelotomić Oršulić, O., Markovinović, D., Varga, M., Bašić, T.: Coseismic ground displacement after the M W 6.2 earthquake in NW Croatia determined from sentinel-1 and GNSS CORS data, Geosciences, 11 (2021) 4, Paper No. 170, https://doi.org/10.3390/geosciences11040170

[19] Tondi, E., Blumetti, A. M., Cicak, M., Di Manna, P., Galli, P., Invernizzi, C., Mazzoli, S., Piccardi, L., Valentini, G., Vittori, E., Volatili, T.: 'Conjugate' coseismic surface faulting related with the 29 December 2020, Mw 6.4, Petrinja earthquake (Sisak-Moslavina, Croatia), Scientific Reports, 11 (2021) 1, https://doi.org/ 10.1038/s41598-021-88378-2

[20] Ustaszewski, K., Herak, M., Tomljenović, B., Herak, D., Matej, S.: Neotectonics of the Dinarides-Pannonian Basin transition and possible earthquake sources in the Banja Luka epicentral area, J. Geodyn., 82 (2014), pp. 52–68, https://doi.org/ 10.1016/j.jog.2014.04.006

[21] Herak, M.: Croatian catalogue and database of focal mechanism solutions, characteristic mechanisms, and stress field properties in the Dinarides and the surrounding regions, Geofizika, 41 (2024) 2, pp. 79-123, https://doi.org/ 10.15233/gfz.2024.41.5

[22] Ustaszewski, K., Kounov, A., Schmid, S.M., Schaltegger, U., Krenn, E., Frank, W., Fügenschuh, B.: Evolution of the Adria–Europe plate boundary in the northern Dinarides: from continent–continent collision to back-arc extension, Tectonics, 29 (2010), TC6017, https://doi.org/ 10.1029/2010TC002668

[23] Schmid, S., Fűgenschuh, B., Kounov, A., Matenco, L., Nievergelt, P., Oberhänsli, R., Pleuger, J., Schefer, S., Schuster, R., Tomljenović, B., Ustaszewski, K., van Hinsbergen, D.J.J.: Tectonic units of the Alpine collision zone between Eastern Alps and western Turkey, Gondwana Res., 78 (2020), pp. 308-374, https://doi.org/10.1016/j.gr.2019.07.005

[24] Saftić, B., Velić, J., Sztanó, O., Juhász, G., Ivković, Ž.: Tertiary subsurface facies, source rocks and hydrocarbon reservoirs in the SW part of the Pannonian Basin (northern Croatia and south-western Hungary). Geologia Croatica, 56 (2003), pp. 101–122, https://hrcak.srce.hr/3793

[25] Tomljenović, B., Csontos, L.: Neogene–Quaternary structures in the border zone between Alps, Dinarides and Pannonian Basin (Hrvatsko zagorje and Karlovac Basins, Croatia), Int J Earth Sci, 90 (2001), pp. 560–578, https://doi.org/ 10.1007/s005310000176

[26] Herak, D., Herak, M., Tomljenović, B.: Seismicity and earthquake focal mechanisms in North-Western Croatia, Tectonophysics, 465 (2009) 1-4, pp. 212-220, https://doi.org/ 10.1016/j.tecto.2008.12.005

[27] Pikija, M.: Basic Geological Map of SFRY 1:100.000, Sisak sheet. Geol. Zavod, Zagreb, Savezni geol. Zavod, Beograd. (in Croatian), 1987

[28] Šikić, K.: Osnovna geološka karta Republike Hrvatske 1: 100.000. Tumač za list Bosanski Novi 1: 100.000, L 33-70 [Basic Geological Map of Republic of Croatia 1: 100000, Geology of the Bosanski Novi sheet–in Croatian]. Hrvatski geološki institut Zagreb, 2014

[29] Tomljenović, B., Stipčević, J., Sečanj, M.: Izvješće o zabilježenim pojavama koseizmičkih površinskih deformacija na području Pokuplja i Banovine nastalih potresnom serijom od 28.12. 2020 do 5.01.2021. Rudarsko-geološko-naftni fakultet, Sveučilište u Zagrebu 2021. (https://www.rgn.unizg.hr/hr/izdvojeno/2790-izvjesce-o-zabiljezenim-pojavama-koseizmickih-povrsinskih-deformacija-na-podrucju-pokuplja-i-banovine-nastalih-potresnom-serijom-od-28-12-2020-do-5-01-2021), 2021

[30] Mihalić Arbanas, S., Arbanas, Ž., Bernat Gazibara, S., Krkač, M.: Preliminary engineering geological and geotechnical investigation of geological hazards induced by Petrinja Earthquake Series 2020-2021, GRAĐEVINAR, 77 (2025) 11, pp. 1071-1082, https://doi.org/ https://doi.org/10.14256/JCE.4422.2025

[31] Kovačević, M.S., Bačić, M., Librić, L., Jurić-Kaćunić, D.: Liquefaction in Croatia: Risk assessment and rapid post-earthquake decision-making – five years later, GRAĐEVINAR, 77 (2025) 11, pp. 1037-1055, https://doi.org/ https://doi.org/10.14256/JCE.4419.2025

[32] Stipčević, J., Poggi, V., Herak, M., Parolai, S., Herak, D., Dasović, I., Bertoni, M., Barnaba, C., Pesaresi, D.: First results from temporary deployment of small seismic network following the Mw= 6.4 Petrinja earthquake, In EGU General Assembly Conference Abstracts (pp. EGU21-16579), 2021

[33] Herak, M., Herak, D., Markušić, S.: Revision of the earthquake catalogue and seismicity of Croatia, 1908–1992, Terra Nova, 8 (1996) 1, pp. 86-94, https://doi.org/ 10.1111/j.1365-3121.1996.tb00728.x

[34] Ross, Z.E., Yue, Y., Meier, M.A., Hauksson, E., Heaton, T.H.: PhaseLink: A deep learning approach to seismic phase association, Journal of Geophysical Research: Solid Earth, 124 (2019) 1, pp. 856-869, https://doi.org/ 10.1029/2018JB016674

[35] Zhu, W., Beroza, G.C.: PhaseNet: a deep-neural-network-based seismic arrival-time picking method, Geophysical Journal International, 216 (2019) 1, pp. 261-273, https://doi.org/ 10.1093/gji/ggy423

[36] Mousavi, S.M., Ellsworth, W.L., Zhu, W., Chuang, L.Y., Beroza, G.C.: Earthquake transformer - an attentive deep-learning model for simultaneous earthquake detection and phase picking, Nature communications, 11 (2020) 1, p.3952, https://doi.org/ 10.1038/s41467-020-17591-w

[37] Šindija, D., Mustać-Brčić, M., Hetényi, G., Stipčević, J.: Enhanced view of the Mw 6.4 Petrinja earthquake sequence (2020-2022) using deep learning. ESS Open Archive. 2025, https://doi.org/ 10.22541/essoar.174982734.45695605/v1

[38] Michelini, A., Cianetti, S., Gaviano, S., Giunchi, C., Jozinović, D., Lauciani, V.: INSTANCE–the Italian seismic dataset for machine learning, Earth System Science Data, 13 (2021) 12, pp. 5509-5544, https://doi.org/ 10.5194/essd-13-5509-2021

[39] Münchmeyer, J.: PyOcto: A high-throughput seismic phase associator, Seismica, 3 (2024) 1, https://doi.org/ 10.26443/seismica.v3i1.1130

[40] Lomax, A., Virieux, J., Volant, P., Berge-Thierry, C.: Probabilistic earthquake location in 3D and layered models: Introduction of a Metropolis-Gibbs method and comparison with linear locations. In Advances in seismic event location (pp. 101-134). Dordrecht: Springer Netherlands, pp. 101-134, 2000, https://doi.org/ 10.1007/978-94-015-9536-0_5

[41] Lomax, A.: Mapping finite-fault slip with spatial correlation between seismicity and point-source Coulomb failure stress change, arXiv preprint, 2024, https://doi.org/ 10.48550/arXiv.2404.05437

[42] Zhu, W., Mousavi, S.M., Beroza, G.C.: Seismic signal denoising and decomposition using deep neural networks, IEEE Transactions on Geoscience and Remote Sensing, 57 (2019) 11, pp. 9476-9488, https://doi.org/ 10.1109/TGRS.2019.2926772

[43] Fonzetti, R., Buttinelli, M., Valoroso, L., De Gori, P., Chiarabba, C.: Fault interaction during large earthquakes as revealed by the L'Aquila 2009 sequence, Journal of Geophysical Research: Solid Earth, 130 (2025) 8, Paper No. e2025JB031245, https://doi.org/ 10.1029/2025JB031245

Primljen / Received: 17.10.2025.
Ispravljen / Corrected: 13.4.2026.
Prihvaćen / Accepted: 7.5.2026.
Dostupno online / Available online: 10.6.2026.

Učinci adhezijskog smrzavanja i F-T ciklusa na posmičnu čvrstoću sučelja između Güngören gline i betona

Autori:

Doc.dr.sc. **Aysenur Aslan Fidan**, dipl.ing.građ.
Sveučilište Dicle, Turska
Odjel za građevinarstvo
aysenur.aslan@dicle.edu.tr
aysenur.asln@gmail.com
Autor za korespondenciju

Doc.dr.sc. **Murat Gulen**, dipl.ing.građ.
Sveučilište Siirt, Turska
Odjel za građevinarstvo
murat.gulen@siirt.edu.tr

Prof.dr.sc. **Suat Akbulut**, dipl.ing.građ.
Tehničko sveučilište Yildiz, Turska
Odjel za građevinarstvo
sakbulut@yildiz.edu.tr

Izvorni znanstveni rad

Aysenur Aslan Fidan, Murat Gulen, Suat Akbulut

Učinci adhezijskog smrzavanja i F-T ciklusa na posmičnu čvrstoću sučelja između Güngören gline i betona

Ciklusi smrzavanja i odmrzavanja (F-T ciklusi) znatno utječu na interakciju tla i konstrukcije jer mogu promijeniti čvrstoću tla i njegovo deformacijsko ponašanje. U ovom se istraživanju analiziraju učinci F-T ciklusa na posmičnu čvrstoću, adheziju i kut trenja na sučelju između Güngören gline i betona pri različitim udjelima vode. Uzorci su pripremljeni s udjelima vode 5 % nižim i 5 % višim od optimalnog udjela te su podvrgnuti 0, 3, 7 i 10 F-T ciklusa u temperaturnome rasponu od -20 °C do +20 °C. Pokusi izravnog smicanja provedeni su u smrznutome stanju i nakon odmrzavanja. Rezultati pokazuju da je adhezijsko smrzavanje, odnosno vezivanje ledom na sučelju, znatno povećalo čvrstoću smrznutih uzoraka. Posmična čvrstoća povećala se od 1,6 do 2,7 puta kod smrznutih uzoraka s većim udjelom vode te od 1,05 do 1,19 puta kod uzoraka s manjim udjelom vode. Nakon odmrzavanja uzorci s manjim udjelom vode pokazali su deformacijsko omekšavanje i smanjenje čvrstoće na 0,80 do 0,95 početne vrijednosti, dok su uzorci s većim udjelom vode uglavnom zadržali svoju čvrstoću. Adhezija se blago povećala kod smrznutih uzoraka s manjim udjelom vode, dok se kod uzoraka s većim udjelom vode nakon trećeg ciklusa povećala gotovo trostruko, a zatim stabilizirala. Kut trenja na sučelju pokazao je različite trendove ovisno o udjelu vode i toplinskome stanju uzorka. Navedene se promjene mogu pripisati zajedničkome djelovanju cementacije ledom, nesmrznute vode, međudjelovanja čestica i preraspodjele vlage na sučelju.

Ključne riječi:
adhezijsko smrzavanje, sučelje glina-beton, ciklusi smrzavanja i odmrzavanja, Güngören glina, posmična čvrstoća

Original research paper

Aysenur Aslan Fidan, Murat Gulen, Suat Akbulut

Adfreezing and freeze-thaw effects on the shear strength of the Güngören clay-concrete interface

The interaction between soil and structures is significantly affected by freeze-thaw (F-T) cycles, which alter soil strength and deformation behaviour. This study investigates the effects of F-T cycles on the shear strength, adhesion, and interface friction angle of the Güngören clay-concrete interface under varying water content. Samples were prepared at 5 % below and 5 % above the optimum water content and subjected to 0, 3, 7, and 10 F-T cycles between -20 °C and +20 °C. Direct shear tests were conducted under both freezing and thawing conditions. The results indicate that adfreezing, ice bonding at the interface, significantly enhanced the strength of frozen samples with shear strength increasing by 1.6-2.7 times in frozen wet-side samples and 1.05-1.19 times in dry-side samples. After thawing, dry-side samples exhibited strain-softening and reduction in strength 0.80-0.95 times the initial value, whereas wet-side samples largely preserved their strength. Adhesion increased slightly in dry-side frozen samples, whereas in wet-side samples, it increased nearly threefold after the third cycle and then stabilised. The interface friction angle exhibits different trends depending on the moisture content and thermal state. These variations are attributed to the combined effects of ice cementation, unfrozen water, particle interactions, and moisture redistribution at the interface.

Key words:
adfreezing, clay-concrete interface, freeze-thaw cycles, Güngören clay, shear strength

1. Uvod

U hladnim područjima interakcija između tla i konstrukcija uvelike je pod utjecajem F-T ciklusa. Smrzavanje vode unutar pora tla dovodi do znatnih promjena u čvrstoći tla i svojstvima deformacije [1, 2]. Osim toga posmična otpornost koja se razvija na sučelju između smrznutog tla i površine konstrukcije, poznata kao adhezijsko smrzavanje, ima ključnu ulogu u stabilnosti infrastrukture ukopane u tlo ili oslonjene na tlo [3, 4].

Ponavljani ciklusi smrzavanja i odmrzavanja mogu promijeniti mehanička svojstva i tla i sučelja tlo-konstrukcija, što rezultira varijacijama u posmičnoj čvrstoći [5, 6]. Te varijacije stvaraju izazove u osiguravanju dugoročnog ponašanja i stabilnosti konstrukcija izloženih takvim uvjetima okružja. Zato je razumijevanje interakcija između tla i konstrukcija u smrznutome stanju i u stanju nakon odmrzavanja ključno za sigurno i isplativo projektiranje geotehničkih sustava kao što su piloti opterećeni trenjem po plaštu, potporni zidovi, sidra, autoceste, nasipi, plitki temelji i zbijeni slojevi [7, 8]. Većina inženjerskih izazova u mehanici smrznutog tla odnosi se na predviđanje ponašanja tla pod spregnutim mehaničkim i toplinskim utjecajima [9, 10].

Ciklus smrzavanja i odmrzavanja obuhvaća četiri faze: stanje prije smrzavanja, smrzavanje, odmrzavanje i konsolidaciju. U stanju prije smrzavanja tlo je zbijeno i pokazuje visoku posmičnu čvrstoću. Tijekom smrzavanja stvaranje leda uzrokuje razdvajanje čestica tla, što dovodi do raspršenije strukture. U fazi odmrzavanja tlo pokazuje veći koeficijent pora i nižu posmičnu čvrstoću. Na kraju, nakon konsolidacije, tlo postupno ponovno dobiva čvrstoću tijekom slijeganja pod opterećenjem, uz smanjeni koeficijent pora u odnosu na stanje nakon odmrzavanja, iako je i dalje veći nego u fazi prije smrzavanja [11, 12].

Posmično ponašanje sučelja između smrznutog tla i konstrukcijskih materijala ključno je za procjenu ponašanja geotehničkih sustava u hladnim područjima. Utjecaj adhezijskog smrzavanja na posmičnu čvrstoću sučelja opsežno je istraživan na različitim vrstama tla, uključujući prah [4], glinu [13, 14], pijesak [15] i pješčenjak [16], u kombinaciji s konstrukcijskim materijalima poput čelika [4, 17, 18], betona [19-21] ili leda [13]. Ta su istraživanja provedena primjenom standardnih ispitivanja s kontroliranom temperaturom [13, 21], velikih posmičnih ispitivanja [14, 19 , 22] i komora s niskim temperaturama [4] pri različitim temperaturama.

Pri konstantnoj temperaturi povećanje početnog udjela vode rezultiralo je većom posmičnom čvrstoćom sučelja. Suprotno tome, pri konstantnome udjelu vode, snižavanje temperature rezultira povećanjem posmične čvrstoće, što ima izraženiji učinak na adheziju [13, 19]. Kako se temperatura smanjivala, tako je način loma prelazio iz deformacijskog očvršćivanja u deformacijsko omekšavanje, ponajprije zbog povećanja udjela leda. Budući da se led ponaša kao krti materijal, on znatno utječe na uočeno ponašanje pri lomu [14, 23].

Nadalje, veća toplinska vodljivost betona u odnosu na tlo potiče migraciju nesmrznute vode prema sučelju. Taj proces dovodi do stvaranja ledenog filma na dodirnoj površini između smrznutog tla i betona. Takva migracija vode i stvaranje ledenog filma znatno utječu na mehaničko ponašanje sučelja tlo-beton [20, 24-26].

Prema meteorološkim podacima Turske državne meteorološke službe (MGM) za razdoblje 2000. – 2022., iako Istanbul općenito ima blagu klimu, minimalne temperature zraka tijekom zimskih mjeseci, osobito u prosincu, siječnju i veljači, često padaju ispod 0 °C i povremeno mogu doseći i do –8 °C. Ti uvjeti dovode do ponavljajućih ciklusa smrzavanja i odmrzavanja u površinskim slojevima tla. Zato je razumijevanje utjecaja takvih toplinskih uvjeta na mehaničko ponašanje Güngören gline ključno za dugoročnu stabilnost građevina koje se nalaze na tome tlu ili su s njim u interakciji. Znatan dio infrastrukture Istanbula, uključujući glavne prometnice, Zračnu luku Atatürk, željezničke pruge i plitke temelje zgrada, izgrađen je na Güngören glini [27, 28].

Ovaj rad istražuje posmično ponašanje sučelja između Güngören gline i betona u smrznutim i odmrznutim uvjetima, uzimajući u obzir utjecaj ciklusa smrzavanja i odmrzavanja, normalnih naprezanja i udjela vode. Cilj ovog istraživanja jest procijeniti utjecaj procesa smrzavanja i odmrzavanja na posmičnu čvrstoću sučelja te pružiti smjernice za poboljšanje sigurnosti i otpornosti urbane infrastrukture.

2. Materijali i metode

2.1. Geotehnička svojstva Güngören gline

U ovome istraživanju uzorci tla prikupljeni su s lokacije u blizini kampusa Tehničkog sveučilišta Yildiz i pripadaju lokalno poznatoj jedinici nazvanoj "Güngören glina". Ta zelenkasta glina visoke plastičnosti sastavni je dio široko rasprostranjene Güngören formacije. Zajedno s Gürpınar formacijom smatra se jednom od najproblematičnijih jedinica tla u Istanbulu zbog visoke plastičnosti i izražene osjetljivosti na uvjete okružja [29]. Güngören formacija široko je rasprostranjena diljem Istanbula i posebno je izražena u područjima kao što su Yedikule, Kazlıçeşme, Osmaniye, Şirinevler, Yenibosna i Halkalı, s debljinama u rasponu od približno 9 do 22 metra [28]. Na slici 1. prikazana je prostorna rasprostranjenost te formacije na europskoj strani Istanbula i ističe njezinu geološku zastupljenost u gradskim četvrtima.

Ta vrsta glina nalazi se ispod ključne infrastrukture, uključujući glavne prometne koridore, zračne luke i gusto naseljene stambene zone [27, 28], zbog čega je posebno važno uzeti u obzir njihovo ponašanje u toplinskim uvjetima.

Rendgenska difrakcija (XRD) provedena je u laboratoriju Tehničkog sveučilišta Yildiz radi određivanja mineralnog sastava uzorka. Rezultati pokazuju da je montmorilonit dominantan mineral, s najvišim intenzitetom vrha. Ostali identificirani minerali uključuju iliti-muskovit, kaolinit i kvarc, različitih intenziteta. Također, supostojanje ilita i montmorilonita potvrđeno je višestrukim karakterističnim vrhovima na XRD dijagramu (slika 2.).

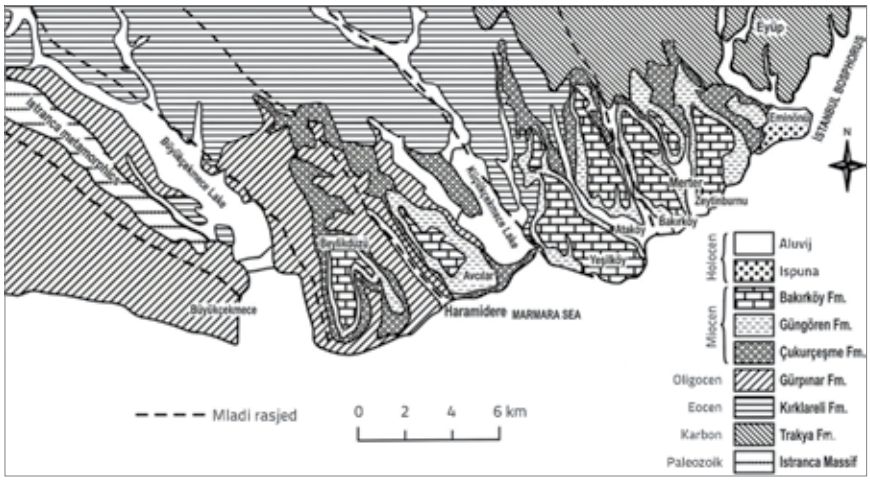

Slika 1. Geološka karta europskog dijela Istanbula [30]

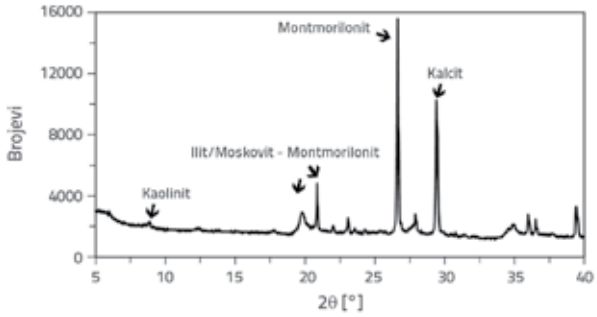

Slika 2. XRD rezultat Güngören gline

Laboratorijska ispitivanja provedena su na uzorcima dobivenim s terena radi određivanja inženjerskih svojstava Güngören gline. Ta ispitivanja uključuju analizu prosijavanjem [31, 32], granice konzistencije [33], specifičnu gustoću čvrstih čestica [34] i ispitivanja zbijanja [35]. Na slici 3. prikazan je položaj Güngören gline na Casagrandeovu dijagramu plastičnosti, a u tablici 1. njezina indeksna svojstva.

Tablica 1. Svojstva Güngören gline

Svojstvo	Vrijednost
Specifična gustoća čvrstih čestica (Gs)	2,63
Granica tečenja, LL [%]	81,50
Granica plastičnosti, PL [%]	35,30
Indeks plastičnosti, PI [%]	46,20
Aktivnost, A	0,71

Prema rezultatima analize prosijavanja i hidrometrijske analize, tlo se sastojalo od približno 95 % finozrnatog materijala s frakcijom gline od 65 %. Analiza prosijavanjem primijenjena je samo na grubu frakciju zadržanu na situ br. 200, dok je frakcija sitnih čestica okarakterizirana hidrometrijskom analizom. Granica tečenja (LL), granica plastičnosti (PL) i indeks plastičnosti (PI) iznosili su 81,5 %, 35,3 % i 46,2 %. Prema ASTM D2487-17 [36], tlo je klasificirano kao glina visoke plastičnosti (CH).

Prema ASTM D4546 [37], gline s PI > 40 % pokazuju vrlo visok potencijal bubrenja. U skladu s time, Güngören glinu karakteriziraju visok potencijal bubrenja, tlak bubrenja i kapacitet zadržavanja vode. Ta svojstva uvelike ovise o mineralnome sastavu, specifičnoj površini i kapacitetu izmjene kationa [38]. Gline bogate montmorilonitom pokazuju najveći potencijal bubrenja i kapacitet zadržavanja vode [39].

Mineralni sastav također utječe na reakciju gline na cikluse smrzavanja i odmrzavanja. Ekspanzija montmorilonita tijekom upijanja vode može uzrokovati strukturnu degradaciju tijekom ciklusa smrzavanja i odmrzavanja te dovesti do omekšavanja tla nakon odmrzavanja [40]. Rezultati prikazani na slikama 2. i 3. dodatno potvrđuju cikluse smrzavanja i odmrzavanja Güngören gline.

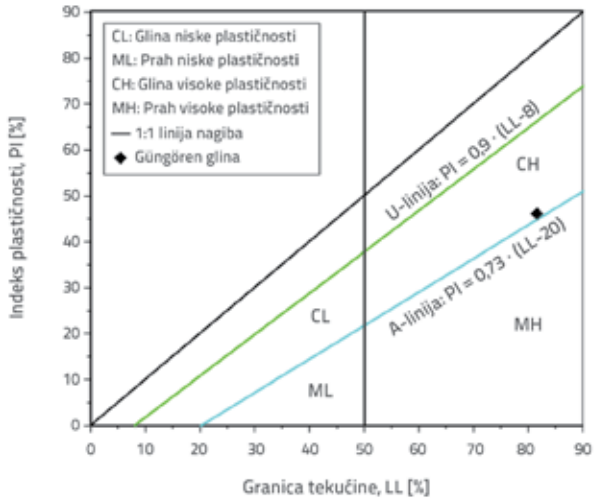

Slika 3. Položaj Güngören gline u Casagrandeovu dijagramu plastičnosti

Svi izravni posmični pokusi provedeni su na uzorcima tla zbijenima na obje strane optimalnog udjela vode (wopt), odnosno na suhoj i mokroj strani. Krivulja zbijanja tla prikazana je na slici 4. Maksimalna suha gustoća iznosila je 1,378 g/cm³, a optimalni udio vode (wopt) 28,3 %. Stupanj zasićenja tla bio je približno 60 % na suhoj strani i 85 % na mokroj strani.

Ispitivanje snižavanja točke smrzavanja provedeno je na zbijenim uzorcima koji predstavljaju suhu (w = 23,3 %) i mokru stranu (w = 33,3 %) krivulje zbijanja. Krivulje temperatura-vrijeme uzoraka, prikazane na slici 5., pokazuju da je točka smrzavanja (FP) –1,1 °C za uzorak sa suhe strane i –0,4 °C za uzorak s mokre strane.

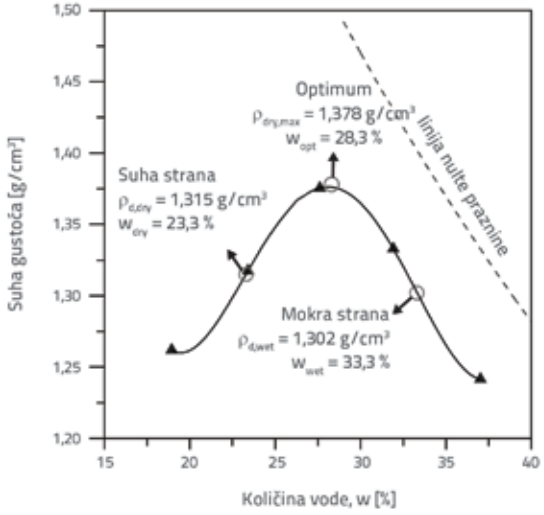

Slika 4. Standardna krivulja zbijanja Güngören gline

Prethodna istraživanja pokazala su da na FP tla utječu brojni čimbenici poput tipa tla, granica konzistencije, udjela vode, sastava i koncentracije soli, uvjeta opterećenja, tlaka bočnog ograničenja i vibracija [5, 41–44].

Niži početni udio vode dovodi do bržeg smrzavanja i većeg sniženja točke smrzavanja zbog promjena tlaka porne vode, dok viši udio vode usporava smrzavanje i blago povećava FP, osobito u blizini zasićenja [16, 45, 46].

Dodatno, viši udio vode rezultirao je izraženijim kašnjenjem napredovanja fronte smrzavanja, dok je niži udio vode doveo do brže stope smrzavanja i kraćeg vremena stabilizacije [45]. FP uzoraka tla nelinearno je rastao s povećanjem udjela vode, približavajući se vrijednosti čiste vode (0 °C) pri visokim razinama zasićenja [16]. Ti učinci pripisuju se prisutnosti slabo vezane vode, koja se smrzava na znatno nižoj temperaturi, te povećanome potencijalu vode u tlima s višim udjelima vode [46].

2.2. Priprema betonskih blokova i karakterizacija hrapavosti površine

Tekstura površine i tvrdoća konstrukcijskih materijala na sučelju imaju ključnu ulogu u određivanju ponašanja sučelja, pri čemu povećana hrapavost površine općenito dovodi do veće posmične čvrstoće [48-50]. Iako su neka istraživanja proučavala glatka sučelja tlo-beton koristeći šperploču ili čelične kalupe [51, 52], druga su ispitivala različite uvjete hrapavosti površine kako bi bolje prikazala terenske primjene [53-55].

Betonski uzorci korišteni za ispitivanje međudjelovanja na sučelju gline i betona izlijevani su u posebno dizajnirane kalupe od šperploče. Smjesa voda-cement-pijesak (2 : 5 : 15 po masi), koja se sastojala od pijeska veličine zrna manje od 4 mm, ugrađena je u kalupe, zbijena i njegovana uranjanjem u vodu (slika 6.a). Tijekom ugradnje betona primijenjene su vibracije kako bi se osigurala odgovarajuća zbijenost betona i uklonili zračni mjehurići koji bi mogli utjecati na čvrstoću i ujednačenost. Nakon izlijevanja kalupi su prekriveni plastičnim folijama kako bi se spriječio gubitak vlage. Nakon vezanja betona (otprilike 18 do 24 sata), uzorci su izvađeni iz kalupa i potom njegovani u vodi pod vlažnom krpom 28 dana radi postizanja pune čvrstoće. Tlačna čvrstoća kockastih uzoraka (15 × 15 × 15 cm) pripremljenih i njegovanih pod istim uvjetima nakon 28 dana iznosila je 51 MPa.

Za procjenu hrapavosti površine uzorci su analizirani pomoću optičkog profilometra AEP Nanomap 1000WLI, koji generira trodimenzionalne profile površine bilježeći varijacije reflektirane svjetlosti. Mjerenja su provedena na više lokacija korištenjem i optičke profilometrije i profilometrije iglom radi osiguranja točnosti i ponovljivosti (slika 6.b).

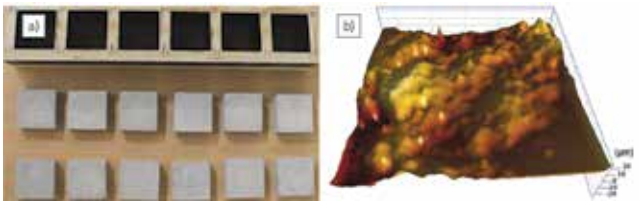

Slika 6. Detalji betonskih blokova: a) betonski uzorci i kalupi od šperploče; b) uzorak za mjerenje hrapavosti površine

U literaturi prikazani su različiti metodološki pristupi za kvantificiranje hrapavosti površine [56-58]. Među njima često se primjenjuju parametri temeljeni na visini poput normaliziranog indeksa hrapavosti (Rn). Normalizirani parametar hrapavosti

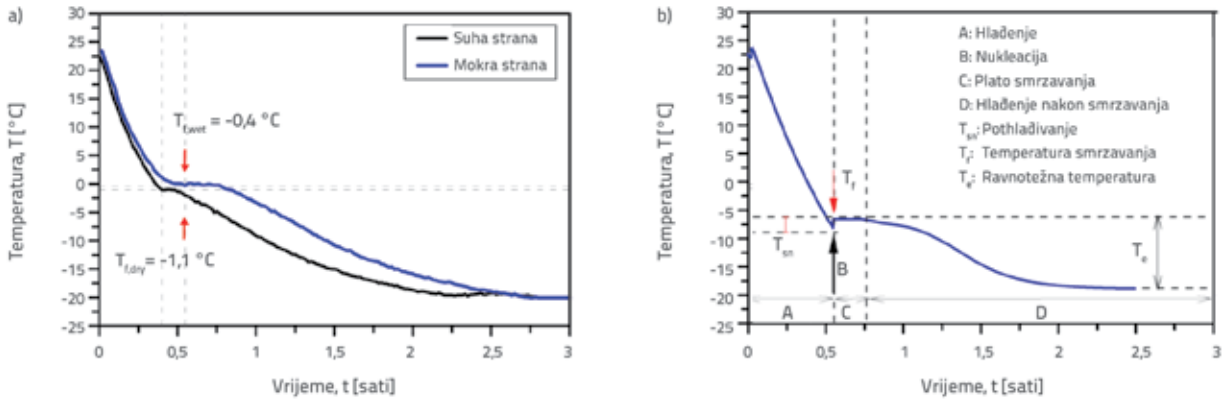

Slika 5. Krivulje temperatura-vrijeme za: a) Güngören glinu (eksperimentalno); b) tipično ponašanje pri smrzavanju, prema [47]

obično se definira kao omjer maksimalne visine neravnina (R_{max}) i srednje veličine čestica (D50), kako je prikazano u izrazu (1). Odgovarajuća vrijednost Rn za glinu korištenu u ovome istraživanju iznosila je približno 10,3, na temelju D50 = 0,0028 mm i Rmax = 0,026 mm.

$$R_n = \frac{R_{max}}{D_{50}} \quad (1)$$

Važno je napomenuti da je izraz (1) ponajprije razvijen za krupnozrnata tla, kod kojih je mehanički odgovor određen interakcijom između veličine čestica i hrapavosti površine. Za sitnozrnata tla poput smjesa gline i praha, gdje je reprezentativna veličina čestica znatno manja, taj parametar postaje manje primjenjiv i ne može se koristiti za smisleno fizikalno tumačenje. U ovom je istraživanju umjesto pristupa temeljenih na jednoj karakterističnoj visini hrapavosti primijenjen površinski pristup kako bi se obuhvatio doprinos cjelokupne teksture površine duž sučelja. Ta formulacija omogućuje reprezentativnije karakteriziranje površina s nepravilnom hrapavošću koje nemaju ujednačenu dubinu, razmak ili raspodjelu.

U toj je formulaciji parametar hrapavosti omjer stvarne površine i projektirane ravninske površine te daje kvantitativnu mjeru nepravilnosti površine, izraz (2). Veće vrijednosti upućuju na hrapaviju površinu s izraženijim asperitetima, što može pojačati mehaničko uklještenje na sučelju. Prema toj metodi izračuna, prosječni parametar hrapavosti (R_{av}) betonskih blokova korištenih u ovome istraživanju iznosio je 1,27.

$$R_{av} = \frac{A_r}{A_0} \quad (2)$$

2.3. Postupak ispitivanja

Za ispitivanja utjecaja smrzavanja i odmrzavanja uzorci su zbijeni u prsten uređaja za izravno smicanje, uz gustoću i udio vode koji odgovaraju suhoj odnosno mokroj strani optimalnog udjela vode (wopt) određenima iz krivulje zbijanja. Mješavina tla i vode najprije je pripremljena i ostavljena da odstoji u plastičnome kalupu 24 sata radi postizanja ujednačenosti. Uzorci su zatim zbijeni u uređaju za izravno smicanje, neposredno na betonsku površinu, čvrsto omotani rastezljivom folijom i smješteni u eksikator radi postizanja homogene raspodjele vlage. Nakon zbijanja posloženi su u spremnike, postavljeni u komoru te podvrgnuti ciklusima smrzavanja i odmrzavanja (slika 7.).

Zbijeni uzorci su zatim podvrgnuti 0, 3, 7 i 10 ciklusa smrzavanja i odmrzavanja. Tijekom faze smrzavanja uzorci su zamrznuti na –20 °C, a potom odmrznuti na 20 °C. Kako bi se spriječio gubitak vlage, relativna vlažnost zraka održavana je na 80 % tijekom cijele faze odmrzavanja. Odabrani temperaturni raspon osigurava potpuno smrzavanje i odmrzavanje porne vode, čime se eliminiraju djelomični učinci promjene faze i smanjuje eksperimentalna varijabilnost.

Slika 7. Faze pripreme uzoraka prikazane na fotografijama: a) pripremljeni uzorci; b) postavljanje uzoraka u eksikator; c) slaganje uzoraka u kutije; d) postavljanje uzoraka u komoru za smrzavanje i odmrzavanje

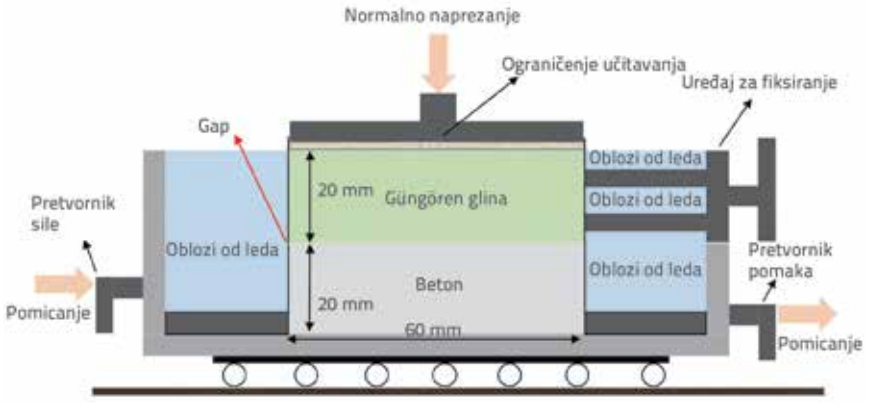

Slika 8. Shematski prikaz uređaja za izravni posmični pokus

U ovome istraživanju izveden je pokus izravnog smicanja, koji je dobro prihvaćena metoda za procjenu posmičnog ponašanja tla i sučelja tlo-konstrukcija [13, 51, 59, 60]. Uzorci sučelja glina-beton ispitivani su pomoću uređaja s kutijom za izravno smicanje dimenzija 6 cm × 6 cm u smrznutome i odmrznutome stanju. Ispitivanja su provedena u skladu s ASTM D3080 [61] primjenom normalnih naprezanja od 50, 100 i 200 kPa uz konstantnu brzinu smicanja od 1,0 mm/min (slika 8.).

Ta metodologija u skladu je s brojnim istraživanjima sučelja tlo-konstrukcija u smrznutim uvjetima i uvjetima smrzavanja i odmrzavanja, uključujući sučelja prah-beton [4], glina-beton [14, 62, 63], prašinasto tlo-čelik [17], pijesak-čelik [18], led-smrznuta glina [13], glina-geotekstil [64] i tlo-georešetka [65]. U većini istraživanja korištene su brzine smicanja između 0,8 i 1,2 mm/min, što je u skladu s 1,0 mm/min primijenjenih u ovome istraživanju [4, 17, 20, 63, 64, 66]. Zato su eksperimentalni parametri, uključujući ispitnu metodu [13, 51, 59, 60], temperaturu [20, 63], brzinu smicanja [4, 17, 20, 63, 64, 66] i primijenjeno normalno naprezanje [4, 13, 14, 17], bili u skladu s onima navedenima u citiranim istraživanjima, što podupire valjanost i usporedivost rezultata.

Uzorcima su dodijeljene oznake prema broju F-T ciklusa i termičkim uvjetima primijenjenima tijekom smicanja. Naprimjer, uzorak "3 ciklusa (smrznuto)" označava uzorak ispitan u smrznutome stanju nakon tri F-T ciklusa, dok "3 ciklusa

Tablica 2. Program ispitivanja

Ispitni materijal	Udio vode [%]	Smrzavanje [°C]	Odmrzavanje [°C]	Ciklusi	σ [kPa]	Stanje
Glina-beton	23,3	–20	+20	0, 3, 7, 10	50, 100, 200	Smrznuto / odmrznuto
Glina-beton	33,3	–20	+20	0, 3, 7, 10	50, 100, 200	Smrznuto / odmrznuto

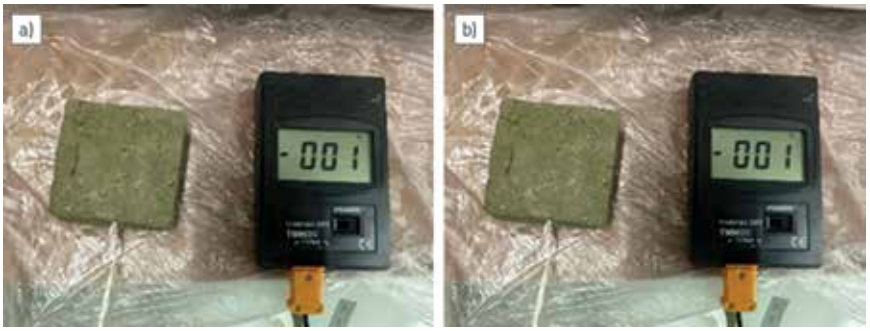

Slika 9. Mjerenje temperature uzoraka tla: a) prije i b) nakon izravnog posmičnog pokusa

(odmrznuto)" označava uzorak ispitan u odmrznutome stanju nakon istog broja ciklusa (tablica 2.).

Kontrolna ispitivanja provedena su prije eksperimentalnog dijela ispitivanja radi procjene ponovljivosti. Pri istim uvjetima varijacija izmjerenoga posmičnog naprezanja bila je ograničena te je iznosila približno 3 do 4 % pri 50 kPa odnosno 2 do 3 % pri 100 i 200 kPa za ispitivanja u smrznutome stanju, dok je za ispitivanja u stanju nakon odmrzavanja ostala na približno 2 % za sve razine normalnog naprezanja. Nakon provjere proveden je planirani program ispitivanja. Osim toga najmanje jedno ispitivanje ponovljeno je za svaku eksperimentalnu varijantu pri normalnim naprezanjima od 50, 100 i 200 kPa.

Prije posmičnog pokusa metalni prsten uređaja za izravno smicanje ohlađen je kako bi se spriječilo topljenje, a tijekom eksperimenta održavana je izolacija pomoću ledenih uložaka i plastičnih pokrova (slika 8.). Temperature uzoraka tla izmjerene prije i nakon pokusa pokazale su porast temperature tijekom posmičnog ispitivanja (slika 9.). Međutim, usporedba s točkom smrzavanja pokazala je da je temperatura tla nakon ispitivanja ostala blizu toj vrijednosti.

U sitnozrnatim tlima dio vode u porama ostaje nesmrznut čak i pri 0 °C [67-70]. Čak i pri vrlo niskim temperaturama poput –20 °C znatne količine nesmrznute vode mogu zaostati, stvarajući tanke filmove oko čestica tla [70, 71]. Prema Konradu [69], količina nesmrznute vode snažno ovisi o strukturnim svojstvima tla. Otvorene strukture tla imaju manje kapilarne nesmrznute vode ispod -2 °C, dok tla izložena većem opterećenju zadržavaju veće količine pod istim temperaturnim uvjetima.

Prisutnost tog filma nesmrznute vode utječe na ponašanje tla, jer se led formira uz adsorbirani sloj, a ne u izravnome kontaktu s česticama tla [12, 72]. Zato rezultate ispitivanja na smrznutim uzorcima gline i uzorcima sučelja glina-beton treba tumačiti uzimajući u obzir zajedničku prisutnost leda i nesmrznute vode. Ispitani uzorci predstavljaju stanje zbijenog tla, a ne prirodnu strukturu tla. Zato se raspodjela nesmrznute vode i njezin utjecaj na mehaničko ponašanje mogu razlikovati od *in situ* uvjeta u kojima struktura tla ima veću ulogu.

3. Rezultati i rasprava

3.1. Vizualno opažanje stvaranja ledenog filma na sučelju

Smrznuti uzorci pripremljeni na mokroj strani optimalnog udjela vode podvrgnuti su izravnome posmičnom pokusu i vizualno pregledani (slika 10.). Uočen je glatki i sjajni kontaktni sloj, što upućuje na stvaranje ledenog sloja s ledenim kristalima unutar pora tla i duž kontaktne površine. Takvo ponašanje pripisuje se toplinskome gradijentu preko sučelja tijekom ciklusa smrzavanja i odmrzavanja. Kako navode He i sur. [20], toplinski gradijent potiče migraciju nesmrznute vode iz okolnog tla prema sučelju, što dovodi do stvaranja ledenih filmova na kontaktnoj površini. Taj mehanizam potvrđuju i prethodna istraživanja [24-26, 73].

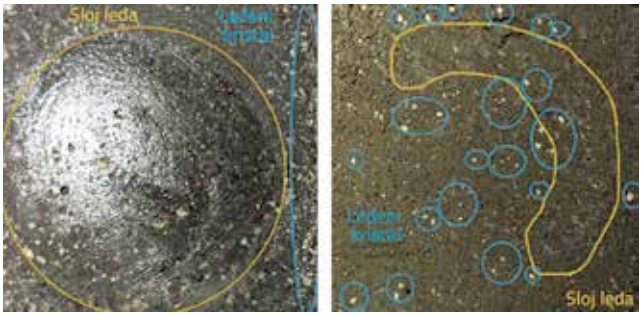

Slika 10. Ledeni sloj i ledeni kristali opaženi na površinama tla i betona nakon 7. ciklusa smrzavanja

3.2. Utjecaj adhezijskog smrzavanja i F-T ciklusa na krivulju naprezanje-deformacija

U ovome istraživanju krivulja naprezanje-deformacija smrznutih uzoraka sučelja glina-beton zbijenih na suhoj strani optimalnog udjela vode pokazuje vrlo sličan višestupanjski proces deformacije kakav su opisali Liu i sur. [19] za smrznuta sučelja tlo-beton (slika 11.). Liu i sur. [19] su primjenom ispitivanja izravnog smicanja velikog mjerila identificirali faze krivulje kao elastičnu deformaciju (a – b), početak plastične deformacije (b – c), klizno slabljenje uz smanjenje posmičnog naprezanja (c – d), deformacijsko očvršćivanje zbog progresivne deformacije (d – e) i rezidualnu posmičnu čvrstoću (e – f). U ovom su istraživanju, tijekom ispitivanja izravnog

smicanja, uzorci pokazali slične faze deformacijskog ponašanja sve do faze deformacijskog očvršćivanja (d – e), ali nisu dosegnuli fazu rezidualne posmične čvrstoće (e – f). To se vjerojatno može pripisati ograničenjima uređaja za izravno smicanje manjeg mjerila. Kako navode Goughnour i Andersland [74], ledena matrica pri uobičajenome tlaku i temperaturi znatno je kruća od skeleta tla te postiže svoju vršnu čvrstoću pri manjim deformacijama. Često se pojavljuju dvije izražene točke popuštanja: jedna pri približno 1 % aksijalne deformacije, a druga pri otprilike 10 % ili više. To dvostruko vršno ponašanje opaženo je i na sučelju glina-beton u pokusima u sklopu ovog istraživanja, što upućuje na to da takav odgovor nije ograničen samo na smrznuta tla. Nakon drugog vrha nije zabilježeno rezidualno ponašanje, a vršna čvrstoća pokazala je blago povećanje u odnosu na početnu vrijednost. Štoviše, to se povećanje izraženije očitovalo s porastom broja ciklusa smrzavanja i odmrzavanja.

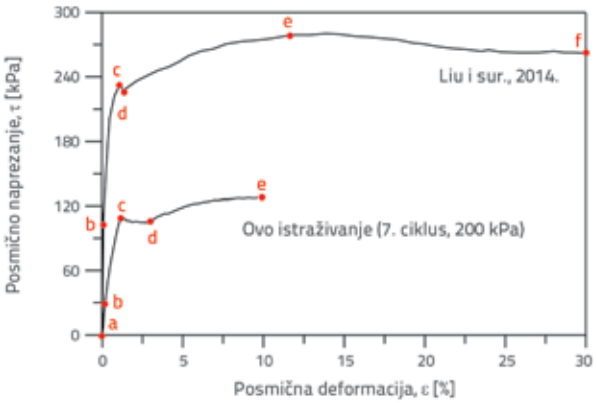

Slika 11. Ponašanje naprezanje-deformacija smrznutog sučelja glina-beton na suhoj strani

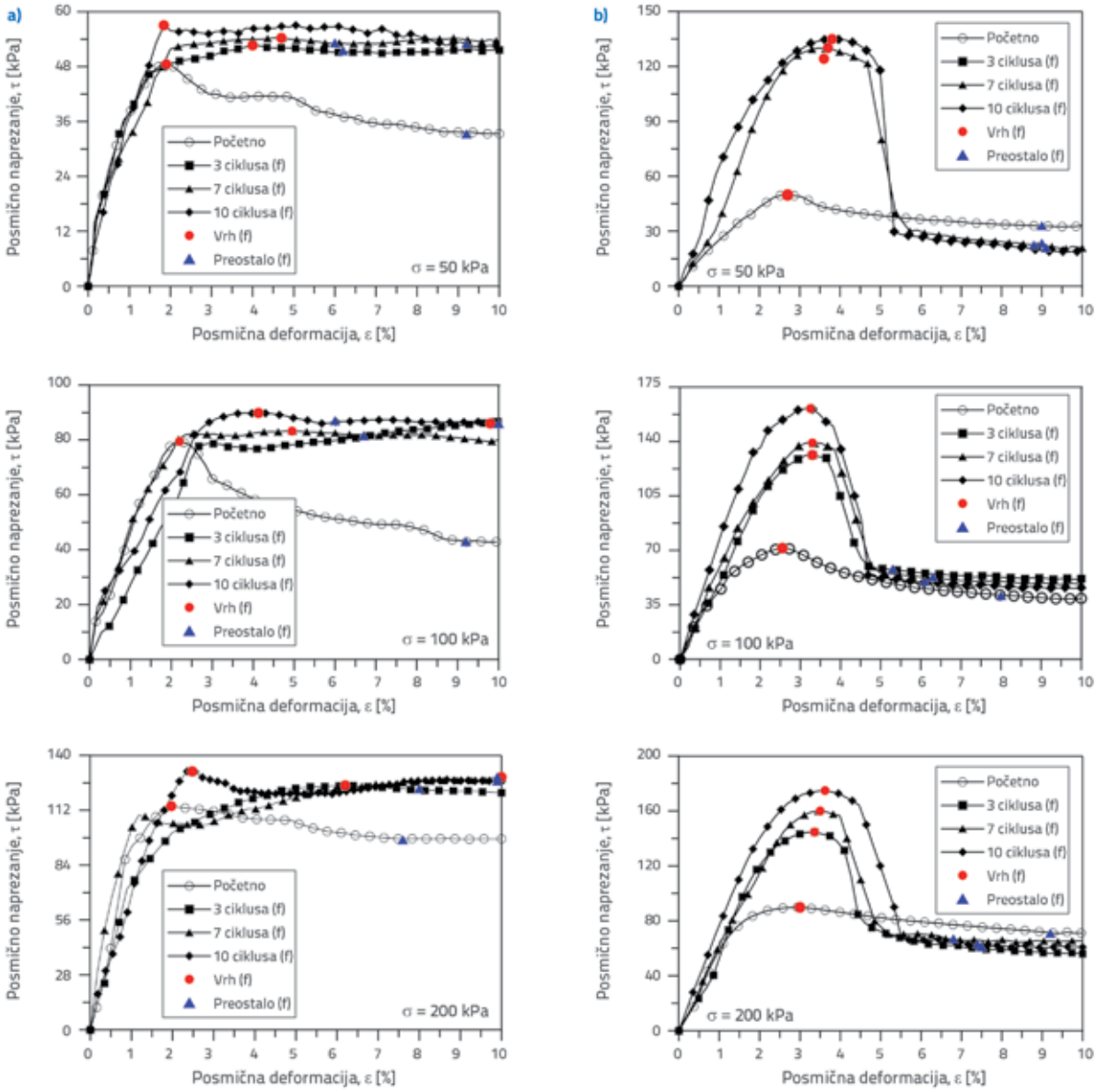

Slika 12. Krivulje naprezanje-deformacija iz izravnih posmičnih pokusa za smrznute uzorke sučelja glina-beton s različitim brojem ciklusa: a) smrznuto – suha strana; b) smrznuto – mokra strana

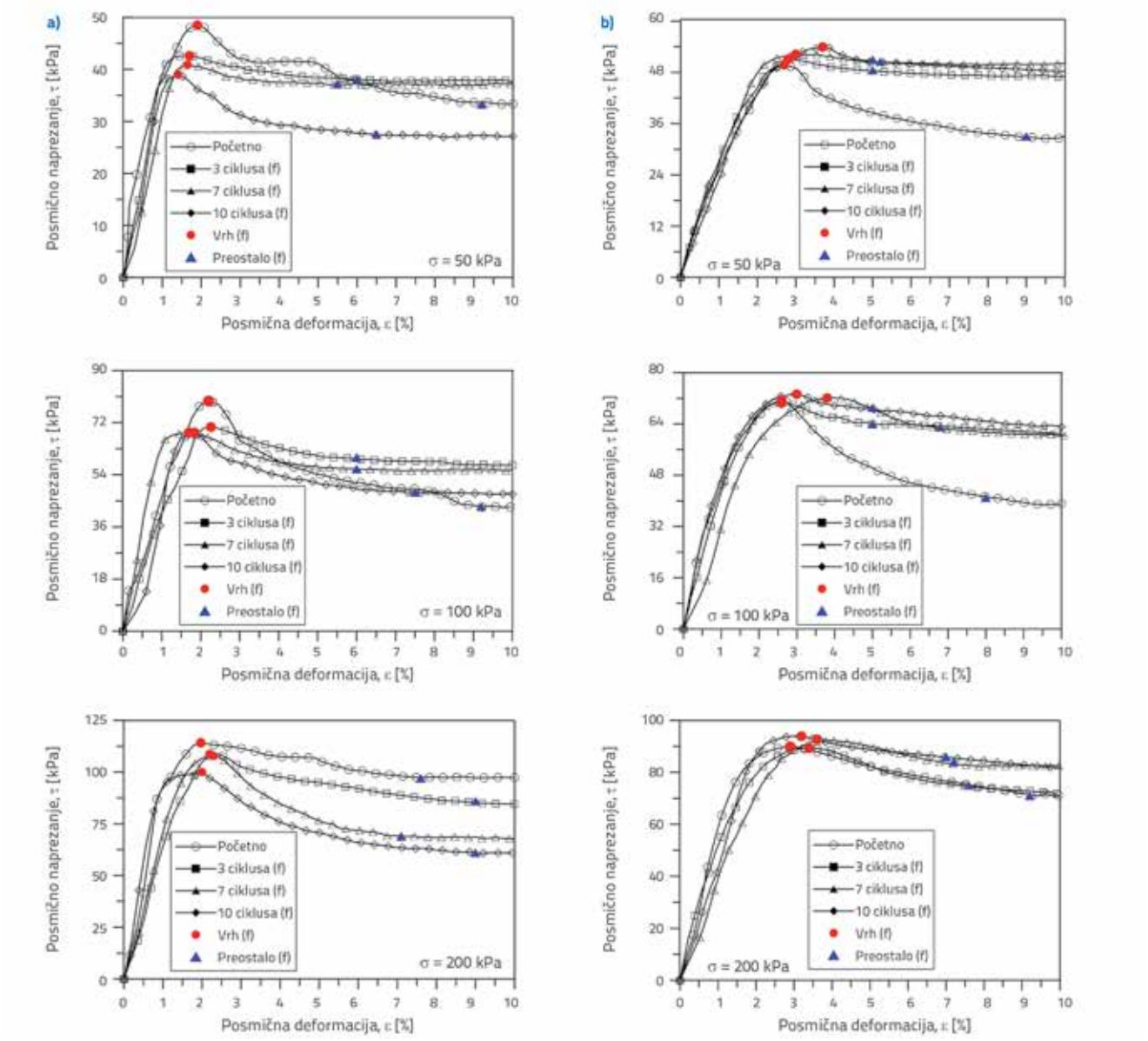

Slika 13. Krivulje naprezanje-deformacija iz izravnoga posmičnog pokusa za uzorke gline i betona nakon odmrzavanja s različitim brojem ciklusa: a) odmrznuto – suha strana; b) odmrznuto – mokra strana

Krivulje odnosa posmično naprezanje-posmična deformacija za smrznuto sučelje glina-beton, za uzorke pripremljene na suhoj i mokroj strani optimalnog udjela vode, prikazane su na slici 12. Za uzorke s mokre strane način loma prešao je iz očvršćivanja pri deformaciji u deformacijsko omekšavanje. Nakon što bi postigli vršno posmično naprezanje, došlo je do naglog smanjenja naprezanja zbog raspada cementirajućeg leda na sučelju, nakon čega je uslijedila stabilizacija na rezidualnoj razini. Takvo ponašanje odražava krti odgovor karakteriziran narušavanjem cementirajućeg leda na sučelju.

Vršno naprezanje povećavalo se s normalnim naprezanjem i brojem ciklusa smrzavanja i odmrzavanja, dok se vršna deformacija kretala između 3 i 4 %. Rezidualno naprezanje raslo je s normalnim naprezanjem, ali nije pokazalo jasnu ovisnost o ciklusima smrzavanja i odmrzavanja, a rezidualna posmična deformacija ostala je u rasponu od 5 – 6 %.

Krivulje odnosa posmičnog naprezanja i posmične deformacije, dobivene iz rezultata pokusa izravnog smicanja za odmrznuto sučelje glina-beton s početnim udjelom vode na suhoj i mokroj strani optimuma, prikazane su na slici 13.

Za odmrznute uzorke na suhoj strani krivulja naprezanje-deformacija pokazala je deformacijsko omekšavanje. U usporedbi sa smrznutim stanjem, krivulja je prešla iz oblika s dvama vrhovima u oblik s jednim vrhom. Vršna deformacija kretala se od 1,5 do 2,5 %, a vršno naprezanje raslo je s normalnim naprezanjem. Međutim, vršno naprezanje niže je nego u početnome stanju i smanjuje se s povećanjem broja ciklusa smrzavanja i odmrzavanja, što upućuje na postupni

gubitak čvrstoće, za razliku od trenda opaženog kod smrznutih uzoraka. Rezidualna deformacija varira između 4 i 6 %, povećava se s normalnim naprezanjem, ali ne pokazuje jasnu ovisnost o broju ciklusa.

Za uzorke odmrznute na mokroj strani također je opaženo ponašanje omekšavanja pri deformaciji. Vršna deformacija, koja se kretala od 2,5 % do 3,5 %, bila je veća nego na suhoj strani. Vršno naprezanje blago je raslo s normalnim naprezanjem i pokazalo je ograničen oporavak s povećanjem broja ciklusa u usporedbi s početnom fazom, ali je i dalje ostalo znatno niže, otprilike na polovici vrijednosti u odnosu na smrznute uzorke. Rezidualna deformacija ostala je unutar raspona 4 do 6 %, dok rezidualno naprezanje raste i s normalnim naprezanjem i s brojem ciklusa smrzavanja i odmrzavanja.

Učinci ciklusa smrzavanja i odmrzavanja na ponašanje sučelja uglavnom su povezani s migracijom vlage, stvaranjem leda i nakupljanjem ledenih filmova na sučelju [20]. Ledeni slojevi imaju ključnu ulogu u adhezijskoj čvrstoći jer je posmična otpornost pri niskim temperaturama uvelike određena cementacijom ledom na sučelju [75]. Veći početni udio vode povećava količinu vode dostupne za smrzavanje, što rezultira jačim vezivanjem ledom [4]. To povećava posmičnu čvrstoću u smrznutim uvjetima, ali također pogoduje krtom slomu zbog vezivanja ledom na sučelju. Prethodna istraživanja [14, 19, 66, 76] pokazala su da povećanje udjela vode mijenja ponašanje iz duktilnog u krto. Slično tome, udio vode (odnosno udio leda u smrznutim uvjetima) znatno utječe na krutost i načine sloma smrznutih tala [13, 77, 78].

Tijekom odmrzavanja degradacija veza leda smanjuje posmičnu čvrstoću sučelja, osobito vršnu čvrstoću [20, 21]. Nasuprot tome, rezidualna čvrstoća ostaje relativno stabilna i uglavnom neovisna o udjelu vode [17] i ciklusima smrzavanja i odmrzavanja [20]. Utjecaj temperature na rezidualnu čvrstoću također je bio ograničen, što su pokazali Zhang i sur. [41].

Pomak pri vršnoj čvrstoći povećava se s početnim udjelom vode, ali na njega ne utječu znatno ciklusi smrzavanja i odmrzavanja, temperatura ni normalno naprezanje. Slično tomu, rezidualni pomak pokazuje malu ovisnost o navedenim čimbenicima [20].

U skladu s navedenim rezultatima rezultati ovog istraživanja pokazuju da se rezidualna posmična čvrstoća tek neznatno mijenja pri različitim udjelima vode i uvjetima smrzavanja i odmrzavanja. Iako se povećava s porastom normalnog naprezanja, ne pokazuje sustavan trend u odnosu na broj ciklusa smrzavanja i odmrzavanja. Prethodna istraživanja pokazala su da je rezidualno posmično naprezanje manje osjetljivo na promjene udjela vode nego vršna posmična čvrstoća [14, 19].

Za razliku od vršne čvrstoće, koja je vrlo osjetljiva na toplinske uvjete i udio vode, rezidualno ponašanje ostaje relativno stabilno. Također je manje pogođeno ciklusima smrzavanja i odmrzavanja [20]. To upućuje na to da je rezidualna posmična čvrstoća uglavnom određena mehanizmima trenja duž sučelja, uz ograničen utjecaj vezivanja ledom ili ciklusa smrzavanja i odmrzavanja.

3.3. Utjecaj adhezijskog smrzavanja i F-T ciklusa na vršnu čvrstoću

Vršno posmično naprezanje, odnosno posmična čvrstoća, pokazalo je izraženu povezanost s normalnim naprezanjem (slika 14.). Taj je odnos opisan linearnom funkcijom prilagodbe za smrznute i odmrznute uzorke pripremljene na suhoj i mokroj strani optimalnog udjela vode (tablica 3.).

Kod smrznutih uzoraka, sa suhe strane optimalnog udjela vode uočeno je povećanje čvrstoće na sučelju zbog adhezijskog smrzavanja. Međutim, povećanje je bilo ograničeno u odnosu na početnu čvrstoću nesmrznutih uzoraka. Vršna čvrstoća rasla je s povećanjem normalnog naprezanja.

Učinak ciklusa smrzavanja i odmrzavanja postaje izraženiji s povećanjem broja ciklusa. To je osobito vidljivo nakon 10 ciklusa. Najviša vrijednost postignuta je pri 200 kPa tijekom 10. ciklusa. Čvrstoća raste sa 114,15 kPa (nesmrznuto) na 131,85 kPa, što je 1,16 puta početna vrijednost. Ukupno, vršna čvrstoća kreće se između 1,05 i 1,19 puta početne čvrstoće. To pokazuje da ponovljeni ciklusi smrzavanja i odmrzavanja postupno povećavaju adhezijsku čvrstoću zahvaljujući cementaciji ledom na sučelju.

Suprotan trend uočen je kod odmrznutih uzoraka sa suhe strane. Nakon 10 ciklusa vršna čvrstoća smanjuje se na 73,95 kPa pri normalnome naprezanju od 200 kPa. To je 0,65 puta početna čvrstoća i 0,56 puta smrznuta čvrstoća. Najniža vrijednost zabilježena je nakon 10 ciklusa, a čvrstoća se postupno smanjivala kako se broj ciklusa povećavao. Nakon odmrzavanja pala je na 0,80 do 0,95 puta početne čvrstoće, ovisno o razini normalnog naprezanja. Taj rezultat naglašava štetan utjecaj ponovljenih F-T ciklusa na strukturni integritet odmrznutih uzoraka sa suhe strane.

Kod smrznutih uzoraka s mokre strane posmična čvrstoća raste 1,6 do 2,7 puta, ovisno o normalnome naprezanju i broju ciklusa, ponajprije zbog cementacije ledom na sučelju uzrokovane migracijom vode uslijed toplinskih gradijenata između gline i betona. Vršna čvrstoća povećavala se s normalnim naprezanjem, a učinak ciklusa bio je ponovno najizraženiji nakon 10 ciklusa. Pri 200 kPa čvrstoća raste s 89,82 kPa na 174,79 kPa, što odgovara 1,95 puta početne vrijednosti. Nakon tri ciklusa vršna posmična čvrstoća doseže 1,61 put početne vrijednosti (144,67 kPa), nakon sedam ciklusa 1,78 puta (160,01 kPa), a nakon 10 ciklusa 1,95 puta (174,79 kPa). To pokazuje da ponovljeno smrzavanje pojačava vezivanje ledom i povećava čvrstoću. Taj je učinak bio izraženiji kod uzoraka s mokre strane, što naglašava važnost početnog udjela vode.

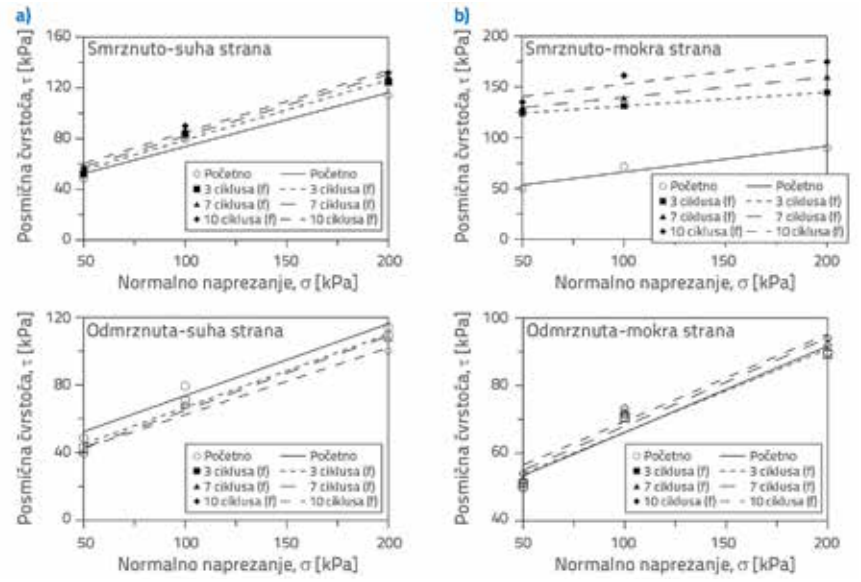

Slika 14. Promjena posmične čvrstoće smrznutih i odmrznutih uzoraka glina-beton u odnosu na normalno naprezanje i broj ciklusa za a) suhu i b) mokru stranu

Tablica 3. Prilagodbeni izrazi za posmičnu čvrstoću smrznutih i odmrznutih uzoraka na suhoj i mokroj strani

Stanje	Uzorak s mokre strane		Uzorak sa suhe strane	
	Jednadžba	R^2	Jednadžba	R^2
Početno	$\tau = 0{,}255\sigma + 40{,}638$	0,944	$\tau = 0{,}425\sigma + 31{,}176$	0,975
3 ciklusa (smrznuto)	$\tau = 0{,}136\sigma + 117{,}516$	0,999	$\tau = 0{,}473\sigma + 31{,}544$	0,989
7 ciklusa (smrznuto)	$\tau = 0{,}201\sigma + 119{,}601$	0,999	$\tau = 0{,}487\sigma + 33{,}238$	0,986
10 ciklusa (smrznuto)	$\tau = 0{,}247\sigma + 128{,}109$	0,869	$\tau = 0{,}487\sigma + 36{,}030$	0,986
3 ciklusa (odmrznuto)	$\tau = 0{,}245\sigma + 41{,}715$	0,961	$\tau = 0{,}433\sigma + 23{,}491$	0,990
7 ciklusa (odmrznuto)	$\tau = 0{,}261\sigma + 41{,}916$	0,968	$\tau = 0{,}440\sigma + 20{,}957$	0,992
10. ciklus (odmrznuto)	$\tau = 0{,}258\sigma + 43{,}620$	0,971	$\tau = 0{,}395\sigma + 22{,}897$	0,972

Nakon odmrzavanja uzorci s mokre strane pokazuju nagli pad čvrstoće. Pri 200 kPa i nakon 10 ciklusa čvrstoća pada sa 174,79 kPa na 93,89 kPa. To je 0,54 puta u odnosu na čvrstoću u smrznutome stanju. Međutim, u usporedbi s početnim nesmrznutim stanjem, nije zabilježen znatan pad nego blagi porast. Čvrstoća raste s 89,82 kPa na 93,89 kPa, što je 1,05 puta početne vrijednosti.

Povećanje čvrstoće u smrznutome stanju rezultat je cementacije ledom na sučelju. Voda migrira prema sučelju zbog toplinskoga gradijenta i smrzava se. Nakon odmrzavanja to dovodi do povećanog udjela vode u blizini sučelja. Primijenjeno normalno naprezanje povećava kontaktnu površinu između tla i betona. Time se smanjuje oslabljivanje uzrokovano ciklusima smrzavanja i odmrzavanja. Umjesto toga čvrstoća ostaje stabilna ili se u nekim slučajevima s ponovljenim ciklusima čak blago poveća.

Kada temperatura padne ispod točke smrzavanja, adhezija leda na sučelju povećava posmičnu otpornost. To se definira kao čvrstoća pri smrzavanju [79]. Taj je učinak povezan s čvrstoćom leda i povećanom adhezijom između smrznutog tla i betona [14, 18, 19, 76]. Wang i sur. [80] pokazali su da vršno naprezanje raste s udjelom vode u smrznutim uvjetima. To je posljedica migracije vode i stvaranja ledenog sloja [17]. Povećano vezivanje ledom također može promijeniti ponašanje materijala iz plastičnog u krto kako raste udio vode [66]. Vršna čvrstoća povećavala se s normalnim naprezanjem, udjelom vode i temperaturom [14]. Nakon odmrzavanja omekšano tlo može ispuniti površinske nepravilnosti i povećati kontakt [24].

3.4. Utjecaj adhezijskog smrzavanja i F-T ciklusa na adheziju i kut trenja na sučelju

Učinci ciklusa smrzavanja i odmrzavanja te adhezijskog smrzavanja na adheziju (ca) i kut trenja na sučelju (δ) između gline i betona jasno su prikazani na slici 15. Vrijednosti adhezije na slici 15.a pokazuju jasne razlike između uzoraka s mokre i suhe strane tijekom ciklusa smrzavanja i odmrzavanja.

Do trećeg ciklusa smrzavanja uzorci sa suhe strane pokazuju samo blago povećanje adhezije. To povećanje nastavlja se postupno s dodatnim ciklusima i doseže ukupno povećanje od 5,00 kPa nakon 10 ciklusa.

To ograničeno povećanje uglavnom je povezano s niskom dostupnošću slobodne vode u uzorcima sa suhe strane. Prisutnost zraka u porama ograničava migraciju vode, a posljedično i opseg cementacije ledom na sučelju.

Nakon trećeg ciklusa smrzavanja adhezija kod uzoraka s većim udjelima vode povećala se na približno trostruku početnu vrijednost. Naknadno povećanje bilo je minimalno, što je dovelo do stabilizacije adhezije na oko 128,11 kPa do desetog ciklusa smrzavanja. Međutim, unatoč toj stabilizaciji, svaki je ciklus i dalje pokazivao trend porasta, pri čemu se adhezija postupno povećavala s povećanjem broja ciklusa.

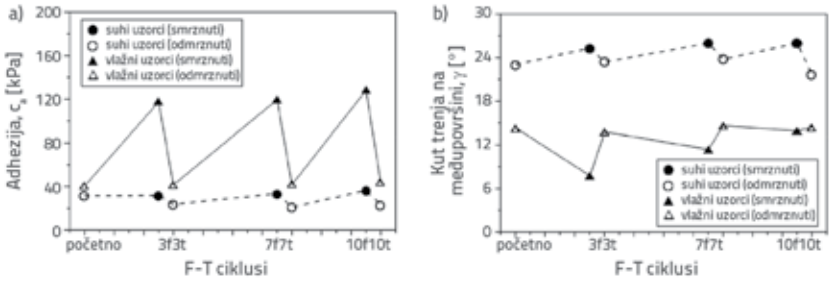

Slika 15. Parametri posmične čvrstoće sučelja na suhoj i mokroj strani: a) adhezija; b) kut trenja na sučelju

Navedeno upućuje na to da, iako je početni utjecaj cementacije ledom izražen, njezino djelovanje nastavlja pridonositi postupnome porastu adhezije s ponavljanjem ciklusa smrzavanja. Takvo ponašanje omogućeno je migracijom slobodne vode prema sučelju.

Tijekom ciklusa odmrzavanja učinak adhezijskog smrzavanja na adheziju postupno je slabio. U uzorcima sa suhe strane adhezija je pokazivala silazni trend u odnosu na početni ciklus, smanjujući se s 31,18 kPa na 22,90 kPa do 10. ciklusa odmrzavanja. To odgovara 0,73 puta početne vrijednosti i upućuje na to da ponovljeno odmrzavanje smanjuje čvrstoću veze na sučelju.

Nasuprot tome, uzorci s mokre strane su nakon odmrzavanja pokazali blagi oporavak u odnosu na početnu vrijednost. Do 10. ciklusa odmrzavanja adhezija se povećala s 40,64 kPa na 43,62 kPa, dosežući 1,07 puta početnu vrijednost. Taj oporavak kod uzoraka s mokre strane može se pripisati migraciji slobodne vode prema sučelju. Taj je učinak postajao izraženiji u ponovljenim ciklusima, a adhezija je bila blago povećana povećanjem udjela vode u blizini sučelja.

Promatrajući kut trenja na sučelju kod smrznutih i odmrznutih uzoraka, uočeni su različiti trendovi. F-T ciklusi ne uzrokuju dosljedan trend u kutu trenja na sučelju, jer i uzorci sa suhe i mokre strane pokazuju kolebanja, koja su izraženija kod uzoraka s mokre strane.

Međutim, u smrznutome stanju uočena su suprotna ponašanja između uzoraka sa suhe i mokre strane. Kod uzoraka sa suhe strane kut trenja na sučelju u smrznutome stanju postupno raste sa svakim ciklusom smrzavanja i odmrzavanja, dosežući najvišu vrijednost u 10. ciklusu. To upućuje na to da ponovljeno smrzavanje potiče međusobno uklapanje čestica ili strukturno preuređenje na sučelju, čime se poboljšava posmična otpornost. Međutim, tijekom odmrzavanja kut trenja na sučelju smanjuje se za otprilike 2°, padajući ispod početne vrijednosti nakon 10 ciklusa, što upućuje na to da je degradacija veze na sučelju tijekom uzastopnih ciklusa odmrzavanja oslabila posmičnu otpornost.

Kod uzoraka s mokre strane smrznuti uzorci su u početku zabilježili nagli pad kuta trenja na sučelju, koji se smanjio na gotovo polovinu početne vrijednosti. Međutim, nakon trećeg ciklusa uočen je postupan oporavak. Vrijednosti su se nakon više ciklusa smrzavanja i odmrzavanja gotovo vratile na početnu razinu.

Taj trend upućuje na to da su migracija vode i nesmrznuta voda u početku smanjile otpornost na sučelju zbog učinka podmazivanja. Međutim, s povećanjem broja ciklusa može doći do veće cementacije ledom ili boljeg preuređenja čestica, što dovodi do poboljšane posmične otpornosti.

U stanju nakon odmrzavanja kut trenja na sučelju znatno se smanjio tijekom početnih ciklusa, a zatim se stabilizirao. Takvo ponašanje vjerojatno je posljedica preraspodjele vode na sučelju. Adhezijska čvrstoća pri smrzavanju na sučelju sastoji se od dviju komponenti: adhezije leda na površinu betona i trenja između zrna tla na sučelju, kako su to opisali He i sur. [14] u svojemu istraživanju. Utjecaj temperature na posmičnu čvrstoću sučelja ponajprije se očituje kroz promjene u kohezivnim silama. S padom temperature i porastom udjela vode adhezija se znatno povećava, što naglašava njezin ključan doprinos posmičnoj čvrstoći u uvjetima smrzavanja.

Nasuprot tome, kut trenja općenito se smatra neosjetljivim na temperaturne promjene. Sadovskiy [81] je uočio da smrzavanje povećava koheziju tla, dok kut posmičnog otpora ostaje praktički nepromijenjen. Slično tome, Wang i sur. [80] izvijestili su da, iako kohezijska sila naglo raste s povećanjem udjela vode, unutarnji kut trenja ima tendenciju smanjenja pri konstantnoj hrapavosti površine [17].

Međutim, u smrznutim uvjetima udio vode ima dvostruki utjecaj. Potiče cementaciju na sučelju stvaranjem ledenih kristala, dok nesmrznuta voda djeluje kao lubrikant. To smanjuje trenje i snižava kut trenja, osobito pri višim udjelima vode [17, 75].

Što se tiče učinaka F-T ciklusa, He i sur. [20] nisu utvrdili znatnu promjenu vršnog ni rezidualnog kuta trenja prije F-T cikliranja ili nakon njega. To opažanje u skladu je s nalazima Ladanyi i Theriault [82], koji su također zaključili da F-T cikliranje pretežno utječe na koheziju, dok otpor trenju ostaje uglavnom stabilan.

Na temelju prethodno prikazanih eksperimentalnih rezultata osnovni fizikalni mehanizmi koji upravljaju ponašanjem sučelja mogu se protumačiti integriranjem opaženih odgovora s postojećim znanjem o procesima smrzavanja i ciklusima smrzavanja i odmrzavanja, kako je to shematski prikazano na slici 16. Rezultati pokazuju da se ponašanje sučelja uvelike razlikuje između suhe i mokre strane. Kod uzoraka s mokre strane visok stupanj zasićenja poticao je migraciju vode prema betonskoj površini tijekom smrzavanja zbog toplinskih gradijenata. To je dovelo do stvaranja neprekinutoga ledenog sloja na sučelju. Time se pojačava adhezijsko smrzavanje i dolazi do znatnog povećanja posmične čvrstoće. Nakon odmrzavanja povećani udio vode poboljšava kontakt čestica pod normalnim naprezanjem, omogućujući sučelju da zadrži svoju posmičnu čvrstoću. Suprotno tome, uzorci sa suhe strane pokazali su ograničenu pokretljivost vode, što je ograničilo razvoj neprekinutoga ledenog sloja. Kao rezultat smrzavanje

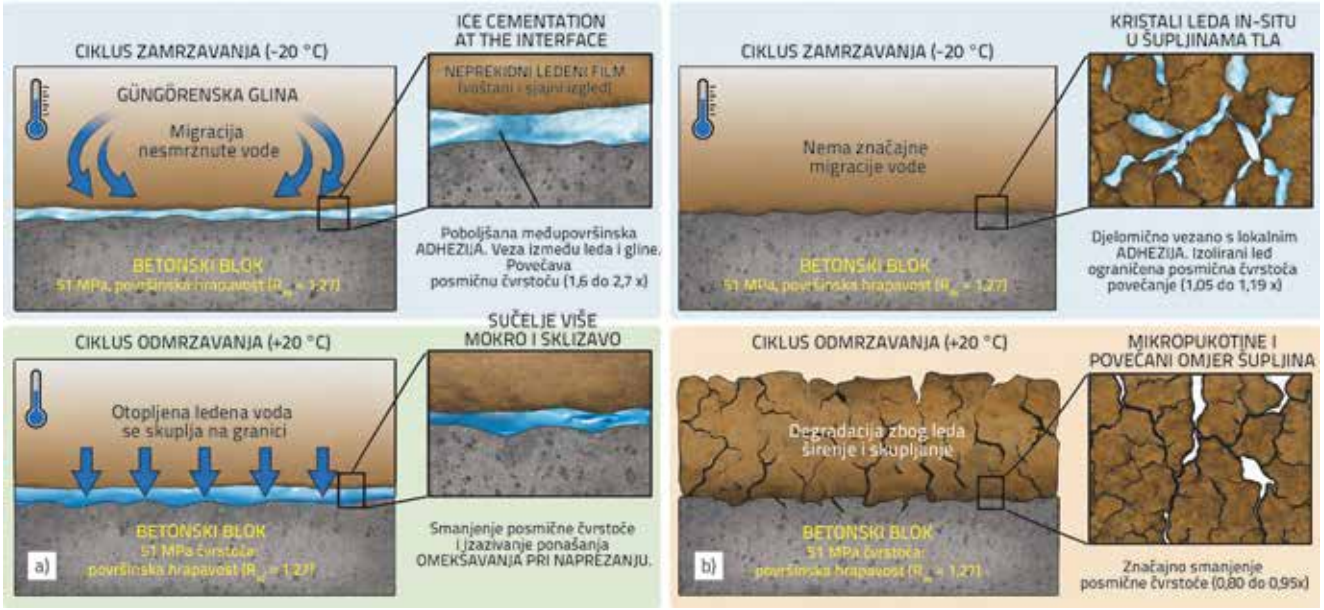

Slika 16. Mehanizmi ponašanja sučelja glina-beton tijekom ciklusa smrzavanja i odmrzavanja: a) mehanizam mokre strane; b) mehanizam suhe strane

je uglavnom bilo ograničeno na pore tla, što je dovelo samo do neznatnog povećanja posmične čvrstoće. Tijekom odmrzavanja mikrostrukturna degradacija i povećani koeficijent pora slabe sučelje, čime se smanjuje posmična čvrstoća.

4. Zaključak

U ovom je istraživanju pokusima izravnog smicanja analizirano ponašanje sučelja Güngören glina–beton pri smicanju, s posebnim naglaskom na učincima ciklusa smrzavanja i odmrzavanja (F-T ciklusa) te adhezijskog smrzavanja. Glavni rezultati istraživanja mogu se sažeti kako slijedi:

- Tijekom smrzavanja toplinski gradijenti između gline i betona uzrokovali su migraciju vode i adhezijsko smrzavanje, što je potvrđeno vidljivim stvaranjem ledenih kristala na sučelju.
- Smrznuti uzorci pripremljeni na suhoj strani optimalnog udjela vode pokazali su višefazno deformacijsko ponašanje s dvama vrhovima, dok su odmrznuti uzorci pokazali deformacijsko omekšavanje. Kod smrznutih uzoraka pripremljenih na mokroj strani optimalnog udjela vode došlo je do krtog loma, dok su odmrznuti uzorci pokazali postupno omekšavanje nakon što su dostigli vršnu čvrstoću.
- Kod smrznutih uzoraka s mokre strane posmična čvrstoća povećala se 1,6 do 2,7 puta, ovisno o normalnome naprezanju i broju ciklusa smrzavanja i odmrzavanja. Odmrznuti uzorci pripremljeni na mokroj strani zadržali su početnu čvrstoću zahvaljujući migraciji vode i povećanoj kontaktnoj površini.
- Kod smrznutih uzoraka pripremljenih na suhoj strani optimalnog udjela vode posmična čvrstoća povećala se 1,05 do 1,19 puta zbog ograničenog udjela vode i slabije cementacije ledom. Nakon odmrzavanja čvrstoća uzoraka pripremljenih na suhoj strani smanjila se na 0,80 do 0,95 početne vrijednosti.
- Nakon 10 ciklusa smrzavanja i odmrzavanja adhezija se kod smrznutih uzoraka pripremljenih na suhoj strani povećala na približno 5 kPa, dok se kod uzoraka pripremljenih na mokroj strani gotovo utrostručila već nakon triju ciklusa. Nakon odmrzavanja adhezija se kod uzoraka pripremljenih na mokroj strani blago oporavila te je premašila početnu vrijednost za približno 3 kPa.
- Kut trenja na sučelju blago se povećao u smrznutim uvjetima kod uzoraka pripremljenih na suhoj strani, ali se smanjio nakon odmrzavanja. Kod uzoraka pripremljenih na mokroj strani tijekom smrzavanja početno se smanjio, a zatim oporavio i stabilizirao tijekom daljnjih ciklusa.

Ograničenja i preporuke

U ovom je istraživanju analizirana posmična čvrstoća sučelja pod utjecajem adhezijskog smrzavanja i F-T ciklusa, s naglaskom na makroskopskome mehaničkom odzivu. Ipak, istraživanje ima nekoliko ograničenja.

Prvo, mikrostrukturna opažanja poput vizualizacije stvaranja leda i razvoja pukotina tijekom odmrzavanja te mjerenje i kontrolirano variranje udjela nesmrznute vode nisu bila uključena, iako ti čimbenici imaju ključnu ulogu u određivanju ponašanja sučelja. Osim toga pokusi su provedeni na zbijenim uzorcima tla, koji ne predstavljaju u cijelosti prirodnu strukturu tla. Zato se raspodjela nesmrznute vode i povezano mehaničko ponašanje mogu razlikovati od *in situ* uvjeta, u kojima struktura tla ima važniju ulogu. Drugo, učinci brzine deformacije i njezine interakcije s temperaturom nisu istraženi, unatoč njihovoj važnosti u određivanju mehaničkog odziva pod različitim opterećenjima

i toplinskim uvjetima. Treće, ponašanje je ispitivano samo pri fiksnim temperaturama smrzavanja i odmrzavanja, a utjecaj različitih temperaturnih razina unutar raspona smrzavanja i odmrzavanja nije razmatran. Važno je napomenuti da ti aspekti zahtijevaju napredne i često specijalizirane eksperimentalne postave. Zato svaki od tih aspekata jest poseban i vrijedan smjer budućih istraživanja. Buduća istraživanja koja bi obuhvatila te čimbenike omogućila bi sveobuhvatnije razumijevanje mehanizama koji upravljaju ponašanjem sučelja tlo-konstrukcija pod uvjetima smrzavanja i odmrzavanja.

LITERATURA

[1] Qi, J., Vermeer, P.A., Cheng, G.: A review of the influence of freeze-thaw cycles on soil geotechnical properties, Permafrost and Periglacial Processes, 17 (2006) 3, pp. 245-252, https://doi.org/10.1002/ppp.559

[2] Hu, J., Zhang, H., Li, Z., Yang, S., Zhang, S., Li, H., Lu, M.: Study on pore-water pressure variation and deformation characteristics of warm frozen soils under confined dynamic loading, Cold Regions Science and Technology, 214 (2023), 103968, https://doi.org/10.1016/j.coldregions.2023.103968

[3] Ding, J., Han, L., Li, Y. et al.: Permafrost engineering characteristics and frozen soil engineering on Qinghai-Tibet railway, Journal of Railway Engineering Society, (2005) s1, pp. 327-332

[4] Sun, T., Gao, X., Liao, Y., Feng, W.: Experimental study on adfreezing strength at the interface between silt and concrete, Cold Regions Science and Technology, 190 (2021), 103346, https://doi.org/10.1016/j.coldregions.2021.103346

[5] Tang, L., Cong, S., Geng, L., Ling, X., Gan, F.: The effect of freeze-thaw cycling on the mechanical properties of expansive soils, Cold Regions Science and Technology, 145 (2018), pp. 197-207, https://doi.org/10.1016/j.coldregions.2017.10.004

[6] Hong, L., Li, M., Du, C. et al.: Bond behaviour of the interface between concrete and basalt fiber reinforced polymer bar after freeze-thaw cycles, Frontiers of Structural and Civil Engineering, 18 (2024), pp. 630-641, https://doi.org/10.1007/s11709-024-0989-y

[7] Tsinker, G.P.: Geotechnical aspects of soil-structure interaction design considerations, in: Handbook of Port and Harbor Engineering, Springer, 1997, https://doi.org/10.1007/978-1-4757-0863-9_4

[8] Pham, T.A., Nadimi, S., Sutman, M.: Critical review of physical-mechanical principles in geostructure-soil interface mechanics, Geotechnical and Geological Engineering, 42 (2024), pp. 6757-6808, https://doi.org/10.1007/s10706-024-02954-7

[9] Kadivar, M., Manahiloh, K.N.: Revisiting parameters that dictate the mechanical behaviour of frozen soils, Cold Regions Science and Technology, 163 (2019), pp. 34-43, https://doi.org/10.1016/j.coldregions.2019.04.005

[10] Shen, M., Zhou, Z., Zhang, S.: Effect of stress path on mechanical behaviours of frozen subgrade soil, Road Materials and Pavement Design, 23 (2021) 5, pp. 1061-1090, https://doi.org/10.1080/14680629.2020.1869583

[11] Sage, J.D., D'Andrea, R.D.: Long term mitigation of frost deterioration of existing roadways, Final Report, NSF Grant No. ECE 85 18813, Worcester, USA, 1988, pp. 1-105

[12] Czurda, K.A., Hohmann, M.: Freezing effect on shear strength of clayey soils, Applied Clay Science, 12 (1997), pp. 165-187, https://doi.org/10.1016/S0169-1317(97)00005-7

[13] Shi, S., Zhang, F., Feng, D., Xu, X.: Experimental investigation on shear characteristics of ice-frozen clay interface, Cold Regions Science and Technology, 176 (2020), 103090, https://doi.org/10.1016/j.coldregions.2020.103090

[14] He, P.F., Mu, Y.H., Ma, W., Huang, Y.T., Dong, J.H.: Testing and modeling of frozen clay-concrete interface behaviour based on large-scale shear tests, Advances in Climate Change Research, 12 (2021) 1, pp. 83-94, https://doi.org/10.1016/j.accre.2020.09.010

[15] Quanbin, S., Ping, Y., Guoliang, W.: Experimental research on adfreezing strength at the interface between frozen sand and structures, Scientia Iranica A, 25 (2018) 2, pp. 663-674, https://doi.org/10.24200/sci.2017.20005

[16] Wang, Q., Qi, J., Wang, S., Xu, J., Yang, Y.: Effect of freeze-thaw on freezing point of a saline loess, Cold Regions Science and Technology, 170 (2020), 102922, https://doi.org/10.1016/j.coldregions.2020.102922

[17] Wang, T.L., Wang, H.H., Hu, T.F., Song, H.F.: Experimental study on the mechanical properties of soil-structure interface under frozen conditions using an improved roughness algorithm, Cold Regions Science and Technology, 158 (2019), pp. 62-68, https://doi.org/10.1016/j.coldregions.2018.10.015

[18] Aldaeef, A.A., Rayhani, M.T.: Pile-soil interface characteristics in ice-poor frozen ground under varying exposure temperature, Cold Regions Science and Technology, 192 (2021), 103377, https://doi.org/10.1016/j.coldregions.2021.103377

[19] Liu, J., Lv, P., Cui, Y., Liu, J.: Experimental study on direct shear behaviour of frozen soil-concrete interface, Cold Regions Science and Technology, 104-105 (2014), pp. 1-6, https://doi.org/10.1016/j.coldregions.2014.04.007

[20] He, P., Mu, Y., Yang, Z., Ma, W., Dong, J., Huang, Y.: Freeze-thaw cycling impact on the shear behaviour of frozen soil-concrete interface, Cold Regions Science and Technology, 173 (2020), 103024, https://doi.org/10.1016/j.coldregions.2020.103024

[21] Zhao, Y., Mao, X., Wu, Q., Huang, W., Wan, Y.: Study on shear characteristics of the interface between frozen soil and pile during thawing process in permafrost area, Advances in Civil Engineering, 2022 (2022), 1755538, https://doi.org/10.1155/2022/1755538

[22] De Guzman, E.M.B., Stafford, D., Alfaro, M.C., Doré, G., Arenson, L.U.: Large-scale direct shear testing of compacted frozen soil under freezing and thawing conditions, Cold Regions Science and Technology, 151 (2018), pp. 138-147, https://doi.org/10.1016/j.coldregions.2018.03.011

[23] Zhao, L., Yang, P., Wang, J.G. et al.: Cyclic direct shear behaviours of frozen soil-structure interface under constant normal stiffness condition, Cold Regions Science and Technology, 102 (2014), pp. 52-62

[24] Volokhov, S.S.: Effect of freezing conditions on the shear strength of soils frozen together with materials, Soil Mechanics and Foundation Engineering, 40 (2003) 6, pp. 1-5, https://doi.org/10.1023/B:SMAF.0000017575.19213.67

[25] Kim, K.H., Jeon, S.E., Kim, J.K. et al.: An experimental study on thermal conductivity of concrete, Cement and Concrete Research, 33 (2003) 3, pp. 363-371, https://doi.org/10.1016/S0008-8846(02)00965-1

[26] Mu, R., Tian, W., Zhou, M.: Moisture migration in concrete exposed to freeze-thaw cycles, Journal of the Chinese Ceramic Society, 38 (2010) 9, pp. 1713-1717

[27] Istanbul Metropolitan Municipality Directorate of Earthquake and Ground Research: Geological-Geotechnical Study Report and Map for the Southern Region of Istanbul's European Side at a 1/5000 Scale for Zoning Plans, Istanbul, 2001

[28] Yılmaz, E.: Güngören formasyonu killerin mühendislik özellikleri ve mineralojik etkiler, Master's thesis, Istanbul University, Institute of Science, Department of Geological Engineering, Istanbul, 2005

[29] Mermutlu, E., Şans, G., Mahmutoğlu, Y.: İstanbul-Ambarlı heyelanının izlenmesi ve analizi, in: KAYAMEK'2011 - X. Bölgesel Kaya Mekaniği Sempozyumu / ROCMEC'2011 - Xth Regional Rock Mechanics Symposium, Ankara, Turkey, 2011

[30] Dalgıç, S.: Factors affecting the greater damage in the Avcılar area of Istanbul during the 17 August 1999 Izmit earthquake, Bulletin of Engineering Geology and the Environment, 63 (2004) 3, pp. 221-232, https://doi.org/10.1007/s10064-004-0234-9

[31] American Society for Testing and Materials (ASTM): ASTM D6913-18: Standard Test Method for Particle-Size Distribution (Gradation) of Soils Using Sieve Analysis, ASTM International, West Conshohocken, PA, USA, 2018

[32] American Society for Testing and Materials (ASTM): ASTM D7928-17: Standard Test Method for Particle-Size Distribution (Gradation) of Fine-Grained Soils Using the Sedimentation (Hydrometer) Analysis, ASTM International, West Conshohocken, PA, USA, 2017

[33] American Society for Testing and Materials (ASTM): ASTM D4318-17: Standard Test Methods for Liquid Limit, Plastic Limit, and Plasticity Index of Soils, ASTM International, West Conshohocken, PA, USA, 2014

[34] American Society for Testing and Materials (ASTM): ASTM D854-14: Standard Test Methods for Specific Gravity of Soil Solids by Water Pycnometer, ASTM International, West Conshohocken, PA, USA, 2014

[35] American Society for Testing and Materials (ASTM): ASTM D698-12: Standard Test Methods for Laboratory Compaction Characteristics of Soil Using Standard Effort (12,400 ft-lb/ft^3), ASTM International, West Conshohocken, PA, USA, 2012

[36] American Society for Testing and Materials (ASTM): ASTM D2487-17(2025): Standard Practice for Classification of Soils for Engineering Purposes (Unified Soil Classification System), ASTM International, West Conshohocken, PA, USA, 2025

[37] American Society for Testing and Materials (ASTM): ASTM D4546-14: Standard Test Methods for One-Dimensional Swell or Collapse of Soils, ASTM International, West Conshohocken, PA, USA, 2014

[38] Tiwari, B., Ajmera, B.: Consolidation and swelling behaviour of major clay minerals and their mixtures, Applied Clay Science, 54 (2011) 3-4, pp. 264-273, https://doi.org/10.1016/j.clay.2011.10.001

[39] Panda, G.P., Bahrami, A., Nagaraju, T.V., Isleem, H.F.: Response of high swelling montmorillonite clays with aqueous polymer, Minerals, 13 (2023) 7, 933, https://doi.org/10.3390/min13070933

[40] Li, X., Zhang, L., Zhang, Y.: Influence of montmorillonite on the freeze-thaw properties of expansive soils, Geotechnical Testing Journal, 34 (2011) 4, pp. 295-306

[41] Zhang, L., Ma, W., Yang, C., Dong, S.: A review and prospect of the thermodynamics of soil subjected to freezing and thawing, Journal of Glaciology and Geocryology, 35 (2013) 6, pp. 1505-1518

[42] Wang, C., Lai, Y., Yu, F., Li, S.: Estimating the freezing-thawing hysteresis of chloride saline soils based on the phase transition theory, Applied Thermal Engineering, 135 (2018), pp. 22-33, https://doi.org/10.1016/j.applthermaleng.2018.02.039

[43] Adorni, E., Ivanov, M., Revetria, R.: Review of the effects of the influence of external vibrations on the freezing point of water, MATEC Web of Conferences, 320 (2020), 00032, https://doi.org/10.1051/matecconf/202032000032

[44] Shah, R., Mir, B.A.: The freezing point of soils and the factors affecting its depression, in: Loon, L.Y., Subramaniyan, M., Gunasekaran, K. (eds): Advances in Construction Management, Lecture Notes in Civil Engineering, vol. 191, Springer, Singapore, 2022, https://doi.org/10.1007/978-981-16-5839-6_14

[45] Mo, C., Hanbing, C., Anyu, L.: Effect of freezing temperature and initial water content on hydrothermal migration of silty soil under freezing, Arabian Journal of Geosciences, 15 (2022) 2, https://doi.org/10.1007/s12517-022-09486-5

[46] Pennisi, S.V., Habteselassie, M.Y.: Laboratory-scale study on the effects of freezing in soils when subjected to different moisture content, Water, 14 (2022), 1892, https://doi.org/10.3390/w14121892

[47] Zhang, L., Yang, C., Wang, D., Zhang, P., Zhang, Y.: Freezing point depression of soil water depending on its non-uniform nature in pore water pressure, Geoderma, 412 (2022), 115724, https://doi.org/10.1016/j.geoderma.2022.115724

[48] Frost, J.D., De Jong, J.T., Recalde, M.: Shear failure behaviour of granular-continuum interfaces, Engineering Fracture Mechanics, 69 (2002), pp. 2029-2048

[49] Gómez, J.E., Filz, G.M., Ebeling, R.M., Dove, J.E.: Sand to concrete interface response to complex load paths in a large displacement shear box, Geotechnical Testing Journal, 31 (2008) 4, pp. 358-369

[50] Martinez, A., Frost, J.D.: The influence of surface roughness form on the strength of sand-structure interfaces, Géotechnique Letters, 7 (2017) 1, pp. 104-111

[51] Di Donna, A., Ferrari, A., Laloui, L.: Experimental investigations of the soil-concrete interface: physical mechanisms, cyclic mobilization, and behaviour at different temperatures, Canadian Geotechnical Journal, 53 (2015) 4, pp. 659-672

[52] Meier, A.L., Faro, V.P., Odebrecht, E.: Shear strength analysis of interfaces between granular soils and concrete cured under stress, Soils and Rocks, 46 (2023) 1, e2023004022

[53] Chang, W.R.: The effect of surface roughness on dynamic friction between neolite and quarry tile, Safety Science, 29 (1998) 2, pp. 89-105

[54] Tehrani, F.S., Han, F., Salgado, R., Prezzi, M., Tovar, R.D., Castro, A.G.: Effect of surface roughness on the shaft resistance of nondisplacement piles embedded in sand, Géotechnique, 66 (2016) 5, pp. 386-400, https://doi.org/10.1680/jgeot.15.P.007

[55] Nardelli, A., Cacciari, P.P., Futai, M.M.: Sand-concrete interface response: The role of surface texture and confinement conditions, Soils and Foundations, 59 (2019) 6, pp. 1675-1694, https://doi.org/10.1016/j.sandf.2019.10.004

[56] Uesugi, M., Kishida, H.: Influential factors of friction between steel and dry sands, Soils and Foundations, 26 (1986) 2, pp. 33-45, https://doi.org/10.3208/sandf1972.26.2_33

[57] Gokhale, M., Underwood, E.E.: A general method for estimation of fracture surface roughness, 1990

[58] ISO 25178-601: Geometrical product specifications (GPS) - Surface texture: Areal - Part 601: Nominal characteristics of contact (stylus) instruments, ISO, 2010

[59] Lemos, L.J.L., Vaughan, P.R.: Clay-interface shear resistance, Géotechnique, 50 (2000) 1, pp. 55-64

[60] Murphy, K.D., McCartney, J.S.: Thermal borehole shear device, Geotechnical Testing Journal, 37 (2014) 6, 20140009, https://doi.org/10.1520/GTJ20140009

[61] American Society for Testing and Materials (ASTM): ASTM D3080/D3080M-22: Standard Test Method for Direct Shear Test of Soils Under Consolidated Drained Conditions, ASTM International, West Conshohocken, PA, USA, 2022

[62] Kou, H., Huang, J., Cheng, Y.: Friction characteristics between marine clay and construction materials, Journal of Ocean University of China, 23 (2024), pp. 427-437, https://doi.org/10.1007/s11802-024-5474-7

[63] Wang, B., Liu, J., Wang, Q., Ling, X., Pan, J., Fang, R., Bai, Z.: Influence of freeze-thaw cycles on the shear performance of silty clay-concrete interface, Cold Regions Science and Technology, 219 (2024), 104120

[64] He, P., Cao, H., Dong, J., Hou, G., Mu, Y., Zhang, J.: Effects of wet-dry-freeze-thaw cycles on the response of the frozen soil-composite geotextile interface in direct shear tests, Case Studies in Thermal Engineering, 63 (2024), 105217, https://doi.org/10.1016/j.csite.2024.105217

[65] Meng, Y., Xu, C., Yang, Y., Du, C., Jia, B., Zhao, C.: Study on the mechanism of freeze-thaw cycles on the shear strength of geogrid-sand interface, Cold Regions Science and Technology, 225 (2024), 104275, https://doi.org/10.1016/j.coldregions.2024.104275

[66] Zhang, K., Yan, J., Mu, Y., Zhu, X., Zhang, L.: Global and local shear behaviour of the frozen soil-concrete interface: Effects of temperature, water content, normal stress, and shear rate, Buildings, 14 (2024) 10, 3319, https://doi.org/10.3390/buildings14103319

[67] Bouyoucos, G.J.: The freezing point method as a new means of measuring the concentration of the soil solution directly in the soil, Michigan Agricultural College Experiment Station Technical Bulletin, 24 (1916), pp. 1-44

[68] Nersesova, Z.A., Tsytovich, A.: Unfrozen water in frozen soils, in: Proceedings of the 1st International Permafrost Conference, Purdue University, Lafayette, Indiana, 1963, pp. 230-234

[69] Konrad, J.M.: Unfrozen water as a function of void ratio in a clayey silt, Cold Regions Science and Technology, 18 (1990), pp. 49-55, https://doi.org/10.1016/0165-232X(90)90037-W

[70] Christ, M., Kim, Y.C.: Experimental study on the physical-mechanical properties of frozen silt, KSCE Journal of Civil Engineering, 13 (2009) 5, pp. 317-324, https://doi.org/10.1007/s12205-009-0317-z

[71] Andersland, O.B., Ladanyi, B.: An Introduction to Frozen Ground Engineering, ASCE & John Wiley & Sons, New York, 1994

[72] Williams, P.J., Smith, M.W.: The Frozen Earth: Fundamentals of Geocryology, Cambridge University Press, Cambridge, 1989, 306 pp.

[73] Ladanyi, B.: Frozen soil-structure interfaces, in: Selvadurai, A.P.S., Boulon, M.J. (eds): Studies in Applied Mechanics, vol. 42, Elsevier, 1995, pp. 3-33, https://doi.org/10.1016/S0922-5382(06)80004-8

[74] Goughnour, R.R., Andersland, O.B.: Mechanical properties of a sand-ice system, Proceedings of the American Society of Civil Engineers, 94 (1968) SM4, pp. 923-950

[75] Shi, Q., Yang, P., Wang, G.: Experimental study on adfreezing strength of the interface between artificial frozen sand and structure, Chinese Journal of Rock Mechanics and Engineering, 35 (2016) 10, pp. 2142-2151

[76] Wen, Z., Yu, Q., Ma, W. et al.: Experimental investigation on the effect of fiberglass reinforced plastic cover on adfreeze bond strength, Cold Regions Science and Technology, 131 (2016), pp. 108-115, https://doi.org/10.1016/j.coldregions.2016.07.009

[77] Xu, X.T., Dong, Y.H., Fan, C.: Laboratory investigation on energy dissipation and damage characteristics of frozen loess during deformation process, Cold Regions Science and Technology, 109 (2015), pp. 1-8, https://doi.org/10.1016/j.coldregions.2014.09.006

[78] Zhu, Z., Liu, Z., Xie, Q.: Dynamic mechanical experiments and microstructure constitutive model of frozen soil with different particle sizes, International Journal of Damage Mechanics, 26 (2017), 105678951770096, https://doi.org/10.1177/1056789517700967

[79] Parameswaran, V.R.: Adfreeze strength of frozen sand to model piles, Canadian Geotechnical Journal, 15 (1978), pp. 494-500

[80] Wang, W., Yang, X., Huang, S., Yin, D., Liu, G.: Experimental study on the shear behaviour of the bonding interface between sandstone and cement mortar under freeze-thaw, Rock Mechanics and Rock Engineering, 53 (2020), pp. 881-907, https://doi.org/10.1007/s00603-019-01951-0

[81] Sadovskiy, A.V.: Adfreeze between ground and foundation materials, in: Proceedings of the 2nd International Conference on Permafrost, Yakutsk, Northern American Volume, 1973, pp. 650-653

[82] Ladanyi, B., Theriault, A.: A study of some factors affecting the adfreeze bond of piles in permafrost, in: Proceedings of the Geotechnical Engineering Congress GSP 27 ASCE, vol. 1, 1990, pp. 213-224

ING-GRAD

Energija koja pokreće budućnost.

više od 330
MW obnovljive energije

više od 50
energetski i infrastrukturnih projekata

Primljen / Received: 12.10.2023.
Ispravljen / Corrected: 3.12.2025.
Prihvaćen / Accepted: 22.5.2026.
Dostupno online / Available online: 10.6.2026.

Eksperimentalno ispitivanje meke stijene po diskontinuitetimu u uvjetima ovisnim o vremenu

Autori:

Mr.sc. **Miodrag Bujišić**, dipl.ing.građ.
Sveučilište Crne Gore , Crna Gora
Građevinski fakultet
miodragb@ucg.ac.me
Autor za korespondenciju

Prof.dr.sc. **Zvonko Tomanović**, dipl.ing.građ.
GeoT d.o.o Podgorica, Crna Gora
zvonko@geot.me

Prethodno priopćenje

Miodrag Bujišić, Zvonko Tomanović

Eksperimentalno ispitivanje meke stijene po diskontinuitetimu u uvjetima ovisnim o vremenu

U okviru eksperimentalnih istraživanja posmične otpornosti po diskontinuitetu pri o vremenu ovisnim uvjetima provedeni su pokusi na tri uzorka meke stijene, laporovitoga vapnenca koja su uzorkovana iz otvorenoga bazena u Pljevljima. Uzorci su istih geometrijskih karakteristika, pravilnoga prizmatičnog oblika, pri čemu je na svakom oblikovana umjetna pukotina, koju odlikuju različite hrapavosti ploha diskontinuiteta (glatka, valovita i umjereno hrapava). Uzorci su ispitivani u laboratorijskim uvjetima, pri čemu je postojeća oprema modificirana i izrađen je dio nove opreme da bi se izveo primjeren eksperiment. Imajući u vidu skroman broj eksperimentalnih istraživanja vremenski ovisnih deformacija mekih stijena po diskontinuitetu (na globalnoj razini) ovim se radomželi dati znanstveni doprinos i prikazati prvi rezultati analizom podataka dobivenih konkretnim eksperimentalnim istraživanjem.

Ključne riječi:
meka stijena, vremenski ovisne deformacije, eksperiment, diskontinuitet, hrapavost

Research Paper

Miodrag Bujišić, Zvonko Tomanović

Experimental investigation of time-dependent deformation of soft rock along discontinuities

This study presents an experimental investigation of the time-dependent shear behaviour of soft rock discontinuities. Three marly limestone specimens obtained from the Pljevlja coal basin were tested under controlled laboratory conditions. The specimens had identical geometric characteristics but differed in discontinuity surface roughness (smooth, undulating and moderately rough). A dedicated experimental apparatus was designed and adapted to perform long-term shear tests under constant normal loading and incremental shear loading. The results demonstrate the significant influence of discontinuity roughness on shear resistance, displacement development and test duration. Given the limited number of published studies addressing time-dependent deformation of soft-rock discontinuities, the presented pilot investigation provides valuable insight into the governing mechanisms and establishes a basis for a comprehensive experimental programme.

Key words:
soft rock, time-dependent deformations, experiment, discontinuity, roughness

1. Uvod

U radu su analizirani rezultati probnih ispitivanja koja čine dio šireg eksperimentalnog istraživanja u okviru znanstvenoga projekta autora ovoga rada. Eksperimentalni dio znanstvenoga projekta čine dvije cjeline, i to: inicijalno (probno) ispitivanje i glavno ispitivanje. Predmet je ovoga rada analiza rezultata probnoga ispitivanja za potrebe definiranja opsega fizičko-mehaničkih parametara i razina opterećenja uzoraka i definiranje najrelevantnijih parametara za glavne nizove eksperimentalnih ispitivanja. Cilj je znanstvenoga projekta eksperimentalnim istraživanjima unaprijediti spoznaje o ponašanjima mekih stijenskih masa. U sljedećim koracima istraživanja u okviru doktorske disertacije želja je da se da znanstveni doprinos u pogledu dobivanja materijalnih karakteristika vremenski ovisnoga ponašanja stijenske mase za uzorke jednostavnoga geometrijskog oblika uz doprinos u pogledu izučavanja fenomena utjecaja diskontinuiteta na dobivanje spomenutih parametara. Plan je da se takvo ispitivanje provede u kontroliranim laboratorijskim uvjetima, pri konstantnom normalnom opterećenju, uz prirast posmičnih naprezanja i mjerenje deformacija, na uzorcima s diskontinuitetom, dimenzija 30 x 15 x15 cm. Važno je naglasiti da se u ovom radu prikazuju rezultati probne faze ispitivanja, osnovni cilj koje nije bilo konačno definiranje reprezentativnih parametara posmične čvrstoće diskontinuiteta, već provjera funkcionalnosti posebno razvijene eksperimentalne aparure, određivanje opsega opterećenja i sagledavanje osnovnih mehanizama vremenski ovisnoga smicanja po umjetno oblikovanom diskontinuitetu. Dobiveni su rezultati osnova za definiranje glavnoga eksperimentalnog niza koji podrazumijeva veći broj uzoraka, kontroliraniji režim opterećivanja i detaljniju analizu mehaničkih i geometrijskih karakteristika diskontinuiteta.

2. Pregled dosadašnjih istraživanja

Pregledom dosadašnjih istraživanja može se konstatirati da je razmjerno mali broj znanstvenika eksperimentalno proučavao učinke utjecaja dugotrajnoga opterećenja i rasterećenja na vremenski ovisne deformacije mekih stijena. Vremenski ovisne deformacije stijenske mase pod djelovanjem konstantnoga naprezanja nazivaju se puzanjem. Puzanje je ovisno o promjeni stanja naprezanja, temperature, vlažnosti, vlage u zraku itd.

Za čvrste (metamorfne i magmatske) stijenske mase deformacija je puzanja zanemariva u pogledu opsega naprezanja i temperatura za realne građevinske situacije, dok je doprinos deformacije puzanja u ukupnoj vrijednosti deformacije vrlo značajan kod mekih stijenskih masa kao što su kamena sol, laporac, anhidrit, flišni sedimenti itd. Ispitivanjima je pokazano da se deformacija puzanja odvija različitom brzinom i definiraju je tri karakteristične faze: primarna, sekundarna i tercijarna.

Većina do sada objavljenih eksperimentalnih istraživanja u svijetu vezanih za ponašanja stijene u uvjetima dugotrajnoga opterećenja pri sobnim temperaturama provedena je na uzorcima kamene soli (Gimm, 1968; Dreyer, 1974; Baar, 1977; Carter et al., 1982; Wallner, 1983; Hunche, 1994, 1995; prikazano u Cristescu N.D & Hunsche U, 1998; itd.). Neusporedivo je manji broj publiciranih eksperimentalnih istraživanja proveden pri sobnim temperaturama na laporcu ili sličnim mekim stijenama koje karakteriziraju znatne deformacije puzanja (glinoviti laporac, Cristescu, 1988; laporac, Kharchafi i Descoeudres, 1995) i koje surealna radna sredina pri izgradnji brojnih podzemnih objekata. U okviru ispitivanja laporovitih materijala mogu se izdvojiti radovi autora iz Crne Gore [1-8].

Kada je riječ o ispitivanjima uzoraka mekih stijenskih masa prožetih diskontinuitetima broj radova je još manji. Za definiranje vremenski ovisnoga ponašanja stijenske mase u početnim koracima proučavanja ove problematike primijenjen je teorijski pristup koji nije dao zadovoljavajuće rezultate [2].

Razvojem računalnih programa usavršavali su se numerički modeli, pa je postalo moguće modelirati složene reološke situacije koje su omogućavale bolje sagledavanje vremenski ovisnoga ponašanja stijenske mase. Određivanje materijalnih parametara i konstanata koji opisuju reološke modele ponašanja stijenske mase općenito se provodi laboratorijski ili ispitivanjima na terenu. Problem je određivanja materijalnih karakteristika posljedica složenosti građe stijenskoga materijala, ali i diskontinuiteta koji izgrađuju i karakteriziraju stijensku masu. U pogledu određivanja karakteristika diskontinuiranih stijenskih masa naročito je važno definiranje opsega hrapavosti posmične plohe diskontinuiteta. Osim standardnih, tradicionalnih metoda opisivanja hrapavosti kvalitativnim i kvantitativnim karakteristikama posljednjih godina, uz tehnološki napredak softverskih alata, moguće je izvršiti definiranje određenih matematičkih zakonitosti koje povezuju posmičnu otpornost diskontinuiteta i hrapavost plohe diskontinuiteta. U tom se pogledu mogu spomenuti radovi [14-17].

Dosadašnja ispitivanja radi formiranja modela kojima će se prikazati vremenski ovisno ponašanje stijenskih masa utemeljena su na analizi monolitnih uzoraka jednostavnih geometrijskih karakteristika i razmjerno jednostavnoga stanja naprezanja. Međutim, uobičajeno je da se tim jednostavnim testovima sa zadovoljavajućom točnošću prikazuje ponašanje znatno složenijega stanja naprezanja I deformacija realne stijenske mase.

3. Eksperimentalno ispitivanje

3.1. Priprema uzoraka i opreme

Materijal za ispitivanje uzorkovan je iz površinskoga kopa Potrlica, rudnika ugljena u Pljevljima. Izvađen je blok veličine oko 3,5 tone, iz dubine od oko 45 m mjereno od površine terena (slika 1.). Materijal je pomoću mehanizacije odmah nakon iskopa utovaren i prevezen iz Pljevalja u Podgoricu (oko 180 km). Prilikom istovara uzorka vodilo se računa da ne dođe do oštećenja stijenske mase, o prirodnoj orijentaciji bloka, pa je ona u neizmijenjenoj geometriji pripremljena za obradu.

Slika 1. a) položaj stepenika iz koga se vadio blok stijene; b) utovar bloka stijenske mase

Slika 2. Uzorci obrađeni do željenih dimenzija 30 x 15 x15 cm

Slika 3. Ispitivanje jednoosne čvrstoće uzoraka

U specijaliziranom postrojenju za obradu kamena izvedena je obrada do formiranja uzoraka oblika kvadra (prizme) dimenzija 30 x 15 x 15 cm (slika 2.). Prilikom oblikovanja uzoraka, zbog vrlo zahtjevne obrade (pucanja prilikom rezanja) meke stijenske mase iz sirovoga (nepravilnog komada stijene) u željeni oblik uzorka, uspješnost obrade iznosila je oko 50 %.

Usporedno je urađena semikvantitativna analiza uzoraka i ustanovljeno je da je riječ o laporovitom vapnencu s dominantnim sudjelovanjem kalcijeva karbonata ($CaCO_3$) od 93,0 %, pri čemu je postotni sadržaj ostalih elemenata (u ukupnom dijelu od 7 %) sljedeći: kvarc 4,80 % (SiO_2), siderit 1,10 % ($FeCO_2$), muskovit 1,10 % ($KAl_3Si_3O_{10}OH_2$).

Za uzorkovani materijal izvršeno je ispitivanje jednoosne tlačne čvrstoće (slika 3.), za različite vlažnosti (od vodozasićenoga do potpuno suhoga uzorka), pri čemu su vrijednosti dobivene za materijal u stanju prirodne vlažnosti dane u tablici 1. U tablici su uzorci označeni s U_1 do U_5. Masa prazne posude označena je s m_p, dok je masa posude s uzorkom u stanju prirodne vlažnosti označena s m_1, a masa posude s osušenim uzorkom s m_2. Jednoosna je čvrstoća označena sa σ_c.

Na svim uzorcima koji su predviđeni za ispitivanje u probnom (a kasnije i u glavnom dijelu eksperimenta), oblikovana je umjetna pukotina (slika 4.). Oblikovanje pukotine je kontrolirano usijecanjem (cijepanjem) uzoraka u duljini od 1 cm na polovini visine (na približno 7,5 cm). Na usječenim žlijebovima uzorci su pod presom (slika 4.c), nanošenjem opterećenja pri kontroliranoj brzini dijeljeni na dvije približno jednake polovine, pri čemu su se oblikovale plohe diskontinuiteta različitih neravnina (slika 5.b).

Tablica 1. Jednoosna čvrstoća na cilindričnim uzorcima 12 x 5 cm

Stanje uzoraka	Uzorci (U1-U5)→	U_1	U_2	U_3	U_4	U_5	W_{sr}, σ_{csr}
Cilindrični uzorci u stanju prirodne vlažnosti, formirani od uzoraka kvadra (prizme) koji su čuvani na dnevnoj temperaturi, parafinirani, umotani u foliju	m_p [g]	4,9	4	5,3	5,4	4	Legenda: U_1-U_5→ uzorci, m_p→ Masa prazne posude, m_1→ masa posude s uzorkom u stanju prirodne vlažnosti, m_2→ masa posude s osušenim uzorkom
	m_1 [g]	41,7	36,7	49,7	36	43,9	
	m_2 [g]	37,4	33,2	45,6	32,7	40	
	m_1-m_2 [g]	4,3	3,5	4,1	3,3	3,9	
	m_2-m_p [g]	32,5	29,2	40,3	27,3	36	
	W [%]	13,2 %	11,9 %	10,1 %	12,1 %	10,8 %	W_{sr} = 11,66 %
	σ_c [MPa]	18,14	17,98	17,11	16,28	17,02	σ_{csr} = 17,31

Slika 4. a) Oblikanje žlijeba na sredini uzorka; b) oblikovani žlijeb dubine 1 cm; c) oblikovanje diskontinuiteta

Svi uzorci su nakon definiranja ploha diskontinuiteta umotani u foliju. Prethodno su nakon oblikovanja geometrije svi uzorci parafinirani radi zadržavanja vlažnosti u prirodnom stanju.

Nakon pripreme uzoraka pristupilo se izradi nove i modifikaciji postojeće opreme koja je korištena za jednoosni i troosno ispitivanje puzanja neporemećenih uzoraka stijene. U okviru probnoga niza planirano je ispitivanje tri uzorka različite hrapavosti, pa je za te potrebe u potpunosti pripremljen jedan postojeći okvir u laboratoriji Građevinskog fakulteta. Okvir za ispitivanje datira iz vremena ispitivanja laporovitog materijala uzorkovanog s iste lokacije za potrebe istraživanja prof. dr. Zvonka Tomanoviča, koje je rađeno prije 20-ak godina. Okviri djeluju na načeku poluge i "mrtvoga" opterećenja. Aparatura je centrirana u pogledu položaja uzorka u kojoj će se provoditi eksperiment, a u skladu s potrebama razine opterećivanja normalnom silom. Da bi se moglo provesti ispitivanje uzoraka po oblikovanim posmičnim plohama napravljeni su čelični kalupi u koje će se postaviti uzorci (slika 5.a).

S obzirom na to da su visine polovina uzoraka približno 7,5 cm, unutarnja je visina kalupa 5 cm kako bi se osiguralo nesmetano smicanje po plohama diskontinuiteta. Debljina zidova i dna čeličnoga kalupa iznosi 1 cm.

Učvršćivanje uzoraka izvedeno je pomoću tvornički proizvedenoga morta za zalijevanje i podlijevanje koji nakon popunjavanja zazora između uzorka i kalupa očvrsne u roku od nekoliko sati i čini uzorak nepomičnim u kalupu. Prilikom učvršćivanja obje polovine uzorka vodilo se računa da one u potpunosti naliježu jedna na drugu radi postizanja što bolje simulacije prirodno stisnutih pukotina .

Radi svladavanja trenja koje se javlja u aparaturi prilikom eksperimenta predviđeno je nalijeganje pokretnih dijelova preko cilindričnih čeličnih elementa koji će biti detaljnije opisani u nastavku teksta u dijelu 3.

Osim uzoraka, okvira, kalupa i valjaka neophodan su dio opreme i elementi za mjerenje promjene naprezanja i deformacija. Za te potrebe konstruirani su čelični prstenasti elementi (dinamometri) s postoljima na kojima su postavljeni uređaji za mjerenje promjena normalnih i posmičnih pomaka.

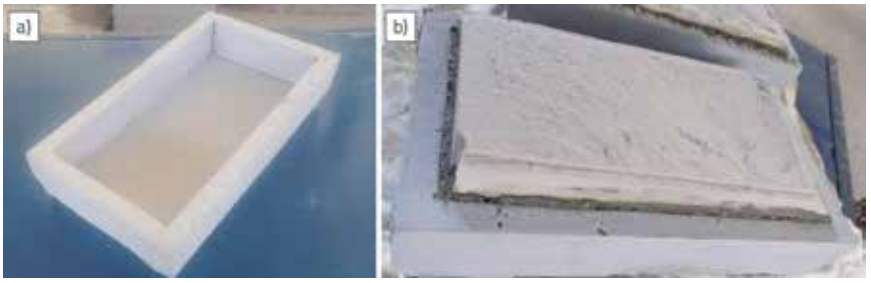

Slika 5. a) Čelični kalup; b) Polovina uzorka postavljena u kalup

Slika 6. a) Prsteni s mjeračima za normalna naprezanja; b) Debljina prstenova 1, 2 i 3 je d = 2,0 cm

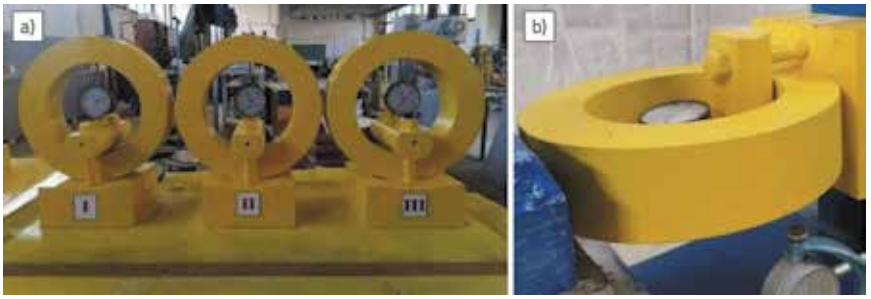

Slika 7. a) Prsteni s mjeračima za posmična naprezanja; b) Debljina prstenova I, II i III je d = 6,0 cm

Čelični prstenovi su istog promjera, ali različite debljine zbog različitoga reda veličine (sila) koji se javljaju u normalnom, odnosno posmičnom smjeru, a koje treba mjeriti dinamometrima (slike 6. i 7.).
Nakon oblikovanja svih pojedinačnih dijelova opreme, pripreme uzoraka i stavljanja u funkciju okvira za ispitivanje stvoreni su uvjeti za početak pokusa.

3.2. Ispitivanje uzoraka

Probno eksperimentalno ispitivanje urađeno je u jednom okviru (slika 8.). U okviru pokusa ispitivana su tri uzorka različitih hrapavosti: 1) potpuno glatka ravnina diskontinuiteta, 2) izrazito valovit diskontinuitet, 3) umjereno hrapava ravnina diskontinuiteta. Za sve tri spomenute ravnine diskontinuiteta ispitivanje je izvedeno za tri različite konstantne razinenormalnih naprezanja. Normalna naprezanja su nanesena u vrijednostima od 0,1 MPa, 0,2 MPa i 0,4 MPa. Ograničenost probnoga niza ogleda se u tome što se u okviru ispitivanja jednoga uzorka za svako sljedeće naneseno vertikalno opterećenje smicanje odvijalo po plohi uzorka koja je u određenoj mjeri izmijenjena zbog smicanja za prethodnu (manju) razinu normalnoga naprezanja. Vertikalno opterećenje nanošeno je sustavom poluge i "mrtvoga tereta". Međutim, relevantnost takvih ispitivanja proizlazi iz načina i redoslijeda odvijanja pokusa. Naime, kako su uzorci u prvoj fazi opterećivani normalnim naprezanjem od 0,1 MPa, a zatim s 0,2 MPa u drugoj fazi, vodilo se računa da se nakon svake faze izvrši pregled ispitanih uzoraka, odnosno da se ustanovi degradiranost ispitivane posmične plohe. S obzirom na to da se u prve dvije faze nije dešavalo da dođe do sloma ili do znatne promjene oblika neravnine diskontinuiteta (promjena se ogledala u obliku površinskih tragova zbog trenja), ustanovljeno je da je ploha diskontuiteta gotovo neporemećena i prikladna za treću fazu ispitivanja.
Treba naglasiti da je eksperimentalna aparatura upotrijebljena u ovom istraživanju posebno razvijen laboratorijski sustav prilagođen dugotrajnim vremenski ovisnim ispitivanjima smicanja po diskontinuitetu. Zbog specifičnosti aparature i velikih dimenzija uzoraka postupak ispitivanja nije u potpunosti odgovarao standardnim ISRM procedurama direktnoga smicanja.
U okviru probne faze istraživanja ispitivanja su provedena uporabom jednoga okvira za smicanje, pri čemu su tri uzorka različitih karakteristika diskontinuiteta uzastopno ispitivana pri normalnim naprezanjima od 0,1 MPa, 0,2 MPa i 0,4 MPa. Nakon završetka pojedinačne faze smicanja uzorak je vraćan u početni položaj, nakon čega je provođeno sljedeće ispitivanje pri većem normalnom naprezanju.
Autori su svjesni da ovakav postupak, naročito kod mekih stijenskih materijala, može dovesti do djelomične degradacije kontaktnih ploha i promjene lokalne kontaktne strukture zbog prethodnoga smicanja. Zbog tog razloga rezultati prikazani u ovom radu imaju preliminarni karakter i ponajprije su korišteni za provjeru funkcionalnosti eksperimentalne aparature, sagledavanje dominantnih mehanizama ponašanja diskontinuiteta i definiranje metodologije glavnoga eksperimentalnog programa.
Glavni eksperimentalni program planiran je uporabom sva tri okvira za smicanje istodobno, pri čemu bi svaki okvir bio opterećen različitom konstantnom razinom normalnoga naprezanja. Na taj bi se način izbjeglo ponovno smicanje istoga diskontinuiteta pri različitim normalnim naprezanjima, što je jedno od glavnih metodoloških ograničenja probne faze istraživanja.
Radi osiguravanja translacijskoga smicanja i ograničavanja neželjenih pomaka i rotacija na gornji su kalup ugrađeni čelični graničnici koji su omogućavali kontrolirano vođenje donjega kalupa tijekom posmičnoga pomicanja. Iako aparatura nije sadržala klasične kuglaste oslonce karakteristične za standardne uređaje direktnoga smicanja, omogućila je stabilan prijenos opterećenja i registriranje dominantnih deformacijskih procesa tijekom eksperimenta.
Horizontalno opterećenje na uzorak naneseno je pomoću velike hidraulične preše postavljene vertikalno u dodatni okvir s "mrtvim" opterećenjem. Željeni pritisak u ulju preše kontroliran je težinom "mrtvoga" tereta na poluzi okvira koja prenosi umnoženo opterećenje "mrtvoga" tereta na klip preše. Na taj je način omogućeno kontrolirano generiranje hidrauličnoga pritiska, koji se dalje prenosio na sustav za smicanje. Sustavom dovođenja ulja iz velike preše (principom spojenih posuda) u sve manje preše na aparaturi za smicanje nanesena je posmična sila na donju polovinu uzorka (na donji kalup koji je pomičan), kako je prikazano na slici 8.

Slika 8. Izgled aparature tijekom trajanja pokusa (vidljivo je smicanje gornje i donje polovine uzorka)

U pokusu nije mjerena masa opterećenja koje se dodaje, već su mjerene vrijednosti horizontalnih sila na uzorku, odnosno posmičnih naprezanja i pomaka. Naime, prilikom dodavanja tereta vodilo se računa da opterećivanjem dođe do pomicanja zbog prirasta posmičnih naprezanja. Iako se opterećenje kojim se izazivalo posmično naprezanje i pomicanja nije brojčano

verificiralo, vođeno je računa da prirasti opterećivanja budu približni. Opterećivanje se vršilo dodavanje betonskih cilindara promjera osnovice 15 cm i visine 30 cm (približno 13 kg), što je približno nakon umnažanja polugama okvira 16 kN/m^2. Opterećivanje se izvodilo dodavanjem jednoga ili dva spomenuta elementa u ovisnosti od vertikalnog opterećenja, odnosno do pokretanja donjega kalupa s uzorkom. Posmično opterećenje nanošeno je dodavanjem spomenutoga tereta u košarama na kraju poluge po sistemu pokretanja ulja iz preše s velikim klipom k prešama s manjim klipovima, kao što je prije objašnjeno.

Svako naredno opterećivanje izvedeno je nakon potpunoga zaustavljanja pomicanja donjega kalupa, do postizanja krajnjega pomaka od 5 cm. S obzirom na duljinu uzorka od 30 cm ustanovljeno je da nakon pomicanja od 5 cm donji kalup osim translacijskoga gibanja počinje "doživljavati" deformaciju rotacije, što nije u skladu s planovima i pretpostavkama pokusa. Veličina pomaka donjeg kalupa tj. diferencijalno pomicanje donjega i gornjega dijela uzorka po diskontinuitetu očitava se na mehaničkom uređaju za mjerenje pomaka (slika 8.).

Kao što je prethodno rečeno, donji kalup i prsten na koji se nanosi vertikalno opterećenje postavljeni su na valjcima kako bi se eliminiralo trenje tijekom trajanja pokusa. Tijekom ispitivanja neophodno je održavanje konstantnosti vertikalnoga opterećenja koje teži promjeni zbog vertikalnih pomaka po neravninama i promjene posmičnih naprezanja i deformacija.

Iz tog je razloga u sklopu ispitivanja glavnoga niza planirano da se oprema upotpuni optičkim kamerama na svim okvirima, koje će 24 sata pratiti ispitivanje. Na početku probnoga niza ustanovljeno je da klip hidraulične preše potpuno izlazi u duljini od 5 cm, pa je ta dužina definirana i kao krajnji pomak uzoraka. Radi sagledavanja i spoznaje pokusa u prvim iteracijama, na uzorku koji nije dio probnoga niza, ustanovljeno je da se na pomaku od približno 7 do 8 cm donja polovina kalupa počinje rotirati oko kraće osi, pa bi pokus koji se provodi izgubio smisao pri takvom stanju aparature. Planiranih, krajnjih 5 cm pomaka približno je 17 % ukupne duljine uzorka (slika 9.).

U okviru ispitivanja probnoga niza uzoraka, u ovisnosti o nanesenom normalnom opterećenju i hrapavosti plohe diskontinuiteta, ovisilo je i trajanje pokusa. Trajanje izvođenja eksperimenta uvjetovalo je očitavanje dobivenih podataka u različitim vremenskim intervalima, u ovisnosti o konkretnom slučaju. Eksperimentalna aparatura upotrijebljena u ovom istraživanju posebno je razvijen laboratorijski sustav prilagođen dugotrajnim ispitivanjima smicanja po diskontinuitetu na uzorcima većih dimenzija. Zbog toga postupak ispitivanja nije u potpunosti odgovarao standardnim uređajima za direktno smicanje, kod kojih se često koriste kuglasti oslonci radi smanjenja utjecaja momenata i omogućavanja rotacija. U ovom probnom ispitivanju cilj je bio da se provjeri funkcionalnost razvijenoga sustava i da se identificiraju problemi koji se moraju uzeti u obzir u glavnom eksperimentalnom nizu.

4. Prikupljanje, obrada i analiza rezultata ispitivanja

U okviru probnoga niza uzoraka ispitana su tri uzorka različitih hrapavosti ploha diskontinuiteta. Za svaki uzorak provedeno je ispitivanje za tri različite konstantne vrijednosti normalnoga opterećenja: 0,1 MPa, 0,2 MPa i 0,4 MPa. Pri ispitivanju uzoraka za manje vrijednosti normalnih naprezanja izazvana su i manja posmična naprezanja, a vrijeme je ispitivanja bilo kraće. To je karakteristika svih ispitivanih uzoraka.

Otežano je i kompleksno održavanje normalne sile konstantnom, jer se zbog smicanja uzorka, tj. promjene posmičnih naprezanja i evidentnih volumetrijskih promjena prilikom smicanja kao i zbog trenja opreme okvira, javljalo stanovito smanjenje ili povećanje vrijednosti zadane normalne sile (kao posljedica težnje k vertikalnom pomicanju uzorka tijekom smicanja), pa se ona morala kontrolirati najviše nakon jednog sata, kako bi se korigirala sila i zadržala nazovi konstantna vrijednost normalnoga naprezanja.

Kod svih uzoraka ispitivanje je počinjalo od najmanjega (0,1 MPa) do najvećega normalnog naprezanja (0,4 MPa), kako bi se što je moguće manje oštetila, odnosno promijenila posmična ploha koja se ispituje. Kod glatkoga uzorka nije postojala bojazan od promjene hrapavosti posmične plohe, dok kod ostale dvije, hrapave površine, nije zabilježena značajnija promjena strukture ispitivane posmične plohe (slika 10.).

Prilikom smicanja na uzorku s glatkim diskontinuitetom vidljivi su tragovi pokusa (uglavnom u obliku plitkih stija na plohi klizanja), odnosno primjetni su tragovi po površini koji upućuju

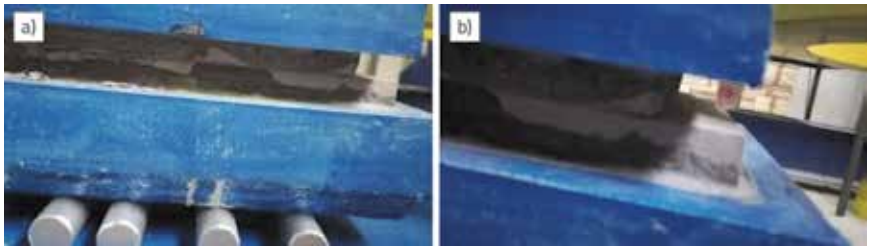

Slika 9. Pomicanje gornje (a) u odnosu na donju (b) polovinu uzorka po posmičnoj plohi

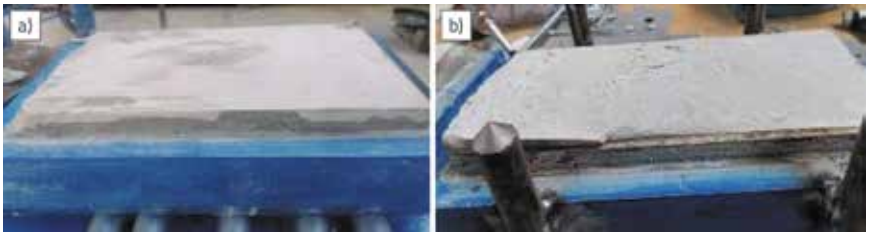

Slika 10. a) Izgled posmične plohe nakon pokusa kod glatkoga uzorka, b) Izgled posmične plohe nakon pokusa kod hrapavoga uzorka

na smicanje ploha, ali bez degradacije i formiranja izlomljenih struktura (slika 10.a).

Kod uzoraka s hrapavim površinama primjetne su okrnjene, slomljene mikrostrukture (dijelovi maloga reda veličine u odnosu na dimenzije uzorka) površine (slika 10.b), pri čemu treba naglasiti da je uzorak s izraženim valom (neravnina u velikoj mjeri) ostao neoštećen u pogledu postojanosti neravnine, dok su se i kod njega i u slučaju uzorka s umjerenom hrapavosti javila oštećenja, osipanje mikrostruktura plohe smicanja. Logično, s povećanjem normalnoga opterećenja, pri čemu se izazivaju i veća posmična naprezanja, povećava se i red veličine razlomljenosti površinske strukture smicanja.

Prilikom ispitivanja uzorka s glatkom plohom diskontinuiteta (S_1') zabilježene su sljedeće maksimalne vrijednosti posmičnih naprezanja za odgovarajuće normalno opterećenje:

σ_n = 0,1 MPa → τ = 0,54 MPa, σ_n = 0,2 MPa → τ = 1,68 MPa, σ_n = 0,4 MPa → τ = 2,46 MPa.

Za uzorak s izraženom neravninom (S_2') dobivene su sljedeće maksimalne vrijednosti posmičnih naprezanja:

σ_n = 0,1 MPa → τ = 3,9 MPa, σ_n = 0,2 MPa → τ = 4,92 MPa, σ_n = 0,4 MPa → τ = 6,72 MPa.

Za uzorak s umjerenom hrapavošću plohe diskontinuiteta (S_3') dobivene su sljedeće maksimalne vrijednosti posmičnih naprezanja:

σ_n = 0,1 MPa → τ = 3,24 MPa, σ_n = 0,2 MPa → τ = 2,70 MPa, σ_n = 0,4 MPa → τ = 4,86MPa.

Dobivene vrijednosti posmičnih naprezanja ne treba neposredno tumačiti kao klasične Mohr–Coulomb parametre neporemećenoga stijenskog materijala. Ispitivanje je provedeno po prethodno formiranim plohama diskontinuiteta, pri čemu je posmična otpornost rezultat kombiniranoga djelovanja trenja, uklještenja neravnina, lokalne dilatacije i djelomične degradacije mikrokontaktnih zona.

Kod diskontinuiteta s izraženim geometrijskim uklještenjem i valovito-nazubljenom kontaktnom plohom, pri razmjerno malim normalnim naprezanjima može doći do pojave visokih prividnih vrijednosti kuta posmične otpornosti i prividne kohezije. Takve su vrijednosti posljedica mehaničkog uklještenja, dilatacije i geometrijski uvjetovane otpornosti pri smicanju, a ne stvarne materijalne konstante neporemećene stijene.

Također, imajući u vidu da je u probnoj fazi isti uzorak ispitivan uzastopno pri više razina normalnoga naprezanja, uz vraćanje u početni položaj između pojedinih faza ispitivanja, moguće su djelomične promjene kontaktne strukture plohe diskontinuiteta. Zbog toga prikazane vrijednosti treba promatrati kao probne rezultate, namijenjene sagledavanju ponašanja sustava i pripremi glavnoga eksperimentalnog programa.

Dodatno, imajući u vidu visok sadržaj kalcijevogakarbonata u ispitivanom laporovitom vapnencu, nije isključena mogućnost da na kontaktnim zonama diskontinuiteta dolazi i do pojave lokalnoga privremenog povezivanja kontaktnih površina, što može dodatno utjecati na izazvanu posmičnu otpornost pri malim normalnim naprezanjima. Međutim, takav učinak u okviru ovoga rada nije posebno eksperimentalno analiziran i zahtijeva dodatna istraživanja.

U pogledu trajanja pokusa, uzorci s hrapavim plohama diskontinuiteta trajali su znatno dulje, i do dva mjeseca, dok je uzorak s glatkom plohom diskontinuiteta dostigao maksimalni pomak za nekoliko sati.

Radi boljeg sagledavanja dobivenih rezultata, a zbog preopširnoga prikazivanja svih dobivenih grafikona ovisnosti, u sljedećim će koracima biti prikazani grafikoni ovisnosti za ispitane uzorke zbog djelovanja maksimalnoga zadanog normalnog opterećenja od oko 0,4 MPa. Na slikama 1., 2. i 3. prikazane su promjene normalnoga i posmičnoga naprezanja i pomaci u ovisnosti o trajanju pokusa.

Dobiveni rezultati pokazuju da se vrijednosti maksimalnih pomaka dostižu u različitim vremenskim intervalima za različite uzorke. Kod uzorka s glatkom plohom diskontonuiteta maksimalni je pomak dostignut u roku od nekoliko sati. Kod uzoraka s hrapavom posmičnim plohom maksimalni se pomak dostiže u vremenskom intervalu mjerenom u danima. Iako je uzorak s izraženom neravninom ispitan u roku od skoro četiri dana, a uzorak s umjerenom hrapavošću u razdoblju od gotovo 65 dana, autori naglašavaju da se pokus kod uzorka S_3' odvijao tako što se svaki sljedeći prirast horizontalnoga opterećenja dodavao tek nakon potpunoga prestanka promjene vrijednosti naprezanja i pomaka.

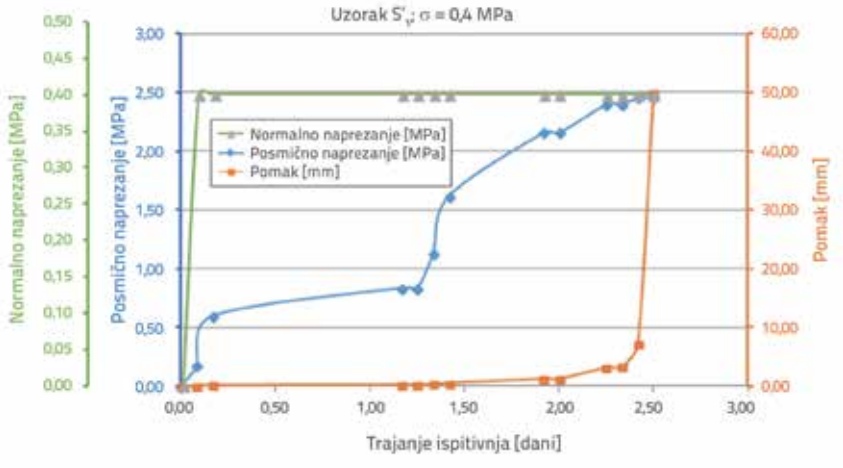

Slika 11. Promjena naprezanja i prirast pomaka u tijeku trajanja pokusa, uzorak S_1'

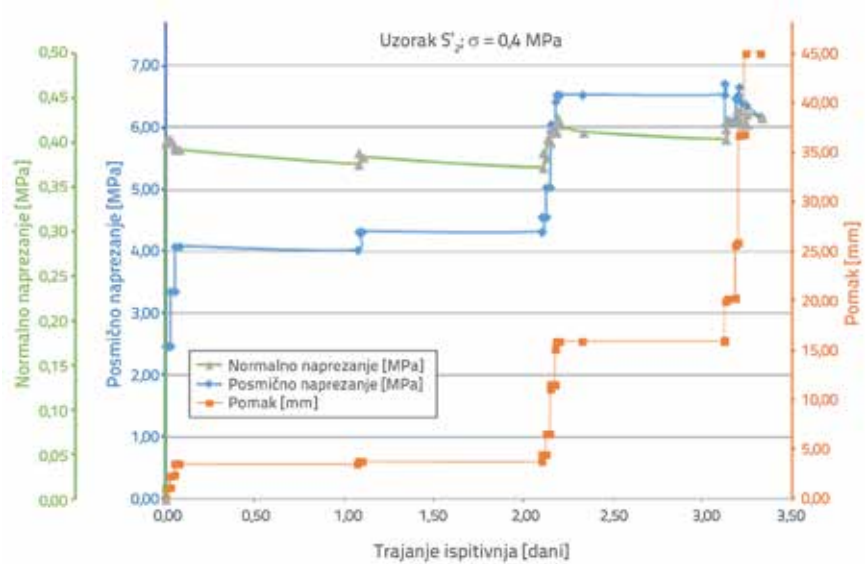

Slika 12. Promjena naprezanja i prirast pomaka u tijeku trajanja pokusa, uzorak S_2'

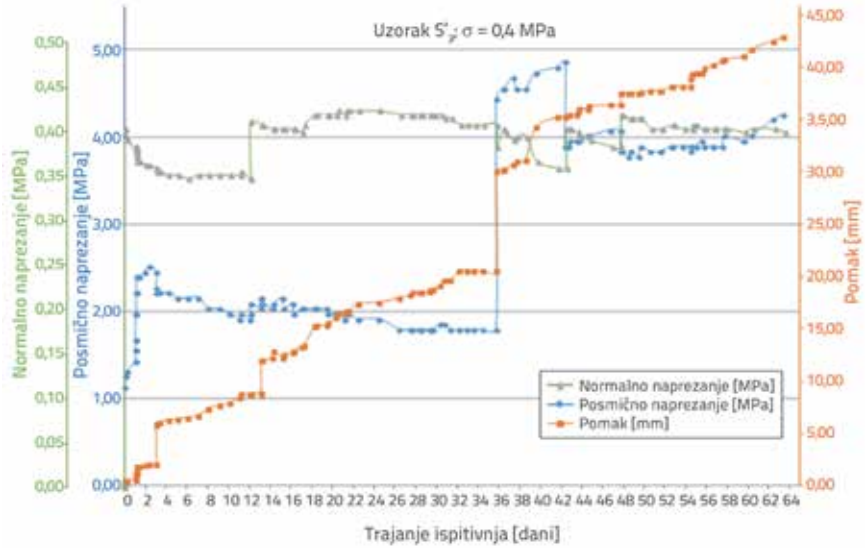

Slika 13. Promjena naprezanja i prirast pomaka u tijeku trajanja pokusa, uzorak S_3'

Za uzorak s izraženom neravninom (S_2') sljedeći je korak opterećivanja izveden nakon postizanja prirasta pomaka manjeg od 0,2 mm/danu. Različiti uvjeti ispitivanja (ponajprije odstupanje normalnih naprezanja od konstantne vrijednosti zbog praćenja posmičnoga ponašanja uzorka) izvedeni su s konkretnom namjerom da se sagledaju svi mogući uvjeti ispitivanja kako bi se u glavnom nizu eksperimenta, prilikom istodobnoga ispitivanja uzoraka u tri okvira, mogli kvalitetno i u statistički dovoljnom broju uzoraka prikupiti odgovarajući podaci s odgovarajućim rezultatima koji omogućavaju sagledavanje fenomenologije ponašanja diskontinuiteta meke stijene pri posmičnim silama-pomacima.

U ovom radu se iznose prvi rezultati testiranja na smicanje diskontinuiteta u mekoj stijeni s vremenski ovisnim učincima. Daljnjim ispitivanjima treba prikupiti dovoljan broj podataka koji mogu biti osnova za reološko modeliranje, a posebno uvođenje vremenski ovisnih deformacija kao parametra pri modeliranju ponašanja stijenske mase, kako matriksa stijene, tako i ponašanja diskontinuiteta.

5. Zaključak

Probnim ispitivanjem pokazalo se da je vrlo zahtjevno istraživanje u pogledu oblikovanja opreme, pripreme i obrade uzoraka urađeno na visokoj razini. Kvalitetna priprema ogleda se i u uspješno dobivenim rezultatima ispitivanja, ali i u minimalnom broju korektivnih aktivnosti koje se moraju uraditi prilikom ispitivanja glavnoga niza eksperimenta, kako na opremi tako i proceduri testiranja. Daljnji rezultati testova trebaju osigurati dovoljan broj podataka za oblikovanje reološkoga modela ponašanja smicanja po diskontinuitetu ispitivane meke stijene, obuhvaćajući kroz numeričku formulaciju i utjecaj hrapavosti ploha diskontinuiteta smicanja na posmičnu čvrstoću materijala i vremenski ovisne deformacije. Ispitivanje uzoraka pokazalo je da vremenski ovisna komponenta posmičnoga pomaka po diskontinuitetu sudjeluje u ukupnoj deformaciji u znatnom postotku, a kod uzorka S_3' i preko 50 %.

Posebno treba naglasiti da prikazani rezultati imaju preliminarni karakter. Probna ispitivanja provedena su radi provjere aparature, opsega opterećenja i osnovnih mehanizama smicanja po diskontinuitetu, a ne radi konačnoga određivanja reprezentativnih parametara posmične čvrstoće. Ponavljanje ispitivanja na istim uzorcima pri uzastopno većim normalnim naprezanjima metodološko je ograničenje probne faze, jer može dovesti do djelomične degradacije i promjene kontaktnih uvjeta uzduž plohe diskontinuiteta. To će ograničenje biti otklonjeno u glavnom nizu eksperimentalnih ispitivanja, provođenjem većega broja pokusa i kontroliranijim režimom opterećivanja.

S obzirom na relativno mali opseg istraživanja, globalno gledano, dosegnute spoznaje u okviru ovoga istraživanja imaju za cilj dati doprinos sagledavanju, spoznaji i izučavanju mekih stijenskih masa i fenomenologije smicanja po diskontinuitetu. Ujedno, opravdanost prethodnih istraživanja istoga materijala, sagledana kroz ustanovljeni doprinos u znanstvenim radovima autora Živaljević, S. & Tomanović, Z. na neporemećenoj stijeni, dokaz su da će rezultati ovih istraživanja ponašanja

diskontinuiteta biti značajan doprinos rasvjetljavanju ponašanja mekih (laporovitih) stijenskih masa prožetih pukotinama i formiranju realnijih reoloških modela.

Zahvala

Autori rada izražavaju zahvalnost zbog financijske I druge pomoći tijekom istraživanja: Fondu za inovacije Crne Gore, koji je prepoznao značaj ovoga istraživanja i dodijelio financijsku potporu prijavljenom timu kojega su činili GeoT d.o.o iz Podgorice i Građevinski fakultet Univerziteta Crne Gore. Rukovodstvu Rudnika uglja A.D. Pljevlja na stručnoj, financijskoj i tehničkoj pomoći prilikom iskopa, utovara i transporta laporovitog materijala. Institutu za ljekove i medicinska sredstva Crne Gore od kojega je dobiven detaljan izvještaj o provedenoj semikvantitativnoj analizi uzoraka, u kojoj se s potpunom preciznošću odredio kemijski, mineraloško-petrološki sastav stijenke mase.

LITERATURA

[1] Zivaljevic, S., Tomanovic, Z.: Experimental research of the effects of preconsolidation on the time-dependent deformations-creep of marl, Mechanics of Time-Dependent Materials, 19 (2015), pp. 43–59, https://doi.org/10.1007/s11043-014-9250-8.

[2] Tomanović, Z.: Initial and time-dependent deformations in marl around small circular opening, GRAĐEVINAR, 66 (2014) 12, pp. 1087-1096, doi: https://doi.org/10.14256/JCE.1120.2014

[3] Tomanović, Z., Miladinović, B., Zivaljević, S.: Criteria for defining the required duration of the creep test, Canadian Geotechnical Journal, 52 (2015) 7, pp. 883–889, https://doi.org/10.1139/cgj-2014-0097.

[4] Tomanović, Z.: Effects of the soft rock pre-consolidation on time-dependent deformations around the tunnel excavation, Technical Gazette, (2014), ISSN 1330-3651.

[5] Tomanović, Z.: The stress and time dependent behaviour of soft rocks, GRAĐEVINAR, 64 (2012) 12, pp. 993–1007, https://doi.org/10.14256/JCE.815.2012.

[6] Tomanović, Z.: Experimental research and complex rheological models of soft rock as a basis for numerical analysis of the stress dependent behavior – Application of innovative techniques in engineering, Proceedings of the Conference Application of Innovative Techniques in Engineering, Niš, Serbia, 25–26 November 2011, pp. 219–243, ISBN 978-86-80295-97-8.

[7] Tomanović, Z.: Influence of K_o on creep properties of marl, Acta Geotechnica Slovenica, (2009), ISSN 1854-0171.

[8] Tomanović, Z.: Rheological model of soft rock creep based on the tests on marl, Mechanics of Time-Dependent Materials, 10 (2006), pp. 135–154, https://doi.org/10.1007/s11043-006-9005-2.

[9] Dusseault, M.B., Fordham, C.J.: Time-dependent behavior of rocks, in: Hudson, J.A. (ed.), Comprehensive Rock Engineering: Principles, Practice and Projects, Vol. 3, Pergamon Press, Oxford, 1993, https://doi.org/10.1016/B978-0-08-042066-0.50013-6.

[10] Cristescu, N.D., Hunsche, U.: Time Effects in Rock Mechanics, John Wiley & Sons, New York, 1998.

[11] Cristescu, N.D., Hunsche, U.: General constitutive equation, in: Time Effects in Rock Mechanics, John Wiley & Sons, New York, 1998, pp. 119–179.

[12] Wallner, M.: Stability calculation concerning a room and pillar design in rock salt, Proceedings of the International Congress for Geotechnics, Melbourne, Australia, 1983.

[13] Kozubal, J., Tomanović, Z., Zivaljević, S.: The soft rock socketed monopile with creep effects – a reliability approach based on wavelet neural networks, Archives of Mining Sciences, 61 (2016) 3, pp. 571–585.

[14] Xu, T., Tang, C.-A., Zhao, J., Li, L., Heap, M.J.: Modelling the time-dependent rheological behaviour of heterogeneous brittle rocks, Geophysical Journal International, 189 (2012) 3, pp. 1781–1796, https://doi.org/10.1111/j.1365-246X.2012.05460.x.

[15] Palmström, A.: Measurement and characterization of rock mass jointing, Chapter 2 in: In-Situ Characterization of Rocks, A.A. Balkema Publishers, Lisse, 2001.

[16] Jandrisevits, C.: Contact-free Measurement of Rock-Mass Structures – Method Comparison, Master's Thesis, Institute of Applied Geosciences, Graz University of Technology, Graz, 2012.

[17] Loiotine, L., Wolff, C., Wyser, E., Andriani, G.F., Derron, M.-H., Jaboyedoff, M., Parise, M.: QDC-2D: A Semi-Automatic Tool for 2D Analysis of Discontinuities for Rock Mass Characterization, Remote Sensing, 13 (2021) 24, Article 5086, https://doi.org/10.3390/rs13245086.

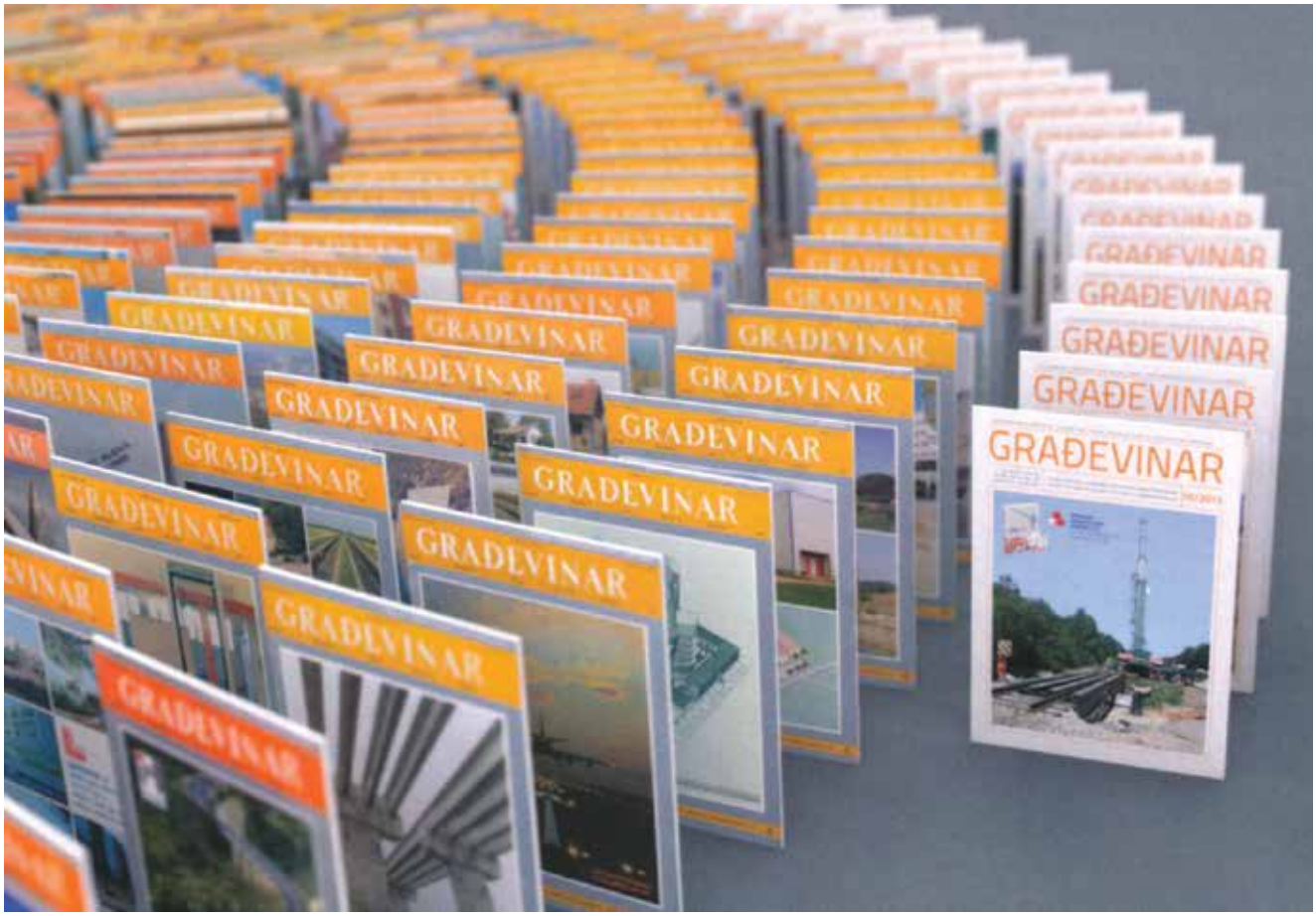

DVD s radovima od 1953. do kraja 1999.

33,00 EUR

DVD se naručuje na:

e-mail: gradjevinar@hsgi.org

Primljen / Received: 26.8.2025.
Ispravljen / Corrected: 6.5.2025.
Prihvaćen / Accepted: 8.5.2026.
Dostupno online / Available online: 10.6.2026.

Okvir za upravljanje rizicima prouzročenima informacijskom asimetrijom u građevinskim projektima

Autori:

Dr.sc. **Ivona Ivić Jazvec**, dipl.ing.građ.
Sveučilište u Zagrebu
Građevinski fakultet
Zavod za organizaciju, tehnologiju i menadžment
ivona.ivic@grad.unizg.hr
Autor za korespondenciju

Prof.dr.sc. **Anita Cerić**, dipl.ing.građ.
Sveučilište u Zagrebu
Građevinski fakultet
Zavod za organizaciju, tehnologiju i menadžment
anita.ceric@grad.unizg.hr

Pregledni rad

Ivona Ivić Jazvec, Anita Cerić

Okvir za upravljanje rizicima prouzročenima informacijskom asimetrijom u građevinskim projektima

Pojava informacijske asimetrije između investitora i izvođača često je uzrok rizika u građevinskim projektima. Kako bi se razvio okvir za upravljanje tim rizicima, napravljeno je sveobuhvatno istraživanje opisano u ovome radu. Primijenjene metode uključivale su analizu sadržaja postojeće literature i intervjue sa stručnjacima sa značajnim radnim iskustvom u fazi izvođenja građevinskih projekata. Istraživanjem je identificirano 20 ključnih rizika koji se pojavljuju prije i nakon potpisa ugovora između investitora i izvođača. Također, identificirane su ključne posljedice tih rizika i 15 ključnih strategija za ublažavanje predmetnih rizika. Na temelju dobivenih rezultata razvijen je okvir za upravljanje tim rizicima koji povezuje identificirane rizike, njihove posljedice i mjere za njihovo ublažavanje. Takav okvir omogućuje strukturiran pristup upravljanju rizicima u različitim fazama građevinskih projekata.

Ključne riječi:
agencijska teorija, informacijska asimetrija, identifikacija rizika, mjere za ublažavanje rizika

Subject review

Ivona Ivić Jazvec, Anita Cerić

Framework for management of risks caused by information asymmetry in construction projects

The occurrence of information asymmetry between clients and contractors is often a source of risk in construction projects. In order to develop a framework for managing these risks, a comprehensive study described in this paper was conducted. The methods employed included content analysis of existing literature and interviews among professionals with significant experience in the execution phase of construction projects. The research identified 20 key risks that arise before and after the signing of a contract between the client and the contractor. It also identified the key consequences of these risks and 15 key strategies for mitigating the risks in question. Based on the obtained results, a framework for managing these risks was developed, linking the identified risks, their consequences, and corresponding mitigation measures. This framework enables a structured approach to risk management across different phases of construction projects.

Key words:
principal-agent theory, information asymmetry, risk identification, risk mitigation measures

1. Uvod

Rizici u građevinskim projektima mogu se razvrstati u različite kategorije ovisno o njihovim uzrocima i prirodi. Na primjer, Thakur i sur. [1] ističu tehničke, logističke, okolišne, financijske, društveno-političke i druge vrste rizika. Među njima komunikacijski rizici predstavljaju jedan od najozbiljnijih izazova budući da su odgovorni za čak 56 % ukupnih troškova rizika u projektima [2]. Ovi rizici mogu nastati u bilo kojoj fazi projekta [3] te ne samo da utječu na povećanje troškova, već mogu ugroziti i ključne projektne ciljeve [4, 5]. Štoviše, komunikacijski rizici često pokreću lančane reakcije koje dovode do drugih vrsta rizika [6].

Ovaj rad usmjeren je na upravljanje rizicima koji proizlaze iz informacijske asimetrije među sudionicima građevinskih projekata. Dosadašnja istraživanja prepoznala su navedene rizike kao značajan problem koji još uvijek nije na odgovarajući način riješen [7, 8]. Informacijska asimetrija podrazumijeva situaciju u kojoj sudionici projekta ne raspolažu jednakom količinom ključnih informacija ili ih međusobno ne dijele, što otežava ostvarenje projektnih ciljeva [9]. Navedeni koncept temelji se na agencijskoj teoriji (engl. *principal-agent theory*), koja opisuje odnos u kojem jedna strana (*principal*) angažira drugu stranu (*agent*) za obavljanje određenog zadatka u njegovo ime [10]. U kontekstu građevinskih projekata investitor ima ulogu *principala*, a izvođač radova preuzima ulogu *agenta*. Takve odnose obilježavaju informacijska asimetrija, različite razine sklonosti prema riziku te nastojanje svakog sudionika da maksimizira vlastitu korist, što može dovesti do oportunističkog ponašanja [11].

Procjena i upravljanje rizicima ključni su elementi u upravljanju projektima. Flanagan i Norman [12] opisuju ga kao sustavni pristup prepoznavanju i kvantificiranju rizika kako bi se omogućilo donošenje svjesnih odluka o njihovom upravljanju. Prema ISO-u, [13] procjena rizika uključuje tri glavna koraka: identifikaciju rizika, analizu rizika i evaluaciju rizika.

Identifikacija rizika obuhvaća prepoznavanje i detaljno opisivanje svih potencijalnih rizika koji mogu pozitivno ili negativno utjecati na ostvarenje ciljeva projekta. Temeljita i precizna identifikacija predstavlja jednu od ključnih faza cjelokupnog procesa upravljanja rizicima. Nakon identificiranja rizika stručnjaci procjenjuju vjerojatnost njihove pojave te njihov mogući utjecaj, odnosno posljedice na projekt. Kombinacija tih dvaju elemenata određuje ukupnu razinu, odnosno težinu rizika prema izrazu: *Rizik* = *vjerojatnost* × *utjecaj*. Po završetku analize rizika raspoloživi su relevantni podaci potrebni za evaluaciju rizika i donošenje odluka o načinu postupanja s njima. Evaluacija rizika predstavlja fazu procesa upravljanja rizicima u kojoj se utvrđuje koji rizici zahtijevaju primjenu mjera ublažavanja, a koji ne zahtijevaju dodatne aktivnosti. Ovaj korak ključan je za učinkovito usmjeravanje resursa i postizanje optimalnog upravljanja rizicima.

Agencijska teorija i problem informacijske asimetrije sve su prisutniji u novijim istraživanjima u građevinskoj industriji [7, 14, 15]. Sustavan pregled literature [16] ukazuje na manjak istraživanja vezanih uz identifikaciju i analizu rizika prouzročenih informacijskom asimetrijom, a istraživanja usmjerena na mjere za ublažavanje tih rizika češća su. Ovaj nedostatak u istraživanju naglašava potrebu za detaljnijim proučavanjem ovih rizika kako bi se unaprijedilo razumijevanje i upravljanje rizicima u građevinskim projektima. Jedan od razloga za nedovoljnu pozornost ovim rizicima leži u njihovoj složenosti i multidisciplinarnoj prirodi koja obuhvaća psihološke, sociološke i ekonomske aspekte [17].

Informacijska asimetrija predstavlja inherentno obilježje odnosa između investitora i izvođača u građevinskim projektima. Sudionici projekta imaju različite ciljeve, razine znanja, interese i pristup informacijama, što rezultira trajnom neravnotežom u raspodjeli informacija. Stoga cilj upravljanja ovim rizicima nije njihovo potpuno uklanjanje, već njihovo prepoznavanje, ograničavanje i učinkovito upravljanje.

Cilj ovog rada jest predstaviti okvir za upravljanje rizicima prouzročenim informacijskom asimetrijom. U okviru su identificirani ključni rizici koji proizlaze iz informacijske asimetrije između investitora i izvođača u građevinskim projektima, klasificirani su prema teorijskim kategorijama informacijske asimetrije te se utvrđuju njihove glavne posljedice i moguće mjere ublažavanja. U drugom poglavlju ovog rada dan je pregled postojeće literature o informacijskoj asimetriji u građevinskim projektima. Također, opisane su tri teorijske skupine rizika informacijske asimetrije. U trećem poglavlju opisana je metodologija istraživanja kojim su predmetni rizici, posljedice i mjere identificirane i klasificirane. U četvrtom poglavlju prikazani su rezultati istraživanja u obliku lista ključnih rizika, njihovih posljedica i mjera za njihovo ublažavanje. U petom poglavlju dan je prijedlog okvira za upravljanje predmetnim rizicima za investitore i izvođače. Okvir povezuje identificirane rizike, njihove posljedice i mjere za njihovo ublažavanje te omogućuje lakše upravljanje ovim rizicima u građevinskim projektima. Rad završava zaključcima o znanstvenom i praktičnom doprinosu ovog istraživanja.

2. Informacijska asimetrija u građevinskim projektima

Teorijska osnova problema informacijske neravnoteže u građevinskim projektima povezana je s agencijskom teorijom i konceptom informacijske asimetrije. Agencijska teorija dolazi iz područja ekonomije i analizira odnose između dviju strana: principala i agenta [18]. Između tih dviju strana problem nastaje zbog informacijske asimetrije. Informacijska asimetrija jest situacija kada jedna strana ima i više informacija o svojim karakteristikama, aktivnostima ili namjerama, ali ih ne dijeli s drugom stranom, često radi vlastite koristi [9]. Ovakva situacija uzrokuje agencijske troškove, koji uključuju nadzor, ugovaranje i druge troškove upravljanja ovim odnosom [19]. Glavni cilj agencijske teorije jest razviti strategije za smanjenje ovih troškova i osigurati da agenti djeluju u skladu s interesima principala, primjerice kroz ugovorne mehanizme, sustave nagrađivanja i nadzora [20].

U građevinskim projektima agencijska teorija identificira odnose između sudionika projekta kao agencijske odnose koji uključuju informacijsku asimetriju, sukob interesa i agencijske troškove [11]. Investitor je glavni principal, a njegovi agenti obuhvaćaju projektante, izvođače, nadzorne inženjere, voditelje projekta i druge sudionike. Također, izvođač može djelovati kao principal prema svojim podizvođačima. S obzirom na broj i različitost sudionika te kompleksnost građevinskih projekata, postoji veliki broj *principal-agent* odnosa, što rezultira brojnim problemima koji proizlaze iz tih odnosa, a koji nastaju kada jedna strana nema potpune informacije o drugoj. Na taj način informacijska asimetrija prisutna u tim odnosima može uzrokovati poteškoće u planiranju, izvođenju i upravljanju projektima. U ovom radu fokusira se na odnos između investitora i izvođača građevinskog projekta, gdje je investitor principal, a izvođač agent koji treba izgraditi građevinu u njegovo ime (slika 1.).

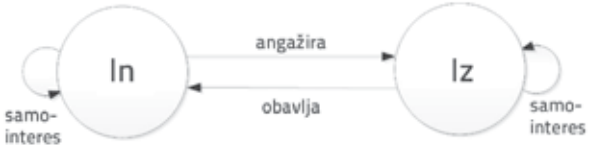

Slika 1. Osnovni agencijski model sudionika u građevinskim projektima (In – investitor; Iz – izvođač) [21]

Osim investitora i izvođača važnu ulogu u upravljanju informacijskom asimetrijom imaju i drugi sudionici projekta, poput projektanta, nadzornog inženjera, voditelja projekta te, u slučaju primjene FIDIC ugovornih modela, inženjera. Projektant je odgovoran za kvalitetu i potpunost projektne dokumentacije, čime izravno utječe na razinu informacijske asimetrije u fazi natječaja i izvođenja radova. Voditelj projekta odgovoran je za planiranje, organizaciju, koordinaciju i kontrolu svih aktivnosti projekta, uključujući upravljanje opsegom, vremenom, troškovima, kvalitetom, rizicima i komunikacijom među svim sudionicima. Nadzorni inženjer i FIDIC inženjer imaju ključnu ulogu u interpretaciji ugovornih odredbi, verifikaciji izvedenih radova i donošenju odluka koje mogu smanjiti ili povećati asimetriju među stranama. Ovi sudionici djeluju kao posrednici u prijenosu informacija i mogu značajno doprinijeti transparentnosti i ravnoteži ugovornih odnosa.

Agencijska teorija prepoznaje nekoliko vrsta problema, a oni se manifestiraju kroz skrivene karakteristike, skrivene aktivnosti i informacije te skrivene namjere [22]. Takvi problemi proizlaze iz asimetrične raspodjele informacija među sudionicima projekta, što može dovesti do različitih rizika. Ako se ti rizici ne prepoznaju i ne upravlja se njima učinkovito, mogu značajno ugroziti ostvarenje projektnih ciljeva [23].

Problem **skrivenih karakteristika** javlja se još prije sklapanja ugovora između principala i agenta, tj. *ex-ante*. Proizlazi iz činjenice da principalu nisu poznate određene osobine agenta, poput njegove izvedbene sposobnosti ili dostupnih resursa [24]. Takva situacija vodi do negativne selekcije (engl. *adverse selection* – AS) [20, 24].

S druge strane, problemi **skrivenih aktivnosti i informacija** nastaju nakon što se ugovor potpiše. Oni se odnose na smanjenje angažmana agenta prilikom izvršavanja zadataka [22]. Ove informacijske asimetrije proizlaze iz toga što principal ne može u potpunosti nadzirati aktivnosti agenta (skrivene aktivnosti) niti točno ocijeniti njegov rad (skrivene informacije) tijekom provedbe zadataka [25]. Iako principal vidi krajnji rezultat, ne može sa sigurnošću znati je li agent uložio maksimalan trud. U tom slučaju govorimo o moralnoj opasnosti (engl. *moral hazard* – MH).

Treći tip problema odnosi se na **skrivene namjere**, koje se otkrivaju tek nakon potpisivanja ugovora [22]. Tada jedna strana postaje svjesna da druga djeluje oportunistički, ali je u slabijoj pregovaračkoj poziciji jer je već uložila određene resurse u suradnju. To je situacija u kojoj partner ostaje u nepovoljnom odnosu zbog već preuzetih obveza, što se na engleskom naziva *hold-up* (HU) [25].

Pitanje informacijske asimetrije u ugovornom odnosu između investitora i izvođača ne predstavlja isključivo tehnički ili organizacijski izazov, već i pravno pitanje. Ugovorni odnos između investitora i izvođača u Republici Hrvatskoj primarno je uređen Zakonom o obveznim odnosima (NN 35/05, 41/08, 125/11, 78/15, 29/18, 126/21, 114/22, 156/22, 145/23, 155/23), koji definira osnovne elemente ugovora o građenju, uključujući prava i obveze ugovornih strana, odgovornost za izvedbu radova te mehanizme zaštite u slučaju neispunjenja ugovornih obveza. U slučaju javnih investicija dodatni regulatorni okvir čini Zakon o javnoj nabavi (NN 120/16, 114/22), kojim se uređuju postupci odabira izvođača, načela transparentnosti, jednakog tretmana i tržišnog natjecanja. Ovaj regulatorni okvir važan je jer se informacijska asimetrija pojavljuje unutar formalno definiranih ugovornih odnosa. Također određuje granice unutar kojih se informacijska asimetrija može smatrati zakonitom, primjerice kada proizlazi iz prirodnih razlika u stručnosti, iskustvu i pristupu informacijama između sudionika projekta. Investitor može imati bolje razumijevanje financijskih aspekata projekta, uključujući budžet, rokove i očekivanja prema izvođaču. To može rezultirati situacijama u kojima izvođač nije u potpunosti upoznat s financijskim ograničenjima ili ciljevima investitora, što može utjecati na planiranje i izvedbu projekta. S druge strane, izvođač ima detaljnije informacije o svom radu, napretku projekta i kvaliteti gradnje, što investitoru može biti teško u potpunosti pratiti, jer svaki oblik kontrole nosi dodatne troškove. Takva je informacijska asimetrija neizbježna u složenim projektima. Nasuprot tome, postoji i mogućnost pojave situacija u kojima jedna strana svjesno uskraćuje ili iskrivljuje ključne informacije s ciljem ostvarivanja nepoštene prednosti, čime se narušavaju načela savjesnosti i poštenja te ravnoteža ugovornih odnosa. U radu se identificirani rizici mogu interpretirati kroz ovu podjelu, pri čemu pojedini oblici informacijske asimetrije prelaze granicu zakonitog ponašanja i ulaze u područje pravno spornih praksi.

Razlika između javnih i privatnih investicija značajno utječe na dinamiku informacijske asimetrije. U javnim projektima regulatorni okvir osigurava formalne mehanizme za smanjenje

asimetrije, uključujući transparentne postupke, mogućnost postavljanja pitanja i žalbene mehanizme. U privatnim projektima takvi formalni mehanizmi često nisu standardizirani, što može povećati fleksibilnost, ali i rizik od neuravnoteženih odnosa.

Na primjer, u kontekstu javne nabave može se pojaviti pitanje odgovornosti izvođača koji prihvaća uvjete natječaja bez postavljanja dodatnih pitanja ili korištenja pravnih sredstava poput žalbe. U takvim slučajevima može se smatrati da je izvođač preuzeo određeni rizik povezan s informacijskom asimetrijom. Međutim, to ne isključuje odgovornost investitora za jasnoću i potpunost dokumentacije, osobito u situacijama gdje nedostatak informacija može dovesti do značajnih odstupanja tijekom realizacije projekta. Stoga se problem informacijske asimetrije u javnoj nabavi ne može jednostrano pripisati jednoj strani, već ga je potrebno promatrati kao rezultat interakcije između regulatornog okvira, kvalitete dokumentacije i ponašanja sudionika.

U praksi su dostupni različiti mehanizmi za ublažavanje i rješavanje posljedica asimetrije, uključujući ugovorne odredbe (npr. klauzule o promjenama radova, raspodjeli rizika), postupke pojašnjenja i dopune dokumentacije, žalbene postupke u javnoj nabavi, kao i sudsku zaštitu u slučaju povrede ugovornih obveza. Iako ovi mehanizmi ne mogu u potpunosti eliminirati asimetriju, oni omogućuju njezino pravno adresiranje i smanjenje negativnih posljedica.

Unatoč postojanju formalnih mehanizama u javnoj nabavi, određeni oblici informacijske asimetrije ostaju prisutni. To se posebno odnosi na implicitne informacije o projektu, budućim promjenama, organizacijskim kapacitetima naručitelja ili stvarnim očekivanjima tijekom izvedbe, koje nije moguće u potpunosti formalizirati kroz natječajnu dokumentaciju. U nastavku ovog rada opisana je metodologija kojom su identificirani rizici uzrokovani informacijskom asimetrijom u građevinskim projektima te je dan okvir za upravljanje njima.

3. Metodologija istraživanja

U prethodnom poglavlju definirani su koncepti informacijske asimetrije te je istaknuto kako informacijska asimetrija među sudionicima građevinskih projekata može generirati različite rizike za projekte. S obzirom na ograničenu primjenu praktičnih metoda upravljanja ovim rizicima, kao i na nedostatak opsežne znanstvene literature koja se njima bavi, nužno je bilo poduzeti prvi korak prema učinkovitom upravljanju – izraditi okvir za upravljanje predmetnim rizicima kroz identifikaciju i klasifikaciju rizika, njihovih posljedica i mjera za njihovo ublažavanje.

U tu je svrhu proveden sustavni pregled relevantne znanstvene literature s ciljem prepoznavanja i kategorizacije rizika povezanih s informacijskom asimetrijom među sudionicima građevinskih projekata. Uz rizike identificirane su i njihove posljedice u građevinskim projektima, kao i mjere za njihovo ublažavanje. Definiranje posljedica i mjera za ublažavanje nužno je za provođenje daljnjih koraka upravljanja rizicima, odnosno za analizu rizika i ublažavanje rizika. Nadalje, provedeni su polustrukturirani intervjui kako bi se dobio uvid u stavove stručnjaka iz prakse o identificiranim rizicima, posljedicama i mjerama te kako bi se preliminarne liste eventualno dopunile novim stavkama. Na temelju prikupljenih podataka formirane su konačne liste ključnih rizika, posljedica i mjera za njihovo ublažavanje.

3.1. Sustavni pregled znanstvenih članaka

Sustavni pregled literature proveden je s ciljem analize prethodnih znanstvenih istraživanja koja su se bavila fenomenom informacijske asimetrije u kontekstu građevinskih projekata. Dio rezultata ove analize prethodno je objavljen u radu [16], a u ovom se članku iznose rezultati koji se odnose na identificiranje ključnih rizika prouzročenih informacijskom asimetrijom, njihovih posljedica i mjera za ublažavanje.

Analizirana literatura preuzeta je iz dviju renomiranih znanstvenih baza podataka – Web of Science Core Collection i Scopus – što je omogućilo sveobuhvatan uvid u problematiku i rizike prouzročene informacijskom asimetrijom u građevinskom sektoru. U pretraživanju su korištene sljedeće ključne riječi: "*asymmetric information*", "*information asymmetry*", "*adverse selection*", "*moral hazard*", "*hold-up*" i "*construction*". Navedeni termini kombinirano su pretraživani unutar naslova, sažetaka i ključnih riječi znanstvenih radova. Nakon pretraživanja dviju elektroničkih baza podataka svi pronađeni zapisi uneseni su u računalni program Mendeley. Sve daljnje faze pregleda literature provedene su unutar tog programa, čime je osigurana objektivna analiza i precizno upravljanje prikupljenim izvorima [26].

Prikupljene publikacije obrađene su prema smjernicama PRISMA metodologije [27], pri čemu su ukupno 94 znanstvena članka zadovoljila kriterije uključivanja jer su sadržavali jedan ili više primjera rizika povezanih s informacijskom asimetrijom, njihovih posljedica ili mjera za ublažavanje. Analizom sadržaja prikupljenih znanstvenih radova formirane su kategorizirane liste rizika za tri kategorije informacijske asimetrije: negativnu selekciju, moralnu opasnost i rizike zadržavanja. Osim toga, formirane su i liste posljedica i mjera za ublažavanje.

Radi dodatne evaluacije podataka dobivenih iz literature, provedeni su polustrukturirani intervjui. Detalji ove faze istraživanja opisani su u nastavku.

3.2. Intervjui

Radi procjene praktične relevantnosti podataka dobivenih iz znanstvene literature, provedeni su intervjui sa stručnjacima s bogatim iskustvom u području građevinskih projekata. Ključna prednost ove metode leži u mogućnosti prikupljanja detaljnih i sadržajno bogatih informacija [28].

Intervjui su provedeni s devet stručnjaka s najmanje 17 godina iskustva u građevinskim projektima, koji trenutačno obnašaju rukovodeće funkcije. Uzorak je odabran svrsishodno, s ciljem dobivanja detaljnih i kvalitetnih podataka od stručnjaka koji su

Tablica 1. Kodovi korišteni u kvalitativnoj analizi sadržaja transkripta intervjua (prilagođeno prema [21])

	Kod	Opis
Prethodno određeni kodovi	+	Slaganje sa stavkom (rizik, posljedica ili mjera za ublažavanje)
	-	Neslaganje sa stavkom
	+/-	Djelomično slaganje sa stavkom
	Razlog	Razlog slaganja, neslaganja ili djelomičnog slaganja sa stavkom
	Dodatak	Nova stavka koju ispitanik dodaje
	Primjer rizika	Primjer iz prakse u kojem je prepoznat rizik prouzročen informacijskom asimetrijom
	Primjer posljedica	Primjer iz prakse u kojem je prepoznata posljedica rizika
	Primjer mjere	Primjer iz prakse u kojem je prepoznata mjera za ublažavanje rizika
Kodovi određeni tijekom analize	Kontekst tržišta	Objašnjenje razlika u pojavi rizika prouzročenih informacijskom asimetrijom ovisno o tržištu na kojem poduzeće nastupa
	Kontekst sudionika	Objašnjenje konteksta pojave rizika zbog uobičajenih obrazaca ponašanja, sposobnosti ili nesposobnosti sudionika u projektu
	Kontekst vrste projekta	Objašnjenje razlika u pojavi rizika prouzročenih informacijskom asimetrijom ovisno o vrsti projekta (javni/privatni)
	Komentar izmjena	Komentar za izmjenom ili nadopunom naziva stavke

sudjelovali u velikim i složenim projektima. Takav mali, homogeni uzorak karakterističan je za kvalitativna istraživanja usmjerena na specifične teme [28]. Nakon devet intervjua zabilježena je saturacija podataka, što je označilo kraj prikupljanja dodatnih informacija. Tri ispitanika dolaze iz organizacija koje djeluju kao javni naručitelji, dvoje dolaze iz privatnih poduzeća za izvođenje građevinskih projekata, a ostali su iz privatnih poduzeća specijaliziranih za konzultantske usluge, nadzor, projektiranje i upravljanje projektima. Svi ispitanici uključeni u istraživanje, iako neki formalno ne dolaze iz izvođačkih organizacija, posjeduju značajno praktično iskustvo u izvođenju građevinskih projekata. Kroz svoje profesionalne uloge bili su izravno uključeni u procese pripreme i realizacije projekata, što podrazumijeva detaljno poznavanje uloge izvođača i investitora, i u fazi prije potpisa ugovora (npr. analiza natječajne dokumentacije, procjena rizika i donošenje odluka o sudjelovanju), i u fazi nakon sklapanja ugovora (upravljanje izvedbom, koordinacija sudionika i rješavanje ugovornih pitanja). Stoga njihovi odgovori reflektiraju i perspektivu izvođača i investitora, unatoč njihovoj formalnoj organizacijskoj pripadnosti. Svi su radili na projektima u Hrvatskoj, pri čemu je četvero imalo i inozemno iskustvo u različitim zemljama. Njihova stručnost najviše obuhvaća javne projekte, a privatne su investicije zastupljene u manjoj mjeri, što je u skladu s fokusom na složene velike projekte, pretežno vezane uz javne investicije u Hrvatskoj.

Pitanja za polustrukturirane intervjue bila su unaprijed definirana radi objektivnije analize, no ispitanicima je pružena mogućnost otvorenih odgovora. Intervjui su se fokusirali na evaluaciju lista rizika, posljedica i mjera prikupljenih iz literature, gdje su stručnjaci komentirali, izražavali slaganje ili neslaganje te davali primjere iz vlastitog iskustva, uz prijedloge za poboljšanje formulacija radi veće jasnoće. Svaki ispitanik sudjelovao je u jednom intervjuu, čije je trajanje variralo od 52 minute do dva sata. Intervjui su se održavali u prostorijama poduzeća, na Građevinskom fakultetu u Zagrebu ili putem *online* platformi, uz posebnu pozornost na stvaranje povjerljive atmosfere koja je poticala otvorenost. Svi intervjui snimljeni su i transkribirani, čime je osigurana bogata baza podataka za daljnju analizu.

Transkripti intervjua analizirani su kvalitativnom analizom sadržaja u MS Wordu. U toj fazi moguće je koristiti se specijaliziranim računalnim alatima, no važno je napomenuti da takvi alati ne mogu samostalno identificirati kodove, već mogu tek djelomično ubrzati analizu teksta [29, 30], stoga je u ovom istraživanju odlučeno da se specijaliziranim programima za kodiranje teksta neće koristiti. Dio kodova definiran je prije analize, a neki su kodovi određeni tijekom same analize. Naime, utvrđeno je da značaj pojedinih rizika, kao i primjenjivost mjera za njihovo ublažavanje, varira s obzirom na vrstu projekta (javni ili privatni). Također je uočeno da se pristup upravljanju rizicima razlikuje ovisno o ulozi sudionika (provodi li ga investitor ili izvođač) i tržištu na kojem poduzeće nastupa. Stoga je bilo važno naknadnim kodovima zabilježiti konkretne komentare stručnjaka o kontekstima u kojima su pričali. Konačni popis kodova vidi se u tablici 1.

4. Rezultati i opis glavnih elemenata okvira

U nastavku su predstavljeni rezultati ovog istraživanja, odnosno identificirani elementi okvira koji se predlaže za upravljanje rizicima prouzročenima informacijskom asimetrijom. Glavni elementi okvira sastoje se od identificiranih rizika, njihovih posljedica i mjera za ublažavanje. Prvo su prikazani rizici identificirani analizom literature i intervjua sa stručnjacima. Ti su rizici klasificirani prema vrstama informacijske asimetrije, s ciljem određivanja faze građevinskog projekta u kojoj se mogu pojaviti te kako bi se omogućila daljnja istraživanja unutar definiranih kategorija. Nakon toga prikazane su identificirane posljedice i moguće mjere za ublažavanje rizika.

4.1. Ključni rizici prouzročeni informacijskom asimetrijom

Prije sklapanja ugovora između investitora (principala) i izvođača (agenta) u građevinskim projektima često postoje okolnosti u kojima jedna strana nema potpun uvid u sposobnosti druge. Javljaju se rizici negativne selekcije (engl. *adverse selection* – AS). U tablici 2. prikazano je osam rizika koji proizlaze iz skrivenih karakteristika, a vezani su uz početnu fazu natjecanja izvođača za dobivanje posla – prvu točku kontakta između agenta i principala. Uobičajeni model izbora izvođača temelji se na prikupljanju ponuda. Zbog jake konkurencije izvođači često nude niže cijene od tržišnih kako bi osigurali ugovor [15, 31], što može rezultirati pogrešnim procjenama, bilo zbog namjere, neiskustva ili nedostatka stručnosti [15]. Osim toga, izvođači često nemaju potpune informacije o projektu, njegovu opsegu ili količinama radova [23, 32–36], osobito kad projekt nije finaliziran, investitor mijenja zahtjeve ili projekt uključuje nove tehnologije [37]. U takvim okolnostima može doći do prijava izvođača koji nisu sposobni realizirati projekt, a investitor može pogrešno procijeniti njihovu sposobnost. Zbog složenosti građevinskih projekata investitori često ne mogu precizno definirati sve zahtjeve, pa se oslanjaju na izvođače da pruže točne informacije, što stvara potencijalnu informacijsku neravnotežu [38]. U tim situacijama ključno je dokazivanje sposobnosti izvođača, primjerice putem certifikata, jamstava i bankovnih garancija. No pouzdanost tih dokaza može biti upitna – zbog smanjene signalne vrijednosti certifikata [37, 39], nedostatka informacija o reputaciji izvođača ili lažnog predstavljanja [23, 35, 36]. Tijekom nadmetanja mogu se pojaviti i drugi rizici, poput tajnih dogovora između investitora i izvođača, između izvođača samih ili između izvođača i podizvođača, što negativno utječe na troškove i tijek projekta [35, 36]. Poseban izazov predstavlja podugovaranje jer investitor često nema potpune informacije o podizvođačima, njihovim sposobnostima ili namjerama [35, 40], a dogovori između izvođača i podizvođača te neadekvatna prijava podizvođača dodatno pojačavaju rizik. Osim rizika identificiranih pregledom literature, stručnjaci su tijekom intervjua naglasili kako financijska nestabilnost izvođača ili investitora predstavlja značajan skriveni rizik prije sklapanja ugovora, koji tijekom izvođenja radova, ali i nakon njih, može uzrokovati ozbiljne negativne posljedice.

Nakon sklapanja ugovora u fazi izgradnje građevinskog projekta često dolazi do situacija u kojima su aktivnosti ili informacije jedne strane djelomično ili potpuno skrivene od druge strane. Rizici povezani s takvom informacijskom asimetrijom u literaturi su prepoznati kao moralna opasnost (engl. *moral hazard* – MH), a izdvojeno je šest ključnih rizika (vidi tablicu 2.). Najčešći primjeri prikrivenih aktivnosti uključuju korištenje materijala lošije kvalitete, smanjenu količinu izvedenih radova, prikrivanje pogrešaka te općenito niži trud izvođača u ispunjavanju ugovornih obveza [35, 36]. To se događa zbog ograničene kontrole investitora, bilo zbog nedostatka stručnosti ili financijskih resursa [38], a izvođač tada može preuzeti veće rizike očekujući da neće biti sankcioniran. Na ponašanje izvođača utječu i nepredviđeni uvjeti kao što su vremenske neprilike [41], a ponekad i svjesno prikrivanje informacija ili odbijanje izvršenja obveza [42]. Kvalitetna razmjena informacija unutar projektnog tima može smanjiti broj pogrešaka [43], no bez jasno definiranih komunikacijskih pravila te suradničkog okruženja informacije često kasne. Kolaboracija se može poboljšati radionicama [44], partnerskim odnosima [45], digitalnim alatima poput informacijskog modeliranja gradnje (engl. *building information modelling* – BIM) i *blockchaina* [9, 45] te ranom uključenosti svih dionika [46]. Razlike između planiranih i izvedenih količina radova uobičajene su [47], a uzroci mogu biti loše planiranje [32–34], nepredviđeni događaji ili investitorove izmjene [23, 35, 36]. Teškoće u kontroli količina uzrokuje loš ili nepravovremen nadzor. Dodatni rizik proizlazi iz narušenih odnosa među sudionicima, posebice kada izostaje povjerenje i spremnost na suradnju [43, 48]. Slaba kolaboracija, neravnomjerno raspodijeljeni rizici i odgovornosti [49] te odsustvo očekivanja o budućoj suradnji mogu potaknuti oportunističko ponašanje izvođača [46, 50]. Poseban izazov predstavlja podugovaranje, gdje izvođač mora prenijeti sustav kontrole i poticaja na podizvođače [51]. Zadnji istaknuti rizik odnosi se na nisku vidljivost određenih građevinskih radova, što otežava naknadnu provjeru kvalitete i količina. U takvim slučajevima, ako je zakonodavni okvir slab, moguće su zloupotrebe i manipulacije u rješavanju sporova [51, 52]. U kategoriji rizika moralne opasnosti nije bilo dodataka od strane stručnjaka tijekom intervjua. Svi rizici identificirani u literaturi verificirani su i kroz intervjue te je njihova priroda dodatno pojašnjena primjerima iz prakse koje su ispitanici dijelili.

Zadnja kategorija informacijskih asimetrija odnosi se na skrivene namjere jedne strane da drugu dovede u nepovoljan položaj, otkrivajući ključne informacije tek kad projekt već uznapreduje. Ako druga strana ne može udovoljiti novim zahtjevima, može doći do obustave radova ili financiranja. Ova situacija poznata je kao rizik zadržavanja (engl. *hold-up* – HU), a ovim istraživanjem identificirano je šest ključnih rizika te vrste (vidi tablicu 2.). Najčešće se manifestira u naknadnim pregovorima, npr. kad investitor traži dodatne ili izmijenjene radove nakon potpisivanja ugovora, a izvođač koristi svoju pregovaračku prednost kako bi ih naplatio skuplje [53, 54]. Zbog ograničenih opcija investitor često pristaje na uvjete kako bi izbjegao prekid projekta. Također, izvođač, zahvaljujući boljem poznavanju izgradnje, može namjerno ne prijaviti nedostatke u projektnoj dokumentaciji kako bi ih poslije iskoristio [38]. Kod velikih infrastrukturnih projekata s visokim stupnjem specifičnosti imovine (engl. *asset specificity*), investitor se nalazi u nepovoljnoj poziciji jer već uložena sredstva ne može lako prenamijeniti, a izvođač koristi svoju prednost za postavljanje dodatnih zahtjeva [50, 55, 56]. To povećava transakcijske troškove produženim pregovorima

Tablica 2. Rizici identificirani pregledom literature i intervjuima sa stručnjacima; AS – rizici negativne selekcije, MH – rizici moralne opasnosti; HU – rizici zadržavanja

ID	Rizik	Izvor	Intervjui
AS1	Loša/manjkava natječajna dokumentacija	[23, 32–37, 58]	verificirano
AS2	Kvalifikacije izvođača nisu poznate/provjerljive	[23, 35 ,37–39, 45, 59]	verificirano
AS3	Nemogućnost prepoznavanja i isključivanja manipulativne niske ponude	[15, 31, 43, 60, 61]	verificirano
AS4	Potajno dogovaranje između sudionika prije ili u tijeku natječaja	[35, 36]	verificirano
AS5	Lažno prikazivanje ili skrivanje podizvođača	[35, 40]	verificirano
AS6	Onemogućen/otežan odabir povjerljivog poslovnog partnera	[46]	verificirano
AS7	Nestabilno financijsko stanje izvođača	intervjui	dodano
AS8	Nestabilno financijsko stanje investitora	intervjui	dodano
MH1	Skrivanje informacija o stvarnoj kvaliteti gradnje	[11, 32–36, 38, 40–42, 45, 50, 60, 62–70]	verificirano
MH2	Otežana razmjena informacija između investitora i izvođača	[23, 35, 36, 40, 43-46, 52, 59, 63, 64, 71–73]	verificirano
MH3	Naknadne izmjene projekta	[23, 32-36 ,47, 58]	verificirano
MH4	Nedostatak razumijevanja i povjerenja između investitora i izvođača	[43, 46, 48–50, 74]	verificirano
MH5	Nedostatak evidencije događaja na gradilištu	[51, 52, 64, 70, 75]	verificirano
MH6	Oportunističko ponašanje zbog jednokratne suradnje	[46, 50]	verificirano
HU1	Zadržavanje radova od strane izvođača	[38, 50, 53, 54, 70, 76–78]	verificirano
HU2	Ograničeno pregovaranje zbog političkog ili javnog utjecaja	[44, 51, 54, 55, 70, 77–79]	verificirano
HU3	Zadržavanje informacija zbog nepovjerenja	[50]	verificirano
HU4	Nepoznavanje stvarnih troškova izvođača	[57]	verificirano
HU5	Zadržavanje plaćanja od strane investitora	intervjui	dodano
HU6	Zadržavanje donošenja odluka od strane investitora	intervjui	dodano

i mogućim sporovima [54]. Dodatni problem nastaje kad nema dugoročne suradnje i povjerenja, pa se obje strane suzdržavaju od istinske suradnje kako ne bi oslabile vlastitu pregovaračku poziciju [50]. Konačno, izostanak mehanizama kontrole troškova omogućava izvođaču da zadrži informacije s ciljem financijske koristi na račun investitora [57]. Unutar ove skupine rizika ispitanici su u intervjuima naglašavali važnost preciznijeg definiranja aktera koji uzrokuju zadržavanje. U literaturi se uočava tendencija da se investitor promatra kao strana koja je pretežito izložena rizicima zadržavanja, međutim analiza prakse upućuje na to da takav odnos nije jednoznačan. Na temelju komentara povezanih s opisom rizika HU1 identificirane su tri zasebne kategorije rizika koje preciznije odražavaju stvarne situacije u građevinskim projektima: zadržavanje radova od strane izvođača, zadržavanje plaćanja od strane investitora te zadržavanje donošenja odluka od strane investitora.

4.2. Ključne posljedice rizika

Rizici koji proizlaze iz informacijske asimetrije mogu negativno utjecati na ostvarenje ciljeva projekta. Osim što ugrožavaju sam projekt, ti rizici imaju šire posljedice poput narušavanja odnosa među dionicima, što često dovodi do konflikata i sporova. Dugoročno gledano informacijska asimetrija u građevinskim projektima također doprinosi smanjenju ukupne produktivnosti sektora.

Nepovoljni učinci na projektne ciljeve uključuju povećanje troškova [43, 47], kašnjenja u realizaciji [53], smanjenu kvalitetu izvedenih radova [80] te poteškoće u implementaciji novih tehnologija i inovacija [11]. Uz to, ovi rizici negativno utječu na buduću suradnju među partnerima [81], izazivaju pravne sporove [55] i narušavaju povjerenje i otvorenu komunikaciju [42, 82].

Na duži rok posljedice informacijske neravnoteže odražavaju se kroz smanjenje učinkovitosti cijele industrije [58]. Kvalificirani izvođači zarađuju manje [31] ili se povlače iz tržišnih natječaja [32–34], a investitori i klijenti gube interes za financiranje projekata [37]. U konačnici tvrtke koje sudjeluju u takvim projektima snose veće transakcijske troškove [55].

Tijekom intervjua ispitanici su s pomoću primjera realizacije rizika povezanih s informacijskom asimetrijom istaknuli još dvije važne posljedice: raskid ugovora i narušavanje reputacije poduzeća uključenih u projekt. Konačna lista ključnih posljedica rizika prouzročenih informacijskom asimetrijom prikazana je u tablici 3.

Tablica 3. Posljedice rizika identificirane pregledom literature i intervjuima sa stručnjacima

ID	Posljedica	Izvor	Intervjui
P1	Povećani troškovi	[15, 31–34, 36, 38, 43, 47, 51, 53–55, 67, 76–78, 83, 84]	verificirano
P2	Pogoršanje odnosa među sudionicima projekta / sporovi	[32–34, 40, 42, 53–55, 81, 82]	verificirano
P3	Smanjena kvaliteta izvedbe	[36, 40, 52, 59–62, 74, 80, 81]	verificirano
P4	Neuspjeh u postizanju učinaka nove tehnologije i inovacija	[11, 37, 39, 45, 52, 66, 72, 73, 85]	verificirano
P5	Produljenje roka izvedbe	[41, 43, 53]	verificirano
P6	Raskid ugovora	intervjui	dodano
P7	Pad reputacije poduzeća	intervjui	dodano

4.3. Ključne mjere za ublažavanje rizika

Mjere za ublažavanje rizika koje se najčešće spominju u relevantnoj literaturi odnose se na izradu tzv. optimalnih ugovora i njihovu kontrolu tijekom provedbe projekta [82]. Unutar tih aktivnosti posebnu ulogu ima definiranje poticaja (engl. *incentive*) za izvođače. Ugovori, primjerice, sadrže klauzule kojima se potiče izvođače da klijentima pružaju točne informacije o troškovima [86, 87], izvršavaju radove u skladu s predviđenim planom [71, 83] reagiraju na nepredviđene okolnosti [41] i prilagođavaju se promjenama u projektu [57, 88, 89]. Također, ugovori bi trebali uključivati uravnoteženu raspodjelu rizika [67], objektivne kriterije za provedbu ugovora [53, 54], jasno izražene namjere ugovornih strana [11], mehanizme za korekciju cijena u skladu s tržišnim promjenama [61], precizno definirane zahtjeve u pogledu izvedbe, tehničke specifikacije i standarde kvalitete [58], kao i zaštitne instrumente poput jamstava [70].

Ugovorne odredbe trebale bi predvidjeti i nagrade za izvođače u slučajevima kada posao završe prije roka i uz zadovoljenje zahtjeva kvalitete [53], kao i kada ostvare uštede u troškovima [48, 85]. Istovremeno, izvođači bi trebali snositi sankcije ako projekt ne dovrše unutar dogovorenog budžeta i vremenskog okvira [52, 85]. Nadalje, projekt bi trebao imati razvijen sustav za izvještavanje i praćenje provedbe ugovora [14, 38], kao i mehanizam za procjenu uspješnosti izvođača [65].

Prije zaključenja ugovora investitor bi trebao primijeniti različite metode kako bi procijenio karakteristike agenata, odnosno izvođača koji su predali svoje ponude (mjera koje se na engleskom jeziku naziva *screening*). To se može provesti na tri načina. Prvi način uključuje istraživanje pozadine, ugleda i ranijih projekata poduzeća koja su se prijavila na natječaj [84]. Drugi način odnosi se na detaljnu analizu dostavljenih ponuda [83], uključujući usporedbu ponuđenih cijena s tržišnim kako bi se ocijenila njihova opravdanost i konkurentnost. Treća je opcija zahtijevanje financijskih garancija od ponuditelja, poput predujmova ili bankovnih jamstava [50], čime se potvrđuje njihova ozbiljnost i financijska sposobnost za izvršenje obveza iz ugovora.

S druge strane, izvođači mogu sami signalizirati svoje kvalitete i pouzdanost investitorima, primjerice kroz predstavljanje certifikata [37] ili putem marketinških aktivnosti [36, 37]. Jedan od značajnih rizika predstavlja damping cijena, zbog čega poznavanje metoda za izračun optimalne ponude može pomoći u njegovom izbjegavanju [31].

Značajan dio rizika koji proizlaze iz informacijske asimetrije može se ograničiti već u fazi odabira izvođača. To se osobito odnosi na situacije u kojima investitor ima mogućnost odabrati izvođača s provjerenom reputacijom [80], usklađenim organizacijskim vrijednostima i poslovnom kulturom [44, 90] ili onoga s kojim već postoji prethodno iskustvo suradnje i uspostavljen partnerski odnos [81].

Učinkovit nadzor kvalitete ima ključnu ulogu u smanjenju rizika povezanih s informacijskom asimetrijom tijekom faze izvođenja [75]. Osim samog nadzora važna je i suradnja sudionika te otvoreno dijeljenje informacija i koristi od samog početka projekta [45]. Komunikacija među akterima trebala bi biti transparentna, odgovorna [14, 70], vjerodostojna [70], iskrena [23] i neformalnija [38]. Povjerenje između sudionika trebalo bi se graditi i njegovati tijekom cijelog trajanja projekta [8].

Investitor bi također trebao omogućiti izvođačima nematerijalne (intrinzične) oblike nagrađivanja, poput jačanja ugleda, većeg stupnja autonomije i odgovornosti, zadovoljstva poslom, stabilnosti te usklađivanja ciljeva [62]. Na kraju, transparentnost u upravljanju informacijama može se postići korištenjem različitih informacijskih sustava [39], uključujući BIM [91, 92], *blockchain* [91], softverske platforme za upravljanje projektima [46] te primjenu principa otvorenog računovodstva [47, 81]. Time se smanjuje prostor za manipulaciju informacijama te se poboljšava koordinacija i donošenje odluka.

U intervjuima su ispitanici identificirali još tri dodatne mjere za ublažavanje rizika uzrokovanih informacijskom asimetrijom: zamjenu predstavnika poduzeća, mirenje sudionika preko treće strane i uspostavu komunikacijskih protokola. Zamjena predstavnika prepoznata je kao učinkovita u slučajevima osobnih sukoba, neslaganja ili narušenog povjerenja među sudionicima projekta. Također je istaknuta mogućnost posredovanja kroz neutralnu treću stranu. Najveći broj ispitanika naglasio je i važnost jasno definiranih komunikacijskih protokola. Iako su u početku bili uključeni unutar mjere M4 – Informacijski sustavi,

Tablica 4. Mjere za ublažavanje rizika identificirane pregledom literature i intervjuima sa stručnjacima (prilagođeno prema [93])

ID	Mjera	Izvor	Intervjui
M1	Novčani poticaji za izvođača (bonusi)	[8, 11, 14, 23, 38, 40, 41, 44, 46–48, 53, 57, 61, 62, 65, 66, 71–73, 75, 80, 82, 83, 86, 88, 89, 94–101]	verificirano
M2	Ponuditelj signalizira svoje karakteristike investitoru (oglašavanje, reputacija)	[8, 36, 37, 44, 50, 53, 55, 58, 59, 65, 66, 70, 80, 84]	verificirano
M3	Kooperacija i izgradnja povjerenja	[8, 14, 23, 37, 38, 44, 45, 48, 70, 74, 77, 81, 87]	verificirano
M4	Informacijski sustavi	[8, 9, 36–40, 43–48, 81, 91, 92]	verificirano
M5	Redovit i temeljit nadzor kvalitete	[11, 40, 42, 60, 66, 72, 73, 75, 80, 102]	verificirano
M6	Ugovorom definirana mjerila za praćenje rada izvođača	[14, 23, 38, 48, 51, 53, 54, 58, 61, 65]	verificirano
M7	Pravedna distribucija rizika između investitora i izvođača	[15, 43, 48, 61, 67, 81, 85, 98, 99]	verificirano
M8	Ugovorne kazne	[23, 46, 48, 52, 53, 75, 101]	verificirano
M9	Investitor provjerava pristigle ponude	[14, 31, 36, 72, 73, 78, 83]	verificirano
M10	Investitor provjerava ponuditelje (certifikati, jamstva, financijska stabilnost)	[14, 36, 61, 70, 84]	verificirano
M11	Ne-financijske nagrade za izvođača (poboljšanje ugleda, zadovoljstvo u radu, autonomija)	[40, 48, 52, 62]	verificirano
M12	Odabir ponuditelja koji ima sličnu organizacijsku kulturu (vrijednosti, ciljeve)	[8, 44, 90]	verificirano
M13	Zamjena predstavnika poduzeća	intervjui	dodano
M14	Mirenje sudionika preko treće strane	intervjui	dodano
M15	Komunikacijski protokoli	intervjui	dodano

odlučeno je da se zasebno istaknu, jer ispitanici su naglasili njihovu ključnu ulogu u prevenciji rizika, neovisno o korištenju informacijskih sustava. Konačna lista ključnih mjera za ublažavanje rizika prouzročenih informacijskom asimetrijom prikazana je u tablici 4.

U kontekstu upravljanja rizicima važno je naglasiti da predložene mjere ne djeluju isključivo na ublažavanje posljedica realiziranih rizika, već i na smanjenje njihove vjerojatnosti. Primjerice, postupci provjere ponuditelja, kvalitetna priprema projektne dokumentacije, jasno definirani ugovorni uvjeti i uspostava sustava nadzora predstavljaju preventivne mehanizme koji mogu značajno smanjiti mogućnost nastanka rizika prouzročenih informacijskom asimetrijom. Međutim, zbog inherentne prirode tih rizika, njihova potpuna eliminacija u pravilu nije moguća, već je cilj upravljanja postići optimalnu ravnotežu između prevencije i ublažavanja posljedica.

5. Okvir za upravljanje rizicima prouzročenima informacijskom asimetrijom

Na temelju analize literature i intervjua s iskusnim stručnjacima iz građevinskih projekata identificirani su ključni rizici povezani s informacijskom asimetrijom, zajedno s njihovim posljedicama i mogućim mjerama za njihovo ublažavanje. Slika 2. predstavlja okvir za upravljanje tim rizicima, čija je struktura oblikovana prema prepoznatim rizicima, njihovim posljedicama i odgovarajućim mjerama koje su nužne za učinkovito upravljanje u građevinskoj praksi.

Rizici povezani sa skrivenim karakteristikama (negativna selekcija) javljaju se prije sklapanja ugovora odnosno u fazi prikupljanja ponuda izvođača. S druge strane, rizici koji proizlaze iz skrivenih informacija i aktivnosti (moralna opasnost) te skrivenih namjera (rizik zadržavanja) nastaju nakon potpisivanja ugovora, tijekom izvođenja radova i mogu trajati do završetka projekta.

Te se vrste rizika najčešće odražavaju na projektne ciljeve, i tijekom izgradnje, i nakon njezina završetka. Za učinkovito upravljanje rizicima nužno je njihovo pravovremeno prepoznavanje, osobito u fazi prikupljanja ponuda, kao i njihovo kontinuirano praćenje i primjena mjera za ublažavanje radi smanjenja njihove učestalosti ili negativnog utjecaja.

Predloženi okvir prikazuje logičku povezanost između rizika, njihovih posljedica i mjera za ublažavanje kroz različite faze projekta. Njegova primjena u praksi podrazumijeva identifikaciju relevantnih rizika u konkretnoj fazi projekta, procjenu njihovog potencijalnog utjecaja te odabir odgovarajućih mjera za njihovo upravljanje.

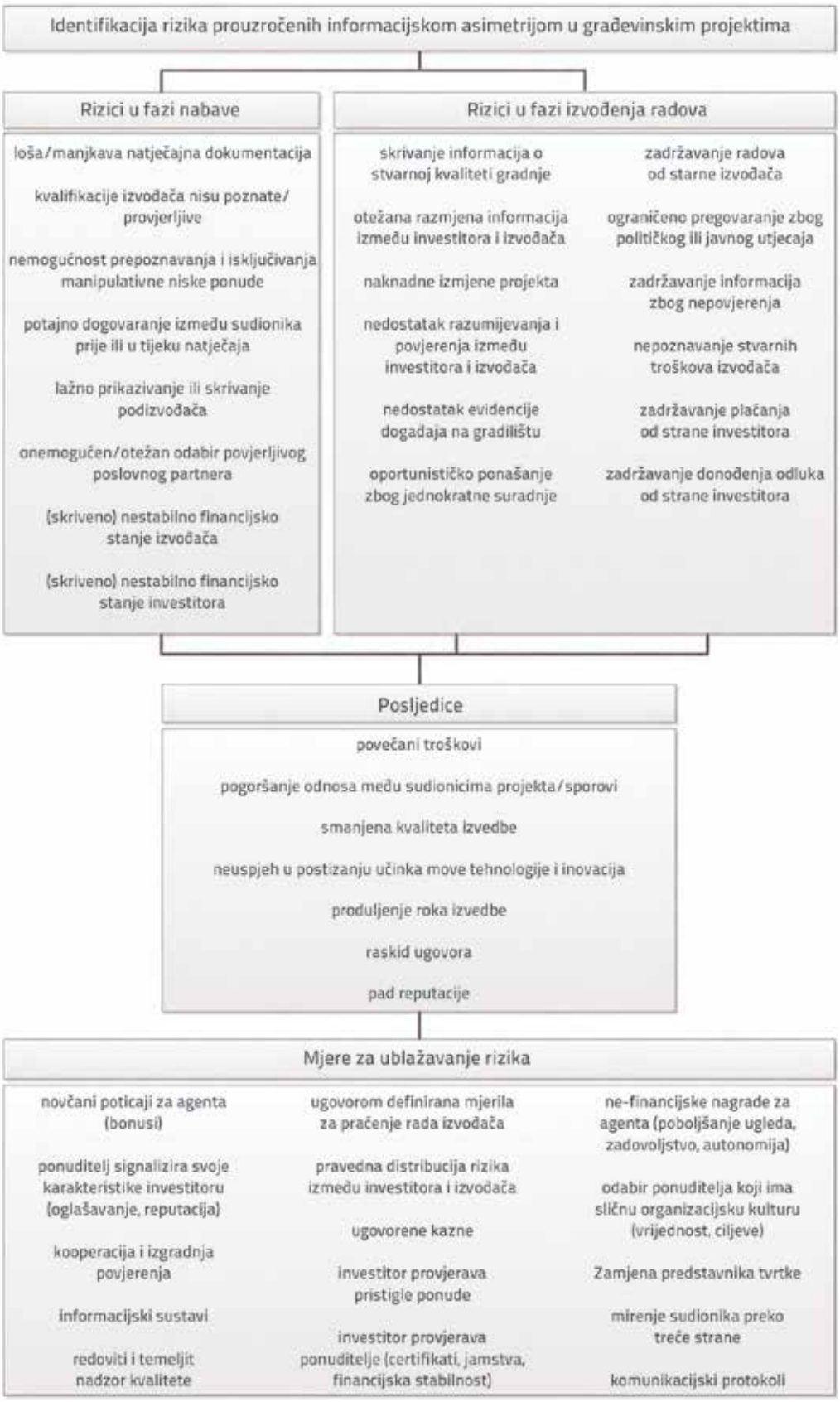

Slika 2. Okvir za upravljanje rizicima prouzročenima informacijskom asimetrijom

6. Zaključak

U radu je predstavljen okvir za upravljanje rizicima prouzročenim informacijskom asimetrijom. Identificirani su i opisani ključni rizici koji proizlaze iz informacijske asimetrije između investitora i izvođača u građevinskim projektima, razvrstani prema teorijskim kategorijama informacijske asimetrije te su određene njihove glavne posljedice i moguće mjere ublažavanja.

Zbog različitosti građevinskih projekata, okvir razvijen u ovom istraživanju ima određena ograničenja u svojoj generalizaciji. Istraživanjem putem intervjua utvrđeno je da značaj pojedinih rizika, kao i primjenjivost mjera za njihovo ublažavanje, varira s obzirom na vrstu projekta (javni ili privatni). Također je uočeno da se pristup upravljanju rizicima razlikuje ovisno o ulozi sudionika – provodi li ga investitor ili izvođač. Stoga je važno okvir primjenjivati prilagođeno različitim vrstama projekata i perspektivama sudionika kako bi se učinkovito povezali rizici, njihove posljedice i odgovarajuće mjere ublažavanja.

Osnovni doprinos ovog istraživanja ogleda se u tome da opisani rizici uzrokovani informacijskom asimetrijom predstavljaju polazište za identifikaciju rizika u budućim građevinskim projektima. Njihove posljedice ukazuju na projektne ciljeve na koje mogu utjecati, što je važno pravodobno prepoznati već u ranim fazama upravljanja rizicima. Nadalje, utvrđene prioritetne mjere za ublažavanje tih rizika mogu poslužiti kao osnova za definiranje odgovarajućih strategija odgovora na rizike. Buduća istraživanja trebala bi biti usmjerena na validaciju prikazanog okvira u stvarnim projektnim uvjetima kako bi se dodatno ispitala povezanost između primjene mjera za ublažavanje rizika informacijskom asimetrijom i uspješnosti ostvarivanja ciljeva građevinskih projekata.

Zahvala

Autori zahvaljuju svim građevinskim stručnjacima koji su sudjelovali u ovom istraživanju te pomogli u oblikovanju rezultata. Posebna zahvala Ladislavu Bevandi, Edvardu Ćozi, Ivani Karačić, Tihomiru Lažeti, Goranu Legcu, Mariju Lovrinčeviću, Tamari Marić, Davoru Periću, Romanu Periću, Siniši Radakoviću i Marku Sokoloviću. Ovaj rad proveden je u okviru institucionalnog istraživačkog projekta BLOCKRUG (Digitalna transformacija kružnog građevinarstva primjenom blockchain tehnologije), financiranog od strane Ministarstva znanosti, obrazovanja i mladih Republike Hrvatske u sklopu Nacionalnog plana oporavka i otpornosti 2021. – 2026., uz sufinanciranje Europske unije kroz program NextGenerationEU.

LITERATURA

[1] Thakur, A.I., Khan, S., Siddiqui, M.J.: Risk management and life cycle costing of infrastructure project, International Journal of Recent Advances in Engineering & Technology, 4 (2016) 3, pp. 70–75.

[2] PMI's Pulse of the Profession In-Depth Report: The High Cost of Low Performance: The Essential Role of Communications, www.pmi.org, 30.5.2019.

[3] Cerić, A.: A Framework for Process-Driven Risk Management in Construction Projects, Research Institute for the Built and Human Environment, University of Salford, 2003.

[4] Assaf, S., Hassanain, M.A., Abdallah, A.: Review and assessment of the causes of deficiencies in design documents for large construction projects, International Journal of Building Pathology and Adaptation, 36 (2018) 3, pp. 300–317.

[5] Choudhry, R.M., Gabriel, H.F., Khan, M.K., Azhar, S.: Causes of discrepancies between design and construction in the Pakistan construction industry, Journal of Construction in Developing Countries, 22 (2018) 2, pp. 1–18.

[6] Dey, P.P., Khan, M., Amin, M., Sinha, B.R., Badkoobehi, H., Jawad, S., Any, L.A.: Managing interacting software project risks, PressAcademia Procedia, Global Business Research Congress (GBRC), Istanbul, 2016.

[7] Cerić, A., Ivić, I.: Network analysis of interconnections between theoretical concepts associated with principal-agent theory concerning construction projects, Organization, Technology and Management in Construction, 13 (2021) 1, pp. 2450–2464.

[8] Cerić, A.: Minimising communication risk in construction: a Delphi study of the key role of project managers, Journal of Civil Engineering and Management, 20 (2014) 6, pp. 829–838.

[9] Cerić, A.: Reducing information asymmetry and building trust in projects using blockchain technology, GRAĐEVINAR, 73 (2021) 10, pp. 967-978, doi: https://doi.org/10.14256/JCE.3310.2021

[10] Jäger, C.: The Principal-Agent Theory within the Context of Economic Sciences, Books on Demand GmbH, 2008.

[11] Liu, J., Ma, G.: Study on incentive and supervision mechanisms of technological innovation in megaprojects based on the principal-agent theory, Engineering, Construction and Architectural Management, 28 (2020) 6, pp. 1593–1614.

[12] Flanagan, R., Norman, G.: Risk Management and Construction, Blackwell Science, Oxford, 1993.

[13] ISO: Risk management - Guidelines, ISO 31000:2018, 2018.

[14] Owusu-Manu, D.-G., Kukah, A.S., Boateng, F., Asumadu, G., Edwards, D.J.: Exploring strategies to reduce moral hazard and adverse selection of Ghanaian public–private partnership (PPP) construction projects, Journal of Engineering, Design and Technology, 19 (2021) 2, pp. 358–372.

[15] Cantarelli, C.C., Chorus, C.G., Cunningham, S.W.: Explaining cost overruns of large-scale transportation infrastructure projects using a signalling game, Transportmetrica A: Transport Science, 9 (2013) 3, pp. 239–258.

[16] Ivić, I., Cerić, A.: Risks caused by information asymmetry in construction projects: a systematic literature review, Sustainability, 15 (2023) 13, 9979.

[17] Cerić, A., Ivić, I.: Management of risks influenced by information asymmetry during construction: Framework for research, 7th International Project and Construction Management Conference (IPCMC2022), eds. C. Budayan, S. Kivrak, S. Ulubeyli, Yildiz Technical University, Istanbul, pp. 1099–1110, 2022.

[18] Lupia, A.: Delegation of power: agency theory, International Encyclopedia of the Social & Behavioral Sciences, ed. J.D. Wright, Elsevier, Amsterdam, pp. 58–60, 2015.

[19] Jensen, M.C., Meckling, W.H.: Theory of the firm: Managerial behavior, agency costs and ownership structure, Journal of Financial Economics, 3 (1976) 4, pp. 305–360.

[20] Eisenhardt, K.M.: Agency theory: An assessment and review, Academy of Management Review, 14 (1989) 1, pp. 57–74.

[21] Ivić, I.: Upravljanje rizicima prouzročenima informacijskom asimetrijom u građevinskim projektima, doktorski rad, Građevinski fakultet, Sveučilište u Zagrebu, 2024.

[22] Bernhold, T., Wiesweg, N.: Principal-agent theory: perspectives and practices for effective workplace solutions, A Handbook of Management Theories and Models for Office Environments and Services, eds. V. Danivska & R.Appel-Meulenbroek, Routledge, Oxon, pp. 117–128, 2022.

[23] Xiang, P., Zhou, J., Zhou, X., Ye, K.: Construction project risk management based on the view of asymmetric information, Journal of Construction Engineering and Management, 138 (2012) 11, pp. 1303–1311.

[24] Ebers, M., Gotsch, W.: Institutionsökonomische Theorien der Organisation, Organisationstheorien, eds. A. Kieser & M. Ebers, Kohlhammer, Stuttgart, pp. 247–308, 2006.

[25] Picot, A., Dietl, H., Franck, E.: Organisation – Eine ökonomische Perspektive, Schäffer-Poeschel, Stuttgart, 1999.

[26] Mendeley, https://www.mendeley.com/search/, 7.8.2025.

[27] Page, M.J., McKenzie, J.E., Bossuyt, P.M., Boutron, I., Hoffmann, T.C., Mulrow, C.D., et al.: The PRISMA 2020 statement: an updated guideline for reporting systematic reviews, BMJ, 372 (2021), n71.

[28] Hansen, S.: Characterizing interview-based studies in construction management research: Analysis of empirical literature evidences, The 2nd International Conference on Innovations in Social Sciences Education and Engineering (ICoISSEE), Bandung, Indonesia.

[29] Bengtsson, M.: How to plan and perform a qualitative study using content analysis, NursingPlus Open, 2 (2016), pp. 8–14.

[30] Forman, J., Damschroder, L.: Qualitative content analysis, Empirical Methods for Bioethics: A Primer (Advances in Bioethics, Vol. 11), eds. L. Jacoby & L.A. Siminoff, Emerald, Bingley, pp. 39–62, 2008.

[31] Ahmed, M.O., El-adaway, I.H., Coatney, K.T., Eid, M.S.: Construction bidding and the winner's curse: game theory approach, Journal of Construction Engineering and Management, 142 (2016), 04015076.

[32] Owusu-Manu, D.G., Kukah, A.S.K., Edwards, D.J., Ameyaw, E.E.: Fuzzy synthetic evaluation of moral hazard and adverse selection of public private partnership projects, International Journal of Construction Management, 23 (2023) 11, pp. 1805–1814.

[33] Owusu-Manu, D.G., Edwards, D.J., Kukah, A.S., Parn, E.A., El-Gohary, H., Hosseini, M.R.: An empirical examination of moral hazards and adverse selection on PPP projects: A case study of Ghana, Journal of Engineering, Design and Technology, 16 (2018) 6, pp. 910–924.

[34] Owusu-Manu, D.G., Kukah, A.S., Edwards, D.J., Pärn, E.A., El-Gohary, H., Aigbavboa, C.: Causal relationships of moral hazard and adverse selection of Ghanaian Public-Private-Partnership (PPP) construction projects, Journal of Engineering, Design and Technology, 16 (2018) 3, pp. 439–460.

[35] Xiang, P., Jia, F., Li, X.: Critical behavioral risk factors among principal participants in the Chinese construction industry, Sustainability, 10 (2018), 3158.

[36] Xiang, P., Huo, X., Shen, L.: Research on the phenomenon of asymmetric information in construction projects - The case of China, International Journal of Project Management, 33 (2015) 3, pp. 589–598.

[37] Feser, D., Runst, P.: Energy efficiency consultants as change agents? Examining the reasons for EECs' limited success, Energy Policy, 98 (2016), pp. 309–317.

[38] Forsythe, P., Sankaran, S., Biesenthal, C.: How far can BIM reduce information asymmetry in the Australian construction context?, Project Management Journal, 46 (2015) 3, pp. 75–87.

[39] Giraudet, L.-G.: Energy efficiency as a credence good: A review of informational barriers to energy savings in the building sector, Energy Economics, 87 (2020), 104698.

[40] Xue, F., Chen, G., Huang, S., Xie, H.: Design of social responsibility incentive contracts for stakeholders of megaprojects under information asymmetry, Sustainability, 14 (2022) 3, 1465.

[41] Lewis, G., Bajari, P.: Moral hazard, incentive contracts, and risk: Evidence from procurement, The Review of Economic Studies, 81 (2014) 3, pp. 1201–1228.

[42] Li, Y., Ning, Y.: Mitigating opportunistic behaviors in consulting projects: Evidence from the outsourced architectural and engineering design, Journal of Construction Engineering and Management, 148 (2022) 7, 04022044.

[43] Pesek, A.E., Smithwick, J.B., Saseendran, A., Sullivan, K.T.: Information asymmetry on heavy civil projects: Deficiency identification by contractors and owners, Journal of Management in Engineering, 35 (2019) 4, 04019008.

[44] Schieg, M.: Strategies for avoiding asymmetric information in construction project management, Journal of Business Economics and Management, 9 (2008) 1, pp. 47–51.

[45] Marinho, A., Couto, J., Teixeira, J.: Relational contracting and its combination with the BIM methodology in mitigating asymmetric information problems in construction projects, Journal of Civil Engineering and Management, 27 (2021) 4, pp. 217–229.

[46] Xu, Q., Chong, H.-Y., Liao, P.-C.: Collaborative information integration for construction safety monitoring, Automation in Construction, 102 (2019), pp. 120–134.

[47] Missbauer, H., Hauber, W.: Bid calculation for construction projects: Regulations and incentive effects of unit price contracts, European Journal of Operational Research, 171 (2006) 3, pp. 1005–1017.

[48] Snippert, T., Witteveen, W., Boes, H., Voordijk, H.: Barriers to realizing a stewardship relation between client and vendor: The Best Value approach, Construction Management and Economics, 33 (2015) 7, pp. 569–586.

[49] Ward, S.C., Chapman, C.B., Curtis, B.: On the allocation of risk in construction projects, International Journal of Project Management, 9 (1991) 3, pp. 140–147.

[50] Tserng, H.P., Ho, S.-P., Chou, J.-S., Lin, C.: Proactive measures of governmental debt guarantees to facilitate Public-Private Partnerships project, Journal of Civil Engineering and Management, 20 (2014) 4, pp. 548–560.

[51] Ive, G., Chang, C.-Y.: The principle of inconsistent trinity in the selection of procurement systems, Construction Management and Economics, 25 (2007) 7, pp. 677–690.

[52] Zhao, H., Liu, X., Wang, Y.: Evolutionary game analysis of opportunistic behavior of Sponge City PPP projects: a perceived value perspective, Scientific Reports, 12 (2022) 1, 8798.

[53] Chang, C.-Y., Ive, G.: Reversal of bargaining power in construction projects: Meaning, existence and implications, Construction Management and Economics, 25 (2007) 8, pp. 845–855.

[54] Chang, C.-Y., Ive, G.: The hold-up problem in the management of construction projects: A case study of the Channel Tunnel, International Journal of Project Management, 25 (2007) 4, pp. 394–404.

[55] Chang, C.-Y.: Understanding the hold-up problem in the management of megaprojects: The case of the Channel Tunnel Rail Link project, International Journal of Project Management, 31 (2013) 4, pp. 628–637.

[56] Williamson, O.E.: Public and private bureaucracies: A transaction cost economics perspectives, Journal of Law, Economics, and Organization, 15 (1999) 1, pp. 306–342.

[57] Yao, M., Wang, F., Chen, Z., Ye, H.: Optimal incentive contract with asymmetric cost information, Journal of Construction Engineering and Management, 146 (2020) 6, 04020054.

[58] Rosenfeld, Y., Geltner, D.: Cost-plus and incentive contracting: Some false benefits and inherent drawbacks, Construction Management and Economics, 9 (1991) 5, pp. 481–490.

[59] Lützkendorf, T., Speer, T.M.: Alleviating asymmetric information in property markets: building performance and product quality as signals for consumers, Building Research & Information, 33 (2005) 2, pp. 182–195.

[60] Liu, D., Xu, W., Li, H., Zhang, W., Wang, W.: Moral hazard and adverse selection in Chinese construction tender market: A case of Wenchuan earthquake, Disaster Prevention and Management, 20 (2011) 4, pp. 363–377.

[61] Xiang, P., Wang, J.: Research on preventing moral hazard of construction project based on information asymmetries, The Open Construction & Building Technology Journal, 8 (2014), pp. 468–475.

[62] Li, H., Lv, L., Zuo, J., Su, L., Wang, L., Yuan, C.: Dynamic reputation incentive mechanism for urban water environment treatment PPP projects, Journal of Construction Engineering and Management, 146 (2020) 8, 04020088.

[63] Liu, J., Wang, Y., Wang, Z.: Multidimensional drivers: exploring contractor rule violations in the construction industry, Engineering, Construction and Architectural Management, 30 (2023) 4, pp. 1496–1518.

[64] Liu, X., Lin, S., Liu, L., Qian, F., Zhang, K.: Exploring the factors triggering occupational ethics risk of technology transaction in Chinese construction industry, International Journal of Environmental Research and Public Health, 17 (2020) 4, 1175.

[65] Ma, L., Zhang, P.: Game analysis on moral hazard of construction project managers in China, International Journal of Civil Engineering, 12 (2014) 4A, pp. 429–438.

[66] Ma, T., Wang, Z., Ding, J.: Governing the moral hazard in China's sponge city projects: A managerial analysis of the construction in the non-public land, Sustainability, 10 (2018) 9, 3018.

[67] Shi, L., He, Y.J., Onishi, M., Kobayashi, K.: Double moral hazard and risk-sharing in construction projects, IEEE Transactions on Engineering Management, 68 (2021) 6, pp. 1919–1929.

[68] Wu, Y., Huang, Y., Luo, W., Li, C.: Construction supervision mechanism for public projects in China: Progress goal-oriented perspective, Journal of Management in Engineering, 30 (2014) 2, pp. 205–213.

[69] Xie, L., Xu, T., Ju, T., Xia, B.: Explaining the alienation of megaproject environmental responsibility behavior: a fuzzy set qualitative comparative analysis study in China, Engineering, Construction and Architectural Management, 30 (2023) 7, pp. 2794–2813.

[70] Xiong, W., Chen, B., Wang, H., Zhu, D.: Transaction hazards and governance mechanisms in Public-Private Partnerships: A comparative study of two cases, Public Performance & Management Review, 42 (2019) 6, pp. 1279–1304.

[71] Cheng, H., Zheng, S.: Incentive compensation mechanism for the infrastructure construction of electric vehicle battery swapping station under asymmetric information, Sustainability, 14 (2022) 12, 7041.

[72] Lampel, J., Miller, R., Floricel, S.: Impact of owner involvement on innovation in large projects: Lessons from power plants construction, International Business Review, 5 (1996) 6, pp. 561–578.

[73] Lampel, J., Miller, R., Floricel, S.: Information asymmetries and technological innovation in large engineering construction projects, R&D Management, 26 (1996) 4, pp. 357–369.

[74] Wu, G., Zuo, J., Zhao, X.: Incentive model based on cooperative relationship in Sustainable construction projects, Sustainability, 9 (2017) 7, 1191.

[75] Du, Y., Zhou, H., Yuan, Y., Xue, H.: Exploring the moral hazard evolutionary mechanism for BIM implementation in an integrated project team, Sustainability, 11 (2019) 20, 5719.

[76] Chen, T.-C., Lin, Y.-C., Wang, L.-C.: The analysis of BOT strategies based on game theory - Case study on Taiwan's high speed railway project, Journal of Civil Engineering and Management, 18 (2012) 5, pp. 662–674.

[77] González-Díaz, M., Arruñada, B., Fernández, A.: Causes of subcontracting: Evidence from panel data on construction firms, Journal of Economic Behavior & Organization, 42 (2000) 2, pp. 167–187.

[78] Ho, P.S., Levitt, R., Tsui, C.-W., Hsu, Y.: Opportunism-focused transaction cost analysis of public-private partnerships, Journal of Management in Engineering, 31 (2015) 6, 04015007.

[79] Montrimas, A., Bruneckienė, J., Gaidelys, V.: Beyond the socio-economic impact of transport megaprojects, Sustainability, 13 (2021) 15, 8547.

[80] Han, H., Shen, J., Liu, B., Han, H.: Dynamic incentive mechanism for large-scale projects based on the reputation effects, SAGE Open, 12 (2022) 4.

[81] Badenfelt, U.: The selection of sharing ratios in target cost contracts, Engineering, Construction and Architectural Management, 15 (2008) 1, pp. 54–65.

[82] Guo, S., Wang, J., Xiong, H.: The influence of effort level on profit distribution strategies in IPD projects, Engineering, Construction and Architectural Management, 30 (2023) 9, pp. 4099–4119.

[83] Chen, W., Li, L.: Incentive contracts for green building production with asymmetric information, International Journal of Production Research, 59 (2021) 6, pp. 1860–1874.

[84] Fernández-Solís, J.L., Rybkowski, Z.K., Xiao, C., Lü, X., Chae, L.S.: General contractor's project of projects – a meta-project: understanding the new paradigm and its implications through the lens of entropy, Architectural Engineering and Design Management, 11 (2015) 3, pp. 213–242.

[85] Zheng, L., Lu, W., Chen, K., Chau, K.W., Niu, Y.: Benefit sharing for BIM implementation: Tackling the moral hazard dilemma in inter-firm cooperation, International Journal of Project Management, 35 (2017) 3, pp. 393–405.

[86] Cao, D., Wang, G.: Contractor–subcontractor relationships with the implementation of emerging interorganizational technologies: roles of cross-project learning and pre-contractual opportunism, International Journal of Construction Education and Research, 10 (2014) 4, pp. 268–284.

[87] Yiyong, L., Yousong, W., Jingkuang, L.: Analysis of adverse selection for motivation mechanism in engineering project cost management, Research Journal of Applied Sciences, Engineering and Technology, 5 (2013), pp. 3777–3782.

[88] Liang, X., Shen, G.Q., Guo, L.: Optimizing incentive policy of energy-efficiency retrofit in public buildings: A principal-agent model, Sustainability, 11 (2019) 12, 3442.

[89] Wu, G.: A multi-objective trade-off model in sustainable construction projects, Sustainability, 9 (2017) 11, 1929.

[90] Warsame, A., Borg, L., Lind, H.: How can clients improve the quality of transport infrastructure projects? The role of knowledge management and incentives, The Scientific World Journal, 2013, 709423.

[91] Singh, A.K., Prasath Kumar, V.R.: Smart contracts and supply chain management using blockchain, Journal of Engineering Research, 9 (2022), pp. 1–11.

[92] Sun, J., Wang, L.: The interaction between BIM's promotion and interest game under information asymmetry, Journal of Industrial and Management Optimization, 11 (2015) 4, pp. 1301–1319.

[93] Ivić, I., Cerić, A.: Mitigation measures for information asymmetry between participants in construction projects: The impact of trust, Sustainability, 16 (2024), 6808.

[94] Hajjej, I., Hillairet, C., Mnif, M., Pontier, M.: Optimal contract with moral hazard for Public Private Partnerships, Stochastics, 89 (2017) 6–7, pp. 1015–1038.

[95] Shi, S., Yin, Y., An, Q., Chen, K.: Optimal build-operate-transfer road contracts under information asymmetry and uncertainty, Transportation Research Part B: Methodological, 152 (2021), pp. 65–86.

[96] Shi, S., Yin, Y., Guo, X.: Optimal choice of capacity, toll and government guarantee for build-operate-transfer roads under asymmetric cost information, Transportation Research Part B: Methodological, 85 (2016), pp. 56–69.

[97] Su, P., Peng, Y., Hu, Q., Tan, R.: Incentive mechanism and subsidy design for construction and demolition waste recycling under information asymmetry with reciprocal behaviors, International Journal of Environmental Research and Public Health, 17 (2020) 12, 4346.

[98] Wang, Y., Cui, P., Liu, J.: Analysis of the risk-sharing ratio in PPP projects based on government minimum revenue guarantees, International Journal of Project Management, 36 (2018) 6, pp. 899–909.

[99] Wang, Y., Gao, H.O., Liu, J.: Incentive game of investor speculation in PPP highway projects based on the government minimum revenue guarantee, Transportation Research Part A: Policy and Practice, 125 (2019), pp. 20–34.

[100] Zhang, R., Zhou, Y., Zhuang, H., Zhu, X.: Study on the project supervision system based on the principal-agent theory, Journal of Industrial Engineering and Management, 8 (2015) 2, pp. 491–508.

[101] Zhao, L., Zhong, S.: Analysis of collusion between contractors and supervisors in constructions, Journal of Southwest Jiaotong University, 48 (2013) 6, pp. 1136–1141.

[102] Nie, X., Wang, Y., Wang, B.: Quality control of water conservancy construction projects considering contractor's credibility, Journal of Coastal Research, 104 (2020), pp. 410–414.

Primljen / Received: 30.10.2025.
Ispravljen / Corrected: 3.5.2026.
Prihvaćen / Accepted: 7.5.2026.
Dostupno online / Available online: 10.6.2026.

Monitoring seismic activity following 2020 Petrinja earthquake

Authors:


Assoc.Prof. **Josip Stipčević**
jstipcevic.geof@pmf.hr
Autor za korespondenciju


Krešimir Kuk, mag.phys.-geophys.
kreso.kuk@gfz.hr


Assoc.Prof. **Iva Dasović**
iva.dasovic@gfz.hr


Dinko Šindija, PhD. Geoph
dsindija@gmail.com


Kristina Šariri, PhD. Geoph
ksariri@gfz.h


Marin Sečanj, PhD. Geoph
msecanj@gfz.hr


Prof. **Davorka Herak**
davorka.herak@gfz.hr


Academician **Marijan Herak**
marijan.herak@gfz.hr

University of Zagreb
Faculty of Science
Department of Geophysics

Original research paper

Josip Stipčević, Krešimir Kuk, Iva Dasović, Dinko Šindija, Kristina Šariri, Marin Sečanj, Davorka Herak, Marijan Herak

Monitoring seismic activity following 2020 Petrinja earthquake

The series of earthquakes in the Petrinja area began on Monday, 28 December 2020, at 6:28 a.m. local time (CET), with an earthquake of magnitude M_L = 5.1 (M_W = 4.9), which was felt across most of central Croatia. Its epicentre was southwest of Petrinja, near Strašnik village. This was soon followed by earthquakes of local magnitude 4.6, 7:49 a.m. and magnitude 3.8 at 7:51 a.m. in the same epicentral area, as well as a series of weaker earthquakes. Unfortunately, these relatively strong earthquakes proved to be just foreshocks, as an even stronger earthquake of local magnitude 6.2 (M_W = 6.4) occurred the next day, 29 December 2020, at 12:19 p.m., also with an epicentre near Strašnik. The cornerstone of this study is the vast amount of seismological data collected. We used both manual and advanced machine learning techniques to analyse the newly collected dataset. This resulted in a substantially expanded seismic catalogue with over 50,000 events. Seismicity analysis confirms that the largest events align with the primary dextral strike-slip Petrinja Fault; however, the aftershock pattern evolved, revealing that stress redistribution activated numerous secondary faults, leading to a complex spatial and temporal distribution of seismicity. The findings provide a detailed seismological record and crucial insights into the tectonic processes of this intraplate region.

Key words:
Petrinja, earthquake, aftershock, seismic network, machine learning

Izvorni znanstveni rad

Josip Stipčević, Krešimir Kuk, Iva Dasović, Dinko Šindija, Kristina Šariri, Marin Sečanj, Davorka Herak, Marijan Herak

Praćenje seizmičke aktivnosti nakon potresa u Petrinji 2020. godine

Niz potresa na području Petrinje započeo je u ponedjeljak 28. prosinca 2020. u 6:28 po lokalnome vremenu (CET) potresom magnitude M_L = 5,1 (M_W = 4,9), koji se osjetio na većemu dijelu središnje Hrvatske. Epicentar se nalazio jugozapadno od Petrinje, u blizini sela Strašnika. Ubrzo su uslijedili potresi lokalne magnitude 4,6 u 7.49 te magnitude 3,8 u 7:51 u istome epicentralnom području, kao i niz slabijih potresa. Nažalost, ti relativno snažni potresi pokazali su se tek prethodnim potresima, jer je već sljedećeg dana, 29. prosinca 2020. u 12:19, zabilježen još jači potres lokalne magnitude 6,2 (M_W = 6,4), također s epicentrom u blizini Strašnika. Temelj ove studije čini velika količina prikupljenih seizmoloških podataka. Za analizu novoprikupljenog skupa podataka korišteni su klasični postupci analize te napredne metode strojnog učenja. Time je dobiven znatno proširen seizmički katalog s više od 50.000 potresa. Analiza seizmičnosti potvrđuje da su najveći potresi usklađeni s glavnim desnim Petrinjskim rasjedom, s pomakom po pružanju, no evolucija naknadnih potresa pokazala je da je preraspodjela naprezanja aktivirala brojne sekundarne rasjede, što je dovelo do složene prostorne i vremenske raspodjele seizmičnosti. Rezultati pružaju detaljan seizmološki uvid u procese u tome žarišnom području unutar tektonske ploče.

Ključne riječi:
Petrinja, potres, naknadni potresi, seizmička mreža, strojno učenje

1. Introduction

The Petrinja earthquake (M_w = 6.4; M_L = 6.2) on 29 December 2020 was one of the most important earthquakes that occurred in Croatia over the last several centuries. The mainshock was preceded by a strong foreshock (M_w = 4.9; M_L = 5.0) that occurred one day earlier, whereas the largest aftershock (M_w = 4.7; M_L = 4.9) was recorded on 6 January 2021. The seismicity of the area and detailed analyses of the famous Kupa Valley earthquake are presented in, for example, u [1, 2].

According to [1], the mainshock caused extensive destruction in the epicentral area. Shaking was felt throughout Croatia and Slovenia, as well as across much of Bosnia and Herzegovina, Serbia, Hungary, Italy, Austria, and Slovakia, with seven fatalities reported. Ground shaking triggered numerous secondary effects, including liquefaction, mud boils, sand volcanoes, landslides, and more than 100 sinkholes near the village of Mečenčani, southeast of the epicentre (Figure 1). Further details on the impact, damage and related effects are provided in, for example, [3-9]. This large intraplate strike-slip event drew considerable attention from the international seismological community. A preliminary analysis of early observations was provided by [10], whereas numerous subsequent studies focused on characterising the seismic source (e.g. [11-16]). The Coulomb stress changes following the main rupture were examined by [1, 14, 15, 17]. Several studies have analysed InSAR satellite data to interpret surface deformation (e.g. [14, 15, 18, 19]). A detailed spatio-temporal analysis of the Petrinja earthquake sequence during its first six months, including the relocation of more than 13,800 events using source-specific station corrections, evaluation of epistemic location uncertainty, computation of focal mechanisms, and assessment of competing finite-fault models, was presented by [1]. In this study, we provide a brief overview of the region's tectonics and describe the rapid deployment of seismic instruments following the Petrinja mainshock. Furthermore, we present an overview of the seismicity in the Petrinja epicentral area from 2020 to 2024. For seismicity monitoring, we employ two types of earthquake detection in seismograms: manual and machine learning (ML) approaches. The overall aim of this study is to outline the seismological work conducted in the five years following the Petrinja earthquake.

2. Tectonics and geology

The Central Croatia region, together with the Petrinja area, lies within the transition zone between the Internal Dinarides and SW Pannonian Basin structural units. This area has been subjected to multiple tectonic phases since the Late Jurassic, resulting in a complex geological and geodynamic setting. The present-day Adria–Europe shortening is predominantly accommodated within the External Dinarides and partly transmitted to the Internal Dinarides and the Dinarides–Pannonian basin transition area [20]. The active NNE-SSW compression within the study area is evidenced by earthquake focal mechanism solutions [21] and predicted by geodynamic modelling. Throughout the Late Cretaceous – Early Palaeogene, the broader Petrinja area formed part of the Sava realm of the Neotethys Ocean and was subjected to the ongoing subduction of remnant oceanic crust beneath European-derived tectonic units. At that time, the Sava oceanic realm was closed along the Sava Suture Zone (SSZ) [22, 23]. Regional compression-related tectonic uplift, folding, and imbrication of older units and associated syn-orogenic deposits were active in the region until the Mid-Eocene [20, 22]. Concurrently, thrusting propagated SW towards the Adriatic foreland and led to the onset of the nappe stack and formation of the Oligocene to Mid-Eocene External Dinarides fold-thrust belt and foreland basin. In the northern Internal Dinarides, a turnover from Late Cretaceous to Mid-Eocene compression to Early Miocene extension occurred along the SSZ, leading to the formation of the Sava Depression, that is, the south-westernmost basin of the Miocene Pannonian back-arc basin system [22]. The Sava Depression began to open during the Early Miocene (c. 18 Ma). This Early Miocene extensional detachment also led to the exhumation of the Internal Dinarides and the SSZ units in its footwall, in the form of core complexes (inselbergs in the present-day morphology).

The opening of regional- and local-scale Miocene basins was accompanied by the deposition of syn- to post-tectonic sedimentary units, which are presently partly exposed along the Sava Depression margins. In the Sava Depression, the Early Miocene syn-rift phase presumably lasted until the Middle Miocene (c. 13.5 Ma; [24]). It was subsequently followed by a post-rift, regionally widespread thermal subsidence phase, which is known to have started across the Pannonian basin system during the late Middle Miocene. Within the sedimentary fill across the Pannonian basin system, this phase is commonly recognized by the substantial thickness of Upper Miocene (Pannonian) sediments (c. 11.6-4.5 Ma) and an almost complete absence of contemporaneous extensional faulting in the central and northwestern parts of the Sava Depression (e.g. [24]).

The termination of the thermal subsidence phase and onset of the successive shortening phase were not uniform across the Pannonian basin system, either spatially or temporally. In the northwestern and central parts of the Sava Depression, this shortening started by the end of the Miocene or during the Early Pliocene c. 6 Ma; [22, 24]).It was driven partly by the The epicentral area of the Petrinja 2020–2021 earthquake series extends for approximately 20 km in a NW-SE direction, at a distance of approximately 7 km to the SW of the town of Petrinja (Figure 1). It corresponds to the Hrastovica Hill, the most prominent morphological structure in the vicinity of Petrinja, whose highest peak, Cepeliš, reaches 415 m a.s.l. According to surface geological data [27], this structure is

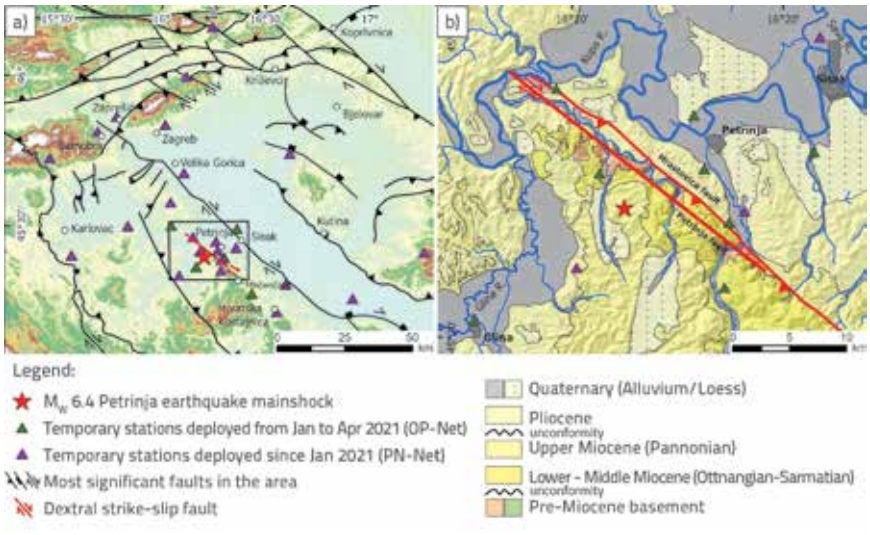

Figure 1. Fault traces are compiled from [20, 23, 25]; simplified geological map of wider Petrinja epicentral area, based on the Basic Geological Map, sheets Sisak [27] and Bosanski Novi [28]

an asymmetric anticline characterised by gently SW-dipping and steeply NE-dipping limb, the latter bounded by a NW-SE striking fault (Figure 1.b). Although the throw on this fault is presumed to be normal [27], a reverse sense of slip was observed during the 1909 earthquake and in the 2020 aftershocks. This raises the question of whether part of the c. 300 m relief represents the thrust component accumulated over several seismic cycles [21]. Locally, along its NE-dipping limb and hinge, this anticline is composed of Upper Cretaceous to Eocene rocks (basalts and pelagic limestones). These are unconformably covered by a concordant succession of Middle to Upper Miocene and Pliocene sediments, which are largely exposed along the SW-dipping limb of the anticline (Figure 1.b). The youngest sediments in the study area are Quaternary gravels, sands, silts, and clays deposited in the Kupa River floodplain and along its tributaries, locally associated with loess deposits mostly preserved in valleys but also found at higher altitudes close to the top of Hrastovica Hill.

Owing to the strength of the earthquake and the specific geological setting, in the aftermath of shaking in the wider epicentral area, a large number of secondary earthquake effects, that is, cosmic deformations on the surface, such as liquefaction, cracks, landslides, and sinkholes, were observed (e.g. [3, 29-31]).

3. Seismic networks

When a strong earthquake occurs, it is crucial for the seismological community to respond rapidly by deploying a dense network of temporary monitoring instruments throughout the broader epicentral region. This setup is essential for detecting even the weakest tremors, many of which would otherwise go undetected. The ability to accurately locate small earthquakes is vital for understanding the size and extent of the activated seismic fault(s). The accurate determination of seismic event depth is one of the most challenging aspects of earthquake analysis, as it is often the least precise and most uncertain parameter. This can be mitigated by enhancing the density and sensitivity of the seismic network, with special focus on the deployment of stations close to the main epicentral area. Moreover, as the highest number of aftershocks occur immediately following a mainshock, prompt installation of instruments in the affected areas is essential to ensure adequate recording of these events.

At the onset of the Petrinja earthquake sequence, the seismic network around the Kupa River was relatively sparse; the two nearest stations to the mainshock were located 32 and 36 km away (blue triangles in Figure 2).

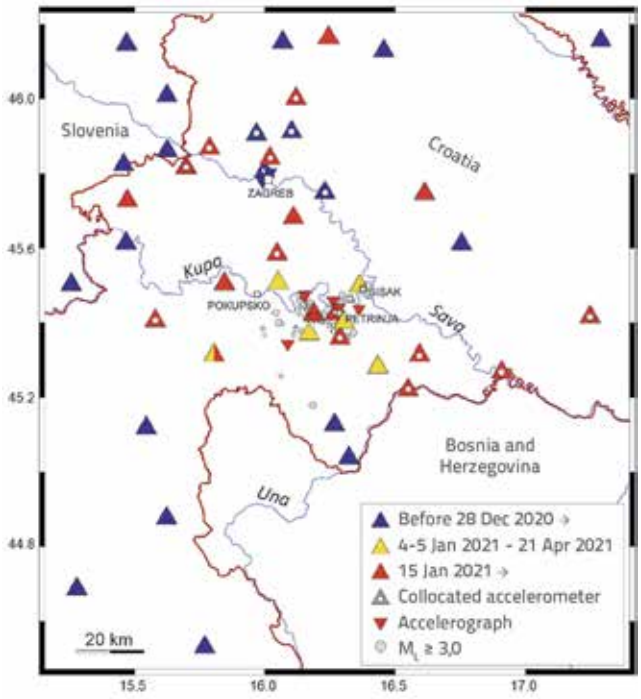

Figure 2. Seismic stations in the greater vicinity of the Petrinja earthquake epicentral area after installation of the OP-Net (yellow triangles) and PN-Net (red triangles, broad-band stations). Blue triangles represent broad-band stations operating within the Croatian CR-Network, the temporary Zagreb network, and stations from the Slovene (SL) and Hungarian (HU) networks. Small, inverted triangles denote strong-motion instruments. White circles within symbols indicate stations with collocated accelerometers. Modified after [1]

Fortunately, on 4–5 January 2021, a temporary six-station network (OP-Net; yellow triangles in Figure 2) was deployed in the epicentral area through collaboration between the National Institute of Oceanography and Applied Geophysics–OGS (Italy) and Department of Geophysics, Faculty of Science, University of Zagreb-despite the travel restrictions imposed by the COVID-19 pandemic. Shortly thereafter, by mid-January 2021, the installation of the Petrinja Network (PN-Net; red symbols in Figure 2) commenced, using newly acquired instruments by the Croatian Seismological Survey (see section 3.2 here and [1] for details). In the following section, we briefly describe the deployment of instruments and other field operations in the aftermath of the Petrinja mainshock and early phase of the aftershock sequence.

3.1. Rapid instrument deployment (OP-Net)

Because of the series of earthquakes in Zagreb that began on 22 March 2020 with M_w = 5.3 (M_L = 5.5) mainshock and the establishment of a monitoring network, Croatian seismologists were left with no free instruments to set up in the Banovina area following the late 2020 Petrinja earthquake. To address this challenge, seismologists from the Department of Geophysics, Faculty of Science, University of Zagreb quickly sought collaboration with their colleagues at the National Institute of Oceanography and Applied Geophysics (OGS, Italy). Through this partnership, the OGS generously provided six seismographs, each equipped with an integrated accelerometer, for rapid installation in the epicentral area. This collaboration was critical in ensuring that the necessary instrumentation was deployed as quickly as possible to monitor the ongoing seismic activity.

On 4–5 January 2021, only six days following the mainshock and amid restrictions imposed by the COVID-19 pandemic, five of these instruments were installed at key locations in the Banovina region at Hotnja, Sisak, Taborište, Novo Selo Glinsko, and Mečenčani (Figure 2, [32]). The placement of the two instruments at the locations in Sisak and Taborište is shown in Figures 3.a and 3.b. Additionally, one broadband seismometer from the Croatian seismic pool was installed at Petrova Gora on 4 January. The strategic placement and rapid deployment of this temporary seismic network augmented the permanent seismic network in the area, thereby improving azimuthal coverage and providing additional near-field observations. This was particularly important, as it helped reduce the uncertainty and instability often associated with the determination of earthquake location, especially focal depth (see Figure 4). With this improved coverage, even smaller earthquakes could be located more reliably, providing valuable data on the ongoing seismic activity in the region. The five short-period instruments from OP-Net were operating until mid-April 2021, when they were removed and returned to Italy.

This collaboration not only contributed to a better understanding of the seismic behaviour of the Banovina area but also highlighted the importance of international cooperation in the field of seismology. By quickly deploying a temporary network of high-quality seismic stations, the team was able to obtain crucial near-field data that was essential for monitoring aftershock activity and future seismic hazard assessments in the region.

Figure 3. Examples of installed temporary stations: a) Temporary stations in Sisak; b) and Taborište equipped with a short period instrument (seismograph with integrated accelerometer *Lunitek Sentinel-Geo*) from rapid deployment of the OP-Net; c) Temporary station in Petrinja cemetery of the Petrinja-Net with collocated seismometer *Kinemetrics MBB-2* (grey insulation box) and accelerometer *Kinemetrics ETNA2* (under green insulation box); d) accelerometer in insulation box shown at close in

3.2. Petrinja temporary seismic network (PN-Net)

Following the initial deployment of the six seismic stations from OP-Net, the Croatian Seismological Survey at the Department of Geophysics, Faculty of Science, University of Zagreb, received a substantial financial donation from the Government of the Republic of Croatia (through the Ministry of Science and Education) for the procurement of a complete set of seismological instruments for seismic monitoring. Within a very short time, 20 modern seismometers with corresponding digitisers and data storage units, as well as 20 accelerometers with all the necessary auxiliary equipment, were acquired. The instruments were purchased and delivered promptly to

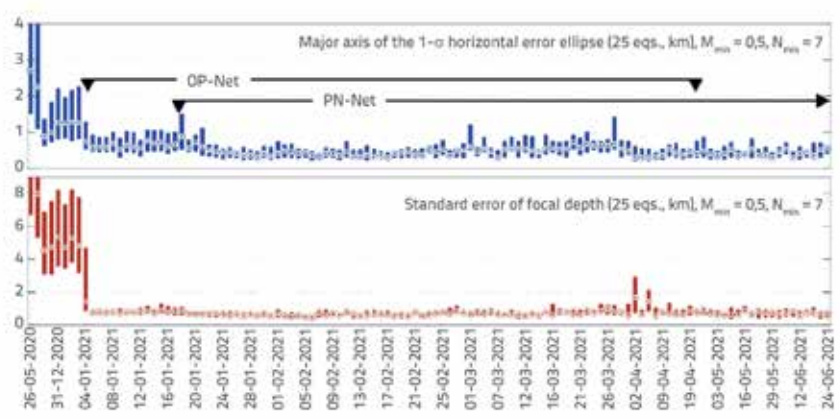

Figure 4. Temporal evolution of the 1-σ confidence radii for hypocentral locations, evaluated in non-overlapping moving windows of 25 consecutive events over the first six months of the Petrinja earthquake sequence. Only earthquakes with local magnitudes $M_L \geq 0.5$ and located with at least seven phase onset times were considered. Circled dots mark the medians, while bars indicate the 25th–75th percentile range. The periods of operation of temporary networks are shown in the top subplot.

enable the rapid commencement of instrumental recording of aftershocks that were occurring in the Petrinja fault area. The equipment was swiftly tested and configured, and the first instruments were deployed in the field only weeks after the mainshock.

In the initial phase, the instruments were installed in the immediate epicentral area, in the town of Petrinja and villages of Brest Pokupski, Hrastovica, Mošćenica, Hrvatski Čuntić, Gora, and Novi Farkašić. In the subsequent phase, temporary seismological stations were installed in the broader epicentral zone at five locations (Pobrđani (Sunja), Jasenovac, Lasinja, Omanovac, and Čazma) to obtain data from a wider geographical distribution relative to the earthquake epicentres. Several instruments were deployed in the wider Zagreb area (Marija Bistrica, Samobor, Žumberak, Ladvenjak, etc.) to monitor the Zagreb earthquake aftershock sequence that started on 22 March 2020, which was still ongoing. In the following months, continuous field inspections of the mobile seismological network were carried out to collect data and verify operational performance. Hundreds of gigabytes of valuable seismological data were collected during this period. Subsequent activities included the acquisition of new data servers, followed by the establishment of a direct real-time data transmission link from all temporary field stations to the operational centre in Zagreb.

3.3. Overall performance of temporary seismic networks

The operation of OP-Net and later PN-Net had a profound impact on the accuracy of aftershock locations. As shown in Figure 4, the establishment of OP-Net improved the confidence of epicentral determinations by roughly 50%, while the average focal-depth uncertainty decreased from about ±5 km to less than ±1 km. The location confidence was further improved after the deployment of PN-Net.

4. Seismicity monitoring following the mainshock

As discussed in the previous section, rapid and robust response to a strong earthquake is crucial, necessitating the swift deployment of a dense, temporary seismic network across the activated fault zone. This enhancement is vital for detecting even the weakest aftershocks and is the primary strategy for improving the accuracy of earthquake location, particularly the challenging task of determining focal depth. The resulting high-resolution data are essential for elucidating the complex tectonics of the sequence. For the Petrinja earthquake, this enhanced monitoring was critical for mapping the spatial distribution of seismicity across the region. While the largest events were clearly associated with the main seismogenic structure-the right-lateral Petrinja Fault-the confident location of thousands of aftershocks revealed that many smaller tremors occurred along several secondary faults activated by stress redistribution. Consequently, the rapid deployment of the OP-Net and, subsequently, the PN-Net was fundamental to capturing this detailed fault geometry and understanding the full extent of the activated zone.

Here, we present two complementary analyses, both based on the rich seismic dataset collected over several years following the Petrinja mainshock. First, we present comprehensive results from the manual analysis of the collected seismograms encompassing permanent and temporary seismic networks. In the second part, we present the results from the automatic analysis using the deep neural network earthquake-signal detector, highlighting the advantages and disadvantages of using this approach compared to manual analysis.

4.1. Petrinja earthquake series – manual catalogue

In this section, we present the results of the manual analysis of seismic records collected between 28 December 2020 and 31 December 2024. During this period, 19,570 earthquakes were located in the wider Petrinja epicentral area (Figure 5). Locations for the first six months of activity are taken from the catalogue as reported in [1], while those for the subsequent period (July 2021–December 2024) are from the Croatian Earthquake Catalogue (CEC) ([33]; latest revision in 2025). The largest events are clearly associated with the main seismogenic structure, the right-lateral Petrinja Fault (red line in Figure 5, top). However, the spatial distribution of seismicity indicates that many aftershocks also occurred along several secondary faults activated by stress redistribution following the mainshock (see also [1]). These include sources between Sisak and Petrinja,

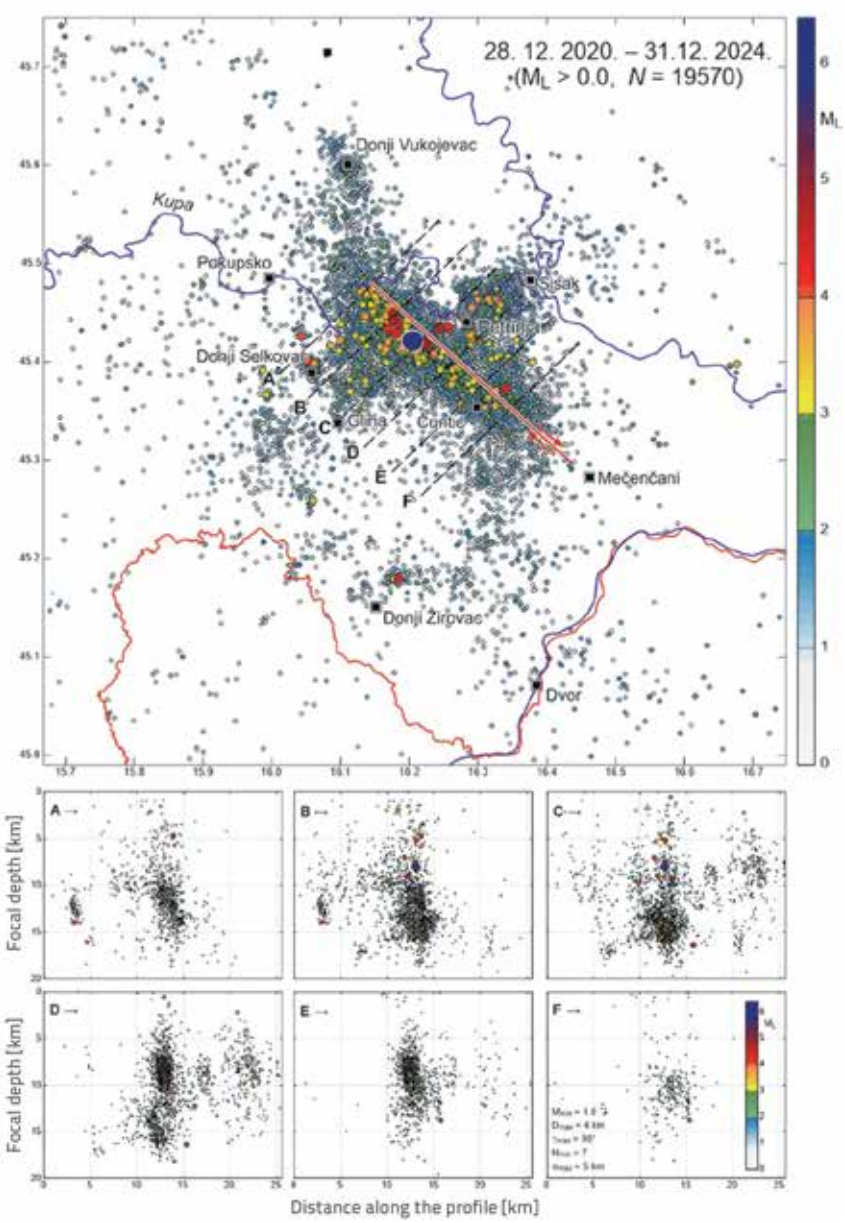

Figure 5. Top: Epicentres of all 19,570 earthquakes with magnitude M_L > 0.0 of the Petrinja sequence (2020–2024). Symbol sizes and colour scale with magnitude. The red straight line shows the simplified surface trace of the Petrinja Fault, and arrows show relative movement of the blocks. Black dashed lines indicate the traces of cross-sections A–F. Bottom: Cross-sections A–F showing vertical profiles of earthquake hypocentres that satisfy the conditions specified in subplot F (minimum magnitude M_{min} = 1.0; maximum distance from the profile D_{max} = 4 km; maximum station azimuthal gap, γ_{max} = 1.0; minimal number of phases used for locations N_{min} = 7; maximum allowed standard error of the hypocentre, σ_{max} = 5 km).

near village Donji Vukojevac, to the northeast and west of Glina, around Donji Selkovac and Donji Žirovac, and to the west of Mečenčani.

Insight into the hypocentral distribution is provided by six cross-sections (A–F) shown in the lower part of Figure 5, which include only reliably located earthquakes that meet the criteria specified in the figure caption. Most hypocentres are concentrated between depths of 5 and 15 km. The profiles delineate several activated faults, all sub-vertical or steeply dipping towards the northeast. Profile D further suggests the presence of a structural discontinuity or detachment within the Petrinja Fault zone at a depth of approximately 11 km. A more detailed analysis of these features lies beyond the scope of this study.

The temporal evolution of the Petrinja earthquake sequence is illustrated in Figure 6. During the first four days (28–31 December 2020), seismicity was almost entirely confined to the Petrinja Fault, which ruptured over a length of approximately 20 km, extending south-westward from the Kupa River towards Čuntić. Notably, several off-Petrinja Fault sources were already active in this early phase, including areas northeast of Petrinja, east of Velika Solina, and near Donji Žirovac-about 25 km from the Petrinja Fault. Most of the activity (approximately 65% of all located events) occurred in 2021. During this period, aftershocks propagated across the Kupa River, delineating a diffuse, approximately N–S-trending fault zone characterised primarily by low-magnitude events, mostly south of Donji Vukojevac. Concurrently, activity along the southeastern segment of the Petrinja Fault intensified, extending towards the village of Mečenčani and thereby increasing the total length of the activated fault segment to more than 30 km. The strongest activity in 2021, aside from that directly along the Petrinja Fault, occurred between Sisak and Petrinja, with additional aftershocks of $M_L \geq 4.0$ near Velika Solina and Donji Žirovac.

Between 2022 and 2024, earthquake activity gradually declined along the north-western part of the aftershock zone and in the Sisak–Petrinja area, while most events persisted in the south-eastern portion of the zone, east and northwest of Čuntić (clusters A and B, Figure 6). During 2022, the initially linear alignment of aftershock epicentres along the Petrinja Fault evolved into a pattern concave towards the northeast. This change reflects continuing activity within a narrow band between Glina and Donji Vukojevac, as well as in the cluster marked B in Figure 6, situated predominantly within the north-eastern block of the Petrinja Fault zone. This contrasts with the

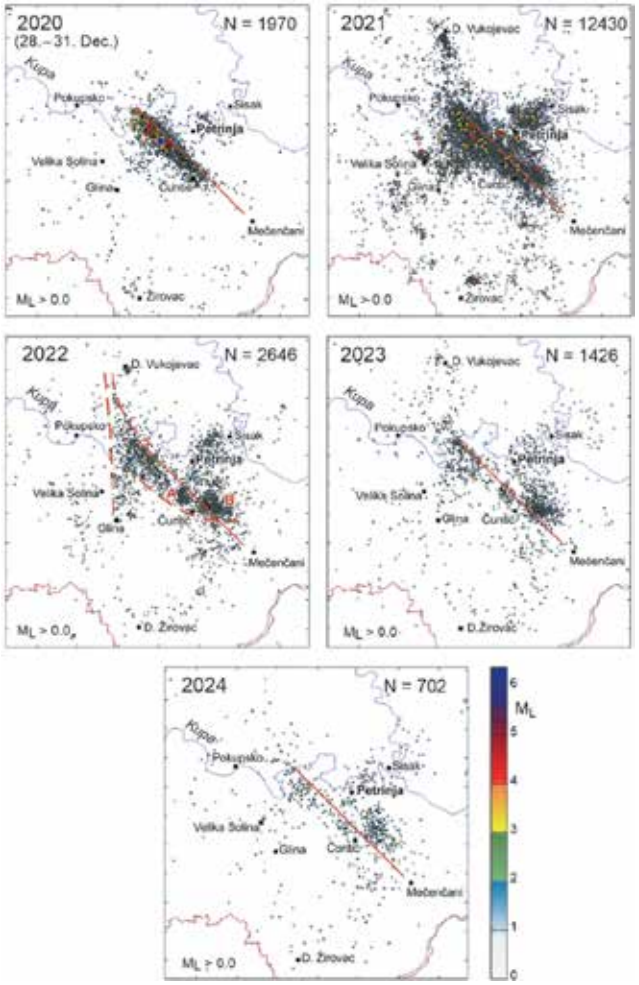

Figure 6. Epicentres of the earthquakes from the Petrinja sequence by year of occurrence (2020–2024). Total number of located events with M_L > 0.0 within each subplot is shown in the upper-right corner. Full red line marks the simplified trace of the Petrinja Fault. Dashed lines indicate observed trends

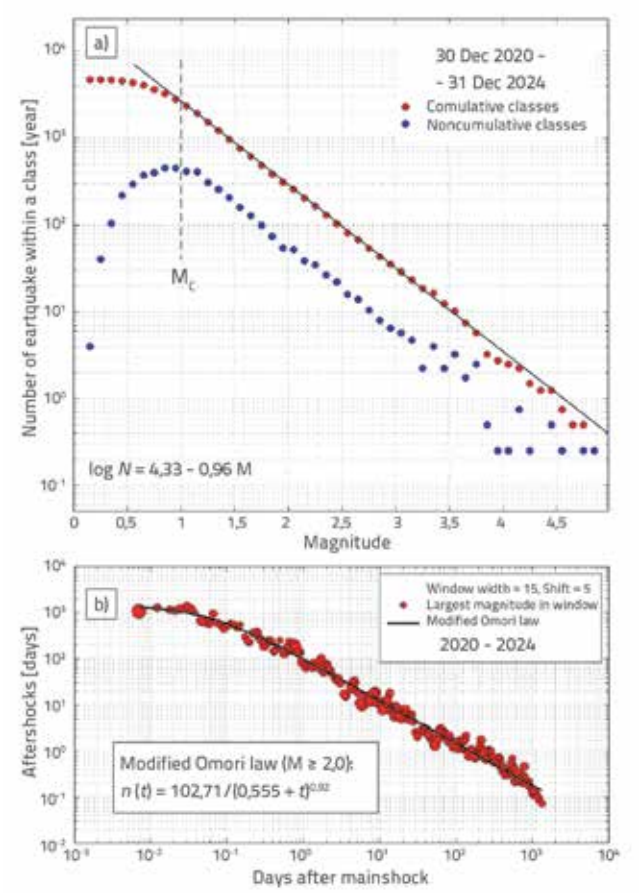

Figure 7. a) Frequency-magnitude distribution for the Petrinja sequence (2020–2024), excluding the mainshock; b) Modified Omori law showing the temporal variation in aftershock activity rates (M_L ≥ 2.0) for the Petrinja sequence (2020–2024)

main Petrinja Fault activity (e.g. cluster A and the north-western segment), where most hypocentres are in the south-western block.

The catalogue for the Petrinja earthquake sequence is found to be complete for M_L ≥ 1.0 (see Figure 7.a) starting from 30 December 2020, that is, approximately 13 hours after the mainshock to avoid the initial period when numerous small aftershocks were obscured by frequent larger events. The Gutenberg-Richter parameter b = 0.96 is slightly higher than b = 0.91 reported by [1] for the first six months and M_L ≥ 1.2. The parameters in the modified Omori law, which describe the decay rate of aftershock occurrence, remained stable throughout the sequence-the coefficients derived for the four-year period (Figure 7.b) are nearly identical to those obtained by [1] for the initial six months. This suggests that aftershock activity will continue to decrease gradually over the coming years, with seismicity unlikely to return to approximately pre-2020 levels before around 2038.

4.2. Automatic earthquake detection and location

The densification of seismic networks, such as that presented in this study, has resulted in a substantial increase in data volume and, consequently, in the time required for manual analysis of the collected data. In recent years, ML methods have emerged as efficient and reliable alternatives to traditional data processing approaches [34-36]. There are several reasons for this, most notably the speed of data analysis: a full day of continuous data can now be processed within minutes, which is particularly beneficial for smaller or underfunded institutions where manual analysis of long seismic sequences would be exceedingly time-consuming. Additionally, ML methods allow for improved and uniform accuracy, as well as the ability to quantify uncertainty in phase picks. Moreover, ML enables the detection of smaller-magnitude events and improves the identification of arrivals on noisier seismograms.

Here, the workflow and initial results from processing nearly two years of seismic data via ML are presented, covering the period from the onset of earthquake sequence to the end of November 2022 [37]. Continuous waveform data from the Croatian Seismograph Network (CR), OP-Net, and PN-Net seismic networks were analysed using the deep neural network earthquake signal detector EQTransformer [36],

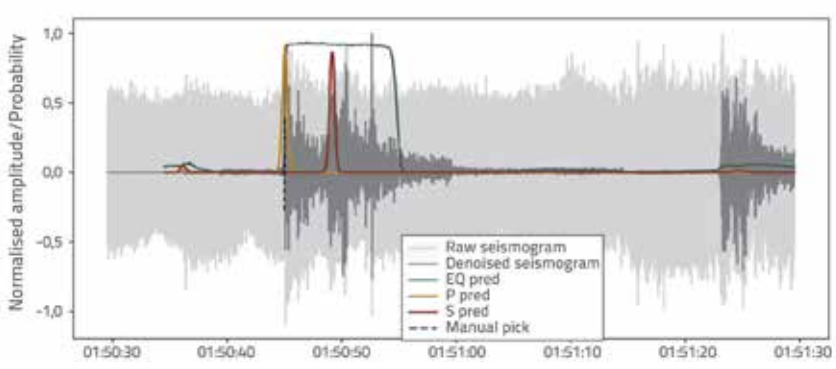

Figure 8. Example of EQTransformer detection and phase picking on a noisy seismogram from station PN03 (OP-Net). The plot shows the raw (grey) and denoised (black) seismograms, EQTransformer earthquake detection probability (green), P-phase (yellow) probability, and S-phase (red) probability, together with the manual pick (black dashed line). The event occurred on 20 January 2021 at 01:50:38 UTC and is considered a newly identified event, as it is not included in the Croatian Earthquake Catalogue

trained on the INSTANCE database [38], for detecting earthquakes and picking P- and S-phases. The detected picks were associated, and initial event locations were obtained using the PyOcto associator [39]. These preliminary locations were subsequently refined using the NonLinLoc algorithm [40], by applying source-specific station travel-time corrections [41] to improve location accuracy. Additionally, the probability output of the EQTransformer for each pick was used so that picks with higher probabilities were assigned smaller pick-time uncertainties during event location.

The initial EQTransformer analysis, with a detection threshold of 0.05 for P- and S-phases, resulted in a total of 8,953,730 seismic phases detected, comprising 6,588,039 P-phases and 2,365,691 S-phases. This large number of detected phases is to be expected, as the probability thresholds for P- and S-phases were set low. For the seismic phase association process, we varied the requirements based on the network density: for the first eight days of the sequence, that is, prior to installation of the first temporary network OP-Net, we required a minimum of five phases per event, and after 4 January 2021, we increased this requirement to a minimum of seven phases per event. After applying these association criteria, we obtained 943,844 valid picks (53% of P- and 47% of S-phases). This resulted in a seismic catalogue of 50,305 events located within the study area (15.7°–16.8° E, 44.8°–45.8° N). Of these, 34,141 events (68%) occurred by the end of June 2021, an additional 9930 events by the end of 2021, and 6,234 events by the end of the study period.

To ensure that the resulting catalogue represents real earthquakes, it was verified against CEC ([33]; latest revision in 2025) for the same study period. Events were classified as 'matched' if their origin times differed by less than two seconds from those in CEC. For events without a corresponding match in the manual catalogue, additional quality criteria were applied: an azimuthal gap smaller than 150°, at least ten associated seismic phases, and a semi-major axis of the confidence ellipsoid (as estimated by NonLinLoc) smaller than 20 km.

An example of such an event and the manner in which the EQTransformer detection and phase picking operate, is shown for station PN03 from the OP-Net network (Figure 8). The two-minute seismogram corresponds to an event with an origin time of 20 January 2021 at 01:50:38 UTC, classified as newly identified since it is absent from the Croatian Earthquake Catalogue (but present in another manual dataset with only a P-phase pick). Despite the high noise level, EQTransformer successfully detected the event and identified both P and S arrivals with peak probabilities of 0.93 and 0.87, respectively. For comparison, the denoised seismogram obtained using the deep neural network denoising/decomposition method [42] is also displayed, illustrating the underlying signal structure and the ability of the model to extract useful information from noisy data by default.

A comparison with CEC shows that 86% of its events have been successfully matched. Of the 50,305 events in the new ML catalogue and 22,386 events in CEC, 19,225 are common to both, whereas 3,161 CEC events are not detected. The analysis also identifies 31,080 new events, of which 9,184 meet the above quality criteria and are considered high-probability detections (Figure 9). The new events are concentrated near the Petrinja fault system and are consistent with the aftershock distribution of the 2020 M_w = 6.4 Petrinja earthquake. The vertical cross-sections indicate that most events are confined to the upper 15 km of the crust, with pronounced clustering at depths of 5–10 km. These depths are, on average, a

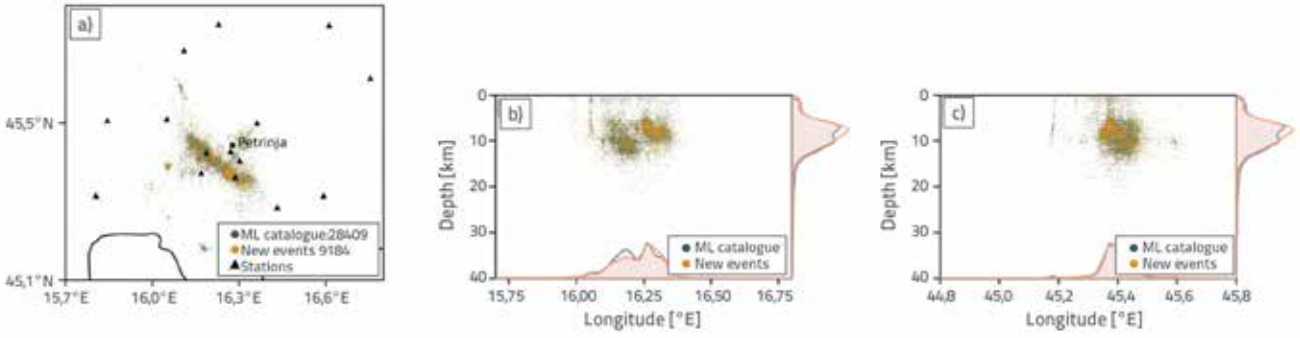

Figure 9. a) Map view of the 28,409 seismic events in our machine learning catalogue, with newly identified high-probability events highlighted in orange. Vertical cross-sections showing the depth distributions of events in the ML catalogue against longitude: b) and latitude; c), for those matching our criteria, with newly identified events highlighted

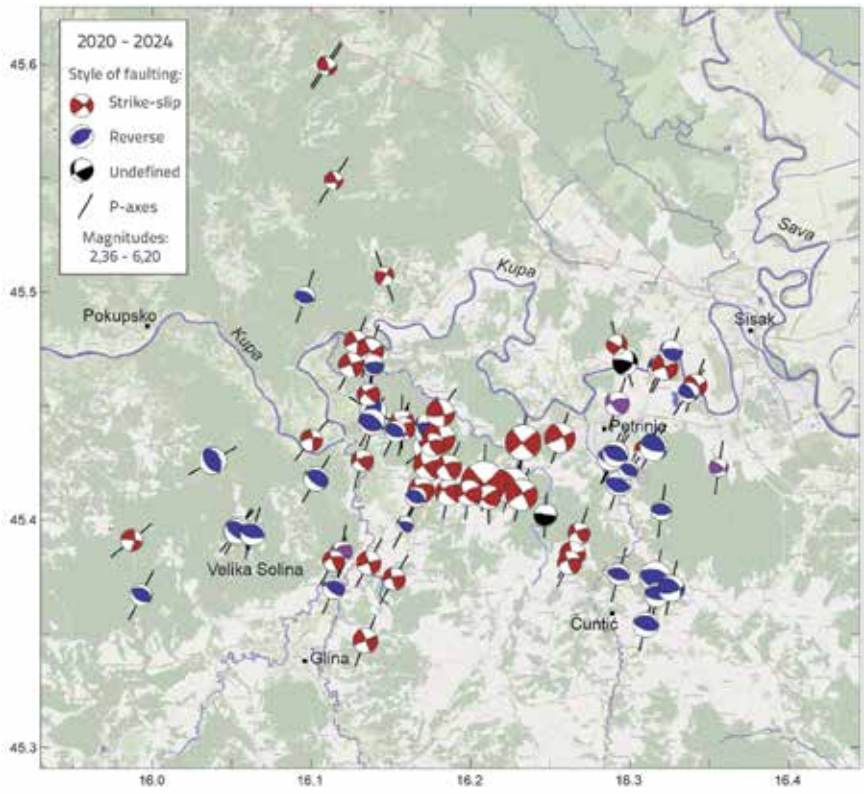

Figure 10. Focal mechanism solutions (FMS) for 2020–2024 from the CroFMS catalogue [21]. The solutions are shown as lower-hemisphere stereographic projection. The colour of the compressional quadrants denotes the style of faulting (see the legend). Short black lines indicate the orientation of the P-axes. The size of each beach-ball scales with magnitude, as shown in the legend. Only solutions of quality ≥ 2 are included.

few kilometres shallower than those in the manual catalogue, a trend also noted in previous ML studies [42].

Our results indicate that the ML workflow reproduces most manually identified events while substantially (over 50%) expanding the catalogue.

5. Focal mechanisms

This section provides a brief report on the available first-motion polarity focal mechanism solutions for the Petrinja epicentral area, collected until the end of 2024, as reported in the CroFMS catalogue [21]. The aim is to give an overview of the complex faulting associated with the Petrinja fault zone after the 2020 Petrinja earthquake.

As noted by [1], the largest events along the Petrinja Fault show predominantly strike-slip faulting (Figure 10). However, almost the same number of aftershocks occurred on reverse faults, most notably near Velika Solina, and in the clusters north-east of Čuntić and south-east of Petrinja. In their study, [1] demonstrated that the distribution of strike-slip and reverse faulting is consistent with the Coulomb failure stress change caused by the mainshock rupture.

The P-axes trend, mostly in the SSW-NNE direction, is comparable with the strike of the maximal horizontal stress (S_{Hmax}) in this area [21]. It is interesting to note that the P-axis of the mainshock strikes almost N–S, which implies an average clockwise rotation of the P-axis in the aftershock sequence of approximately 16° [1].

6. Discussion and conclusion

The comprehensive analysis of the Petrinja earthquake sequence from 2020 to 2024, supported by both manual and advanced ML techniques, provides a significantly enhanced view of the seismic and tectonic processes active in this crucial transition zone between the Internal Dinarides and the SW Pannonian Basin.

A critical element of this work was the rapid and collaborative deployment of temporary seismic networks, specifically the Italian-Croatian OP-Net and subsequent PN-Net. These deployments augmented the sparse permanent network, leading to significant improvements in the number of stations and data quality. The enhanced network density was instrumental in reducing the uncertainty of hypocentral locations, particularly focal depth, which is essential for accurate fault-plane mapping (Figure 4).

It is unfortunate that the earthquake struck an area that had not been adequately monitored, largely due to funding limitations in previous years. In particular, the absence of strong-motion instruments (accelerographs) meant that a unique opportunity to collect ground-acceleration data in the near-field of a large strike-slip earthquake was lost. Such data would have been the most valuable addition to the database of strong-motion records in Croatia. However, the deployment of the OP-Net (comprising both geophones and accelerographs), and later PN-Net, enabled the recording of acceleration during the strongest aftershock on 6 January 2021, as well as during all subsequent significant events.

The ability to swiftly deploy instruments enabled the capture of the highest-intensity aftershock period immediately following the mainshock. Furthermore, the immense data volume was efficiently processed using ML techniques, which substantially expanded the earthquake catalogue by over 50%, successfully detecting thousands of low-magnitude events missed by manual analysis and thereby validating the use of advanced methods in post-seismic monitoring.

The detailed analysis of nearly 20,000 manually located and over 50,000 ML-detected events (Figures 5 and 9) confirms that the largest earthquakes occurred along the right-lateral Petrinja fault, an active structure in the complex transition zone between the Dinarides and the Pannonian Basin. However, the seismicity distribution evolved over time, showing a complex pattern in which stress redistribution after the main rupture activated numerous secondary faults extending beyond the main fault trace. While activity has generally decayed following the Modified Omori Law (Figure 7.b), which predicts a gradual return to background levels around 2038, clusters of activity have persisted in the south-eastern areas.

An investigation into the focal mechanism solutions (CroFMS catalogue) revealed a complex interplay of faulting styles (Figure 10). While the major events show the expected strike-slip faulting, a substantial number of aftershocks exhibit reverse faulting in specific clusters. This heterogeneous pattern is consistent with the change in the Coulomb failure stress caused by the mainshock, which validates current models of static stress triggering. Additionally, the study highlights an important observation: the P-axes of the aftershocks, which align with the regional maximal horizontal stress (S_{Hmax}), exhibit a noticeable clockwise rotation relative to the mainshock's P-axis. This rotation provides vital constraints on the local stress field and its variations.

In conclusion, the five years of intense monitoring following the Petrinja earthquake have yielded a remarkably detailed and robust understanding of this significant intraplate strike-slip event. The successful collaboration and rapid deployment of the seismic networks, complemented by a powerful ML workflow, have created a uniquely rich dataset. This dataset not only defines the primary and secondary faults activated by the event but also provides compelling evidence that the heterogeneous aftershock faulting is a direct, predictable consequence of stress redistribution. The insights gained into the geometry and kinematics of the Petrinja fault system, aftershock productivity, and short-term variability of tectonic stress are important for refining seismic hazard models. These findings enable a more reliable characterisation of the main seismogenic faults, including their recurrence parameters, maximum expected magnitudes, and typical focal mechanisms. This, in turn, provides a stronger foundation for deterministic modelling of realistic earthquake scenarios in the Banovina area, thus supporting the development of long-term earthquake risk mitigation strategies in Central Croatia.

Acknowledgements

The Croatian Seismological Survey at the Department of Geophysics, Faculty of Science, University of Zagreb acknowledges financial donation from the Government of the Republic of Croatia (through the Ministry of Science and Education) for the procurement of a complete set of seismological instruments for seismic monitoring: 20 modern seismometers and 20 accelerometers with all the necessary auxiliary equipment. Seismologists from the Andrija Mohorovičić Geophysical Institute at the Department of Geophysics, Faculty of Science, University of Zagreb acknowledge the help of colleagues from the National Institute of Oceanography and Applied Geophysics (OGS, Italy) and their generous provision of six seismographs with integrated accelerometer for rapid deployment. The stations of the permanent Croatian network and those from the mobile pool (PN-Net) were managed by the Croatian Seismological Survey, Department of Geophysics, Faculty of Science, University of Zagreb. Automatic earthquake detection and location was performed within the project 'Investigation of seismically vulnerable areas in Croatia and seismic ground motion assessment – CRONOS' funded by the Norwegian Grants (Norwegian Financial Mechanism 2014-2021, grant 04-UBS-U-0002/22-90). The temporary stations of the OP-Net were managed by seismologists from the Andrija Mohorovičić Geophysical Institute, Department of Geophysics, Faculty of Science, University of Zagreb. We thank all our colleagues who helped with station deployment and maintenance, as well as seismograms and data analyses.

REFERENCES

[1] Herak, M., Herak, D.: Properties of the Petrinja (Croatia) earthquake sequence of 2020–2021–Results of seismological research for the first six months of activity. Tectonophysics, 858 (2023), Paper No. 229885, https://doi.org/10.1016/j.tecto.2023.229885

[2] Herak, D., Herak M.: The Kupa Valley (Croatia) Earthquake of 8 October 1909 - 100 Years Later, Seismological Research Letters 81 (2010), pp. 30–36, https://doi.org/ 10.1785/gssrl.81.1.30

[3] Pollak, D., Gulam, V., Novosel, T., Avanić, R., Tomljenović, B., Hećej, N., Terzić, J., Stipčević, J., Bačić, M., Kurečić, T., Dolić, M.: The preliminary inventory of coseismic ground failures related to December 2020–January 2021 Petrinja earthquake series, Geologia Croatica, 74(2) (2021), pp. 189-208, https://doi.org/10.4154/gc.2021.08

[4] Tomac, I., Vlahovic, I., Parlov, J., Matoš, B., Matešic, D., Kosovic, I., Pavicic, I., Frangen, T., Terzic, J., Pavelic, D.: Geotechnical Reconnaissance and Engineering Effects of the December 29, 2020, M6. 4 Petrinja, Croatia Earthquake, and Associated Seismic Sequence, Technical report of Geotechnical Extreme Event Reconnaissance (GEER) Association: Petrinja, Croatia, 2021, pp. 49-96, https://doi.org/10.18118/G63T0

[5] Tomac, I., Kovačević Zelić, B., Perić, D., Domitrović, D., Štambuk Cvitanović, N., Vučenović, H., Parlov, J., Stipčević, J., Matešić, D., Matoš, B., Vlahović, I.: Geotechnical reconnaissance of an extensive cover-collapse sinkhole phenomena of 2020–2021 Petrinja earthquake sequence (Central Croatia), Earthquake spectra, 39 (2023) 1, pp. 653-686, https://doi.org/10.1177/87552930221115759

[6] Atalić, J., Uroš, M., Šavor Novak, M., Demšić, M., Baniček, M., Kadić, A., Oreb, J.: The Croatian Centre for Earthquake Engineering: establishment, activities and future opportunities, in 3rd European Conference on Earthquake Engineering & Seismology (3ECEES), (2022), pp. 2088-2097

[7] Atalić, J., Demšić, M., Baniček, M., Uroš, M., Dasović, I., Prevolnik, S., Kadić, A., Šavor Novak, M., Nastev, M.: The December 2020 magnitude (Mw) 6.4 Petrinja earthquake, Croatia: seismological aspects, emergency response and impacts, Bulletin of earthquake engineering, 21 (2023) 13 , pp. 5767-5808, https://doi.org/10.1007/s10518-023-01758-z

[8] Mihaljević, I., Zlatović, S.: Embankments damaged in the magnitude Mw 6.4 Petrinja earthquake and remediation, Geosciences, 13 (2023) 2, Paper No. 48, https://doi.org/ 10.3390/geosciences13020048

[9] Mijić, Z., Zlatović, S., Montgomery, J., Ziotopoulou, K., Gjetvaj, V.: Liquefaction effects in the 2020 Mw 6.4 Petrinja, Croatia, earthquake, Soil Dynamics and Earthquake Engineering, 193 (2025), Paper No. 109262 https://doi.org/ 10.1016/j.soildyn.2025.109262

[10] Markušić, S., Stanko, D., Penava, D., Ivančić, I., Bjelotomić Oršulić, O., Korbar, T., Sarhosis, V.: Destructive M6. 2 Petrinja earthquake (Croatia) in 2020 - Preliminary multidisciplinary research, Remote Sensing, 13 (2021) 6, Paper No. 1095, https://doi.org/ 10.3390/rs13061095

[11] Kastelic, V., Atzori, S., Carafa, M., Govorčin, M., Herak, D., Herak, M., Matoš, B., Stipčević, J., Tomljenović, B.: Petrinja Seismogenic Source and its 2020-2021 Earthquake Sequence (central Croatia). in EGU General Assembly Conference Abstracts (2021), Paper No. EGU21-16585

[12] Baize, S., Amoroso, S., Belić, N., Benedetti, L., Boncio, P., Budić, M., Cinti, F.R., Henriquet, M., Jamšek Rupnik, P., Kordić, B., Markušić, S.: Environmental effects and seismogenic source characterization of the December 2020 earthquake sequence near Petrinja, Croatia, Geophysical Journal International, 230 (2022) 2, pp. 1394-1418, https://doi.org/ 10.1093/gji/ggac123

[13] Henriquet, M., Kordic, B., Métois, M., Lasserre, C., Baize, S., Benedetti, L., Spelić, M., Vukovski, M.: Rapid remeasure of dense civilian networks as a game-changer tool for surface deformation monitoring: The case study of the Mw 6.4 2020 Petrinja Earthquake, Croatia, Geophysical Research Letters, 49 (2022) 24, Paper No. e2022GL100166, https://doi.org/10.1029/2022GL100166

[14] Xiong, W., Yu, P., Chen, W., Liu, G., Zhao, B., Nie, Zh., Qiao, X.: The 2020 Mw 6.4 Petrinja earthquake: a dextral event with large coseismic slip highlights a complex fault system in northwestern Croatia, Geophys. J. Int., 228 (2022), pp. 1935–1945, https://doi.org/10.1093/gji/ggab440

[15] Zhu, S., Wen, Y., Gong, X., Liu, J.: Coseismic and Early Postseismic Deformation of the 2020 Mw 6.4 Petrinja Earthquake (Croatia) Revealed by InSAR, Remote Sensing, 15(10) (2023), 2617. https://doi.org/10.3390/rs15102617

[16] Žilić, I., Causse, M., Vallee, M., Markušić, S.: High Stress Drop and Slow Rupture During the 2020 MW6.4 Intraplate Petrinja Earthquake, Croatia, Journal of Geophysical Research-Solid Earth, 130 (2025) 1, 10.1029/2024JB029107

[17] Sardeli, E., Michas, G., Pavlou, K., Zaccagnino, D., Vallianatos, F.: Spatiotemporal properties of the 2020–2021 Petrinja (Croatia) earthquake sequence, Journal of Seismology, 28 (2024) 4, pp. 899-920, https://doi.org/ 10.1007/s10950-024-10228-1

[18] Bjelotomić Oršulić, O., Markovinović, D., Varga, M., Bašić, T.: Coseismic ground displacement after the M W 6.2 earthquake in NW Croatia determined from sentinel-1 and GNSS CORS data, Geosciences, 11 (2021) 4, Paper No. 170, https://doi.org/10.3390/geosciences11040170

[19] Tondi, E., Blumetti, A. M., Cicak, M., Di Manna, P., Galli, P., Invernizzi, C., Mazzoli, S., Piccardi, L., Valentini, G., Vittori, E., Volatili, T.: 'Conjugate' coseismic surface faulting related with the 29 December 2020, Mw 6.4, Petrinja earthquake (Sisak-Moslavina, Croatia), Scientific Reports, 11 (2021) 1, https://doi.org/ 10.1038/s41598-021-88378-2

[20] Ustaszewski, K., Herak, M., Tomljenović, B., Herak, D., Matej, S.: Neotectonics of the Dinarides-Pannonian Basin transition and possible earthquake sources in the Banja Luka epicentral area, J. Geodyn., 82 (2014), pp. 52–68, https://doi.org/ 10.1016/j.jog.2014.04.006

[21] Herak, M.: Croatian catalogue and database of focal mechanism solutions, characteristic mechanisms, and stress field properties in the Dinarides and the surrounding regions, Geofizika, 41 (2024) 2, pp. 79-123, https://doi.org/ 10.15233/gfz.2024.41.5

[22] Ustaszewski, K., Kounov, A., Schmid, S.M., Schaltegger, U., Krenn, E., Frank, W., Fügenschuh, B.: Evolution of the Adria–Europe plate boundary in the northern Dinarides: from continent–continent collision to back-arc extension, Tectonics, 29 (2010), TC6017, https://doi.org/ 10.1029/2010TC002668

[23] Schmid, S., Fűgenschuh, B., Kounov, A., Matenco, L., Nievergelt, P., Oberhänsli, R., Pleuger, J., Schefer, S., Schuster, R., Tomljenović, B., Ustaszewski, K., van Hinsbergen, D.J.J.: Tectonic units of the Alpine collision zone between Eastern Alps and western Turkey, Gondwana Res., 78 (2020), pp. 308-374, https://doi.org/10.1016/j.gr.2019.07.005

[24] Saftić, B., Velić, J., Sztanó, O., Juhász, G., Ivković, Ž.: Tertiary subsurface facies, source rocks and hydrocarbon reservoirs in the SW part of the Pannonian Basin (northern Croatia and south-western Hungary). Geologia Croatica, 56 (2003), pp. 101–122, https://hrcak.srce.hr/3793

[25] Tomljenović, B., Csontos, L.: Neogene–Quaternary structures in the border zone between Alps, Dinarides and Pannonian Basin (Hrvatsko zagorje and Karlovac Basins, Croatia), Int J Earth Sci, 90 (2001), pp. 560–578, https://doi.org/ 10.1007/s005310000176

[26] Herak, D., Herak, M., Tomljenović, B.: Seismicity and earthquake focal mechanisms in North-Western Croatia, Tectonophysics, 465 (2009) 1-4, pp. 212-220, https://doi.org/ 10.1016/j.tecto.2008.12.005

[27] Pikija, M.: Basic Geological Map of SFRY 1:100.000, Sisak sheet. Geol. Zavod, Zagreb, Savezni geol. Zavod, Beograd. (in Croatian), 1987

[28] Šikić, K.: Osnovna geološka karta Republike Hrvatske 1: 100.000. Tumač za list Bosanski Novi 1: 100.000, L 33-70 [Basic Geological Map of Republic of Croatia 1: 100000, Geology of the Bosanski Novi sheet–in Croatian]. Hrvatski geološki institut Zagreb, 2014

[29] Tomljenović, B., Stipčević, J., Sečanj, M.: Izvješće o zabilježenim pojavama koseizmičkih površinskih deformacija na području Pokuplja i Banovine nastalih potresnom serijom od 28.12. 2020 do 5.01.2021. Rudarsko-geološko-naftni fakultet, Sveučilište u Zagrebu 2021. (https://www.rgn.unizg.hr/hr/izdvojeno/2790-izvjesce-o-zabiljezenim-pojavama-koseizmickih-povrsinskih-deformacija-na-podrucju-pokuplja-i-banovine-nastalih-potresnom-serijom-od-28-12-2020-do-5-01-2021), 2021

[30] Mihalić Arbanas, S., Arbanas, Ž., Bernat Gazibara, S., Krkač, M.: Preliminary engineering geological and geotechnical investigation of geological hazards induced by Petrinja Earthquake Series 2020-2021, GRAĐEVINAR, 77 (2025) 11, pp. 1071-1082, https://doi.org/ https://doi.org/10.14256/JCE.4422.2025

[31] Kovačević, M.S., Bačić, M., Librić, L., Jurić-Kaćunić, D.: Liquefaction in Croatia: Risk assessment and rapid post-earthquake decision-making – five years later, GRAĐEVINAR, 77 (2025) 11, pp. 1037-1055, https://doi.org/ https://doi.org/10.14256/JCE.4419.2025

[32] Stipčević, J., Poggi, V., Herak, M., Parolai, S., Herak, D., Dasović, I., Bertoni, M., Barnaba, C., Pesaresi, D.: First results from temporary deployment of small seismic network following the Mw= 6.4 Petrinja earthquake, In EGU General Assembly Conference Abstracts (pp. EGU21-16579), 2021

[33] Herak, M., Herak, D., Markušić, S.: Revision of the earthquake catalogue and seismicity of Croatia, 1908–1992, Terra Nova, 8 (1996) 1, pp. 86-94, https://doi.org/ 10.1111/j.1365-3121.1996.tb00728.x

[34] Ross, Z.E., Yue, Y., Meier, M.A., Hauksson, E., Heaton, T.H.: PhaseLink: A deep learning approach to seismic phase association, Journal of Geophysical Research: Solid Earth, 124 (2019) 1, pp. 856-869, https://doi.org/ 10.1029/2018JB016674

[35] Zhu, W., Beroza, G.C.: PhaseNet: a deep-neural-network-based seismic arrival-time picking method, Geophysical Journal International, 216 (2019) 1, pp. 261-273, https://doi.org/ 10.1093/gji/ggy423

[36] Mousavi, S.M., Ellsworth, W.L., Zhu, W., Chuang, L.Y., Beroza, G.C.: Earthquake transformer - an attentive deep-learning model for simultaneous earthquake detection and phase picking, Nature communications, 11 (2020) 1, p.3952, https://doi.org/ 10.1038/s41467-020-17591-w

[37] Šindija, D., Mustać-Brčić, M., Hetényi, G., Stipčević, J.: Enhanced view of the Mw 6.4 Petrinja earthquake sequence (2020-2022) using deep learning. ESS Open Archive. 2025, https://doi.org/ 10.22541/essoar.174982734.45695605/v1

[38] Michelini, A., Cianetti, S., Gaviano, S., Giunchi, C., Jozinović, D., Lauciani, V.: INSTANCE–the Italian seismic dataset for machine learning, Earth System Science Data, 13 (2021) 12, pp. 5509-5544, https://doi.org/ 10.5194/essd-13-5509-2021

[39] Münchmeyer, J.: PyOcto: A high-throughput seismic phase associator, Seismica, 3 (2024) 1, https://doi.org/ 10.26443/seismica.v3i1.1130

[40] Lomax, A., Virieux, J., Volant, P., Berge-Thierry, C.: Probabilistic earthquake location in 3D and layered models: Introduction of a Metropolis-Gibbs method and comparison with linear locations. In Advances in seismic event location (pp. 101-134). Dordrecht: Springer Netherlands, pp. 101-134, 2000, https://doi.org/ 10.1007/978-94-015-9536-0_5

[41] Lomax, A.: Mapping finite-fault slip with spatial correlation between seismicity and point-source Coulomb failure stress change, arXiv preprint, 2024, https://doi.org/ 10.48550/arXiv.2404.05437

[42] Zhu, W., Mousavi, S.M., Beroza, G.C.: Seismic signal denoising and decomposition using deep neural networks, IEEE Transactions on Geoscience and Remote Sensing, 57 (2019) 11, pp. 9476-9488, https://doi.org/ 10.1109/TGRS.2019.2926772

[43] Fonzetti, R., Buttinelli, M., Valoroso, L., De Gori, P., Chiarabba, C.: Fault interaction during large earthquakes as revealed by the L'Aquila 2009 sequence, Journal of Geophysical Research: Solid Earth, 130 (2025) 8, Paper No. e2025JB031245, https://doi.org/ 10.1029/2025JB031245

Primljen / Received: 17.10.2025.
Ispravljen / Corrected: 13.4.2026.
Prihvaćen / Accepted: 7.5.2026.
Dostupno online / Available online: 10.6.2026.

Adfreezing and freeze-thaw effects on the shear strength of the Güngören clay-concrete interface

Authors:

Assist.Prof. **Aysenur Aslan Fidan**, PhD. CE
Dicle University, Turkey
Department of Engineering
aysenur.aslan@dicle.edu.tr
aysenur.asln@gmail.com
Corresponding author

Assist.Prof. **Murat Gulen**, PhD. CE
Siirt University, Turkey
Department of Engineering
murat.gulen@siirt.edu.tr

Prof. **Suat Akbulut**, PhD. CE
Yildiz Technical University, Turkey
Department of Engineering
sakbulut@yildiz.edu.tr

Original research paper

Aysenur Aslan Fidan, Murat Gulen, Suat Akbulut

Adfreezing and freeze-thaw effects on the shear strength of the Güngören clay-concrete interface

The interaction between soil and structures is significantly affected by freeze-thaw (F-T) cycles, which alter soil strength and deformation behaviour. This study investigates the effects of F-T cycles on the shear strength, adhesion, and interface friction angle of the Güngören clay-concrete interface under varying water content. Samples were prepared at 5 % below and 5 % above the optimum water content and subjected to 0, 3, 7, and 10 F-T cycles between -20 °C and +20 °C. Direct shear tests were conducted under both freezing and thawing conditions. The results indicate that adfreezing, ice bonding at the interface, significantly enhanced the strength of frozen samples with shear strength increasing by 1.6-2.7 times in frozen wet-side samples and 1.05-1.19 times in dry-side samples. After thawing, dry-side samples exhibited strain-softening and reduction in strength 0.80-0.95 times the initial value, whereas wet-side samples largely preserved their strength. Adhesion increased slightly in dry-side frozen samples, whereas in wet-side samples, it increased nearly threefold after the third cycle and then stabilised. The interface friction angle exhibits different trends depending on the moisture content and thermal state. These variations are attributed to the combined effects of ice cementation, unfrozen water, particle interactions, and moisture redistribution at the interface.

Key words:
adfreezing, clay-concrete interface, freeze-thaw cycles, Güngören clay, shear strength

Izvorni znanstveni rad

Aysenur Aslan Fidan, Murat Gulen, Suat Akbulut

Učinci adhezijskog smrzavanja i F-T ciklusa na posmičnu čvrstoću sučelja između Güngören gline i betona

Ciklusi smrzavanja i odmrzavanja (F-T ciklusi) znatno utječu na interakciju tla i konstrukcije jer mogu promijeniti čvrstoću tla i njegovo deformacijsko ponašanje. U ovom se istraživanju analiziraju učinci F-T ciklusa na posmičnu čvrstoću, adheziju i kut trenja na sučelju između Güngören gline i betona pri različitim udjelima vode. Uzorci su pripremljeni s udjelima vode 5 % nižim i 5 % višim od optimalnog udjela te su podvrgnuti 0, 3, 7 i 10 F-T ciklusa u temperaturnome rasponu od -20 °C do +20 °C. Pokusi izravnog smicanja provedeni su u smrznutome stanju i nakon odmrzavanja. Rezultati pokazuju da je adhezijsko smrzavanje, odnosno vezivanje ledom na sučelju, znatno povećalo čvrstoću smrznutih uzoraka. Posmična čvrstoća povećala se od 1,6 do 2,7 puta kod smrznutih uzoraka s većim udjelom vode te od 1,05 do 1,19 puta kod uzoraka s manjim udjelom vode. Nakon odmrzavanja uzorci s manjim udjelom vode pokazali su deformacijsko omekšavanje i smanjenje čvrstoće na 0,80 do 0,95 početne vrijednosti, dok su uzorci s većim udjelom vode uglavnom zadržali svoju čvrstoću. Adhezija se blago povećala kod smrznutih uzoraka s manjim udjelom vode, dok se kod uzoraka s većim udjelom vode nakon trećeg ciklusa povećala gotovo trostruko, a zatim stabilizirala. Kut trenja na sučelju pokazao je različite trendove ovisno o udjelu vode i toplinskome stanju uzorka. Navedene se promjene mogu pripisati zajedničkome djelovanju cementacije ledom, nesmrznute vode, međudjelovanja čestica i preraspodjele vlage na sučelju.

Ključne riječi:
adhezijsko smrzavanje, sučelje glina-beton, ciklusi smrzavanja i odmrzavanja, Güngören glina, posmična čvrstoća

1. Introduction

In cold regions, the interaction between the soil and structures is highly influenced by the F-T cycles. The freezing of water within soil pores leads to significant changes in the soil strength and deformation characteristics [1, 2]. In addition, the shear resistance developed at the interface between frozen soil and structural surfaces, known as adfreezing, plays a critical role in the stability of the infrastructure embedded in or supported by soil [3, 4].

Repeated F-T cycles can change the mechanical properties of both the soil and the soil-structure interface, resulting in variations in the shear strength [5, 6]. These variations create challenges in maintaining the long-term performance and stability of structures subjected to such environmental conditions. Therefore, understanding soil-structure interactions under freezing and thawing conditions is essential for the safe and cost-effective design of geotechnical systems such as friction piles, retaining walls, anchors, highways, embankments, shallow foundations, and compacted layers [7, 8]. Most engineering problems in frozen soil mechanics are related to predicting the behaviour of soil under coupled mechanical and thermal effects [9, 10].

The F-T cycle has four stages: prefreezing, freezing, thawing, and consolidation. In the pre-freezing stage, the soil was compact and exhibited high shear strength. During freezing, ice formation causes separation of soil particles, leading to a more dispersed structure. During the thawing stage, the soil exhibited a higher void ratio and lower shear strength. Finally, after consolidation, the soil gradually regains strength as it settles under load, with a reduced void ratio compared to the thawed condition, although it remains higher than that in the prefreezing state [11, 12].

The shear behaviour of the interface between the frozen soil and structural materials is critical for evaluating the performance of geotechnical systems in cold regions. The effect of adfreezing on the interface shear strength has been extensively investigated using different soil types, including silt [4], clay [13, 14], sand [15], and sandstone [16], in combination with structural materials such as steel [4, 17, 18], concrete [19-21] or ice [13]. These studies were conducted using temperature-controlled standard tests [13, 21], large shear tests [14, 19, 22] and low-temperature chambers [4] at different temperatures.

At a constant temperature, an increase in the initial water content resulted in a higher interface shear strength. Conversely, at a constant water content, decreasing the temperature results in an increase in shear strength, which has a more pronounced effect on adhesion [13, 19]. As the temperature decreased, the failure mode transitioned from strain hardening to strain softening, primarily because of the increase in ice content. As ice behaves as a brittle material, it significantly influences the observed failure behaviour [14, 23].

Furthermore, the higher thermal conductivity of concrete compared to that of soil promotes the migration of unfrozen water toward the interface. This process leads to the formation of an ice film at the contact surface between the frozen soil and concrete. Such moisture migration and ice film formation significantly affect the mechanical behaviour of the soil-concrete interface [20, 24-26].

According to meteorological data from the Turkish State Meteorological Service (MGM) for the period 2000-2022, although Istanbul generally exhibits a mild climate, minimum air temperatures during winter months-particularly in December, January, and February-frequently fall below 0 °C and can occasionally reach as low as –8 °C. These conditions led to repeated F-T cycles in the near-surface layers. Therefore, understanding the effects of such thermal conditions on the mechanical behaviour of Güngören clay is critical for ensuring the long-term stability of structures found on or interacting with this soil. A significant portion of Istanbul's infrastructure, including major roads, Atatürk Airport, railway lines, and shallow building foundations, has been constructed using Güngören clay [27, 28].

This study investigates the shear behaviour of the Güngören clay-concrete interface under frozen and thawed conditions, considering the effects of F-T cycles, normal stresses, and water content. The objective of this study is to evaluate the effects of freezing and thawing processes on the interface shear strength and to provide insights for improving the safety and resilience of urban infrastructure.

2. Materials and methods

2.1. Geotechnical properties of Güngören clay

In this study, the soil samples were collected from a site near the Yildiz Technical University campus and belonging to a locally known unit referred to as "Güngören clay". This high-plasticity green clay is a constituent of the widely distributed Güngören Formation. Along with the Gürpınar Formation, it is considered one of the most problematic soil units in Istanbul because of its high plasticity and pronounced sensitivity to environmental conditions [29]. The Güngören Formation is extensively distributed across Istanbul and is particularly prominent in areas such as Yedikule, Kazlıçeşme, Osmaniye, Şirinevler, Yenibosna, and Halkalı, with thicknesses ranging from approximately 9 to 22 meters [28]. Figure 1 illustrates the spatial distribution of this formation on the European side of Istanbul and highlights its geological prevalence across the urban districts.

These clays underlie critical infrastructure, including major transportation corridors, airports, and densely populated residential zones [27, 28], making their behaviour under thermal conditions particularly important to consider.

X-ray diffraction (XRD) analysis was conducted in the laboratory of the Yildiz Technical University to determine the mineralogical composition of the sample. The results indicate that montmorillonite was the dominant mineral, exhibiting the highest peak intensity. Other identified minerals included illite-muscovite, kaolinite, and quartz, which were observed at varying intensities. In addition, the coexistence of illite and montmorillonite was confirmed by the multiple characteristic peaks in the XRD pattern (Figure 2).

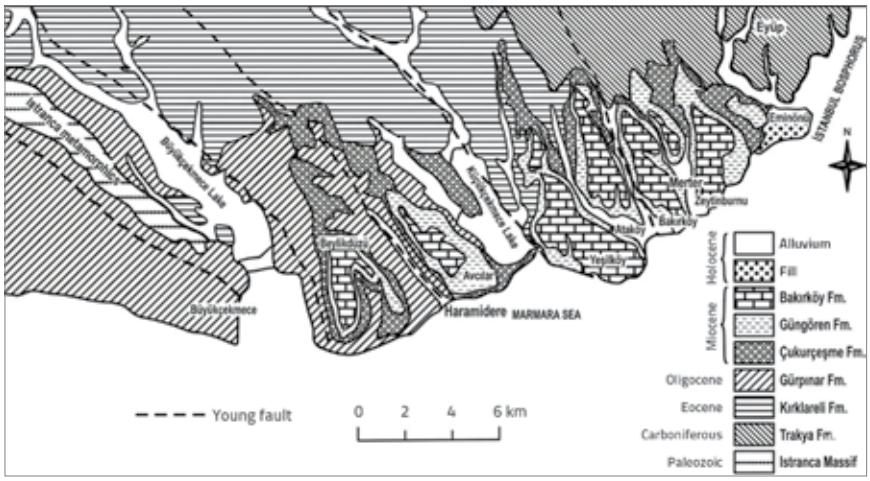

Figure 1. Geology map of the European part of Istanbul [30]

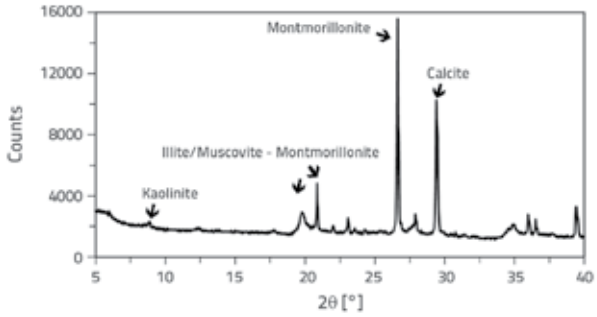

Figure 2. XRD result of Güngören clay

Laboratory tests were conducted on samples obtained from the site to determine the engineering properties of the Güngören clay. These tests include sieve analysis [31, 32], consistency limits [33], specific gravity [34] and compaction tests [35]. Figure 3 shows the location of the Güngören clay on the Casagrande plasticity chart, and Table 1 presents its index properties.

Table 1. Properties of Güngören clay

Property	Value
Specific gravity (Gs)	2.63
Liquid limit, LL [%]	81.50
Plastic limit, PL [%]	35.30
Plasticity index, PI [%]	46.20
Activity, A	0.71

The soil consisted of approximately 95 % fine-grained material with a clay fraction of 65 % based on sieve and hydrometer analyses. Sieve analysis was applied only to the coarse fraction retained on sieve no. 200, whereas the fine particle fraction was characterised using hydrometer analysis. The liquid limit (LL), plastic limit (PL) and plasticity index (PI) were 81.5 %, 35.3 %, and 46.2 %, respectively. According to ASTM D2487-17 [36], the soil was classified as high-plasticity clay (CH).

According to ASTM D4546 [37], clays with a PI > 40 % exhibit a very high swelling potential. Accordingly, Güngören clay is characterised by a high swelling potential, swelling pressure, and water retention capacity. These properties are largely governed by the mineral composition, specific surface area, and cation exchange capacity [38]. Montmorillonite-rich clays exhibit the highest swelling and water-retention capacities [39].

Mineral composition also influences the response of clay to freeze-thaw cycles. The expansion of montmorillonite during water absorption can induce structural degradation during freeze-thaw cycles and lead to softening of the soil upon thawing [40]. The results presented in Figure 2 and 3 further confirm the freeze-thaw cycles of Güngören clay.

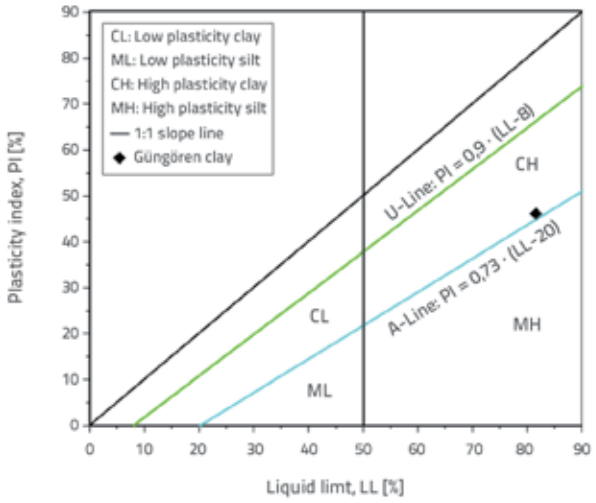

Figure 3. Location of Güngören clay on the Casagrande plasticity chart

All direct shear tests were conducted on soil samples compacted on both the dry and wet-sides of the optimum water content (wopt). The soil compaction curve is shown in Figure 4. The maximum dry density was 1.378 g/cm^3 and the optimum water content (wopt) was 28.3 %. The degree of soil saturation was approximately 60 % on the dry-side and 85 % on the wet-side.

A freezing-point depression test was conducted on compacted samples representing both the dry-side (w = 23.3 %) and wet-side (w = 33.3 %) of the compaction curve. The temperature-characteristic curves of the samples, shown in Figure 5, indicate that the freezing point (FP) is –1.1 °C for the dry-side sample and –0.4 °C for the wet-side sample.

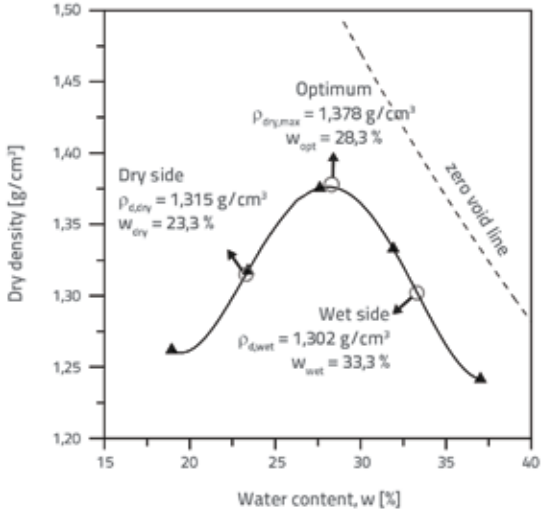

Figure 4. Standard compaction curve of Güngören clay

Previous studies have shown that the FP of soils is influenced by factors such as soil type, consistency limits, water content, salt composition and concentration, loading conditions, confining pressure, and vibrations [5, 41–44]. A lower initial water content leads to faster freezing and greater freezing-point depression due to changes in pore water pressure, whereas a higher water content delays freezing and slightly increases FP, particularly near saturation [16, 45, 46].

In addition, a higher water content resulted in a more pronounced delay in the advancement of the freezing front, whereas a lower moisture content led to a faster freezing rate and shorter stabilization time [45]. The FP of soil samples increased nonlinearly with increasing water content, approaching that of pure water (0°C) at high saturation levels [16]. These effects are attributed to the presence of loosely bound water, which freezes at a much lower temperature, and to the increased water potential in soils with a higher moisture content [46].

2.2. Concrete blocks preparation and surface roughness characterization

The surface texture and hardness of construction materials at the contact interface play critical roles in governing the interface behaviour, with increased surface roughness generally leading to enhanced shear strength [48-50]. Although some studies have investigated smooth soil - concrete interfaces using plywood or steel moulds [51, 52], others have examined a range of surface roughness conditions to better represent field applications [53-55].

The concrete samples used to investigate the clay-concrete interfacial interactions were cast in specially designed plywood moulds. A water-cement-sand mixture (2:5:15 by mass) consisting of sand with particle sizes smaller than 4 mm was poured into the moulds, compacted, and cured by immersion in water (Figure 6a). During casting, vibration was applied to ensure adequate compaction and eliminate air voids, which could affect strength and uniformity.

After casting, the moulds were covered with plastic sheets to prevent the loss of moisture. Once the concrete had set (approximately 18-24 hours), the samples were demolded and subsequently cured in water under a moist cloth for 28 days to achieve full strength. The 28-day compressive strength of the cubic specimens (15 × 15 × 15 cm) prepared and cured under the same conditions was determined to be 51 MPa.

To evaluate surface roughness, the samples were analysed using an AEP Nanomap 1000WLI optical profilometer, which generates three-dimensional surface profiles by capturing variations in reflected light. Measurements were performed at multiple locations using both optical and stylus profilometry to ensure accuracy and repeatability (Figure 6.b).

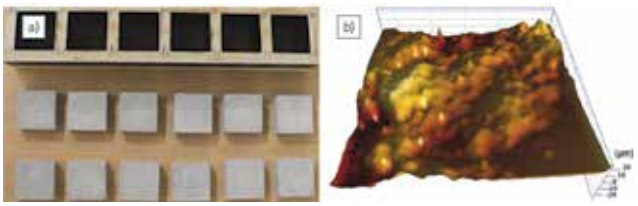

Figure 6. Details of concrete blocks: a) concrete samples and plywood molds b) surface roughness measurement sample

Various methodological approaches for quantifying surface roughness have been reported [56-58]. Among these, height-based parameters such as the normalised roughness index () are commonly used. The normalised roughness index (R_n) is

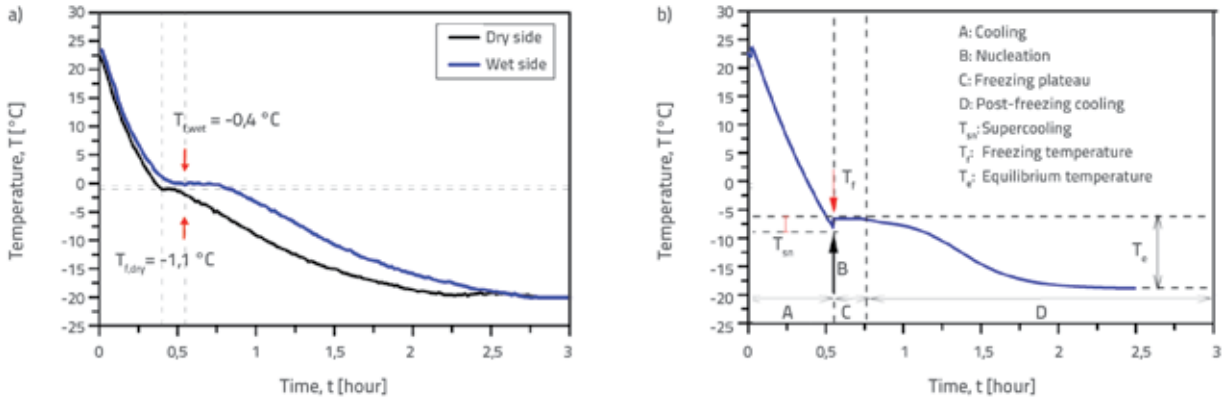

Figure 5. Temperature-time curves of: a) Güngören clay (experimental); b) typical freezing behaviour, according to [47]

commonly defined as the ratio of the maximum asperity height (R_{max}) to the mean particle size (D_{50}), as expressed in Equation (1): The corresponding R_n value for the clay used in this study was approximately 10.3, based on D_{50} = 0.0028 mm and R_{max} = 0.026 mm.

$$R_n = \frac{R_{max}}{D_{50}} \quad (1)$$

It is important to note that Equation (1) was primarily developed for granular soils, where the mechanical response is governed by the interaction between particle size and surface roughness. For fine-grained soils, such as clay-silt mixtures, where the representative particle size is significantly smaller, this parameter becomes less applicable and cannot be used to make a meaningful physical interpretation. In this study, instead of using approaches based on a single characteristic roughness height, an area-based formulation is adopted to account for the contribution of the entire surface texture along the interface. This formulation provides a more representative characterisation of surfaces with irregular roughness that do not exhibit consistent depth, spacing, or distribution.

In this formulation, the roughness parameter represents the ratio of the actual surface area to the projected planar area and provides a quantitative measure of the surface irregularity. Higher values indicate a rougher surface with more pronounced asperities, which may enhance mechanical interlocking at the interface. Based on this calculation method, the average roughness parameter (R_{av}) of the concrete blocks used in this study was determined to be 1.27.

$$R_{av} = \frac{A_r}{A_0} \quad (2)$$

2.3. Test procedure

For the freeze-thaw tests, the samples were compacted in a shear box ring, considering the density and water content for both the dry and wet-sides of the wopt determined from the compaction curve. The soil-water mixture was initially prepared and allowed to rest in a plastic mould for 24 h to ensure uniformity. The mixture was compacted into shear boxes directly onto the concrete surface, securely wrapped with a stretch film, and placed in a desiccator to ensure homogeneous moisture distribution after compaction. After compaction, the samples were arranged in boxes, placed in a cabinet in an orderly manner, and subjected to F-T cycles (Figure 7).

Figure 7. Stages in sample preparation shown in photos: a) prepared samples b) placing samples in a desiccator c) arranging sample in boxes d) placing samples in the freeze-thaw cabinet

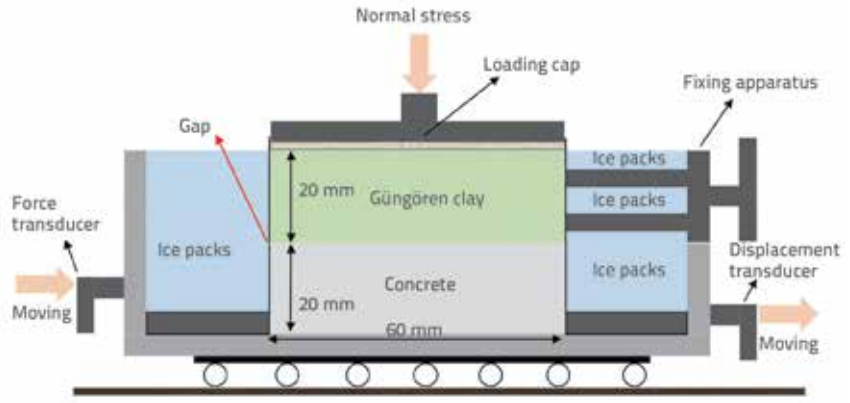

Figure 8. Schematic representation of the direct shear test apparatus

The compacted samples were then subjected to 0, 3, 7, and 10 F-T cycles. During the freezing stage, the samples were frozen at -20 °C and subsequently thawed at 20 °C. To prevent moisture loss, ambient humidity was maintained at 80 % throughout the thawing stage. The selected temperature range ensures complete freezing and thawing of the pore water, thereby eliminating partial phase change effects and reducing experimental variability.

The direct shear test, which is a well-established method for evaluating the shear behaviour of soils and soil-structure interfaces [13, 51, 59, 60], was employed in this study. The clay-concrete interface samples were tested using a shear box apparatus with dimensions of 6 cm × 6 cm under both freezing and thawing conditions. The tests were performed in accordance with ASTM D3080 [61] by applying normal stresses of 50, 100, and 200 kPa at a constant shear rate of 1.0 mm/min (Figure 8).

This methodology is consistent with numerous studies on soil-structure interfaces under frozen and freeze-thaw conditions, including silt-concrete [4], clay-concrete [14, 62, 63], silty soil-steel [17], sand-steel [18], ice-frozen clay [13], clay-geotextile [64], and soil-geogrid interfaces [65]. Most studies used shear rates between 0.8 to 1.2 mm/min, consistent with the 1.0 mm/min applied in this study [4, 17, 20, 63, 64, 66]. Therefore, the experimental parameters, including the test method [13, 51, 59, 60], temperature [20, 63], shear rate [4, 17, 20, 63, 64, 66], and applied normal stress [4,13, 14,17] were consistent with those reported in the cited studies, supporting the validity and comparability of the results.

The samples were labelled according to the number of F-T cycles and thermal conditions applied during shearing. For instance, a "3-cycles (frozen)" sample refers to a specimen tested in a frozen

Table 2. Testing programme

Test material	Water ratio [%]	Freezing [°C]	Thawing [°C]	Cycles	σ [kPa]	Condition
Clay-concrete	23.3	–20	+20	0, 3, 7, 10	50, 100, 200	Frozen / Thawed
Clay-concrete	33.3	–20	+20	0, 3, 7, 10	50, 100, 200	Frozen / Thawed

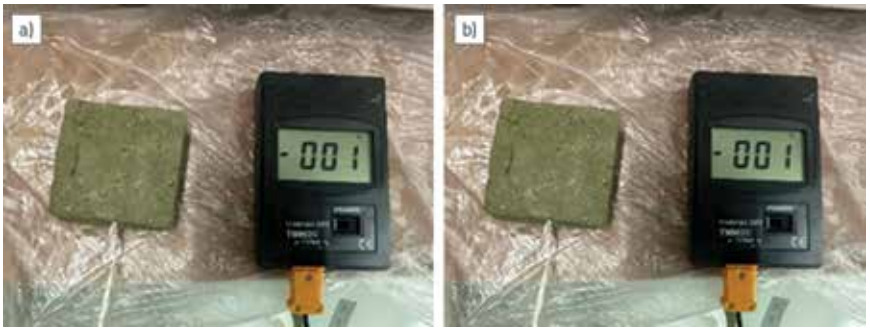

Figure 9. Temperature measurements of soil samples: a) before and b) after the direct shear test

state after three F-T cycles, whereas a "3-cycles (thawed)" sample denotes one tested in the thawed state after the same number of cycles (Table 2).

Control tests were conducted prior to the experimental program to assess repeatability. Under identical conditions, the variation in the measured shear stress was found to be limited, reaching approximately 3-4 % at 50 kPa, 2-3 % at 100 and 200 kPa for frozen tests, whereas for thawed tests, it remained at approximately 2 % for all normal stress levels. Following the verification, a planned test program was conducted. In addition, at least one test was repeated for each experimental condition under normal stresses of 50, 100, and 200 kPa.

Prior to the shear test, the metal ring of the shear box was cooled to prevent melting, and insulation was maintained during the experiment using ice packs and plastic covers (Figure 8). The temperatures of the soil samples measured before and after the test indicated an increase in temperature during shear testing (Figure 9). However, comparison with the freezing point indicated that the soil temperature remained close to it after testing.

In fine-grained soils, a portion of pore water remains unfrozen even at 0°C [67-70]. Even at very low temperatures, such as -20°C, considerable amounts of unfrozen water can persist, forming thin films around soil particles [70, 71]. According to Konrad [69], the amount of unfrozen water is strongly influenced by soil structure; open soil structures contain less capillary unfrozen water below -2°C, whereas soils subjected to higher loading retain larger amounts under the same temperature conditions.

The presence of this unfrozen water film affects the soil behaviour, as ice forms adjacent to the adsorbed layer rather than in direct contact with the soil particles [12, 72]. Therefore, the results of the tests on frozen on clay and clay-concrete samples should be interpreted by considering the combined presence of ice and unfrozen water. The tested samples represent compacted soil conditions rather than natural soil structures. Therefore, the distribution of unfrozen water and its influence on the mechanical behaviour may differ from in situ conditions, where the soil structure plays a more significant role.

3. Results and discussion

3.1. Visual observation of ice film formation at the interface

Frozen samples prepared on the wet-side with the optimum water content were subjected to direct shear testing and visually examined (Figure 10). A smooth and glossy interface was observed, indicating the formation of an ice layer with ice crystals present within the soil voids and along the contact surface. This behaviour is attributed to the thermal gradient across the interface during freeze-thaw cycling. As reported by He et al. [20], this thermal gradient drives the migration of unfrozen water from the surrounding soil toward the interface, leading to the formation of ice films at the contact surface. This mechanism is supported by previous studies [24-26, 73].

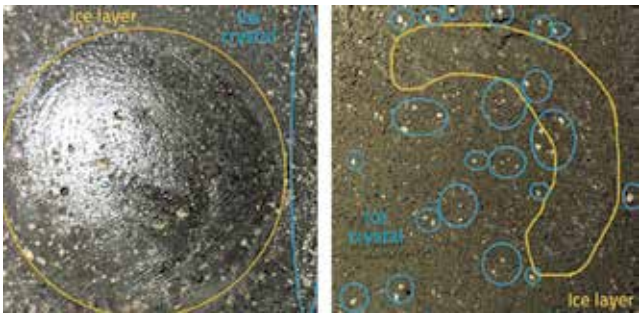

Figure 10. Ice layer and ice crystals observed on the soil and concrete surfaces after the 7th freezing cycle

3.2. Adfreezing and F-T cycles effect on stress-strain curve

In this study, the stress-strain curve of frozen clay-concrete samples compacted on the dry-side of the optimum water content closely aligns with the multi-stage deformation process described by Liu et al. [19] for frozen soil-concrete interfaces (Figure 11). Using large-scale direct shear tests, Liu et al. [19] identified the curve stages as elastic deformation (a-b), plastic deformation onset (b-c), sliding failure with shear stress reduction (c-d), strain hardening owing to progressive deformation (d-e), and residual shear strength (e-f). In our study, which was

conducted using direct shear tests, the samples exhibited similar stages up to strain hardening (d-e), but did not reach the residual shear strength stage (e-f), likely because of the limitations of the smaller shear apparatus. As noted by Goughnour and Andersland [74], the ice matrix under typical pressure and temperature conditions is significantly more rigid than the soil skeleton, reaching its peak strength at lower strains. They often exhibit two distinct yield points: one at approximately 1 % axial strain, and the other at approximately 10 % or higher. This dual-peak behaviour was also observed at the clay-concrete interface in our tests, indicating that such a response is not limited to frozen soils alone. No residual behaviour was observed after the second peak, and the peak strength showed a slight increase compared with the initial value. Moreover, this increase became more pronounced with the number of freeze-thaw cycles.

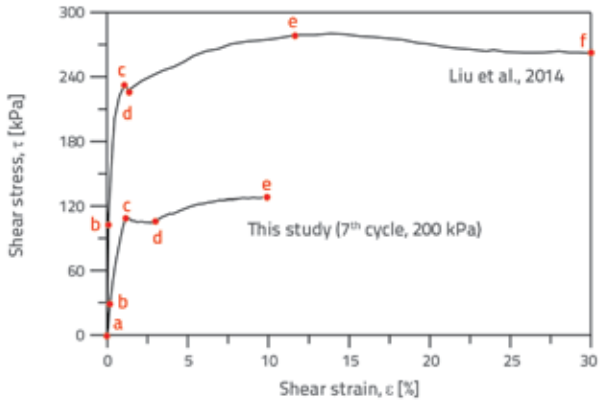

Figure 11. Stress-strain behaviour of frozen clay-concrete interface on the dry-side

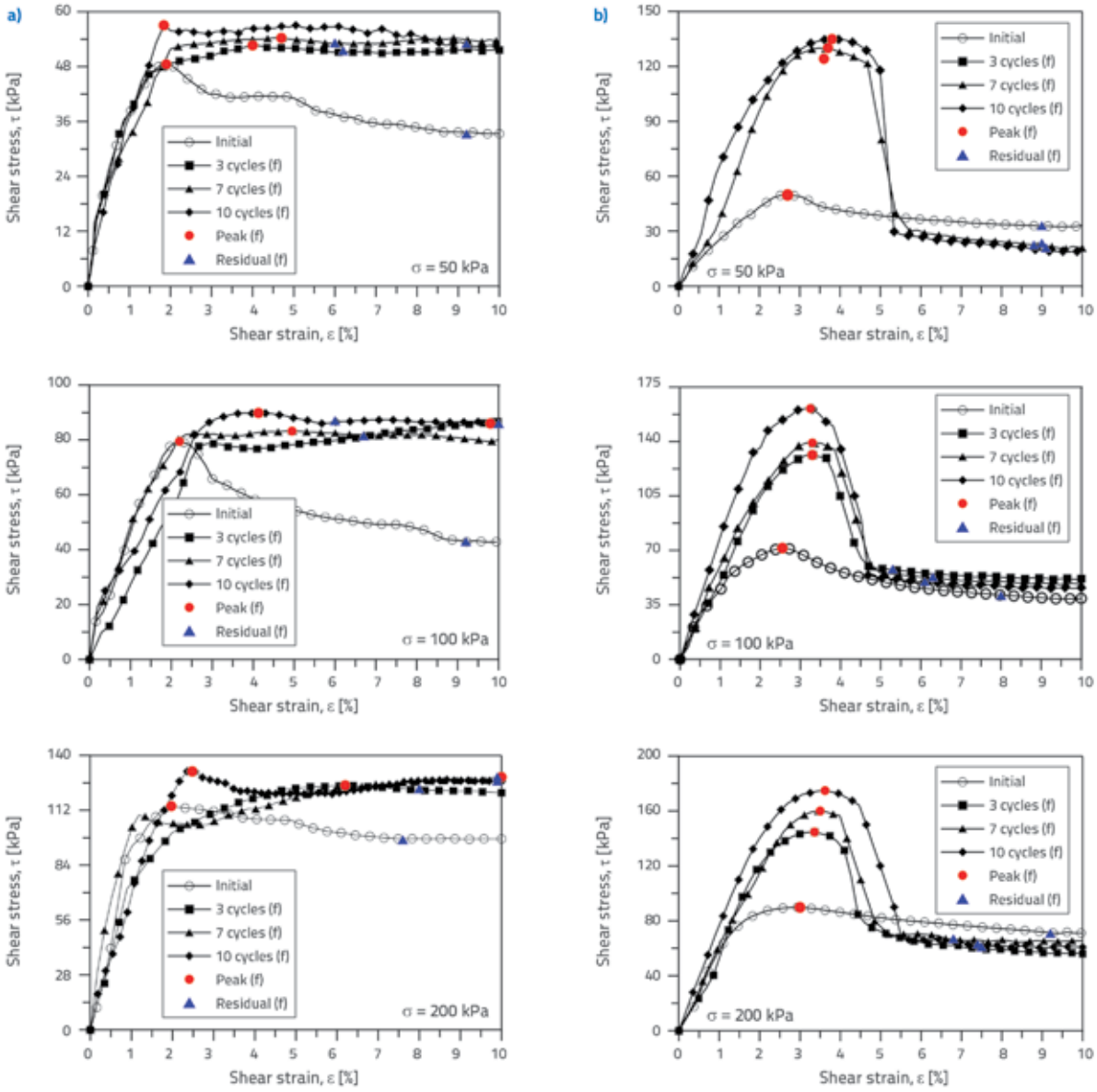

Figure 12. Stress-strain curves from direct shear tests for frozen clay-concrete samples with varying numbers of cycles: a) Frozen - Dry-side; b) Frozen - Wet-side

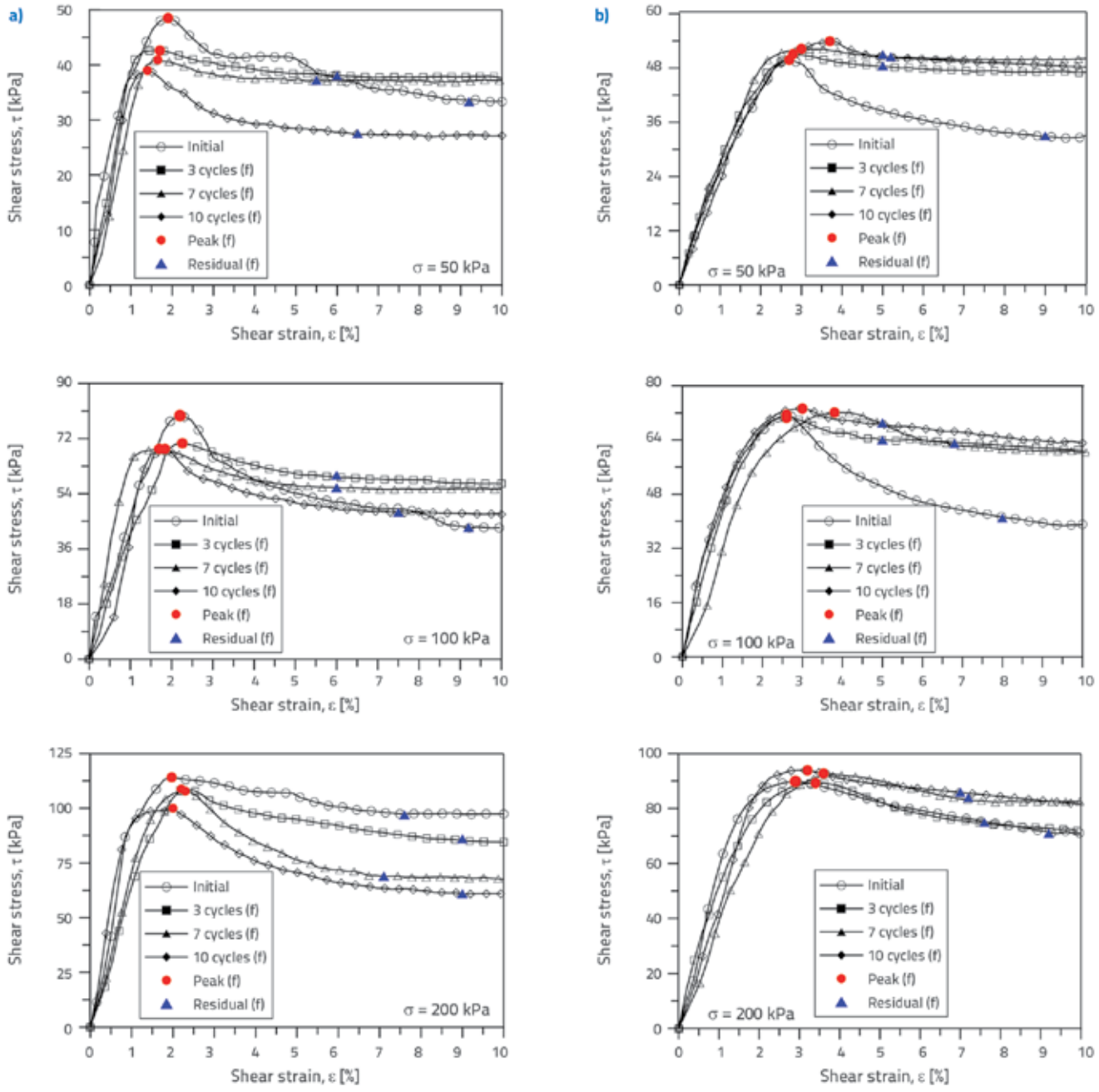

Figure 13. Stress-strain curves from direct shear tests for thawed clay-concrete samples with varying numbers of cycles: a) Thawed - Dry-side b) Thawed - Wet-side

The shear stress-strain curves of the frozen clay-concrete interface for the samples prepared on the dry and wet-sides of the optimum water content are presented in Figure 12.

For the wet-side samples, the failure mode shifted from strain hardening to strain softening. After reaching the peak shear stress, rapid stress reduction occurred owing to the breakdown of the cementing ice at the interface, followed by stabilisation at a residual level. This behaviour reflects a brittle response characterised by the disruption of the cementing ice at the interface.

The peak stress increased with the normal stress and number of F-T cycles, whereas the peak strain ranged between 3 to 4 %. Residual stress increased with normal stress but showed no clear dependence on freeze-thaw cycles, and residual strain remained within the range of 5 to 6 %.

The shear stress-strain curves obtained from the direct shear test results for the thawed clay-concrete interface with the initial water content on the dry and wet-sides of the optimum are presented in Figure 13.

For thawed samples on the dry-side, the stress-strain curve showed a strain-softening behaviour. Compared to the frozen condition, the curve shifted from a dual-peak shape to a single-peak shape. The peak strain ranges between 1.5-2.5 %, and the peak stress increased with the normal stress. However, the peak stress is lower than the initial state and decreases with an increasing number of freeze-thaw cycles, indicating progressive strength loss, in contrast to the trend observed in the frozen samples. The residual strain varies between 4-6 %, increasing with normal stress but showing no clear dependence on the number of cycles.

For samples thawed on the wet-side, strain-softening behaviour was also observed. The peak strain, which ranged from 2.5 % to 3.5 %, was higher than that on the dry-side. Peak stress slightly increased with normal stress and showed limited recovery with increasing cycles compared to the initial stage, but it remained significantly lower at approximately half of that of the frozen samples. Residual strain remained within 4-6 %, while residual stress increases with both normal stress and the number of freeze-thaw cycles.

The effects of freeze-thaw cycling on the interface behaviour are mainly related to moisture migration, ice formation, and the accumulation of ice films at the interface [20]. Ice layers play a key role in adfreezing strength because the shear resistance at low temperatures is largely controlled by ice cementation at the interface [75]. Higher initial moisture content increases the amount of water available for freezing, resulting in stronger ice bonding [4]. This enhances the shear strength under frozen conditions, but also promotes brittle failure owing to interfacial ice bonding. Previous studies [14, 19, 66, 76] have shown that increasing the water content shifts the behaviour from plastic to brittle. Similarly, the water content (or ice content under frozen conditions) significantly affects the stiffness and failure modes of frozen soils [13, 77, 78].

During thawing, the degradation of ice bonds reduces interface shear strength, particularly peak strength [20, 21]. In contrast, the residual strength remains relatively stable and is largely independent of the moisture content [17] and freeze-thaw cycles [20]. The influence of temperature on the residual strength was also limited, as shown by Zhang et al. [41].

Peak displacement increases with initial moisture content but is not strongly affected by freeze-thaw cycles, temperature, or normal stress. Similarly, the residual displacement showed little dependence on these factors [20].

In agreement with these findings, the results indicate that the residual shear strength varies only slightly under different moisture and freeze-thaw conditions. It increases with the normal stress but shows no systematic trend with the number of cycles. Studies have shown that the residual shear stress is less sensitive to changes in water content than the peak shear strength [14, 19].

Unlike the peak strength, which is highly sensitive to thermal conditions and moisture content, the residual behaviour remains relatively stable. It is also less affected by F-T cycles [20]. This suggests that the residual shear strength is mainly governed by frictional mechanisms at the interface, with limited influence from ice bonding or freeze-thaw cycling.

3.3. Adfreezing and F-T cycles effect on peak strength

The peak shear stress, defined as shear strength, demonstrated a strong correlation with the normal stress (Figure 14). This relationship followed a linear fitting function for both frozen and thawed samples prepared on the wet and dry-sides of the optimum water content (Table 3).

In the frozen dry-side samples, the interface strength exhibited an adfreezing effect. However, the increase was limited compared with the initial unfrozen strength. The peak strength increased with the normal stress.

The effect of the F-T cycles became more noticeable as the number of cycles increased. This is particularly evident after 10 cycles. The highest value was obtained at 200 kPa during the 10^{th} cycle. The strength increases from 114.15 kPa (unfrozen) to 131.85 kPa, which is 1.16 times the initial value. Overall, the peak strength ranges between 1.05 to 1.19 times the initial strength. This indicates that repeated F-T cycles gradually increase the adfreezing strength owing to ice cementation at the interface.

The opposite trend was observed for the thawed dry-side samples. After 10 cycles, the peak strength decreases to 73.95 kPa at 200 kPa normal stress. This is 0.65 times the initial strength and 0.56 times the frozen strength. The lowest value occurred after 10 cycles, and the strength gradually decreased as the number of cycles increased. After thawing, it dropped to 0.80-0.95 times the initial strength, depending on the normal stress level. This result highlights the detrimental impact of repeated F-T cycles on the structural integrity of the thawed dry-side samples.

In frozen wet-side samples, shear strength increases 1.6 to 2.7 times depending on normal stress and the cycle number, primarily due to ice cementation at the interface driven by water migration caused by thermal gradients between clay and concrete. The peak strength increased with the normal stress, and the effect of the cycles was again most visible at 10 cycles. At 200 kPa, strength increases from 89.82 kPa to 174.79 kPa, corresponding to 1.95 times the initial value.

After three cycles, the peak shear strength reaching 1.61 times the initial value (144.67 kPa), 1.78 times after seven cycles (160.01 kPa), and 1.95 times after 10 cycles (174.79 kPa).

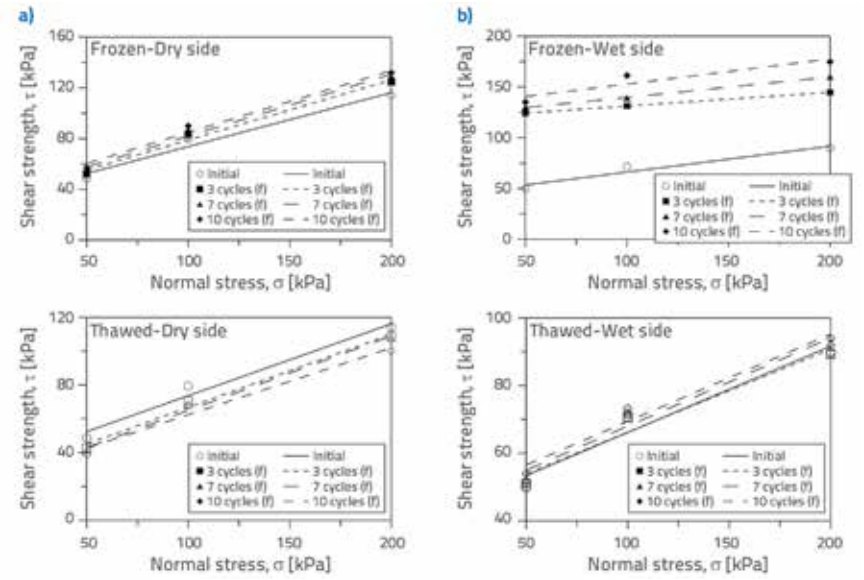

Figure 14. Change in shear strength of frozen and thawed clay-concrete samples with respect to normal stress and number of cycles for a) Dry-side b) Wet-side

Table 3. Shear strength fitting equations for frozen and thawed samples on the wet and dry-sides

Condition	Wet-side sample		Dry-side sample	
	Equation	R^2	Equation	R^2
Initial	$\tau = 0.255\sigma + 40.638$	0.944	$\tau = 0.425\sigma + 31.176$	0.975
3 cycle (frozen)	$\tau = 0.136\sigma + 117.516$	0.999	$\tau = 0.473\sigma + 31.544$	0.989
7 cycle (frozen)	$\tau = 0.201\sigma + 119.601$	0.999	$\tau = 0.487\sigma + 33.238$	0.986
10 cycle (frozen)	$\tau = 0.247\sigma + 128.109$	0.869	$\tau = 0.487\sigma + 36.030$	0.986
3 cycle (thawed)	$\tau = 0.245\sigma + 41.715$	0.961	$\tau = 0.433\sigma + 23.491$	0.990
7 cycle (thawed)	$\tau = 0.261\sigma + 41.916$	0.968	$\tau = 0.440\sigma + 20.957$	0.992
10 cycle (thawed)	$\tau = 0.258\sigma + 43.620$	0.971	$\tau = 0.395\sigma + 22.897$	0.972

This shows that repeated freezing enhances ice-bonding and increases strength. This effect was stronger in wet samples, highlighting the role of the initial water content.

After thawing, the wet samples exhibited a sharp decrease in strength. At 200 kPa and 10 cycles, strength drops from 174.79 kPa to 93.89 kPa. This is 0.54 times the frozen strength. However, compared with the initial unfrozen state, there was no significant decrease. However, only a slight increase was observed. Strength, increases from 89.82 kPa to 93.89 kPa which is 1.05 times the initial value.

The increase in the frozen strength was due to ice cementation at the interface. Water migrates toward the interface owing to the thermal gradient and freezes. After thawing, this led to a higher moisture content near the interface. The applied normal stress enhanced the contact surface between the soil and concrete. This reduced the weakening effects of the F-T cycles. Instead, the strength remained stable, or in some cases, increased slightly with repeated cycles.

When the temperature falls below freezing, ice adhesion at the interface increases the shear resistance. This was defined as the freezing strength [79]. This effect is related to the strength of ice and the increased adhesion between the frozen soil and concrete [14, 18, 19, 76]. Wang et al. [80] showed that the peak stress increases with moisture content under frozen conditions. This is due to water migration and ice layer formation [17]. Increased ice bonding may also change the behaviour from plastic to brittle as the moisture content increases [66]. The peak strength increased with normal stress, water content, and temperature [14]. After thawing, the softened soil can fill surface irregularities and increase contact [24].

3.4. Adfreezing and F-T cycles effect on adhesion and interface friction angle

The effects of freeze-thaw cycles and adfreezing on the adhesion (c_a) and interface friction angle (δ) between clay and concrete are clearly presented in Figure 15. The adhesion values in Figure 15a show clear differences between the wet- and dry-side samples under F-T cycles.

By the 3rd freezing cycle, the dry-side samples exhibited only a slight increase in adhesion. This increase continues gradually with additional cycles and reaches a total increase of 5.00 kPa after 10 cycles.

This limited increase was mainly related to the low availability of free water in the dry-side samples. The presence of air in the voids restricts water migration, and consequently, the extent of ice cementation at the interface.

After the third freezing cycle, the adhesion of the wet samples increased to three times its initial value. The subsequent increase was minimal, leading to stabilization at approximately 128.11 kPa by the 10th freeze cycle. However, despite this stabilisation,

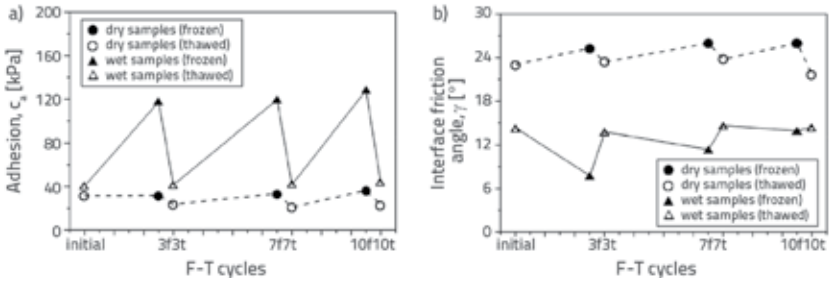

Figure 15. Shear strength parameters of the interface at dry-side and wet-side: a) adhesion; b) interface friction angle

each cycle still showed an increasing trend, with the adhesion gradually increasing as the number of cycles increased.

This suggests that although the initial impact of ice cementation is significant, its influence continues to contribute to a steady increase in adhesion with repeated freeze cycles. This behaviour was facilitated by the movement of free water toward the interface.

During the thawing cycles, the adfreezing effect on adhesion gradually weakened. In dry samples, adhesion shows a decreasing trend compared to the initial cycle, dropping from 31.18 kPa to 22.90 kPa by the 10th thawing cycle. This corresponds to 0.73 times the initial value and indicates that repeated thawing reduces the interfacial bond strength.

In contrast, the wet samples showed a slight recovery after thawing compared to the initial value. By the 10th thawing cycle, adhesion increases from 40.64 kPa to 43.62 kPa reaching 1.07 times the initial value. This recovery in the wet samples may be attributed to the free water migration toward the interface. This effect became more pronounced with repeated cycles, and the adhesion was slightly enhanced by increasing the moisture content near the interface.

When considering the interface friction angle of both the frozen and thawed samples, varied trends were observed. F-T cycles do not produce a consistent trend in interface friction, as both dry and wet samples show fluctuations, which are more pronounced in wet samples.

However, contrasting behaviours were observed between the dry- and wet-side samples in the frozen state. In dry samples, the interface friction angle in the frozen state shows a gradual increase with each freeze-thaw cycle, reaching its highest value at 10th cycle. This suggests that repeated freezing enhances interlocking or structural rearrangement at the interface, thereby improving shear resistance.

However, during thawing, the interface friction angle decreases by approximately 2°, falling below the initial value after 10 cycles, indicating that the degradation of interfacial bonding over successive thawing cycles weakened the shear resistance.

Among the wet samples, the frozen samples initially experienced a sharp drop in the interface friction angle, which reduced it to nearly half of the initial value. However, after 3rd cycle, gradual recovery was observed. The values nearly returned to the initial level after multiple freeze-thaw cycles. This trend suggests that water migration and unfrozen water initially reduced the interfacial resistance owing to the lubricating effect. However, with an increasing number of cycles, higher ice cementation or better particle rearrangement may occur, leading to an improved shear resistance.

In the thawed state, the interface friction angle significantly decreased in the initial cycles and then stabilised. This behaviour was likely due to the redistribution of water at the interface.

The freeze bond strength at the interface consists of two components: ice adhesion to the concrete surface and friction between the soil grains at the interface, as described by He et al. [14] in their study. The influence of temperature on the interface shear strength is primarily reflected in changes in the cohesive forces. As the temperature decreased and the moisture content increased, the adhesion increased significantly, highlighting its crucial contribution to the shear strength under frozen conditions.

In contrast, the friction angle is generally considered insensitive to temperature variations. Sadovskiy [81] observed that freezing increases the soil cohesion, whereas the angle of shearing resistance remains virtually unchanged. Similarly, Wang et al. [80] reported that, although the cohesive force increases sharply with increasing moisture content, the internal friction angle tends to decrease under constant surface roughness [17]. However, under frozen conditions, the moisture content exerts a dual influence. It enhances the interface cementation through the formation of ice crystals, whereas unfrozen water acts as a lubricant. This reduces friction and lowers the friction angle, particularly at higher moisture levels [17, 75].

Regarding the effects of F-T cycles, He et al. [20] found no significant variation in the peak or residual friction angles before or after F-T cycling. This observation aligns with the findings of Ladanyi and Theriault [82], who also concluded that F-T cycling predominantly affects cohesion, whereas frictional resistance remains largely stable.

Based on the experimental findings presented above, the underlying physical mechanisms governing interface behaviour can be interpreted by integrating the observed responses with established knowledge of freezing and freeze-thaw processes, as illustrated schematically in Figure 16. The results indicate that the interface behaviour differs fundamentally between wet- and dry-side conditions. For the wet-side samples, a high degree of saturation promoted water migration towards the concrete surface during freezing owing to thermal gradients. This led to the formation of a continuous ice layer at the interface. This enhances adfreezing and results in a significant increase in the shear strength. Following thawing, the elevated

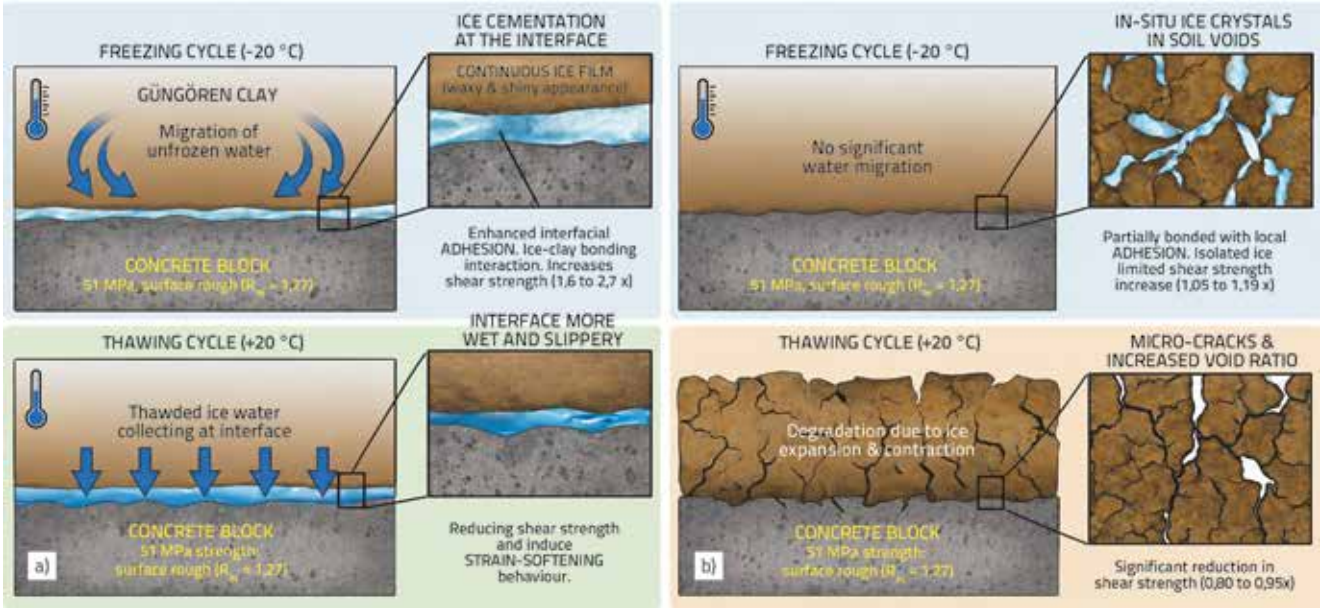

Figure 16. Mechanisms of clay-concrete interface behaviour under freeze-thaw cycles: a) wet-side mechanism; b) dry-side mechanism

moisture content improves particle contact under normal stress, enabling the interface to retain its shear strength. By contrast, the dry-side samples exhibited limited water mobility, which restricted the development of a continuous ice layer. As a result, freezing was primarily confined to the soil pores, leading to only a marginal increase in shear strength. During thawing, microstructural degradation and an increased void ratio weaken the interface, thereby reducing the shear strength.

4. Conclusion

This study examined the shear behaviour of the Güngören clay-concrete interface through direct shear tests, focusing on the effects of F-T cycling and adfreezing. The results obtained for the Güngören clay-concrete interface are as follows.

- During freezing, thermal gradients between clay and concrete induced water migration and adfreezing, as evidenced by visible ice crystal formation at the interface.
- Dry-side frozen samples showed double-peak, multi-stage deformation, whereas thawed samples exhibited strain softening. The frozen wet-side samples failed in a brittle manner, whereas the thawed samples exhibited gradual post-peak softening.
- In frozen wet-side samples, the shear strength increased by 1.6 to 2.7 times depending on the normal stress and the number of freeze-thaw cycles. The samples thawed on the wet-side retained their initial strength owing to water migration and an increased contact surface.
- In frozen dry-side samples, the shear strength increased 1.05 to 1.19 times due to limited water content and restricted ice cementation. After thawing, dry-side samples decreased to 0.80 to 0.95 times their initial values.
- Adhesion increased to ~5 kPa in the frozen dry-side samples after 10 freeze-thaw cycles and tripled in the wet-side samples after three cycles. After thawing, the adhesion slightly recovered in the wet-side samples, exceeding the initial value by approximately 3 kPa.
- The interface friction angle increased slightly under frozen conditions for dry-side samples but declined after thawing. In the wet-side samples, it initially decreased during freezing and then recovered and stabilised across cycles.

Limitations and recommendations

This study evaluated the shear strength under the adfreezing effect and F-T cycles, focusing on the macroscopic mechanical response. However, this study had several limitations.

First, microstructural observations, such as the visualisation of ice formation and crack development during thawing as well as the measurement and controlled variation of unfrozen water content, were not included, although these factors play a critical role in governing the interface behaviour. In addition, experiments were conducted on compacted soil samples, which do not fully represent the natural soil structure. Therefore, the distribution of unfrozen water and the associated mechanical behaviour may differ from in situ conditions, where the soil structure plays a more significant role. Second, the effects of strain rate and its interaction with temperature were not investigated, despite their importance in defining the mechanical response under different loading and thermal conditions. Third, the behaviour was examined only at fixed

freezing and thawing temperatures, and the influence of different temperature levels across the freeze-thaw range was not considered.

It should be noted that these aspects require advanced and often specialized experimental setups. Therefore, each study presented a distinct and valuable research direction. Future studies addressing these factors would provide a more comprehensive understanding of the mechanisms governing the soil-structure interface behaviour under freeze-thaw conditions.

REFERENCES

[1] Qi, J., Vermeer, P.A., Cheng, G.: A review of the influence of freeze-thaw cycles on soil geotechnical properties, Permafrost and Periglacial Processes, 17 (2006) 3, pp. 245-252, https://doi.org/10.1002/ppp.559

[2] Hu, J., Zhang, H., Li, Z., Yang, S., Zhang, S., Li, H., Lu, M.: Study on pore-water pressure variation and deformation characteristics of warm frozen soils under confined dynamic loading, Cold Regions Science and Technology, 214 (2023), 103968, https://doi.org/10.1016/j.coldregions.2023.103968

[3] Ding, J., Han, L., Li, Y. et al.: Permafrost engineering characteristics and frozen soil engineering on Qinghai-Tibet railway, Journal of Railway Engineering Society, (2005) s1, pp. 327-332

[4] Sun, T., Gao, X., Liao, Y., Feng, W.: Experimental study on adfreezing strength at the interface between silt and concrete, Cold Regions Science and Technology, 190 (2021), 103346, https://doi.org/10.1016/j.coldregions.2021.103346

[5] Tang, L., Cong, S., Geng, L., Ling, X., Gan, F.: The effect of freeze-thaw cycling on the mechanical properties of expansive soils, Cold Regions Science and Technology, 145 (2018), pp. 197-207, https://doi.org/10.1016/j.coldregions.2017.10.004

[6] Hong, L., Li, M., Du, C. et al.: Bond behaviour of the interface between concrete and basalt fiber reinforced polymer bar after freeze-thaw cycles, Frontiers of Structural and Civil Engineering, 18 (2024), pp. 630-641, https://doi.org/10.1007/s11709-024-0989-y

[7] Tsinker, G.P.: Geotechnical aspects of soil-structure interaction design considerations, in: Handbook of Port and Harbor Engineering, Springer, 1997, https://doi.org/10.1007/978-1-4757-0863-9_4

[8] Pham, T.A., Nadimi, S., Sutman, M.: Critical review of physical-mechanical principles in geostructure-soil interface mechanics, Geotechnical and Geological Engineering, 42 (2024), pp. 6757-6808, https://doi.org/10.1007/s10706-024-02954-7

[9] Kadivar, M., Manahiloh, K.N.: Revisiting parameters that dictate the mechanical behaviour of frozen soils, Cold Regions Science and Technology, 163 (2019), pp. 34-43, https://doi.org/10.1016/j.coldregions.2019.04.005

[10] Shen, M., Zhou, Z., Zhang, S.: Effect of stress path on mechanical behaviours of frozen subgrade soil, Road Materials and Pavement Design, 23 (2021) 5, pp. 1061-1090, https://doi.org/10.1080/14680629.2020.1869583

[11] Sage, J.D., D'Andrea, R.D.: Long term mitigation of frost deterioration of existing roadways, Final Report, NSF Grant No. ECE 85 18813, Worcester, USA, 1988, pp. 1-105

[12] Czurda, K.A., Hohmann, M.: Freezing effect on shear strength of clayey soils, Applied Clay Science, 12 (1997), pp. 165-187, https://doi.org/10.1016/S0169-1317(97)00005-7

[13] Shi, S., Zhang, F., Feng, D., Xu, X.: Experimental investigation on shear characteristics of ice-frozen clay interface, Cold Regions Science and Technology, 176 (2020), 103090, https://doi.org/10.1016/j.coldregions.2020.103090

[14] He, P.F., Mu, Y.H., Ma, W., Huang, Y.T., Dong, J.H.: Testing and modeling of frozen clay-concrete interface behaviour based on large-scale shear tests, Advances in Climate Change Research, 12 (2021) 1, pp. 83-94, https://doi.org/10.1016/j.accre.2020.09.010

[15] Quanbin, S., Ping, Y., Guoliang, W.: Experimental research on adfreezing strength at the interface between frozen sand and structures, Scientia Iranica A, 25 (2018) 2, pp. 663-674, https://doi.org/10.24200/sci.2017.20005

[16] Wang, Q., Qi, J., Wang, S., Xu, J., Yang, Y.: Effect of freeze-thaw on freezing point of a saline loess, Cold Regions Science and Technology, 170 (2020), 102922, https://doi.org/10.1016/j.coldregions.2020.102922

[17] Wang, T.L., Wang, H.H., Hu, T.F., Song, H.F.: Experimental study on the mechanical properties of soil-structure interface under frozen conditions using an improved roughness algorithm, Cold Regions Science and Technology, 158 (2019), pp. 62-68, https://doi.org/10.1016/j.coldregions.2018.10.015

[18] Aldaeef, A.A., Rayhani, M.T.: Pile-soil interface characteristics in ice-poor frozen ground under varying exposure temperature, Cold Regions Science and Technology, 192 (2021), 103377, https://doi.org/10.1016/j.coldregions.2021.103377

[19] Liu, J., Lv, P., Cui, Y., Liu, J.: Experimental study on direct shear behaviour of frozen soil-concrete interface, Cold Regions Science and Technology, 104-105 (2014), pp. 1-6, https://doi.org/10.1016/j.coldregions.2014.04.007

[20] He, P., Mu, Y., Yang, Z., Ma, W., Dong, J., Huang, Y.: Freeze-thaw cycling impact on the shear behaviour of frozen soil-concrete interface, Cold Regions Science and Technology, 173 (2020), 103024, https://doi.org/10.1016/j.coldregions.2020.103024

[21] Zhao, Y., Mao, X., Wu, Q., Huang, W., Wan, Y.: Study on shear characteristics of the interface between frozen soil and pile during thawing process in permafrost area, Advances in Civil Engineering, 2022 (2022), 1755538, https://doi.org/10.1155/2022/1755538

[22] De Guzman, E.M.B., Stafford, D., Alfaro, M.C., Doré, G., Arenson, L.U.: Large-scale direct shear testing of compacted frozen soil under freezing and thawing conditions, Cold Regions Science and Technology, 151 (2018), pp. 138-147, https://doi.org/10.1016/j.coldregions.2018.03.011

[23] Zhao, L., Yang, P., Wang, J.G. et al.: Cyclic direct shear behaviours of frozen soil-structure interface under constant normal stiffness condition, Cold Regions Science and Technology, 102 (2014), pp. 52-62

[24] Volokhov, S.S.: Effect of freezing conditions on the shear strength of soils frozen together with materials, Soil Mechanics and Foundation Engineering, 40 (2003) 6, pp. 1-5, https://doi.org/10.1023/B:SMAF.0000017575.19213.67

[25] Kim, K.H., Jeon, S.E., Kim, J.K. et al.: An experimental study on thermal conductivity of concrete, Cement and Concrete Research, 33 (2003) 3, pp. 363-371, https://doi.org/10.1016/S0008-8846(02)00965-1

[26] Mu, R., Tian, W., Zhou, M.: Moisture migration in concrete exposed to freeze-thaw cycles, Journal of the Chinese Ceramic Society, 38 (2010) 9, pp. 1713-1717

[27] Istanbul Metropolitan Municipality Directorate of Earthquake and Ground Research: Geological-Geotechnical Study Report and Map for the Southern Region of Istanbul's European Side at a 1/5000 Scale for Zoning Plans, Istanbul, 2001

[28] Yılmaz, E.: Güngören formasyonu killerin mühendislik özellikleri ve mineralojik etkiler, Master's thesis, Istanbul University, Institute of Science, Department of Geological Engineering, Istanbul, 2005

[29] Mermutlu, E., Şans, G., Mahmutoğlu, Y.: İstanbul-Ambarlı heyelanının izlenmesi ve analizi, in: KAYAMEK'2011 - X. Bölgesel Kaya Mekaniği Sempozyumu / ROCMEC'2011 - Xth Regional Rock Mechanics Symposium, Ankara, Turkey, 2011

[30] Dalgıç, S.: Factors affecting the greater damage in the Avcılar area of Istanbul during the 17 August 1999 Izmit earthquake, Bulletin of Engineering Geology and the Environment, 63 (2004) 3, pp. 221-232, https://doi.org/10.1007/s10064-004-0234-9

[31] American Society for Testing and Materials (ASTM): ASTM D6913-18: Standard Test Method for Particle-Size Distribution (Gradation) of Soils Using Sieve Analysis, ASTM International, West Conshohocken, PA, USA, 2018

[32] American Society for Testing and Materials (ASTM): ASTM D7928-17: Standard Test Method for Particle-Size Distribution (Gradation) of Fine-Grained Soils Using the Sedimentation (Hydrometer) Analysis, ASTM International, West Conshohocken, PA, USA, 2017

[33] American Society for Testing and Materials (ASTM): ASTM D4318-17: Standard Test Methods for Liquid Limit, Plastic Limit, and Plasticity Index of Soils, ASTM International, West Conshohocken, PA, USA, 2014

[34] American Society for Testing and Materials (ASTM): ASTM D854-14: Standard Test Methods for Specific Gravity of Soil Solids by Water Pycnometer, ASTM International, West Conshohocken, PA, USA, 2014

[35] American Society for Testing and Materials (ASTM): ASTM D698-12: Standard Test Methods for Laboratory Compaction Characteristics of Soil Using Standard Effort (12,400 ft-lb/ft^3), ASTM International, West Conshohocken, PA, USA, 2012

[36] American Society for Testing and Materials (ASTM): ASTM D2487-17(2025): Standard Practice for Classification of Soils for Engineering Purposes (Unified Soil Classification System), ASTM International, West Conshohocken, PA, USA, 2025

[37] American Society for Testing and Materials (ASTM): ASTM D4546-14: Standard Test Methods for One-Dimensional Swell or Collapse of Soils, ASTM International, West Conshohocken, PA, USA, 2014

[38] Tiwari, B., Ajmera, B.: Consolidation and swelling behaviour of major clay minerals and their mixtures, Applied Clay Science, 54 (2011) 3-4, pp. 264-273, https://doi.org/10.1016/j.clay.2011.10.001

[39] Panda, G.P., Bahrami, A., Nagaraju, T.V., Isleem, H.F.: Response of high swelling montmorillonite clays with aqueous polymer, Minerals, 13 (2023) 7, 933, https://doi.org/10.3390/min13070933

[40] Li, X., Zhang, L., Zhang, Y.: Influence of montmorillonite on the freeze-thaw properties of expansive soils, Geotechnical Testing Journal, 34 (2011) 4, pp. 295-306

[41] Zhang, L., Ma, W., Yang, C., Dong, S.: A review and prospect of the thermodynamics of soil subjected to freezing and thawing, Journal of Glaciology and Geocryology, 35 (2013) 6, pp. 1505-1518

[42] Wang, C., Lai, Y., Yu, F., Li, S.: Estimating the freezing-thawing hysteresis of chloride saline soils based on the phase transition theory, Applied Thermal Engineering, 135 (2018), pp. 22-33, https://doi.org/10.1016/j.applthermaleng.2018.02.039

[43] Adorni, E., Ivanov, M., Revetria, R.: Review of the effects of the influence of external vibrations on the freezing point of water, MATEC Web of Conferences, 320 (2020), 00032, https://doi.org/10.1051/matecconf/202032000032

[44] Shah, R., Mir, B.A.: The freezing point of soils and the factors affecting its depression, in: Loon, L.Y., Subramaniyan, M., Gunasekaran, K. (eds): Advances in Construction Management, Lecture Notes in Civil Engineering, vol. 191, Springer, Singapore, 2022, https://doi.org/10.1007/978-981-16-5839-6_14

[45] Mo, C., Hanbing, C., Anyu, L.: Effect of freezing temperature and initial water content on hydrothermal migration of silty soil under freezing, Arabian Journal of Geosciences, 15 (2022) 2, https://doi.org/10.1007/s12517-022-09486-5

[46] Pennisi, S.V., Habteselassie, M.Y.: Laboratory-scale study on the effects of freezing in soils when subjected to different moisture content, Water, 14 (2022), 1892, https://doi.org/10.3390/w14121892

[47] Zhang, L., Yang, C., Wang, D., Zhang, P., Zhang, Y.: Freezing point depression of soil water depending on its non-uniform nature in pore water pressure, Geoderma, 412 (2022), 115724, https://doi.org/10.1016/j.geoderma.2022.115724

[48] Frost, J.D., De Jong, J.T., Recalde, M.: Shear failure behaviour of granular-continuum interfaces, Engineering Fracture Mechanics, 69 (2002), pp. 2029-2048

[49] Gómez, J.E., Filz, G.M., Ebeling, R.M., Dove, J.E.: Sand to concrete interface response to complex load paths in a large displacement shear box, Geotechnical Testing Journal, 31 (2008) 4, pp. 358-369

[50] Martinez, A., Frost, J.D.: The influence of surface roughness form on the strength of sand-structure interfaces, Géotechnique Letters, 7 (2017) 1, pp. 104-111

[51] Di Donna, A., Ferrari, A., Laloui, L.: Experimental investigations of the soil-concrete interface: physical mechanisms, cyclic mobilization, and behaviour at different temperatures, Canadian Geotechnical Journal, 53 (2015) 4, pp. 659-672

[52] Meier, A.L., Faro, V.P., Odebrecht, E.: Shear strength analysis of interfaces between granular soils and concrete cured under stress, Soils and Rocks, 46 (2023) 1, e2023004022

[53] Chang, W.R.: The effect of surface roughness on dynamic friction between neolite and quarry tile, Safety Science, 29 (1998) 2, pp. 89-105

[54] Tehrani, F.S., Han, F., Salgado, R., Prezzi, M., Tovar, R.D., Castro, A.G.: Effect of surface roughness on the shaft resistance of nondisplacement piles embedded in sand, Géotechnique, 66 (2016) 5, pp. 386-400, https://doi.org/10.1680/jgeot.15.P.007

[55] Nardelli, A., Cacciari, P.P., Futai, M.M.: Sand-concrete interface response: The role of surface texture and confinement conditions, Soils and Foundations, 59 (2019) 6, pp. 1675-1694, https://doi.org/10.1016/j.sandf.2019.10.004

[56] Uesugi, M., Kishida, H.: Influential factors of friction between steel and dry sands, Soils and Foundations, 26 (1986) 2, pp. 33-45, https://doi.org/10.3208/sandf1972.26.2_33

[57] Gokhale, M., Underwood, E.E.: A general method for estimation of fracture surface roughness, 1990

[58] ISO 25178-601: Geometrical product specifications (GPS) - Surface texture: Areal - Part 601: Nominal characteristics of contact (stylus) instruments, ISO, 2010

[59] Lemos, L.J.L., Vaughan, P.R.: Clay-interface shear resistance, Géotechnique, 50 (2000) 1, pp. 55-64

[60] Murphy, K.D., McCartney, J.S.: Thermal borehole shear device, Geotechnical Testing Journal, 37 (2014) 6, 20140009, https://doi.org/10.1520/GTJ20140009

[61] American Society for Testing and Materials (ASTM): ASTM D3080/D3080M-22: Standard Test Method for Direct Shear Test of Soils Under Consolidated Drained Conditions, ASTM International, West Conshohocken, PA, USA, 2022

[62] Kou, H., Huang, J., Cheng, Y.: Friction characteristics between marine clay and construction materials, Journal of Ocean University of China, 23 (2024), pp. 427-437, https://doi.org/10.1007/s11802-024-5474-7

[63] Wang, B., Liu, J., Wang, Q., Ling, X., Pan, J., Fang, R., Bai, Z.: Influence of freeze-thaw cycles on the shear performance of silty clay-concrete interface, Cold Regions Science and Technology, 219 (2024), 104120

[64] He, P., Cao, H., Dong, J., Hou, G., Mu, Y., Zhang, J.: Effects of wet-dry-freeze-thaw cycles on the response of the frozen soil-composite geotextile interface in direct shear tests, Case Studies in Thermal Engineering, 63 (2024), 105217, https://doi.org/10.1016/j.csite.2024.105217

[65] Meng, Y., Xu, C., Yang, Y., Du, C., Jia, B., Zhao, C.: Study on the mechanism of freeze-thaw cycles on the shear strength of geogrid-sand interface, Cold Regions Science and Technology, 225 (2024), 104275, https://doi.org/10.1016/j.coldregions.2024.104275

[66] Zhang, K., Yan, J., Mu, Y., Zhu, X., Zhang, L.: Global and local shear behaviour of the frozen soil-concrete interface: Effects of temperature, water content, normal stress, and shear rate, Buildings, 14 (2024) 10, 3319, https://doi.org/10.3390/buildings14103319

[67] Bouyoucos, G.J.: The freezing point method as a new means of measuring the concentration of the soil solution directly in the soil, Michigan Agricultural College Experiment Station Technical Bulletin, 24 (1916), pp. 1-44

[68] Nersesova, Z.A., Tsytovich, A.: Unfrozen water in frozen soils, in: Proceedings of the 1st International Permafrost Conference, Purdue University, Lafayette, Indiana, 1963, pp. 230-234

[69] Konrad, J.M.: Unfrozen water as a function of void ratio in a clayey silt, Cold Regions Science and Technology, 18 (1990), pp. 49-55, https://doi.org/10.1016/0165-232X(90)90037-W

[70] Christ, M., Kim, Y.C.: Experimental study on the physical-mechanical properties of frozen silt, KSCE Journal of Civil Engineering, 13 (2009) 5, pp. 317-324, https://doi.org/10.1007/s12205-009-0317-z

[71] Andersland, O.B., Ladanyi, B.: An Introduction to Frozen Ground Engineering, ASCE & John Wiley & Sons, New York, 1994

[72] Williams, P.J., Smith, M.W.: The Frozen Earth: Fundamentals of Geocryology, Cambridge University Press, Cambridge, 1989, 306 pp.

[73] Ladanyi, B.: Frozen soil-structure interfaces, in: Selvadurai, A.P.S., Boulon, M.J. (eds): Studies in Applied Mechanics, vol. 42, Elsevier, 1995, pp. 3-33, https://doi.org/10.1016/S0922-5382(06)80004-8

[74] Goughnour, R.R., Andersland, O.B.: Mechanical properties of a sand-ice system, Proceedings of the American Society of Civil Engineers, 94 (1968) SM4, pp. 923-950

[75] Shi, Q., Yang, P., Wang, G.: Experimental study on adfreezing strength of the interface between artificial frozen sand and structure, Chinese Journal of Rock Mechanics and Engineering, 35 (2016) 10, pp. 2142-2151

[76] Wen, Z., Yu, Q., Ma, W. et al.: Experimental investigation on the effect of fiberglass reinforced plastic cover on adfreeze bond strength, Cold Regions Science and Technology, 131 (2016), pp. 108-115, https://doi.org/10.1016/j.coldregions.2016.07.009

[77] Xu, X.T., Dong, Y.H., Fan, C.: Laboratory investigation on energy dissipation and damage characteristics of frozen loess during deformation process, Cold Regions Science and Technology, 109 (2015), pp. 1-8, https://doi.org/10.1016/j.coldregions.2014.09.006

[78] Zhu, Z., Liu, Z., Xie, Q.: Dynamic mechanical experiments and microstructure constitutive model of frozen soil with different particle sizes, International Journal of Damage Mechanics, 26 (2017), 105678951770096, https://doi.org/10.1177/1056789517700967

[79] Parameswaran, V.R.: Adfreeze strength of frozen sand to model piles, Canadian Geotechnical Journal, 15 (1978), pp. 494-500

[80] Wang, W., Yang, X., Huang, S., Yin, D., Liu, G.: Experimental study on the shear behaviour of the bonding interface between sandstone and cement mortar under freeze-thaw, Rock Mechanics and Rock Engineering, 53 (2020), pp. 881-907, https://doi.org/10.1007/s00603-019-01951-0

[81] Sadovskiy, A.V.: Adfreeze between ground and foundation materials, in: Proceedings of the 2nd International Conference on Permafrost, Yakutsk, Northern American Volume, 1973, pp. 650-653

[82] Ladanyi, B., Theriault, A.: A study of some factors affecting the adfreeze bond of piles in permafrost, in: Proceedings of the Geotechnical Engineering Congress GSP 27 ASCE, vol. 1, 1990, pp. 213-224

Primljen / Received: 12.10.2023.
Ispravljen / Corrected: 3.12.2025.
Prihvaćen / Accepted: 22.5.2026.
Dostupno online / Available online: 10.6.2026.

Experimental investigation of time-dependent deformation of soft rock along discontinuities

Authors:

Miodrag Bujišić, MSc. CE
University of Montenegro, Montenegro
Faculty of Civil Engineering
miodragb@ucg.ac.me
Corresponding author

Prof. **Zvonko Tomanović**, PhD. CE
GeoT d.o.o Podgorica, Montenegro
zvonko@geot.me

Research Paper

Miodrag Bujišić, Zvonko Tomanović

Experimental investigation of time-dependent deformation of soft rock along discontinuities

This study presents an experimental investigation of the time-dependent shear behaviour of soft rock discontinuities. Three marly limestone specimens obtained from the Pljevlja coal basin were tested under controlled laboratory conditions. The specimens had identical geometric characteristics but differed in discontinuity surface roughness (smooth, undulating and moderately rough). A dedicated experimental apparatus was designed and adapted to perform long-term shear tests under constant normal loading and incremental shear loading. The results demonstrate the significant influence of discontinuity roughness on shear resistance, displacement development and test duration. Given the limited number of published studies addressing time-dependent deformation of soft-rock discontinuities, the presented pilot investigation provides valuable insight into the governing mechanisms and establishes a basis for a comprehensive experimental programme.

Key words:
soft rock, time-dependent deformations, experiment, discontinuity, roughness

Prethodno priopćenje

Miodrag Bujišić, Zvonko Tomanović

Eksperimentalno ispitivanje meke stijene po diskontinuitetimu u uvjetima ovisnim o vremenu

U okviru eksperimentalnih istraživanja posmične otpornosti po diskontinuitetu pri o vremenu ovisnim uvjetima provedeni su pokusi na tri uzorka meke stijene, laporovitoga vapnenca koja su uzorkovana iz otvorenoga bazena u Pljevljima. Uzorci su istih geometrijskih karakteristika, pravilnoga prizmatičnog oblika, pri čemu je na svakom oblikovana umjetna pukotina, koju odlikuju različite hrapavosti ploha diskontinuiteta (glatka, valovita i umjereno hrapava). Uzorci su ispitivani u laboratorijskim uvjetima, pri čemu je postojeća oprema modificirana i izrađen je dio nove opreme da bi se izveo primjeren eksperiment. Imajući u vidu skroman broj eksperimentalnih istraživanja vremenski ovisnih deformacija mekih stijena po diskontinuitetu (na globalnoj razini) ovim se radomželi dati znanstveni doprinos i prikazati prvi rezultati analizom podataka dobivenih konkretnim eksperimentalnim istraživanjem.

Ključne riječi:
meka stijena, vremenski ovisne deformacije, eksperiment, diskontinuitet, hrapavost

1. Introduction

This paper provides analysis of the results from pilot test, constituting more extensive experimental research within the scope of a scientific project by authors Miodrag Bujisic, MSc and Prof Zvonko Tomanovic, PhD. Experimental part of the scientific project includes two segments – initial (trial) test and main test. The objective of this paper is to analyse the results obtained during a pilot experimental programme pilot test for the purposes of defining the scope of physical-mechanical parameters and the specimen loading level and determining most relevant parameters for key series of experimental tests. The primary objective of the project is to improve the understanding of behaviour of soft rock mass through experimental research. The next steps of the research within the scope of a PhD thesis, aim to add scientific value in terms of obtaining material characteristics of time-dependent behaviour of rock mass for the specimens of a simple geometric shape, while contributing to the examination of phenomenon of discontinuity impact on obtaining the foregoing parameters. The experimental programme was designed to investigate specimens with discontinuities, specimen size 30x15x15(cm) under controlled laboratory conditions, at constant normal loading with incremental shear stress and measurement of deformations. It is important to emphasize that this paper presents the results of a preliminary testing phase, whose primary objective was not the final determination of representative shear strength parameters of discontinuities, but rather the verification of the functionality of a specially developed experimental apparatus, determination of the loading range, and identification of the fundamental mechanisms governing time-dependent shearing along artificially created discontinuities. The obtained results represent the basis for defining the main experimental program, which includes a larger number of specimens, a more controlled loading regime, and a more detailed analysis of the mechanical and geometrical characteristics of discontinuities.

2. Overview of previous research studies

Overview of previous research studies suggests that relatively small number of scientists has engaged in experimental research of effects of long-term loading and unloading on time-dependent deformation of soft rocks. Time-dependent deformation of rock mass under constant stress is defined as creep. Creep depends on changes in stress state, temperature, moisture, air humidity etc.

With regards to a solid rock mass (metamorphic and igneous rocks), creep deformation is insignificant. However, contribution of creep deformation to total value of deformation is considerable in case of soft rock mass, such as rock salt, marl, anhydrite, flysch sediment etc. The tests have shown that creep deformation occurs at different rates and is characterised by three stages, referred to as primary, secondary and tertiary creep. Most of the previously published experimental research in the world addressing the rock behaviour under long-term loading at room temperatures was conducted on the rock salt specimens. (Gimm, 1968; Dreyer, 1974; Baar, 1977; Carter et al., 1982; Wallner, 1983; Hunche, 1994, 1995; presented by Cristescu N.D & Hunsche U, 1998; etc.). An incomparably smaller number of the published experimental research was conducted at room temperatures on marl or similar soft rocks that are characterised by significant creep deformations (clayey-marl, Cristescu, 1988; marl, Kharchafi and Descoeudres, 1995), which represent a realistic work environment for construction of numerous underground structures. Within the examination of marly materials, the papers of authors from Montenegro can be singled out, according [1-8].

When it comes to testing of soft rock specimens intersected by discontinuities, the number of published papers is even smaller. A theoretical approach applied in the initial stage of research of this subject-matter to define time-dependent behaviour of rock mass has not yielded satisfactory results [2].

With advances in development of software tools, numerical modelling has been improved, thus enabling modelling of complex rheological situations which has allowed for better perspective of time-dependent behaviour of rock mass. Determining material parameters and constants which define rheological models of the rock mass behaviour is generally performed by means of laboratory or in-situ tests. A challenging task to determine material characteristics is a consequence of not only complex composition of rock material but also discontinuities which form and characterise the rock mass.

In terms of determining the characteristics of discontinuous rock masses, it is particularly important to define the range of roughness of the shearing, discontinuous surface. In addition to the standard, traditional methods of describing roughness with qualitative and quantitative characteristics, in recent years, with the technological progress of software tools, it is possible to define certain mathematical methods that connect the shear resistance of discontinuities and the roughness of discontinuous surfaces. In this regard, the following papers can be mentioned [14-17].

Previous tests conducted to form models that will represent time-dependent behaviour of rock mass are based on the analysis of monolith specimens of simple geometric characteristics and relatively simple stress state. Nevertheless, it is common practice to use these simple tests to represent with a satisfactory level of accuracy the behaviour of a far more complex stress-strain state of a real rock mass.

3. Experimental tests

3.1. Specimen and equipment preparation

Material used for testing has been sampled from the open pit Potrlica of the coal mine Pljevlja. A block of approximately 3.5 tons was extracted from the open pit mine, at depth of approx. 25m, measured from the terrain surface (Figure 1). Immediately upon excavation, the material was loaded on transport equipment and transported from Pljevlja to Podgorica (approx.

Figure 1. a) position of a bench from which the rock mass block was extracted, b) loading of the rock mass block

Figure 2. Specimens processed to target dimensions 30 x 15 x 15 cm

Figure 3. Examination of uniaxial strength of specimens

180 km). Special care was taken during transportation and unloading to preserve the in-situ structure and orientation of the extracted block., hence rock mass with unchanged geometry was prepared for processing.

A specialised plant for processing of stone was used to process material and form cuboid (prism) shaped specimens with dimensions 30 x 15 x 15 cm (Figure 2). During the preparation of the specimens, due to the very demanding processing (specimens splitting during cutting) of the soft rock mass from nature (irregular shape of rock specimen) into the desired shape of specimen, the processing success rate was approximately 50 %. Simultaneously, a semi-quantitative analysis of specimens was conducted the results of which confirmed the specimens are marly limestone, dominantly composed (93.0 %) of calcium carbonate ($CaCO_3$), while the remaining 7 % includes the following components: quartz 4.80 % (SiO_2), siderite 1.10 % ($FeCO_2$), muscovite 1.10 % ($KAl_3Si_3O_{10}OH_2$).

Sampled material was subjected to uniaxial compression strength tests (Figure 3), for different moisture content (from water-saturated to completely dry specimen). Resulting values for the material with natural moisture content are presented in Table 1. In the table, the specimens are marked with U_1 to U_5. Weight of an empty container is marked with m_p, weight of a container holding a specimen with natural moisture content is marked with m_1, and weight of a container holding a dried specimen is marked with m_2. Uniaxial strength is marked with σ_c.

An artificial crack (Figure 4) was formed on each specimen intended to be tested in a trial (and subsequently in the main part of the experiment). Crack-forming was controlled by cutting (splitting) of specimen in the length of 1 cm at half height (at

Table 1. Uniaxial strength of cylinder-shaped specimens 12 x 5 cm

Specimen condition	Specimens (U1-U5)→	U_1	U_2	U_3	U_4	U_5	$W_{sr.}$ σ_{csr}
Cylinder-shaped specimens with natural moisture content, formed from the cuboid (prism) shaped specimens, stored at day temperature, paraffin-coated, wrapped in foil	m_p [g]	4.9	4	5.3	5.4	4	Key: U_1-U_5 → specimens m_p → Weight of empty container, m_1 → weight of container with specimen with natural moisture content m_2 → weight of container with dried specimen
	m_1 [g]	41.7	36.7	49.7	36	43.9	
	m_2 [g]	37.4	33.2	45.6	32.7	40	
	m_1-m_2 [g]	4.3	3.5	4.1	3.3	3.9	
	m_2-m_p [g]	32.5	29.2	40.3	27.3	36	
	W [%]	13.2 %	11.9 %	10.1 %	12.1 %	10.8 %	W_{sr} = 11.66 %
	σ_c [MPa]	18.14	17.98	17.11	16.28	17.02	σ_{csr} = 17.31

Figure 4. a) Cutting a groove at the specimen centre; b) Cut groove of 1 cm depth; c) Forming of discontinuity

approximately 7.5 cm). At the cut grooves, using a cylinder (Figure 4c) to apply loading at a controlled rate, the specimens were divided into two, approximately equal halves (Figure 3), followed by forming of discontinuity planes of different roughness (Figure 5.b).

Upon defining discontinuity planes, all specimens were wrapped in foil. Previously, after the geometry had been formed, all the specimens were paraffin-coated to preserve their natural moisture content.

With the specimens prepared, the next step was to design new and modify the existing equipment to be used for uniaxial and triaxial creep testing of the intact rock specimens. The scope of pilot programme provided for testing of three specimens of different roughness. For this purpose, one existing frame was specifically prepared at the laboratory of the Faculty of Civil Engineering.

This test frame dates to about 20 years ago, when it was used for testing of marly material which was sampled from the same site for the purposes of the research conducted by Prof Zvonko Tomanovic, PhD. The frame operates on the principle of lever arm and deadweight. The apparatus is centred in relation to the position of a specimen to be subjected to the test and according to the needs of the normal force loading level. Enabling for testing of specimens along the formed shear surfaces, steel moulds were formed for placement of the specimens (Figure 4.a).

Considering the height of the half-specimen is approx. 7.5, the internal height of the mould is 5 cm, to allow for the undisturbed shear behaviour along the discontinuity planes. Thickness of walls and bottom of the steel mould is 1 cm.

The specimens are fixed using a factory produced mortar for casting and grouting, which takes several hours to set after having been poured to fill the voids between the specimen and the mould, making the specimen immovable in the mould. When fixing both halves of the specimen, attempts were made to have the two halves tight fitted to enable as much better simulation of the naturally closely spaced cracks.

To overcome friction that occurs in the apparatus, the experiment provided for adjustment of movable parts to fit over

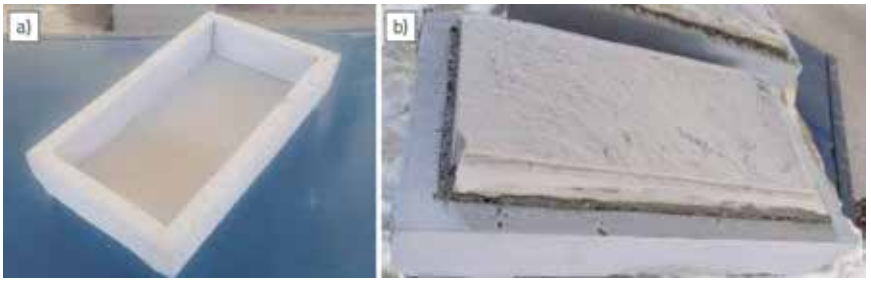

Figure 5. a) Steel mould; b) Half-specimen placed in the mould

Figure 6. a) Rings with gauges for normal stress; b) Thickness of rings 1, 2 and 3 is d = 2.0 cm

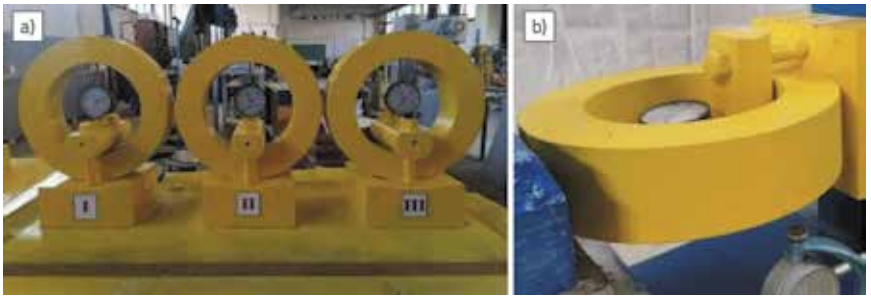

Figure 7. a) Rings with gauges for shear stress; b) Thickness of rings I, II and III is d = 6.0 cm

the cylinder-shaped steel elements, which will be described in detail in part 3 of this paper.
In addition to the specimens, frames, benches and rollers, key components of the equipment are elements for measurement of change in stress and strain. For this purpose, steel rings (dynamometers) were developed with a base plate on which gauges for measurement of normal and shear displacements were mounted. The steel rings are of the same diameter but different thickness due to a different order of magnitude (forces) occurring in the normal and shear direction respectively, which are the subject of measurement by dynamometers (Figures 6 and 7).
With setting of all components of the equipment, specimens prepared, and frames put in operation, all the conditions required for commencement of the experiment were fulfilled.

3.2. Specimen testing

Trial experimental test was performed using one frame (Figure 8). The experiment included testing of three specimens of different roughness, particularly 1) completely smooth plane of discontinuity, 2) extremely undulating discontinuity, and 3) moderately rough plane of discontinuity. For all three foregoing discontinuity planes, the testing was performed under three different constant levels of normal stress. Normal stresses of 0.1 MPa, 0.2 MPa and 0.4 MPa were applied. Limitation of the pilot programme of the experiment is reflected in the fact that within testing of one specimen, for each subsequently applied vertical loading, the shear occurred along the specimen surface that was altered to a certain extent because of the shear occurring for the previous (lower) level of normal stress. The vertical loading was applied using the system of lever arm and deadweight. However, the relevance of such tests derives from the way and sequence of tests. Namely, as the specimens were loaded with a normal stress of 0.1 MPa in the first phase, and then with 0.2 MPa in the second phase, care was taken to inspect the tested specimens after each phase, in fact, to establish the degradation of the tested shear surface. Given that in the first two phases there was no breakage or significant change in the shape of the discontinuity surface (the change was reflected in the form of surface marks due to friction), it was found that the discontinuous surface was almost undisturbed and suitable for the third phase of testing.
It should be emphasized that the experimental apparatus used in this research represents a specially developed laboratory system adapted for long-term time-dependent shear testing along discontinuities. Due to the specific configuration of the apparatus and the large dimensions of the specimens, the testing procedure did not fully correspond to standard ISRM direct shear testing procedures.
Within the preliminary phase of the investigation, testing was carried out using one shear frame, while three specimens with different discontinuity characteristics were successively tested under normal stresses of 0.1 MPa, 0.2 MPa and 0.4 MPa. After completion of each individual shearing phase, the specimen was returned to its initial position, after which the next testing stage was performed under a higher normal stress level.
The authors are aware that such a procedure, particularly in the case of soft rock materials, may lead to partial degradation of the contact surfaces and changes in the local contact structure due to previous shearing. For this reason, the results presented in this paper have a preliminary character and were primarily used for verification of the experimental apparatus functionality, identification of the dominant mechanisms governing discontinuity behaviour, and definition of the methodology for the main experimental program.
The main experimental program was planned to use all three shear frames simultaneously, with each frame subjected to a different constant normal stress level. In this way, repeated shearing of the same discontinuity under different normal stresses would be avoided, which represents one of the main methodological limitations of the preliminary testing phase.
In order to ensure translational shearing and to limit undesirable displacements and rotations, steel guiding restraints were installed on the upper shear box, enabling controlled guidance of the lower box during shear displacement. Although the apparatus did not contain classical spherical seats characteristic of standard direct shear devices, it enabled stable load transfer and registration of the dominant deformation processes during the experiment.
Horizontal loading was applied to the specimen by a large hydraulic cylinder positioned vertically in an additional frame with deadweight. The preferred pressure of hydraulic oil was controlled by weight of the deadweight on the lever arm of the frame which transferred a multiplied load of the deadweight onto the cylinder pivot. In this way, controlled generation of hydraulic pressure was achieved, which was further transferred to the shearing system. By means of the oil supply system from the large cylinder (principle of communicating vessels) and all smaller vessels on the shear apparatus, the shear force was applied to the lower half of the specimen (lower fixed mould), as illustrated in Figure 8.

Figure 8. View of the apparatus during the experiment (visible shearing of upper and lower half of the specimen)

In the experiment, the mass of the added load was not measured, but the horizontal forces, namely shear stress and displacement values were measured. Namely, during the load adding, care was taken to ensure that the loading causes displacement due to the increase in shear stresses. Although the load causing shear stress and displacement was not numerically verified, care was taken to ensure that the load increments were approximate. The loading was done by adding concrete cylinders with a base diameter of 15 cm and a height of 30 cm (approx. 13 kg), which is approximately 16 kN/m^2 after multiplying by the frame levers. The loading was carried out by adding one or two mentioned elements, depending on the vertical load, that is, until the lower mold with the specimen was started. The shear load was applied by adding the mentioned load in the basket at the end of the lever, according to the system of moving the oil from the press with large clip to the presses with smaller clips, as previously explained.

Each subsequent loading was performed after the movement of the lower mold had completely stopped, until the final movement of 5 cm had been reached. Considering the length of the specimen of 30 cm, it was found that after a displacement of 5 cm, the lower mold, in addition to translational movement, begins to "experience" rotation, which is not in accordance with the plans and assumptions of the experiment.

Value of displacement of the lower mould, meaning differential displacement of the lower and upper half of the specimen along discontinuity was recorded by the mechanical device for displacement measurement (Figure 8).

As previously mentioned, the lower mould and the ring to which vertical loading is applied are placed on rollers to eliminate friction during the experiment duration. During the testing, it is required to maintain vertical loading constant, as it tends to change because of the vertical movement over the rough surfaces and changes in shear stress and strain. For such a reason, testing of the main series provides for introduction of complementary components – equipping each load frame with optic cameras to enable 24h coverage of the testing. At the beginning of the trail series, it was observed that the hydraulic cylinder piston was fully extended in the length of 5cm. Therefore, this length was defined as the final displacement of the specimen. For the purposes of consideration and understanding of the experiment, it was identified that at approximately 7-8cm of displacement, the lower half of the mould started rotating about a shorter axis, hence the intended experiment would lose its meaning with such condition of the apparatus. The defined ultimate 5cm of displacement represents approximately 17 % of the total specimen length (Figure 8).

Within testing of the pilot programme of specimens, the experiment duration depended on the applied normal loading and the roughness of the discontinuity planes. The duration of the experiment conditioned recording of the data obtained in different time intervals, depending on a specific case.

The experimental apparatus used in this research represents a specially developed laboratory system adapted for long-term shear testing along discontinuities on large-scale specimens. Therefore, the testing procedure did not fully correspond to conventional direct shear devices, where spherical seats are commonly used to reduce moment effects and allow rotations. In this preliminary investigation, the objective was to verify the functionality of the developed system and identify the issues that must be taken into consideration in the main experimental series.

4. Collection, processing and analysis of the test results

Within the pilot programme of specimens, three specimens of different roughness of discontinuity planes were tested. For each specimen, tests were performed for three different constant values of normal loading of 0.1 MPa, 0.2 MPa and 0.4 MPa. At specimen testing for lower values of normal stress lower shear stress was also induced, with a shorter testing time. This is a common feature for all tested specimens.

Maintaining the normal force constant proved to be demanding and complex, considering that because of the specimen shearing, meaning changes in shear stress and evident volumetric changes resulting from shearing as well as due to the friction of the load frame equipment, certain reduction or increase in value of the defined normal force occurred (as a consequence of intention towards vertical displacement of specimen in the course of shearing), requiring the force to be controlled not later than after one hour so as to adjust the force and retain a quasi-constant value of the normal stress.

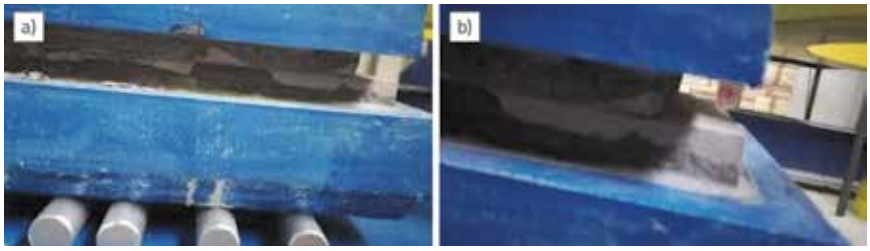

Figure 9. Displacement of upper half (a) in relation to the lower half (b) of the specimen along the shear surface

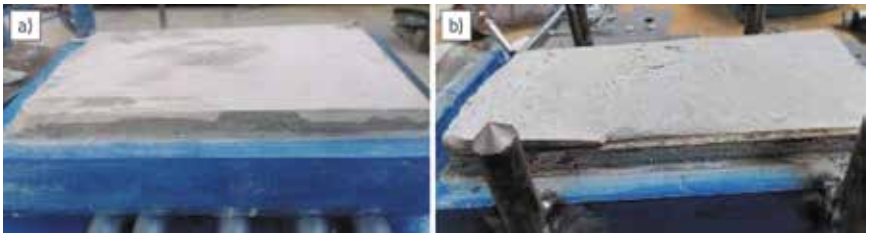

Figure 10. a) View of the shear surface after test on a smooth specimen; b) View of the shear surface after test on a rough specimen

For all specimens, the testing was performed starting from the lowest (0.1 MPa) to the highest normal stress (0.4 MPa), to minimise damage or altering of the tested shear surface. In case of a smooth specimen there was no concern about eventual change in the roughness of the shear surface, while the other two rough surfaces were not observed for any significant change in structure of the tested shear surface (Figure 10).

As a result of shear, the specimen with smooth discontinuity showed visible traces of the experiment (mainly in a form of shallow striations on the sliding surface), meaning visible traces on the surface which indicate to the shear displacement of surfaces, however without degradation or forming of fractured structures (Figure 10.a).

Specimens with rough discontinuities exhibited local asperity damage and fragmentation of microstructural features along the shear surface (fragments of small order of magnitude compared to the specimen dimensions) (Figure 10b). These observations suggest that the specimen with a distinctive waviness (unevenness) largely remained undamaged with a view to the consistency of the unevenness. This specimen as well as the specimen with moderate roughness were observed for damages, scattering of microstructures of the shear surface. As expected, increasing normal stress resulted in more pronounced damage to surface asperities.

During testing of the specimen with a smooth discontinuity surface (S_1'), the following maximum values of shear stress for corresponding normal stress were recorded:

σ_n = 0.1 MPa → τ = 0.54 MPa, σ_n = 0.2 MPa → τ = 1.68 MPa, σ_n = 0.4 MPa → τ = 2.46 MPa.

For the specimen with a distinctive unevenness (S_2'), the following maximum values of shear stress were obtained:

σ_n = 0.1 MPa → τ = 3.9 MPa, σ_n = 0.2 MPa → τ = 4.92 MPa, σ_n = 0.4 MPa → τ = 6.72 MPa.

For the specimen with moderate roughness of the discontinuity surface (S_3'), the following maximum values of shear stress were obtained::

σ_n = 0.1 MPa → τ = 3.24 MPa, σ_n = 0.2 MPa → τ = 2.70 MPa, σ_n = 0.4 MPa → τ = 4.86MPa.

The obtained shear stress values should not be directly interpreted as classical Mohr–Coulomb parameters of intact rock material. The tests were performed along previously formed discontinuity surfaces, where the shear resistance resulted from the combined effects of friction, asperity interlocking, local dilation and partial degradation of micro-contact zones.

In discontinuities characterized by pronounced geometrical interlocking and undulating rough contact surfaces, relatively low normal stress levels may lead to the occurrence of high apparent values of shear resistance angle and apparent cohesion. Such values are a consequence of mechanical interlocking, dilation and geometrically controlled shear resistance, rather than true material constants of intact rock.

Also, considering that during the preliminary phase the same specimen was successively tested under several normal stress levels, with repositioning between individual testing stages, partial changes in the contact structure of the discontinuity surfaces may have occurred. Therefore, the presented values should be regarded as preliminary results intended for understanding system behaviour and preparation of the main experimental program.

Additionally, considering the high calcium carbonate content of the tested marly limestone, the possibility of local temporary bonding effects at the discontinuity contact zones may have contributed to the observed response, which may additionally influence the mobilized shear resistance under low normal stress levels. However, such effects were not specifically investigated within the scope of this study and require further research.

In terms of the experiment duration, the specimens with rough surfaces of discontinuity lasted significantly longer, even up to two months, while the specimen with a smooth surface of discontinuity achieved maximum displacement for couple of hours.

For better comprehension of the obtained results and due to an extensive scope of all obtained correlation graphs, the next steps will show correlation graphs obtained for the tested specimens subjected to a maximum defined normal loading of approximately 0.4 MPa. Figures 1 to 3 display changes in normal and shear stress and displacements in correlation with the experiment duration.

The obtained results show that the values of maximum displacements are achieved in different time intervals for different specimens. In case of specimens for smooth

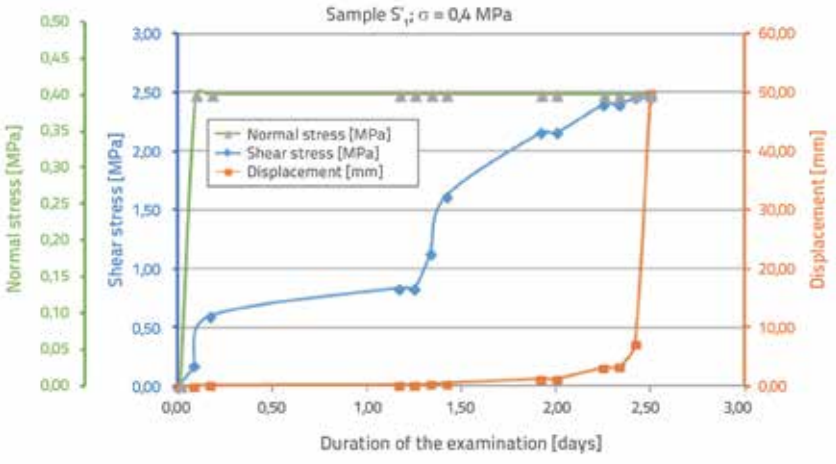

Figure 11. Change in stress and displacement increment during the experiment time, specimen S_1'

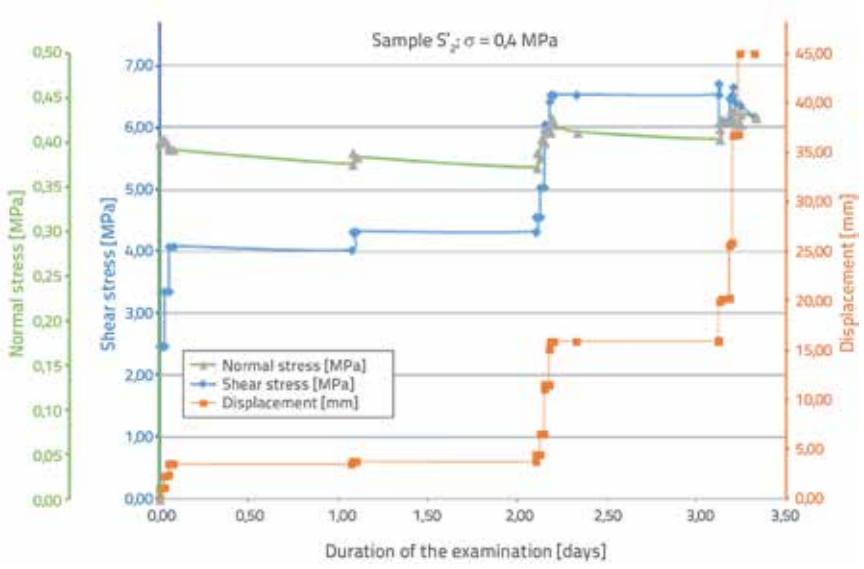

Figure 12. Change in stress and displacement increment during the experiment time, specimen S_2'

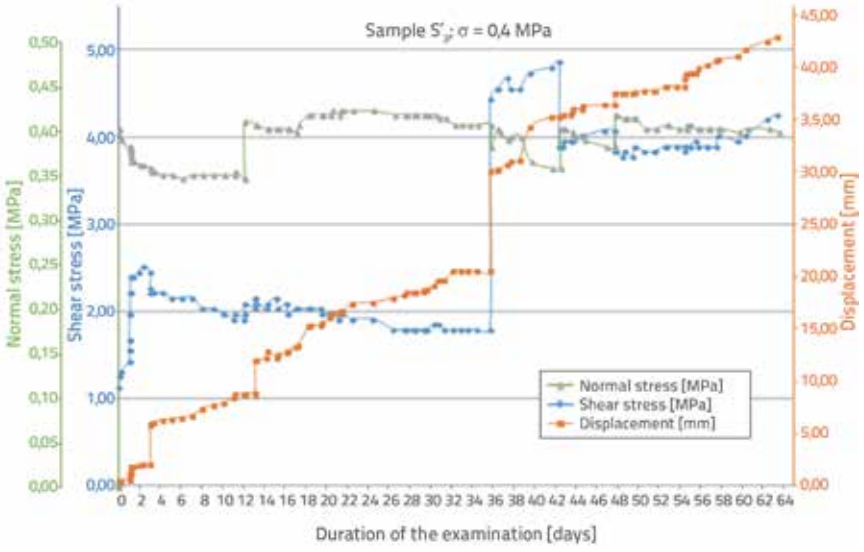

Figure 13. Change in stress and displacement increment during the experiment time, specimen S_3'

discontinuity surface, a maximum displacement is achieved within couple of hours. In case of specimens with a rough shear surface, a maximum displacement is achieved in a time interval measured by days.

Notwithstanding the specimen with a distinctive unevenness was tested within almost four days and the specimen with moderate roughness in almost 65-day period, the authors emphasize that the experiment in case of the specimen S_3' was conducted in the way that each subsequent increment of horizontal loading was added only after there were no more changes in the value of stress and displacement.

As regards the specimen with a distinctive unevenness (S_2'), the next loading step was carried out after the displacement increment below 0.2 mm/day was achieved. Different testing conditions (mainly deviation of normal stresses from the constant value in order to monitoring the shearing behaviour of the specimen) were designed with an intention to consider all possible testing conditions, so that during simultaneous testing of specimens in three loading frames within the scope of the main series of the experiment, it would be possible to collect all data with adequate results that would allow for consideration of the phenomenology of behaviour of the soft rock discontinuity at shear forces – displacements in a good quality manner and with a sufficient number of specimens in terms of statistics.

This paper reports initial test results for shear of discontinuities in soft rock with a time-dependent effects. Further tests should provide for enough data that would form basis for rheological modelling, and especially introduction of time-dependent deformation as a parameter for modelling of the behaviour of rock mass, both the rock matrix and the behaviour of discontinuities.

5. Conclusions

The pilot experimental programme confirmed the functionality of the developed testing apparatus and demonstrated the feasibility of long-term shear testing on large-scale soft-rock specimens containing artificial discontinuities. A high-quality preparation is also reflected in the successfully obtained test results as well as in a minimum number of corrective activities that will be required for the purposes of testing of the main series of the experiment relating to both equipment and testing protocol. Further test results should provide sufficient data for forming of a rheological model of shear behaviour along discontinuity of the tested soft rock, where a numerical formulation should also include the impact of roughness of the shear discontinuity surfaces on the shear strength of material and time-dependent deformation. The specimen testing showed that the time-dependent component of the shear displacement along discontinuity participates in the total deformation in a significantly high percent, being more than 50 % in case of the specimen S_3'.

It should be particularly emphasized that the presented results have a preliminary character. The pilot tests were conducted for the purpose of verifying the apparatus, determining the loading range, and identifying the fundamental mechanisms

of shearing along discontinuities, rather than for the final determination of representative shear strength parameters. Repeated testing of the same specimens under successively increasing normal stress levels represents a methodological limitation of the preliminary phase, since it may lead to partial degradation and changes in the contact conditions along the discontinuity surfaces. This limitation will be eliminated in the main experimental testing series through a larger number of tests and a more controlled loading regime.

Considering a relatively narrow scope of research, from a general point of view, the purpose of knowledge acquired within this research is to contribute to the understanding, perception and studying of soft rock mass and phenomenology of shear along discontinuity. At the same time, justification of previous research of the same material viewed through the acknowledged contribution in scientific papers of Prof Slobodan Zivaljevic, S. & Tomanovic, Z., addressing the intact rock, are another proof that the results of these researches of behaviour of discontinuities will greatly contribute to a better understanding of the behaviour of soft (marly) rock mass intersected by fissures and formation of more realistic rheological models.

Acknowledgements

The authors of the paper extend their gratitude for financial help and other kind of assistance during the research, in particular to: The Innovation Fund of Montenegro for having recognised the importance of this research and awarded a financial grant to the team which submitted the application, consisting of GeoT d.o.o from Podgorica and Faculty of Civil Engineering, University of Montenegro. Management of the Coal Mine Pljevlja for their expert, financial and technical assistance during the excavation, loading and transport of the marly material. Montenegrin Institute for Medicines and Medical Devices which provided a detailed report on the conducted semi-quantitative analysis of specimens, and defined a chemical, mineralogical-petrological composition of rock mass with a pinpoint accuracy.

REFERENCES

[1] Zivaljevic, S., Tomanovic, Z.: Experimental research of the effects of preconsolidation on the time-dependent deformations-creep of marl, Mechanics of Time-Dependent Materials, 19 (2015), pp. 43–59, https://doi.org/10.1007/s11043-014-9250-8.

[2] Tomanović, Z.: Initial and time-dependent deformations in marl around small circular opening, GRAĐEVINAR, 66 (2014) 12, pp. 1087-1096, doi: https://doi.org/10.14256/JCE.1120.2014

[3] Tomanović, Z., Miladinović, B., Zivaljević, S.: Criteria for defining the required duration of the creep test, Canadian Geotechnical Journal, 52 (2015) 7, pp. 883–889, https://doi.org/10.1139/cgj-2014-0097.

[4] Tomanović, Z.: Effects of the soft rock pre-consolidation on time-dependent deformations around the tunnel excavation, Technical Gazette, (2014), ISSN 1330-3651.

[5] Tomanović, Z.: The stress and time dependent behaviour of soft rocks, GRAĐEVINAR, 64 (2012) 12, pp. 993–1007, https://doi.org/10.14256/JCE.815.2012.

[6] Tomanović, Z.: Experimental research and complex rheological models of soft rock as a basis for numerical analysis of the stress dependent behavior – Application of innovative techniques in engineering, Proceedings of the Conference Application of Innovative Techniques in Engineering, Niš, Serbia, 25–26 November 2011, pp. 219–243, ISBN 978-86-80295-97-8.

[7] Tomanović, Z.: Influence of K_o on creep properties of marl, Acta Geotechnica Slovenica, (2009), ISSN 1854-0171.

[8] Tomanović, Z.: Rheological model of soft rock creep based on the tests on marl, Mechanics of Time-Dependent Materials, 10 (2006), pp. 135–154, https://doi.org/10.1007/s11043-006-9005-2.

[9] Dusseault, M.B., Fordham, C.J.: Time-dependent behavior of rocks, in: Hudson, J.A. (ed.), Comprehensive Rock Engineering: Principles, Practice and Projects, Vol. 3, Pergamon Press, Oxford, 1993, https://doi.org/10.1016/B978-0-08-042066-0.50013-6.

[10] Cristescu, N.D., Hunsche, U.: Time Effects in Rock Mechanics, John Wiley & Sons, New York, 1998.

[11] Cristescu, N.D., Hunsche, U.: General constitutive equation, in: Time Effects in Rock Mechanics, John Wiley & Sons, New York, 1998, pp. 119–179.

[12] Wallner, M.: Stability calculation concerning a room and pillar design in rock salt, Proceedings of the International Congress for Geotechnics, Melbourne, Australia, 1983.

[13] Kozubal, J., Tomanović, Z., Zivaljević, S.: The soft rock socketed monopile with creep effects – a reliability approach based on wavelet neural networks, Archives of Mining Sciences, 61 (2016) 3, pp. 571–585.

[14] Xu, T., Tang, C.-A., Zhao, J., Li, L., Heap, M.J.: Modelling the time-dependent rheological behaviour of heterogeneous brittle rocks, Geophysical Journal International, 189 (2012) 3, pp. 1781–1796, https://doi.org/10.1111/j.1365-246X.2012.05460.x.

[15] Palmström, A.: Measurement and characterization of rock mass jointing, Chapter 2 in: In-Situ Characterization of Rocks, A.A. Balkema Publishers, Lisse, 2001.

[16] Jandrisevits, C.: Contact-free Measurement of Rock-Mass Structures – Method Comparison, Master's Thesis, Institute of Applied Geosciences, Graz University of Technology, Graz, 2012.

[17] Loiotine, L., Wolff, C., Wyser, E., Andriani, G.F., Derron, M.-H., Jaboyedoff, M., Parise, M.: QDC-2D: A Semi-Automatic Tool for 2D Analysis of Discontinuities for Rock Mass Characterization, Remote Sensing, 13 (2021) 24, Article 5086, https://doi.org/10.3390/rs13245086.

Primljen / Received: 26.8.2025.
Ispravljen / Corrected: 6.5.2025.
Prihvaćen / Accepted: 8.5.2026.
Dostupno online / Available online: 10.6.2026.

Framework for management of risks caused by information asymmetry in construction projects

Authors:

Ivona Ivić Jazvec, PhD. CE
University of Zagreb
Faculty of Civil Engineering
Department of Organization, Technology and Management
ivona.ivic@grad.unizg.hr
Corresponding author

Prof. **Anita Cerić**, PhD. CE
University of Zagreb
Faculty of Civil Engineering
Department of Organization, Technology and Management
anita.ceric@grad.unizg.hr

Subject review

Ivona Ivić Jazvec, Anita Cerić

Framework for management of risks caused by information asymmetry in construction projects

The occurrence of information asymmetry between clients and contractors is often a source of risk in construction projects. In order to develop a framework for managing these risks, a comprehensive study described in this paper was conducted. The methods employed included content analysis of existing literature and interviews among professionals with significant experience in the execution phase of construction projects. The research identified 20 key risks that arise before and after the signing of a contract between the client and the contractor. It also identified the key consequences of these risks and 15 key strategies for mitigating the risks in question. Based on the obtained results, a framework for managing these risks was developed, linking the identified risks, their consequences, and corresponding mitigation measures. This framework enables a structured approach to risk management across different phases of construction projects.

Key words:
principal-agent theory, information asymmetry, risk identification, risk mitigation measures

Pregledni rad

Ivona Ivić Jazvec, Anita Cerić

Okvir za upravljanje rizicima prouzročenima informacijskom asimetrijom u građevinskim projektima

Pojava informacijske asimetrije između investitora i izvođača često je uzrok rizika u građevinskim projektima. Kako bi se razvio okvir za upravljanje tim rizicima, napravljeno je sveobuhvatno istraživanje opisano u ovome radu. Primijenjene metode uključivale su analizu sadržaja postojeće literature i intervjue sa stručnjacima sa značajnim radnim iskustvom u fazi izvođenja građevinskih projekata. Istraživanjem je identificirano 20 ključnih rizika koji se pojavljuju prije i nakon potpisa ugovora između investitora i izvođača. Također, identificirane su ključne posljedice tih rizika i 15 ključnih strategija za ublažavanje predmetnih rizika. Na temelju dobivenih rezultata razvijen je okvir za upravljanje tim rizicima koji povezuje identificirane rizike, njihove posljedice i mjere za njihovo ublažavanje. Takav okvir omogućuje strukturiran pristup upravljanju rizicima u različitim fazama građevinskih projekata.

Ključne riječi:
agencijska teorija, informacijska asimetrija, identifikacija rizika, mjere za ublažavanje rizika

1. Introduction

Risks in construction projects can be classified into various categories depending on their causes and nature. For example, Thakur et al. [1] highlight technical, logistical, environmental, financial, socio-political, and other types of risk. Among these, communication risks represent one of the most serious challenges, as they account for as much as 56 % of the total risk costs in projects [2]. These risks may arise at any stage of a project [3] and not only contribute to increased costs, but may also jeopardise key project objectives [4, 5]. Moreover, communication risks often trigger chain reactions leading to other types of risk [6].

This paper focuses on the management of risks related to information asymmetry among participants in construction projects. Previous studies have identified these risks as a significant issue that has still not been adequately addressed [7, 8]. Information asymmetry refers to a situation in which project participants do not possess the same amount of primary information or fail to share such information with one another, thereby hindering the achievement of project objectives [9]. This concept is based on principal-agent theory, which describes a relationship in which one party (the principal) engages another party (the agent) to perform a specific task on its behalf [10]. In the context of construction projects, the investor assumes the role of the principal, while the contractor acts as the agent. Such relationships are characterized by information asymmetry, differing levels of risk aversion, and the tendency of each participant to maximize their own benefit, which may lead to opportunistic behaviour [11].

Risk assessment and management are major elements of project management. Flanagan and Norman [12] describe it as a systematic approach to identifying and quantifying risks to enable informed decision-making regarding their management. According to International Organization for Standardization [13], risk assessment includes three main steps: risk identification, risk analysis, and risk evaluation.

Risk identification involves recognizing and providing a detailed description of all potential risks that may positively or negatively affect the achievement of project objectives. Thorough and precise identification represents one of the critical phases of the overall risk management process. After risks have been identified, experts assess the likelihood of their occurrence and their potential impact, i.e., the consequences for the project. The combination of these two elements determines the overall level or severity of risk, expressed as: Risk = probability × impact. Upon completion of risk analysis, relevant data are available for risk evaluation and for making decisions on how to address the identified risks. Risk evaluation is a phase of the risk management process in which it is determined which risks require mitigation measures and which do not require any further action. This step is essential for the effective allocation of resources and achieving optimal risk management.

Principal-agent theory and the problem of information asymmetry have become increasingly prominent in recent research within the construction industry [7, 14, 15]. A systematic literature review [16] indicates a lack of research related to the identification and analysis of risks caused by information asymmetry, whereas studies focusing on mitigation measures are more common. This research gap highlights the need for a more detailed examination of these risks to improve the understanding and management of risks in construction projects. One of the reasons for the insufficient attention given to these risks lies in their complexity and multidisciplinary nature, encompassing psychological, sociological, and economic aspects [17].

Information asymmetry represents an inherent characteristic of the relationship between clients and contractors in construction projects. Project participants possess different objectives, levels of knowledge, interests, and access to information, resulting in a persistent imbalance in the distribution of information. Therefore, the objective of managing these risks is not their complete elimination, but rather their identification, limitation, and effective management.

The aim of this paper is to present a framework for managing risks caused by information asymmetry. The framework identifies primary risks arising from information asymmetry between investors and contractors in construction projects, classifies them according to theoretical categories of information asymmetry, and determines their main consequences as well as corresponding mitigation measures. The second chapter of this paper provides an overview of the existing literature on information asymmetry in construction projects. In addition, the three theoretical groups of information asymmetry risks are described. The third chapter describes the research methodology through which the relevant risks, consequences, and measures were identified and classified. The fourth chapter presents the research results in the form of lists of key risks, their consequences, and measures for their mitigation. The fifth chapter proposes a framework for managing the relevant risks for clients and contractors. The framework connects the identified risks, their consequences, and mitigation measures, thereby facilitating the management of these risks in construction projects. The paper concludes with findings regarding the scientific and practical contribution of this research.

2. Information asymmetry in construction projects

The theoretical foundation of the problem of information imbalance in construction projects is associated with principal-agent theory and the concept of information asymmetry. Principal-agent theory originates from the field of economics and analyses relationships between two parties: the principal and the agent [18]. The problem between these two parties arises due to information asymmetry. Information asymmetry is a situation in which one party possesses more information regarding its characteristics, activities, or intentions, but does not share it with the other party, often for its own benefit [9]. Such a situation gives rise to agency costs, which include monitoring, contracting, and other costs associated with managing this relationship [19]. The primary objective of principal-agent theory is to develop strategies for reducing these costs and ensuring that agents act in accordance with the interests of the principal, for example through contractual mechanisms and systems of incentives and supervision [20].

In construction projects, principal-agent theory identifies the relationships between project participants as agency relationships involving information asymmetry, conflicts of interest, and agency costs [11]. The client is the primary principal, while its agents include designers, contractors, supervising engineers, project managers, and other participants. Furthermore, the contractor may act as a principal in relation to its subcontractors. Given the number and diversity of participants, as well as the complexity of construction projects, there exists a large number of principal-agent relationships, resulting in numerous problems arising from such relationships when one party does not possess complete information about the other. In this way, the information asymmetry present in these relationships may cause difficulties in project planning, execution, and management. This paper focuses on the relationship between the client and the contractor in a construction project, where the client is the principal and the contractor is the agent responsible for constructing the facility on its behalf (Figure 1).

Figure 1. Basic principal-agent model of participants in construction projects (CI – Client; Co – Contractor) [21]

In addition to the client and the contractor, other project participants also play an important role in managing information asymmetry, including the designer, supervising engineer, project manager, and, in the case of the application of FIDIC contract models, the engineer. The designer is responsible for the quality and completeness of the design documentation, thereby directly influencing the level of information asymmetry during the tendering and construction phases. The project manager is responsible for the planning, organisation, coordination, and control of all project activities, including the management of scope, time, costs, quality, risks, and communication among all participants. The supervising engineer and the FIDIC engineer play a primary role in the interpretation of contractual provisions, verification of completed works, and decision-making processes that may reduce or increase asymmetry between the parties. These participants act as intermediaries in the transfer of information and may significantly contribute to the transparency and balance of contractual relationships.

Principal-agent theory recognises several types of problems, which manifest through hidden characteristics, hidden activities and information, and hidden intentions [22]. Such problems arise from the asymmetric distribution of information among project participants, which may lead to various risks. If these risks are not recognised and managed effectively, they may significantly jeopardise the achievement of project objectives [23].

The problem of hidden characteristics arises even before **signing a contract** between the principal and the agent, that is, *ex ante*. It stems from the fact that the principal is unaware of certain characteristics of the agent, such as its performance capability or available resources [24]. Such a situation leads to **adverse selection** (AS) [20, 24].

On the other hand, problems related to hidden activities and information arise after the contract has been signed. They refer to a reduction in the agent's level of effort during task execution [22]. These information asymmetries arise because the principal cannot fully monitor the agent's activities (hidden activities), nor accurately assess its performance (hidden information) during task implementation [25]. Although the principal can observe the outcome, it cannot know with certainty whether the agent has exerted maximum effort. In such cases, this is referred to as **moral hazard** (MH).

The third type of problem relates to hidden intentions, which become apparent only after the signing of the contract [22]. In such situations, one party becomes aware that the other is acting opportunistically but remains in a weaker bargaining position because it has already committed certain resources to the cooperation. This represents a situation in which a partner remains in an unfavourable relationship due to obligations already undertaken, commonly referred as **hold-up** (HU) [25].

The issue of information asymmetry in the contractual relationship between the client and the contractor does not represent solely a technical or organisational challenge, but also a legal issue. The contractual relationship between the client and the contractor in the Republic of Croatia is primarily regulated by the Obligations Act (Official Gazette Nos. 35/05, 41/08, 125/11, 78/15, 29/18, 126/21, 114/22, 156/22, 145/23, 155/23), which defines the fundamental elements of construction contracts, including the rights and obligations of the contracting parties, responsibility for the **construction phase**, and protection mechanisms in cases of non-performance of contractual obligations. In the case of public investments, the additional regulatory framework is provided by the Public Procurement Act (Official Gazette Nos. 120/16, 114/22), which regulates contractor selection procedures, as well as the principles of transparency, equal treatment, and market competition. This regulatory framework is important because information asymmetry arises within formally defined contractual relationships. It also determines the boundaries within which information asymmetry may be considered lawful, for example when it arises from natural differences in expertise, experience, and access to information among project participants. The client may possess a better understanding of the financial aspects of the project, including the budget, deadlines, and expectations towards the contractor. This may result in situations in which the contractor is not fully aware of the client's financial constraints or objectives, which may affect project planning and execution. On the other hand, the contractor possesses more detailed information regarding its work, project progress, and construction quality, which may be difficult for the client to monitor fully, as every form of control entails additional costs. Such information asymmetry is unavoidable in complex projects. In contrast, situations may also arise in which one party deliberately withholds or distorts key information to gain an unfair advantage, thereby violating the principles of good faith and fair dealing, as well as the balance of contractual relationships. In this paper, the identified risks may be interpreted through this distinction, whereby

certain forms of information asymmetry exceed the boundaries of lawful conduct and enter the domain of legally disputable practices.
The difference between public and private investments significantly affects the dynamics of information asymmetry. In public projects, the regulatory framework provides formal mechanisms for reducing asymmetry, including transparent procedures, the possibility of submitting questions, and appeal mechanisms. In private projects, such formal mechanisms are often not standardised, which may increase flexibility, but also the risk of unbalanced relationships.
For example, in the context of public procurement, the issue of contractor responsibility may arise when a contractor accepts the tender conditions without submitting additional questions or using legal remedies such as appeals. In such cases, it may be considered that the contractor has assumed a certain level of risk associated with information asymmetry. However, this does not exclude the client's responsibility for the clarity and completeness of the documentation, particularly in situations where a lack of information may lead to significant deviations during project implementation. Therefore, the problem of information asymmetry in public procurement cannot be attributed unilaterally to one party, but must instead be viewed as the result of an interaction between the regulatory framework, the quality of documentation, and the behaviour of the participants.
In practice, various mechanisms are available for mitigating and resolving the consequences of asymmetry, including contractual provisions (e.g. clauses relating to variations, risk allocation), procedures for clarification and amendment of documentation, appeal procedures in public procurement, as well as judicial protection in cases involving breaches of contractual obligations. Although these mechanisms cannot eliminate asymmetry entirely, they enable its legal addressing and the reduction of its negative consequences.
Despite the existence of formal mechanisms in public procurement, certain forms of information asymmetry remain present. This particularly relates to implicit information concerning the project, future changes, the organisational capacities of the contracting authority, or actual expectations during project execution, which cannot be fully formalised through tender documentation. The following section of this paper describes the methodology used to identify risks caused by information asymmetry in construction projects and presents a framework for their management.

3. Research methodology

The previous chapter defined the concepts of information asymmetry and highlighted how information asymmetry among participants in construction projects may generate various project risks. Given the limited application of practical methods for managing these risks, as well as the lack of extensive scientific literature addressing them, it was necessary to undertake the first step towards effective management by developing a framework for managing the relevant risks through the identification and classification of risks, their consequences, and mitigation measures. For this purpose, a systematic review of the relevant scientific literature was conducted with the aim of identifying and categorising risks associated with information asymmetry among participants in construction projects. In addition, their consequences in construction projects, as well as measures for their mitigation, were identified. Defining consequences and mitigation measures is necessary for carrying out subsequent stages of risk management, namely risk analysis and risk mitigation. Furthermore, semi-structured interviews were conducted to gain insight into the views of industry experts regarding the identified risks, consequences, and mitigation measures, as well as to supplement the preliminary lists with additional items where appropriate. Based on the collected data, final lists of major risks, consequences, and mitigation measures were established.

3.1. Systematic literature review

The systematic literature review was conducted with the aim of analysing previous scientific research addressing the phenomenon of information asymmetry in the context of construction projects. Part of the results of this analysis was previously published in paper [16], whereas this article presents the results relating to the identification of key risks caused by information asymmetry, their consequences, and mitigation measures.
The analysed literature was retrieved from two renowned scientific databases – Web of Science Core Collection and Scopus – which enabled a comprehensive insight into the issue and the risks caused by information asymmetry in the construction sector. The following keywords were used in the search process: "*asymmetric information*", "*information asymmetry*", "*adverse selection*", "*moral hazard*", "*hold-up*", and "*construction*". These terms were searched in combination within the titles, abstracts, and keywords of scientific papers. Following the search of the two electronic databases, all retrieved records were imported into the Mendeley software. All subsequent stages of the literature review were conducted within this software, thereby ensuring objective analysis and precise management of the collected sources [26].
The collected publications were processed in accordance with the guidelines of the PRISMA methodology [27], whereby a total of 94 scientific articles met the inclusion criteria because they contained one or more examples of risks associated with information asymmetry, their consequences, or mitigation measures. Through content analysis of the collected scientific papers, categorised lists of risks were developed for the three categories of information asymmetry: adverse selection, moral hazard, and hold-up. In addition, lists of consequences and mitigation measures were also established. For additional evaluation of the data obtained from the literature, semi-structured interviews were conducted.

3.2. Interviews

To assess the practical relevance of the data obtained from the scientific literature, interviews were conducted with experts possessing extensive experience in the field of construction projects. The key advantage of this method lies in its ability to collect detailed and content-rich information [28].

Table 1. Codes used in the qualitative content analysis of interview transcripts (adapted from [21])

	Code	Description
Predefined codes	+	Agreement with the item (risk, consequence, or mitigation measure)
	-	Disagreement with the Item
	+/-	Partial agreement with the item
	Reason	Reason for agreement, disagreement, or partial agreement with the item
	Addition	New item added by the respondent
	Example of a risk	Practical example in which a risk caused by information asymmetry was identified
	Example of a consequence	Practical example in which a risk consequence was identified
	Example of a mitigation measure	Practical example in which a risk mitigation measure was identified
Codes identified during the analysis	Market context	Explanation of differences in the occurrence of risks caused by information asymmetry depending on the market in which the company operates
	Participant context	Explanation of the context of risk occurrence due to common behavioural patterns, capabilities, or inabilities of project participants
	Project type context	Explanation of differences in the occurrence of risks caused by information asymmetry depending on the type of project (public / private)
	Modification	Modification or supplementation of the item

The interviews were conducted with nine experts with at least 17 years of experience in construction projects, all of whom currently hold managerial positions. The sample was selected purposively, with the aim of obtaining in-depth and high-quality data from experts who had participated in large and complex projects. Such a small, homogeneous sample is characteristic of qualitative research focused on specific topics [28]. After nine interviews, data saturation was observed, marking the end of further data collection. Three respondents came from organisations operating as public clients, two were from private construction contracting companies, while the remaining respondents came from private companies specialising in consultancy services, supervision, design, and project management. All respondents included in the study, although some did not formally belong to contracting organisations, possessed significant practical experience in the execution of construction projects. Through their professional roles, they were directly involved in project preparation and implementation processes, which included detailed knowledge of the roles of contractors and clients, both in the pre-contract phase (e.g. analysis of tender documentation, risk assessment, and decision-making regarding participation) and in the post-contract phase (management of execution, coordination of participants, and resolution of contractual issues). Therefore, their responses reflected both the contractor's and the client's perspectives, despite their formal organisational affiliation. All respondents had worked on projects in Croatia, while four of them also possessed international experience in various countries. Their expertise predominantly related to public projects, whereas private investments were represented to a lesser extent, which is consistent with the focus on large and complex projects, predominantly associated with public investments in Croatia.

The questions used in the semi-structured interviews were mostly predefined to ensure a more objective analysis; however, respondents were given the opportunity to provide open-ended answers. The interviews focused on the evaluation of the lists of risks, consequences, and mitigation measures collected from the literature, whereby the experts provided comments, expressed agreement or disagreement, and shared examples from their own experience, together with suggestions for improving formulations to enhance clarity. Each respondent participated in one interview, the duration of which ranged from 52 minutes to two hours. The interviews were conducted at company premises, at the Faculty of Civil Engineering, University of Zagreb, or via online platforms, with particular attention devoted to creating a confidential atmosphere that encouraged openness. All interviews were recorded and transcribed, thereby ensuring a rich database for further analysis.

The interview transcripts were analysed using qualitative content analysis in Microsoft Word. At this stage, specialised software tools may be used; however, such tools cannot independently identify codes, but may only partially accelerate text analysis [29, 30]. Therefore, it was decided that specialised text-coding software would not be used in this research. Some of the codes were defined prior to the analysis, whereas others were determined during the analysis itself. Specifically, it was established that the significance of particular risks, as well as the applicability of mitigation measures, varies depending on the type of project (public or private). It was also observed that the approach to risk management differs depending on the role of the participant (whether implemented by the client or the contractor) and the market in which the company operates. Consequently, it was important to use additional codes to record the experts' specific comments regarding the contexts in which they were speaking. The final list of codes is presented in Table 1.

4. Results and description of the main elements of the framework

The following section presents the results of this research, namely the identified elements of the framework proposed for managing risks caused by information asymmetry. The main elements of the framework consist of the identified risks, their consequences, and mitigation measures. First, the risks

identified through the literature analysis and interviews with experts are presented. These risks were classified according to the types of information asymmetry, with the aim of determining the phase of the construction project in which they may occur and enabling further research within the defined categories. Subsequently, the identified consequences and corresponding mitigation measures are presented.

4.1. Primary risks caused by information asymmetry

Before signing a contract between the client (principal) and the contractor (agent) in construction projects, circumstances often arise in which one party does not possess complete insight into the capabilities of the other. In such situations, adverse selection (AS) risks occur. Table 2 presents eight risks arising from hidden characteristics, associated with the initial phase of contractors competing for the award of a contract – the first point of contact between the agent and the principal. The usual contractor selection model is based on the tenders. Owing to strong competition, contractors frequently offer prices below market levels to secure a contract [15, 31], which may result in inaccurate estimates, whether due to intention, inexperience, or lack of expertise [15]. In addition, contractors often do not possess complete information regarding the project, its scope, or quantities of work [23, 32–36], particularly when the project has not been finalised, when the client changes requirements, or when the project involves new technologies [37]. Under such circumstances, contractors who are incapable of delivering the project may submit bids, while the client may incorrectly assess their capabilities.

Due to the complexity of construction projects, clients are often unable to define all requirements precisely and therefore rely on contractors to provide accurate information, thereby creating potential information imbalance [38]. In such situations, demonstrating the contractor's capability is essential, for example through certificates, warranties, and bank guarantees. However, the reliability of such evidence may be questionable owing to the reduced signalling value of certificates [37, 39], lack of information regarding the contractor's reputation, or misrepresentation [23, 35, 36]. During the tendering process, other risks may also arise, such as collusion between the client and the contractor, among contractors themselves, or between contractors and subcontractors, which negatively affects project costs and implementation [35, 36]. Subcontracting represents a particular challenge because the client often does not possess complete information regarding subcontractors, their capabilities, or intentions [35, 40], while arrangements between contractors and subcontractors, together with inadequate disclosure of subcontractors, further increase the risk. In addition to the risks identified through the literature review, the experts interviewed emphasised that the financial instability of either the contractor or the client represents a significant hidden risk prior to contract signing, which may cause serious negative consequences during project execution as well as after project completion.

After the contract is signed, during the construction phase of a project, situations frequently arise in which the activities or information of one party are partially or completely concealed from the other party. Risks associated with such information asymmetry are identified in the literature as moral hazard (MH), and six key risks have been identified (see Table 2). The most common examples of hidden activities include the use of lower-quality materials, reduced quantities of executed works, concealment of errors, and, in general, a lower level of effort by the contractor in fulfilling contractual obligations [35 ,36]. This occurs due to the client's limited ability to control, whether because of a lack of expertise or financial resources [38], whereby the contractor may assume greater risks in the expectation that sanctions will not follow. Contractor behaviour is also influenced by unforeseen conditions, such as adverse weather conditions [41], and sometimes by the deliberate concealment of information or refusal to fulfil obligations [42]. High-quality information exchange within the project team can reduce the number of errors [43]; however, in the absence of clearly defined communication rules and a collaborative environment, information is often delayed. Collaboration may be improved through workshops [44], partnering relationships [45], digital tools such as building information modelling (BIM) and blockchain [9, 45], as well as the early involvement of all stakeholders [46]. Differences between planned and executed quantities of work are common [47], and their causes may include poor planning [32–34], unforeseen events, or changes introduced by the client [23, 35, 36]. Difficulties in controlling quantities arise from inadequate or untimely supervision. An additional risk stems from deteriorated relationships among participants, particularly where trust and willingness to cooperate are lacking [43, 48]. Poor collaboration, unevenly distributed risks and responsibilities [49], and the absence of expectations regarding future cooperation may encourage opportunistic behaviour by the contractor [46, 50]. Subcontracting represents a particular challenge, as the contractor must transfer the system of control and incentives to subcontractors [51]. The final highlighted risk relates to the low visibility of certain construction works, which complicates the subsequent verification of quality and quantities. In such cases, where the legislative framework is weak, abuses and manipulations in dispute resolution may occur [51 ,52]. Within the category of moral hazard risks, no additional items were proposed by the experts during the interviews. All risks identified in the literature were verified through the interviews, and their nature was further clarified through practical examples shared by the respondents.

The final category of information asymmetry relates to the hidden intentions of one party to place the other party in an unfavourable position by revealing key information only once the project has already significantly progressed. If the other party is unable to comply with the new requirements, suspension of works or financing may occur. This situation is known as hold-up (HU) risk, and this research identified six key risks of this type (see Table 2). It most commonly manifests itself during subsequent negotiations, for example when the client requests additional or modified works after the signing of the contract, while the contractor exploits its bargaining advantage to charge higher prices for such works [53, 54]. Due to limited alternatives, the client often accepts such conditions to avoid project interruption. Owing to its superior knowledge of

Table 2. Risks identified through the literature review and interviews with experts; AS – adverse selection risks, MH – moral hazard risks, HU – hold-up risks

ID	Risk	Source	Interviews
AS1	Poor / deficient tender documentation	[23, 32–37, 58]	verified
AS2	Contractor qualifications are unknown / unverifiable	[23, 35 ,37–39, 45, 59]	verified
AS3	Inability to identify and exclude a manipulative low bid	[15, 31, 43, 60, 61]	verified
AS4	Collusion between participants before or during the tendering process	[35, 36]	verified
AS5	Misrepresentation or concealment of subcontractors	[35, 40]	verified
AS6	Prevented / hindered selection of a trustworthy business partner	[46]	verified
AS7	(Hidden) unstable financial condition of the contractor	interviews	added
AS8	(Hidden) unstable financial condition of the client	interviews	added
MH1	Concealment of information regarding the actual quality of construction	[11, 32–36, 38, 40–42, 45, 50, 60, 62–70]	verified
MH2	Restricted information exchange between the client and the contractor	[23, 35, 36, 40, 43-46, 52, 59, 63, 64, 71–73]	verified
MH3	Subsequent project modifications	[23, 32-36 ,47, 58]	verified
MH4	Lack of mutual trust and understanding	[43, 46, 48–50, 74]	verified
MH5	Inadequate documentation of site events on the construction site	[51, 52, 64, 70, 75]	verified
MH6	Opportunistic behaviour due to one-off cooperation	[46, 50]	verified
HU1	Suspension of work by the contractor	[38, 50, 53, 54, 70, 76–78]	verified
HU2	Restricted negotiation due to political or public influence	[44, 51, 54, 55, 70, 77–79]	verified
HU3	Suspension of information due to distrust	[50]	verified
HU4	Lack of knowledge regarding the contractor's actual costs	[57]	verified
HU5	Withholding of payments by the client	interviews	added
HU6	Delays in client decision-making	interviews	added

the construction process, the contractor may intentionally fail to report deficiencies in the design documentation to exploit them at a later stage [38]. In large infrastructure projects with a high degree of asset specificity, the client is placed in an unfavourable position because the resources already invested cannot easily be reallocated, while the contractor uses its advantage to impose additional demands [50, 55, 56]. This increases transaction costs through prolonged negotiations and potential disputes [54]. An additional problem arises in the absence of long-term cooperation and trust, as both parties refrain from genuine collaboration to avoid weakening their own bargaining positions [50]. Finally, the absence of cost-control mechanisms enables the contractor to withhold information for the purpose of achieving financial gain at the client's expense [57]. Within this group of risks, the interview respondents emphasised the importance of defining more precisely the actors responsible for causing hold-up situations. The literature demonstrates a tendency to view the client as the party predominantly exposed to hold-up risks; however, the analysis of practical examples indicates that such a relationship is not unambiguous. Based on comments related to the description of risk HU1, three separate categories of risks were identified that more accurately reflect real situations in construction projects: withholding of work by the contractor, withholding of payments by the client, and withholding of decision-making by the client.

4.2. Key consequences

Risks arising from information asymmetry may negatively affect the achievement of project objectives. In addition to jeopardising the project itself, these risks have broader consequences, such as deteriorating relationships among stakeholders, which often leads to conflicts and disputes. In the long term, information asymmetry in construction projects also contributes to a reduction in the overall productivity of the sector.

Adverse effects on project objectives include increased costs [43, 47], delays in project implementation [53], reduced quality of executed works [80], and difficulties in the implementation of new technologies and innovations [11]. In addition, these risks negatively affect future cooperation among partners [81], give rise to legal disputes [55], and undermine trust and open communication [42, 82].

In the longer term, the consequences of information imbalance are reflected in reduced efficiency across the entire industry [58]. Qualified contractors earn lower profits [31] or withdraw from competitive tendering procedures [32–34], while clients lose interest in financing projects [37]. Ultimately, companies participating in such projects bear higher transaction costs [55].

During the interviews, respondents highlighted two additional important consequences through real examples of risks

Table 3. Consequences of risks identified through the literature review and interviews with experts

ID	Consequence	Source	Interviews
P1	Increased costs	[15, 31–34, 36, 38, 43, 47, 51, 53–55, 67, 76–78, 83, 84]	verified
P2	Deterioration of relationships among project participants / disputes	[32–34, 40, 42, 53–55, 81, 82]	verified
P3	Reduced quality	[36, 40, 52, 59–62, 74, 80, 81]	verified
P4	Failure to achieve the benefits of new technologies and innovations	[11, 37, 39, 45, 52, 66, 72, 73, 85]	verified
P5	Project delays	[41, 43, 53]	verified
P6	Contract termination	interviews	added
P7	Damage to organisational reputation	interviews	added

associated with information asymmetry: contract termination and damage to the reputation of companies involved in the project. The final list of key consequences of risks caused by information asymmetry is presented in Table 3.

4.3. Key mitigation measures

The mitigation measures most frequently mentioned in the relevant literature relate to the so-called optimal contracts and their control during project implementation [82]. Within these, the design of incentive mechanisms for contractors plays a particularly important role. Contracts, for example, contain clauses intended to encourage contractors to provide clients with accurate information regarding costs [86, 87], execute works in accordance with the planned schedule [71, 83], respond to unforeseen circumstances [41], and adapt to project changes [57, 88, 89]. Additionally, contracts should include a balanced allocation of risks [67], clearly defined performance criteria for contract implementation [53, 54], clearly expressed intentions of the contracting parties [11], mechanisms for price adjustments in accordance with market changes [61], precisely defined performance requirements, technical specifications and quality standards [58], as well as protective instruments such as guarantees [70].

Contractual provisions should also provide rewards for contractors in cases where works are completed ahead of schedule while satisfying quality requirements [53], as well as where cost savings are achieved [48, 85]. At the same time, contractors should bear sanctions if the project is not completed within the agreed budget and timeframe [52, 85]. Moreover, the project should have a developed system for reporting and monitoring contract implementation [14, 38], as well as a mechanism for evaluating contractor performance [65].

Prior to contract signing, the client should apply various methods to assess the characteristics of agents, contractors who compete in tenders (screening). This may be carried out in three ways. The first involves investigating the background, reputation, and previous projects of companies participating in the tender procedure [84]. The second relates to the detailed analysis of submitted tenders [83], including comparison of offered prices with market prices to assess their justification and competitiveness. The third option is to require financial guarantees from tenderers, such as advance payment guarantees or bank guarantees [50], thereby confirming their seriousness and financial capability to fulfil contractual obligations.

On the other hand, contractors may themselves signal their quality and reliability to clients, for example through the presentation of certificates [37] or through marketing activities [36, 37]. One significant risk is price dumping, which is why knowledge of methods for calculating the optimal tender price may help to avoid it [31].

A significant proportion of risks arising from information asymmetry may already be limited during the contractor selection phase. This particularly applies to situations in which the client has the possibility of selecting a contractor with a verified reputation [80], aligned organisational values and business culture [44, 90], or one with whom there is already previous experience of cooperation and an established partnering relationship [81].

Effective quality control plays a key role in reducing risks associated with information asymmetry during the execution phase [75]. In addition to supervision itself, the cooperation of participants and the open sharing of information and benefits from the very beginning of the project are also important [45]. Communication among stakeholders should be transparent, accountable [14, 70], credible [70], honest [23], and more informal in nature [38]. Trust between participants should be established and maintained throughout the entire duration of the project [8].

The client should also provide contractors with non-financial (intrinsic) forms of reward, such as enhancement of reputation, a greater degree of autonomy and responsibility, job satisfaction, stability, and alignment of objectives [62]. Finally, transparency in information management may be achieved using various information systems [39], including BIM [91, 92], blockchain [91], software platforms for project management [46], and the application of open-book accounting principles [47, 81]. This reduces the scope for information manipulation and improves coordination and decision-making.

During the interviews, respondents recognised three additional mitigation measures for risks caused by information asymmetry: replacement of company representatives, mediation between participants through a third party, and the establishment of communication protocols. Replacement of representatives was recognised as effective in cases of personal conflicts, disagreements, or impaired trust among project participants. The possibility of mediation through a neutral third party was also

Table 4. Mitigation measures determined through the literature review and interviews with experts, according [93]

ID	Mitigation measure	Source	Interviews
M1	Financial incentives for the contractor (bonuses)	[8, 11, 14, 23, 38, 40, 41, 44, 46–48, 53, 57, 61, 62, 65, 66, 71–73, 75, 80, 82, 83, 86, 88, 89, 94–101]	verified
M2	The tenderer signals its characteristics to the client (advertising, reputation)	[8, 36, 37, 44, 50, 53, 55, 58, 59, 65, 66, 70, 80, 84]	verified
M3	Cooperation and trust-building	[8, 14, 23, 37, 38, 44, 45, 48, 70, 74, 77, 81, 87]	verified
M4	Information systems	[8, 9, 36–40, 43–48, 81, 91, 92]	verified
M5	Regular and thorough quality control	[11, 40, 42, 60, 66, 72, 73, 75, 80, 102]	verified
M6	Contractually defined criteria for monitoring contractor performance	[14, 23, 38, 48, 51, 53, 54, 58, 61, 65]	verified
M7	Fair distribution of risks between the client and the contractor	[15, 43, 48, 61, 67, 81, 85, 98, 99]	verified
M8	Contractual penalties	[23, 46, 48, 52, 53, 75, 101]	verified
M9	The client reviews submitted tenders	[14, 31, 36, 72, 73, 78, 83]	verified
M10	The client verifies tenderers (certificates, guarantees, financial stability)	[14, 36, 61, 70, 84]	verified
M11	Non-financial rewards for the contractor (enhancement of reputation, job satisfaction, autonomy)	[40, 48, 52, 62]	verified
M12	Selection of a tenderer with a similar organisational culture (values, objectives)	[8, 44, 90]	verified
M13	Replacement of company representatives	interviews	added
M14	Mediation between participants through a third party	interviews	added
M15	Communication protocols	interviews	added

emphasised. The largest number of respondents additionally highlighted the importance of clearly defined communication protocols. Although these were initially included within measure M4 – Information systems, it was decided to present them separately because the respondents emphasised their key role in risk prevention, regardless of the use of information systems. The final list of key mitigation measures for risks caused by information asymmetry is presented in Table 4.

In the context of risk management, it is important to emphasise that the proposed measures do not operate solely to mitigate the consequences of realised risks, but also to reduce their probability of occurrence. For example, tenderer verification procedures, high-quality preparation of project documentation, clearly defined contractual conditions, and the establishment of supervision systems represent preventive mechanisms that may significantly reduce the likelihood of risks caused by information asymmetry arising. However, due to the inherent nature of such risks, their complete elimination is generally not possible; rather, the objective of management is to achieve an optimal balance between prevention and consequence mitigation.

5. Framework for managing risks caused by information asymmetry

Based on the literature analysis and interviews with experienced construction project experts, key risks associated with information asymmetry were identified, together with their consequences and possible mitigation measures. Figure 2 illustrates a framework for managing these risks, the structure of which was developed according to the highlighted risks, their consequences, and the corresponding measures necessary for effective management in construction practice.

Risks associated with hidden characteristics (adverse selection) arise prior to contract signing, during the tendering phase. On the other hand, risks arising from hidden information and activities (moral hazard) and hidden intentions (hold-up) occur after contract signing, during the construction phase, and may persist throughout project delivery.

These types of risks most commonly affect project objectives, both during construction and after its completion. Effective risk management requires their timely identification, particularly during the tendering phase, as well as their continuous monitoring and the application of mitigation measures to reduce their frequency or negative impact.

The proposed framework illustrates the logical relationship between risks, their consequences, and mitigation measures throughout different project phases. Its application in practice involves the identification of relevant risks in a specific project phase, assessment of their potential impact, and selection of appropriate measures for their management.

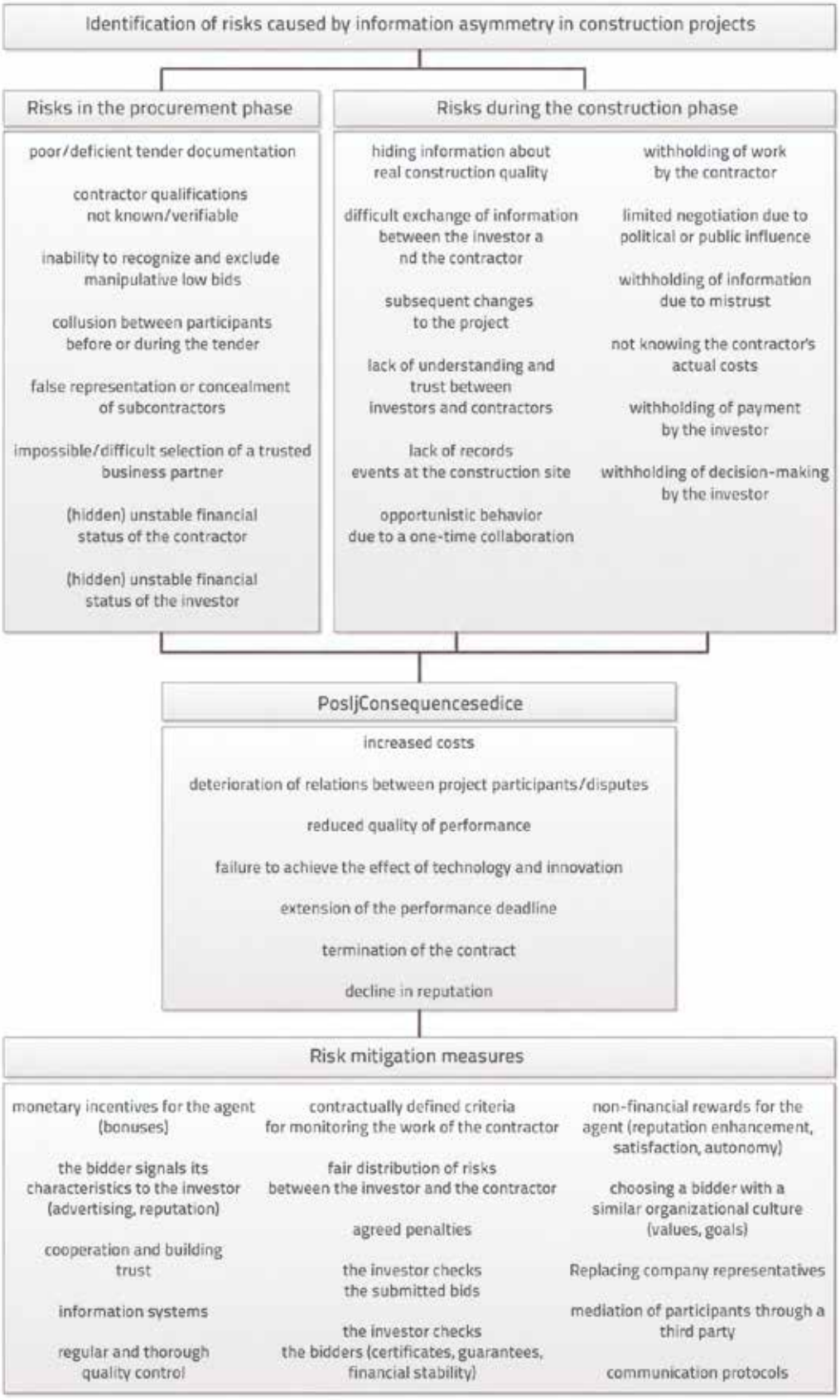

Figure 2. Framework for managing risks caused by information asymmetry

6. Conclusion

This paper presents a framework for managing risks arising from information asymmetry in construction projects. The study identified and classified the principal risks associated with information asymmetry between clients and contractors according to the theoretical categories of principal–agent theory. It further identified their principal consequences and corresponding mitigation measures, thereby providing a structured basis for systematic risk management throughout the project life cycle.

Due to the diversity of construction projects, the framework developed in this research has certain limitations regarding its generalisation. The interview-based research established that the significance of risks, as well as the applicability of mitigation measures, varies depending on the type of project (public or private). It was also observed that the approach to risk management differs depending on the role of the participant – whether it is implemented by the client or the contractor. Therefore, it is important to apply the framework in a manner adapted to different project types and participant perspectives to effectively connect risks, their consequences, and the corresponding mitigation measures.

The primary contribution of this research is the establishment of a foundation for the identification of risks arising from information asymmetry in future construction projects. The established consequences indicate the project objectives that may be affected, emphasising the importance of their timely recognition during the early stages of the risk management process. In addition, the prioritised mitigation measures identified in this study may serve as a basis for the development of appropriate risk response strategies. Future research should validate the proposed framework using empirical evidence obtained from completed construction projects and evaluate its applicability across different procurement systems, contractual arrangements, and national construction markets

Acknowledgements

The authors thank all construction experts who participated in this research whose expertise significantly contributed to the successful completion of this research. Special thanks are extended to Ladislav Bevanda, Edvard Ćoza, Ivana Karačić, Tihomir Lažeta, Goran Legac, Mario Lovrinčević, Tamara Marić, Davor Perić, Roman Perić, Siniša Radaković, and Marko Sokolović. This paper was carried out within the institutional research project BLOCKRUG (Digital Transformation of Circular Construction Using Blockchain Technology), funded by the Ministry of Science, Education and Youth of the Republic of Croatia under the National Recovery and Resilience Plan 2021–2026, with co-financing from the European Union through the NextGenerationEU programme.

REFERENCES

[1] Thakur, A.I., Khan, S., Siddiqui, M.J.: Risk management and life cycle costing of infrastructure project, International Journal of Recent Advances in Engineering & Technology, 4 (2016) 3, pp. 70–75.

[2] PMI's Pulse of the Profession In-Depth Report: The High Cost of Low Performance: The Essential Role of Communications, www.pmi.org, 30.5.2019.

[3] Cerić, A.: A Framework for Process-Driven Risk Management in Construction Projects, Research Institute for the Built and Human Environment, University of Salford, 2003.

[4] Assaf, S., Hassanain, M.A., Abdallah, A.: Review and assessment of the causes of deficiencies in design documents for large construction projects, International Journal of Building Pathology and Adaptation, 36 (2018) 3, pp. 300–317.

[5] Choudhry, R.M., Gabriel, H.F., Khan, M.K., Azhar, S.: Causes of discrepancies between design and construction in the Pakistan construction industry, Journal of Construction in Developing Countries, 22 (2018) 2, pp. 1–18.

[6] Dey, P.P., Khan, M., Amin, M., Sinha, B.R., Badkoobehi, H., Jawad, S., Any, L.A.: Managing interacting software project risks, PressAcademia Procedia, Global Business Research Congress (GBRC), Istanbul, 2016.

[7] Cerić, A., Ivić, I.: Network analysis of interconnections between theoretical concepts associated with principal-agent theory concerning construction projects, Organization, Technology and Management in Construction, 13 (2021) 1, pp. 2450–2464.

[8] Cerić, A.: Minimising communication risk in construction: a Delphi study of the key role of project managers, Journal of Civil Engineering and Management, 20 (2014) 6, pp. 829–838.

[9] Cerić, A.: Reducing information asymmetry and building trust in projects using blockchain technology, GRAĐEVINAR, 73 (2021) 10, pp. 967-978, doi: https://doi.org/10.14256/JCE.3310.2021

[10] Jäger, C.: The Principal-Agent Theory within the Context of Economic Sciences, Books on Demand GmbH, 2008.

[11] Liu, J., Ma, G.: Study on incentive and supervision mechanisms of technological innovation in megaprojects based on the principal-agent theory, Engineering, Construction and Architectural Management, 28 (2020) 6, pp. 1593–1614.

[12] Flanagan, R., Norman, G.: Risk Management and Construction, Blackwell Science, Oxford, 1993.

[13] ISO: Risk management - Guidelines, ISO 31000:2018, 2018.

[14] Owusu-Manu, D.-G., Kukah, A.S., Boateng, F., Asumadu, G., Edwards, D.J.: Exploring strategies to reduce moral hazard and adverse selection of Ghanaian public–private partnership (PPP) construction projects, Journal of Engineering, Design and Technology, 19 (2021) 2, pp. 358–372.

[15] Cantarelli, C.C., Chorus, C.G., Cunningham, S.W.: Explaining cost overruns of large-scale transportation infrastructure projects using a signalling game, Transportmetrica A: Transport Science, 9 (2013) 3, pp. 239–258.

[16] Ivić, I., Cerić, A.: Risks caused by information asymmetry in construction projects: a systematic literature review, Sustainability, 15 (2023) 13, 9979.

[17] Cerić, A., Ivić, I.: Management of risks influenced by information asymmetry during construction: Framework for research, 7th International Project and Construction Management Conference (IPCMC2022), eds. C. Budayan, S. Kivrak, S. Ulubeyli, Yildiz Technical University, Istanbul, pp. 1099–1110, 2022.

[18] Lupia, A.: Delegation of power: agency theory, International Encyclopedia of the Social & Behavioral Sciences, ed. J.D. Wright, Elsevier, Amsterdam, pp. 58–60, 2015.

[19] Jensen, M.C., Meckling, W.H.: Theory of the firm: Managerial behavior, agency costs and ownership structure, Journal of Financial Economics, 3 (1976) 4, pp. 305–360.

[20] Eisenhardt, K.M.: Agency theory: An assessment and review, Academy of Management Review, 14 (1989) 1, pp. 57–74.

[21] Ivić, I.: Upravljanje rizicima prouzročenima informacijskom asimetrijom u građevinskim projektima, doktorski rad, Građevinski fakultet, Sveučilište u Zagrebu, 2024.

[22] Bernhold, T., Wiesweg, N.: Principal-agent theory: perspectives and practices for effective workplace solutions, A Handbook of Management Theories and Models for Office Environments and Services, eds. V. Danivska & R.Appel-Meulenbroek, Routledge, Oxon, pp. 117–128, 2022.

[23] Xiang, P., Zhou, J., Zhou, X., Ye, K.: Construction project risk management based on the view of asymmetric information, Journal of Construction Engineering and Management, 138 (2012) 11, pp. 1303–1311.

[24] Ebers, M., Gotsch, W.: Institutionsökonomische Theorien der Organisation, Organisationstheorien, eds. A. Kieser & M. Ebers, Kohlhammer, Stuttgart, pp. 247–308, 2006.

[25] Picot, A., Dietl, H., Franck, E.: Organisation – Eine ökonomische Perspektive, Schäffer-Poeschel, Stuttgart, 1999.

[26] Mendeley, https://www.mendeley.com/search/, 7.8.2025.

[27] Page, M.J., McKenzie, J.E., Bossuyt, P.M., Boutron, I., Hoffmann, T.C., Mulrow, C.D., et al.: The PRISMA 2020 statement: an updated guideline for reporting systematic reviews, BMJ, 372 (2021), n71.

[28] Hansen, S.: Characterizing interview-based studies in construction management research: Analysis of empirical literature evidences, The 2nd International Conference on Innovations in Social Sciences Education and Engineering (ICoISSEE), Bandung, Indonesia.

[29] Bengtsson, M.: How to plan and perform a qualitative study using content analysis, NursingPlus Open, 2 (2016), pp. 8–14.

[30] Forman, J., Damschroder, L.: Qualitative content analysis, Empirical Methods for Bioethics: A Primer (Advances in Bioethics, Vol. 11), eds. L. Jacoby & L.A. Siminoff, Emerald, Bingley, pp. 39–62, 2008.

[31] Ahmed, M.O., El-adaway, I.H., Coatney, K.T., Eid, M.S.: Construction bidding and the winner's curse: game theory approach, Journal of Construction Engineering and Management, 142 (2016), 04015076.

[32] Owusu-Manu, D.G., Kukah, A.S.K., Edwards, D.J., Ameyaw, E.E.: Fuzzy synthetic evaluation of moral hazard and adverse selection of public private partnership projects, International Journal of Construction Management, 23 (2023) 11, pp. 1805–1814.

[33] Owusu-Manu, D.G., Edwards, D.J., Kukah, A.S., Parn, E.A., El-Gohary, H., Hosseini, M.R.: An empirical examination of moral hazards and adverse selection on PPP projects: A case study of Ghana, Journal of Engineering, Design and Technology, 16 (2018) 6, pp. 910–924.

[34] Owusu-Manu, D.G., Kukah, A.S., Edwards, D.J., Pärn, E.A., El-Gohary, H., Aigbavboa, C.: Causal relationships of moral hazard and adverse selection of Ghanaian Public-Private-Partnership (PPP) construction projects, Journal of Engineering, Design and Technology, 16 (2018) 3, pp. 439–460.

[35] Xiang, P., Jia, F., Li, X.: Critical behavioral risk factors among principal participants in the Chinese construction industry, Sustainability, 10 (2018), 3158.

[36] Xiang, P., Huo, X., Shen, L.: Research on the phenomenon of asymmetric information in construction projects - The case of China, International Journal of Project Management, 33 (2015) 3, pp. 589–598.

[37] Feser, D., Runst, P.: Energy efficiency consultants as change agents? Examining the reasons for EECs' limited success, Energy Policy, 98 (2016), pp. 309–317.

[38] Forsythe, P., Sankaran, S., Biesenthal, C.: How far can BIM reduce information asymmetry in the Australian construction context?, Project Management Journal, 46 (2015) 3, pp. 75–87.

[39] Giraudet, L.-G.: Energy efficiency as a credence good: A review of informational barriers to energy savings in the building sector, Energy Economics, 87 (2020), 104698.

[40] Xue, F., Chen, G., Huang, S., Xie, H.: Design of social responsibility incentive contracts for stakeholders of megaprojects under information asymmetry, Sustainability, 14 (2022) 3, 1465.

[41] Lewis, G., Bajari, P.: Moral hazard, incentive contracts, and risk: Evidence from procurement, The Review of Economic Studies, 81 (2014) 3, pp. 1201–1228.

[42] Li, Y., Ning, Y.: Mitigating opportunistic behaviors in consulting projects: Evidence from the outsourced architectural and engineering design, Journal of Construction Engineering and Management, 148 (2022) 7, 04022044.

[43] Pesek, A.E., Smithwick, J.B., Saseendran, A., Sullivan, K.T.: Information asymmetry on heavy civil projects: Deficiency identification by contractors and owners, Journal of Management in Engineering, 35 (2019) 4, 04019008.

[44] Schieg, M.: Strategies for avoiding asymmetric information in construction project management, Journal of Business Economics and Management, 9 (2008) 1, pp. 47–51.

[45] Marinho, A., Couto, J., Teixeira, J.: Relational contracting and its combination with the BIM methodology in mitigating asymmetric information problems in construction projects, Journal of Civil Engineering and Management, 27 (2021) 4, pp. 217–229.

[46] Xu, Q., Chong, H.-Y., Liao, P.-C.: Collaborative information integration for construction safety monitoring, Automation in Construction, 102 (2019), pp. 120–134.

[47] Missbauer, H., Hauber, W.: Bid calculation for construction projects: Regulations and incentive effects of unit price contracts, European Journal of Operational Research, 171 (2006) 3, pp. 1005–1017.

[48] Snippert, T., Witteveen, W., Boes, H., Voordijk, H.: Barriers to realizing a stewardship relation between client and vendor: The Best Value approach, Construction Management and Economics, 33 (2015) 7, pp. 569–586.

[49] Ward, S.C., Chapman, C.B., Curtis, B.: On the allocation of risk in construction projects, International Journal of Project Management, 9 (1991) 3, pp. 140–147.

[50] Tserng, H.P., Ho, S.-P., Chou, J.-S., Lin, C.: Proactive measures of governmental debt guarantees to facilitate Public-Private Partnerships project, Journal of Civil Engineering and Management, 20 (2014) 4, pp. 548–560.

[51] Ive, G., Chang, C.-Y.: The principle of inconsistent trinity in the selection of procurement systems, Construction Management and Economics, 25 (2007) 7, pp. 677–690.

[52] Zhao, H., Liu, X., Wang, Y.: Evolutionary game analysis of opportunistic behavior of Sponge City PPP projects: a perceived value perspective, Scientific Reports, 12 (2022) 1, 8798.

[53] Chang, C.-Y., Ive, G.: Reversal of bargaining power in construction projects: Meaning, existence and implications, Construction Management and Economics, 25 (2007) 8, pp. 845–855.

[54] Chang, C.-Y., Ive, G.: The hold-up problem in the management of construction projects: A case study of the Channel Tunnel, International Journal of Project Management, 25 (2007) 4, pp. 394–404.

[55] Chang, C.-Y.: Understanding the hold-up problem in the management of megaprojects: The case of the Channel Tunnel Rail Link project, International Journal of Project Management, 31 (2013) 4, pp. 628–637.

[56] Williamson, O.E.: Public and private bureaucracies: A transaction cost economics perspectives, Journal of Law, Economics, and Organization, 15 (1999) 1, pp. 306–342.

[57] Yao, M., Wang, F., Chen, Z., Ye, H.: Optimal incentive contract with asymmetric cost information, Journal of Construction Engineering and Management, 146 (2020) 6, 04020054.

[58] Rosenfeld, Y., Geltner, D.: Cost-plus and incentive contracting: Some false benefits and inherent drawbacks, Construction Management and Economics, 9 (1991) 5, pp. 481–490.

[59] Lützkendorf, T., Speer, T.M.: Alleviating asymmetric information in property markets: building performance and product quality as signals for consumers, Building Research & Information, 33 (2005) 2, pp. 182–195.

[60] Liu, D., Xu, W., Li, H., Zhang, W., Wang, W.: Moral hazard and adverse selection in Chinese construction tender market: A case of Wenchuan earthquake, Disaster Prevention and Management, 20 (2011) 4, pp. 363–377.

[61] Xiang, P., Wang, J.: Research on preventing moral hazard of construction project based on information asymmetries, The Open Construction & Building Technology Journal, 8 (2014), pp. 468–475.

[62] Li, H., Lv, L., Zuo, J., Su, L., Wang, L., Yuan, C.: Dynamic reputation incentive mechanism for urban water environment treatment PPP projects, Journal of Construction Engineering and Management, 146 (2020) 8, 04020088.

[63] Liu, J., Wang, Y., Wang, Z.: Multidimensional drivers: exploring contractor rule violations in the construction industry, Engineering, Construction and Architectural Management, 30 (2023) 4, pp. 1496–1518.

[64] Liu, X., Lin, S., Liu, L., Qian, F., Zhang, K.: Exploring the factors triggering occupational ethics risk of technology transaction in Chinese construction industry, International Journal of Environmental Research and Public Health, 17 (2020) 4, 1175.

[65] Ma, L., Zhang, P.: Game analysis on moral hazard of construction project managers in China, International Journal of Civil Engineering, 12 (2014) 4A, pp. 429–438.

[66] Ma, T., Wang, Z., Ding, J.: Governing the moral hazard in China's sponge city projects: A managerial analysis of the construction in the non-public land, Sustainability, 10 (2018) 9, 3018.

[67] Shi, L., He, Y.J., Onishi, M., Kobayashi, K.: Double moral hazard and risk-sharing in construction projects, IEEE Transactions on Engineering Management, 68 (2021) 6, pp. 1919–1929.

[68] Wu, Y., Huang, Y., Luo, W., Li, C.: Construction supervision mechanism for public projects in China: Progress goal-oriented perspective, Journal of Management in Engineering, 30 (2014) 2, pp. 205–213.

[69] Xie, L., Xu, T., Ju, T., Xia, B.: Explaining the alienation of megaproject environmental responsibility behavior: a fuzzy set qualitative comparative analysis study in China, Engineering, Construction and Architectural Management, 30 (2023) 7, pp. 2794–2813.

[70] Xiong, W., Chen, B., Wang, H., Zhu, D.: Transaction hazards and governance mechanisms in Public-Private Partnerships: A comparative study of two cases, Public Performance & Management Review, 42 (2019) 6, pp. 1279–1304.

[71] Cheng, H., Zheng, S.: Incentive compensation mechanism for the infrastructure construction of electric vehicle battery swapping station under asymmetric information, Sustainability, 14 (2022) 12, 7041.

[72] Lampel, J., Miller, R., Floricel, S.: Impact of owner involvement on innovation in large projects: Lessons from power plants construction, International Business Review, 5 (1996) 6, pp. 561–578.

[73] Lampel, J., Miller, R., Floricel, S.: Information asymmetries and technological innovation in large engineering construction projects, R&D Management, 26 (1996) 4, pp. 357–369.

[74] Wu, G., Zuo, J., Zhao, X.: Incentive model based on cooperative relationship in Sustainable construction projects, Sustainability, 9 (2017) 7, 1191.

[75] Du, Y., Zhou, H., Yuan, Y., Xue, H.: Exploring the moral hazard evolutionary mechanism for BIM implementation in an integrated project team, Sustainability, 11 (2019) 20, 5719.

[76] Chen, T.-C., Lin, Y.-C., Wang, L.-C.: The analysis of BOT strategies based on game theory - Case study on Taiwan's high speed railway project, Journal of Civil Engineering and Management, 18 (2012) 5, pp. 662–674.

[77] González-Díaz, M., Arruñada, B., Fernández, A.: Causes of subcontracting: Evidence from panel data on construction firms, Journal of Economic Behavior & Organization, 42 (2000) 2, pp. 167–187.

[78] Ho, P.S., Levitt, R., Tsui, C.-W., Hsu, Y.: Opportunism-focused transaction cost analysis of public-private partnerships, Journal of Management in Engineering, 31 (2015) 6, 04015007.

[79] Montrimas, A., Bruneckienė, J., Gaidelys, V.: Beyond the socio-economic impact of transport megaprojects, Sustainability, 13 (2021) 15, 8547.

[80] Han, H., Shen, J., Liu, B., Han, H.: Dynamic incentive mechanism for large-scale projects based on the reputation effects, SAGE Open, 12 (2022) 4.

[81] Badenfelt, U.: The selection of sharing ratios in target cost contracts, Engineering, Construction and Architectural Management, 15 (2008) 1, pp. 54–65.

[82] Guo, S., Wang, J., Xiong, H.: The influence of effort level on profit distribution strategies in IPD projects, Engineering, Construction and Architectural Management, 30 (2023) 9, pp. 4099–4119.

[83] Chen, W., Li, L.: Incentive contracts for green building production with asymmetric information, International Journal of Production Research, 59 (2021) 6, pp. 1860–1874.

[84] Fernández-Solís, J.L., Rybkowski, Z.K., Xiao, C., Lü, X., Chae, L.S.: General contractor's project of projects – a meta-project: understanding the new paradigm and its implications through the lens of entropy, Architectural Engineering and Design Management, 11 (2015) 3, pp. 213–242.

[85] Zheng, L., Lu, W., Chen, K., Chau, K.W., Niu, Y.: Benefit sharing for BIM implementation: Tackling the moral hazard dilemma in inter-firm cooperation, International Journal of Project Management, 35 (2017) 3, pp. 393–405.

[86] Cao, D., Wang, G.: Contractor–subcontractor relationships with the implementation of emerging interorganizational technologies: roles of cross-project learning and pre-contractual opportunism, International Journal of Construction Education and Research, 10 (2014) 4, pp. 268–284.

[87] Yiyong, L., Yousong, W., Jingkuang, L.: Analysis of adverse selection for motivation mechanism in engineering project cost management, Research Journal of Applied Sciences, Engineering and Technology, 5 (2013), pp. 3777–3782.

[88] Liang, X., Shen, G.Q., Guo, L.: Optimizing incentive policy of energy-efficiency retrofit in public buildings: A principal-agent model, Sustainability, 11 (2019) 12, 3442.

[89] Wu, G.: A multi-objective trade-off model in sustainable construction projects, Sustainability, 9 (2017) 11, 1929.

[90] Warsame, A., Borg, L., Lind, H.: How can clients improve the quality of transport infrastructure projects? The role of knowledge management and incentives, The Scientific World Journal, 2013, 709423.

[91] Singh, A.K., Prasath Kumar, V.R.: Smart contracts and supply chain management using blockchain, Journal of Engineering Research, 9 (2022), pp. 1–11.

[92] Sun, J., Wang, L.: The interaction between BIM's promotion and interest game under information asymmetry, Journal of Industrial and Management Optimization, 11 (2015) 4, pp. 1301–1319.

[93] Ivić, I., Cerić, A.: Mitigation measures for information asymmetry between participants in construction projects: The impact of trust, Sustainability, 16 (2024), 6808.

[94] Hajjej, I., Hillairet, C., Mnif, M., Pontier, M.: Optimal contract with moral hazard for Public Private Partnerships, Stochastics, 89 (2017) 6–7, pp. 1015–1038.

[95] Shi, S., Yin, Y., An, Q., Chen, K.: Optimal build-operate-transfer road contracts under information asymmetry and uncertainty, Transportation Research Part B: Methodological, 152 (2021), pp. 65–86.

[96] Shi, S., Yin, Y., Guo, X.: Optimal choice of capacity, toll and government guarantee for build-operate-transfer roads under asymmetric cost information, Transportation Research Part B: Methodological, 85 (2016), pp. 56–69.

[97] Su, P., Peng, Y., Hu, Q., Tan, R.: Incentive mechanism and subsidy design for construction and demolition waste recycling under information asymmetry with reciprocal behaviors, International Journal of Environmental Research and Public Health, 17 (2020) 12, 4346.

[98] Wang, Y., Cui, P., Liu, J.: Analysis of the risk-sharing ratio in PPP projects based on government minimum revenue guarantees, International Journal of Project Management, 36 (2018) 6, pp. 899–909.

[99] Wang, Y., Gao, H.O., Liu, J.: Incentive game of investor speculation in PPP highway projects based on the government minimum revenue guarantee, Transportation Research Part A: Policy and Practice, 125 (2019), pp. 20–34.

[100] Zhang, R., Zhou, Y., Zhuang, H., Zhu, X.: Study on the project supervision system based on the principal-agent theory, Journal of Industrial Engineering and Management, 8 (2015) 2, pp. 491–508.

[101] Zhao, L., Zhong, S.: Analysis of collusion between contractors and supervisors in constructions, Journal of Southwest Jiaotong University, 48 (2013) 6, pp. 1136–1141.

[102] Nie, X., Wang, Y., Wang, B.: Quality control of water conservancy construction projects considering contractor's credibility, Journal of Coastal Research, 104 (2020), pp. 410–414.